The role of chemerin and chemerin derived peptides in inflammation

A thesis submitted for the degree of Doctor of Philosophy in Pathology

University of Oxford

Trinity Term 2015



Daniel Regan-Komito

Lincoln College
Sir William Dunn School of Pathology

Abstract

The role of chemerin and chemerin derived peptides in inflammation

Daniel Regan-Komito, Lincoln College & Sir William Dunn School of Pathology

Submitted for the degree of D.Phil of Pathology, Trinity Term 2015

Inflammation is a normal physiological response to invading pathogens or tissue injury. However, if the inciting stimulus is not efficiently cleared, the inflammatory response is not resolved and becomes chronic. Chronic inflammation plays an important role in the pathology of a variety of diseases including atherosclerosis, rheumatoid arthritis, multiple sclerosis, psoriasis, colitis and cancer. Understanding this disease process and its regulation is of paramount importance for the development of novel therapies for these diseases.

Chemerin was originally isolated from inflammatory exudate fluid and found to be a ligand for the orphan G-protein coupled receptor, ChemR23. Secreted in an inactive pro-form, pro-chemerin, the carboxyl terminus can be cleaved by different proteases to generate active chemerin isoforms. Active chemerin is a chemoattractant for immature dendritic cells, natural killer cells and macrophages. The role played by chemerin during chronic inflammation remains controversial. It has been reported to be elevated in patients with a number of inflammatory and metabolic diseases but chemerin and shorter chemerin derived peptides have also been reported to exert anti-inflammatory effects in pre-clinical murine models.

In this thesis, I set out to investigate what role chemerin plays during inflammation. I demonstrated that chemerin can exert both pro- and anti-inflammatory effects depending on the time of intervention. During a standard model of acute inflammation (zymosan induced peritonitis), pre-treatment of animals with recombinant murine chemerin increased neutrophil recruitment while administration of chemerin into an already inflamed peritoneum significantly reduced monocyte recruitment. These effects are likely due to further proteolytic processing of active chemerin as demonstrated by the incubation of active chemerin with neutrophil derived proteases, which produced shorter bioactive peptides.

Chemerin binds to three receptors, ChemR23, GPR1 and CCRL2. Both ChemR23 and GPR1 have been demonstrated to induce downstream signalling following chemerin binding but CCRL2 does not. CCRL2 is expressed on a range of cell types and its expression is rapidly increased following inflammatory stimuli. However, its role in inflammation remains largely unknown. I have demonstrated that animals lacking the CCRL2 chemerin receptor display exaggerated monocyte and neutrophil recruitment during acute inflammatory responses. This phenotype does not seem to be due to increased levels of total chemerin either locally or systemically, nor does it seem to be due to differences in local inflammatory mediator production. I observed increased neutrophils in the blood of these animals during acute inflammatory responses, indicating CCRL2 may play a role in dampening neutrophil mobilisation from bone marrow rather then exerting effects locally.

Taken together the experiments presented in this thesis suggest that targeting chemerin therapeutically may be of benefit in certain contexts but not in others. In addition, the non-signalling chemerin receptor CCRL2 plays a non-redundant role in regulating neutrophil and monocyte recruitment to local sites of inflammation as well as mobilisation of neutrophils into the blood stream.

Acknowledgments

There are so many people who without which, this thesis would not exist.

Firstly I would like thank my supervisor David Greaves for giving me the wonderful opportunity to study for a D.Phil in his laboratory, for always making time for one to one meetings to discuss my data, for allowing me to pursue my own research directions, for giving me the opportunity to teach during my D.Phil which I thoroughly enjoyed and for always being available to offer important career advice, despite his insane teaching schedule.

My second supervisor Asif Iqbal for constant support, advice and encouragement throughout my D.Phil studies, for help with all the *in vivo* experiments, for always being around for a drink in the University Club when experiments weren't working and finally for being a great friend who always does everything he can to help, no matter the situation.

I would like to thank the British Heart Foundation for funding my D.Phil and allowing me the opportunity to study and work at the Dunn School for four years.

To all other members of the Greaves lab, past and present. Gemma for being the source of all knowledge, laughter and helpful advice, Theo for teaching me as many Greek words as possible and educating me on how to properly pronounce words of the Irish language, Lewis for never letting an awkward silence take place, for coming out with the most ridiculous and hilarious jokes and for his never ending computer skills (without whom, the headings of this thesis would be in God knows what order), Max and Jamie for providing constant hilarious conversations and Sophia for expanding my knowledge of chemerin peptide biology through her own experiments.

To all my friends in Lincoln MCR as well as all members of 85 Marlborough Road, past and present for random nights ending in the MCR.

To my friends back home in Dublin, particularly Conor and Bob for making numerous trips over to Oxford and always taking time out to meet up whenever I was home. I couldn't ask for better friends.

To my family, without whom I can't imagine where I would be today. To my grandparents, John and Esther, for pushing me to keep learning, for their patience and sage advice. To my parents, Vera and Lee, for their constant and unwavering support, understanding, encouragement and advice both during these last four years and also throughout my entire life.

Last but not least, my girlfriend Lucy, for putting up with my grumpiness during the last few months, for always cheering me up, for making me take time off when I needed it and for generally making my time in Oxford more meaningful then I could have imagined.

Abbreviations

ACN	Acetyl nitrile
ADP	Adenosine triphosphate
AP-1	Activator protein 1
Apo E	Apoliprotein E
Arg-1	Arginase-1
ASO	Anti-sense oligonucleotide
ATP	Adenosine triphosphate
BAL	Broncheolar lavage
BMI	Body mass index
BSA	Bovine serum albumin
cAMP	Cyclic adenosine monophosphate
CCRL2	CC chemokine receptor like-2
CHO-K1	Chinese hamster ovary cell 1
CI	Cell Index
CMKLR1	Chemokine like receptor 1
CNS	Central nervous system
COX-2	Cycloxygenase 2
CRP	C-reactive protein
DC	Dendritic cell
DMEM	Dulbeccos modified eagle medium
DNA	Deoxyribonucleic acid
DNP	2,4-Dinitrophenol
DSS	Dextran sodium sulphate
EAE	Experimental autoimmune encephalomyelitis
EDTA	Ethylenediaminetetraacetic acid
ELISA	Enzyme-linked immunosorbent assay
ERK	Extracellular regulated kinase
FACS	Flow assisted cell sorting
FBS	Fetal bovine serum
FFA	Free fatty acid
FITC	Fluorescein isothiocyanate
FLS	Fibroblast like synoviocytes
fMLP	N-formylmethionyl-leucyl-phenylalanine
FoxP3	Forkhead box P3
FPR1	Formyl peptide receptor 1
FPR2	Formyl peptide receptor 2
G-CSF	Granulocyte colony stimulating factor
GDP	Guanine diphosphate
GFP	Green fluorescent protein
GPCR	G-protein coupled receptor
GPR1	G-protein coupled receptor 1
GTP-	Guanine triphosphate
H&E	Haemotoxylin and Eosin
HEPES	4-(2-hydroxyethyl)-1-piperazineethanesulfonic acid
HEV	High endothelial venules
HPLC	High performance liquid chromatography
HUVEC	Human umbilical vein endothelial cell
I.P.	Intraperitoneal

I.V.	Intravenous
IBD	Inflammatory bowel disease
ICAM-1	Intercellular adhesion molecule 1
IFN-γ	Interferon-γ
Ig	immunoglobulin
IL	Interleukin
LDL	Low density lipoprotein
LFA-1	Lymphocyte function-associated antigen-1
LPS	Lipopolysaccharide
LTB_4	Leukotriene B_4
LXA_4	Lipoxin A_4
MAC-1	Macrophage antigen 1
M-CSF	Macrophage colony stimulating factor
MEK	Mitogen-activated protein kinase kinase
MMP	Matrix metalloproteinase
MPO	Myeloperoxidase
MS	Multiple sclerosis
NF_KB	Nuclear factor kappa-light-chain-enhancer of activated B cells
NK	Natural killer
NLR	Nod like receptor
NLRP3	NLR family, pyrin domain containing 3
OVA	Ovalbumin
PAMP	Pathogen associated molecular pattern
PBS	Phosphate buffered saline
PCR	Polymerase chain reaction
pDC	Plasmacytoid dendritic cell
PEC	Peritoneal exudate cells
PGD2	Prostaglandin D_2
PGE_2	Prostaglandin E_2
PI3K	Phosophatidylinositol 3-kinase
Poly I:C	Polyinosinic:polycytidylic acid
PPAR-γ	Peroxisome proliferator-activated receptor-ϒ
PRR	Pathogen recognition receptors
PSGL-1	P-selectin glycoprotein ligand 1
PTX	Pertussis toxin
PUFA	Polyunsaturated fatty acids
RA	Retinoid acid
RAG	Recombinase activating gene
RIG-I	Retinoic acid inducible gene-1
RNA	Ribonucleic acid
ROCK	Rho-associated protein kinase
Rpm	Revolusions per minute
RPMI	Rosswell Park Memorial Institute
SCID	Severe combined immunodeficient
siRNA	Small interfering ribonucleic acid
SR-A1	Steroid receptor RNA activator 1
SREBP2	Sterol regulatory element-binding protein 2
TBE	Tris-borate-EDTA
TFA	Trifluoroacetic acid
TFG-β	Transforming Growth Factor-β

TIG2	Tazarotene induced gene 2
TLR	Toll like receptor
TMB	3,3',5,5'–Tetramethylbenzidine
TNF-α	Tumour necrosis factor- α
Treg	Regulatory T cells
VCAM-1	Vascular cell adhesion protein 1
VEGF	Vascular endothelial growth factor
VLA-4	Very late antigen-4
ZIP	Zymosan induced peritonitis

Table of Contents

Abstract i

Acknowledgments ii

Abbreviations iii

Table of Contents vi

List of Figures xiii

List of Tables xvi

1 Introduction 1

1.1 Acute inflammation 1

1.1.1 Endothelial cells. 2

1.1.2 Neutrophils 3

1.1.3 Monocytes 5

1.1.4 Mast cells 6

1.2 Macrophages; Sentinels of the immune system 7

1.3 Atherosclerosis: An example of macrophage dominated chronic inflammation 9

1.4 The resolution of inflammation 13

1.4.1 Pro-resolving eicosanoids 14

1.4.2 Cytokines 16

1.4.3 Adenosine 17

1.4.4 Annexin A1 and the annexin peptide Ac2-26 17

1.4.5 Return to tissue homeostasis 18

1.5 Leukocyte recruitment and chemotaxis in inflammation 20

1.5.1 Neutrophil mobilisation during inflammation 20

1.5.2 Monocyte mobilisation during inflammation 21

1.5.3 Non-classical chemoattractants 22
1.5.4 Targeting chemokines for the treatment of inflammatory diseases. 23
1.6 Chemerin 25
1.6.1 Historical overview and structure 25
1.6.2 Regulation of chemerin expression by steroid hormones, metabolic cues and cytokines. 26
1.6.3 Chemerin bioactivity regulation by proteolytic cleavage 29
1.6.4 The role of chemerin in chemotaxis and recruitment of immune cells to sites of inflammation 32
1.6.5 The role of endogenous chemerin in inflammatory diseases 35
1.6.6 The function of chemerin as an adipokine and its role in metabolic disease 40
1.6.7 The role of chemerin in host defence 43
1.6.8 Anti-inflammatory effects of chemerin 45
1.7 Chemerin receptors 50
1.7.1 ChemR23 50
1.7.2 GPR1 52
1.7.3 CCRL2 54
1.8 Original hypotheses for this thesis 57
1.9 Experimental Aims. 57
2 Materials and Methods 58
2.1 Materials 58
2.1.1 Proteins and peptides used 58
2.2 *In vivo* procedures 58
2.3 Antibodies 60
2.4 In vivo models 61
2.4.1 Zymosan induced peritonitis 61
2.4.2 Thioglycollate induced peritonitis 62

2.4.3 LPS endotoxemia 63
2.4.4 Dextran Sodium Sulphate (DSS) induced colitis 63
2.5 Biogel-elicited peritoneal exudate cell isolation. 64
2.6 Bone marrow derived macrophage isolation 65
2.7 Electrical impedance sensing assays 66
2.8 Real time chemotaxis assay 68
2.9 ChemR23 β-arrestin recruitment assays. 69
2.10 Macrophage activation assays 70
2.11 ELISA assays 70
2.12 Luminex assays 72
2.13 Mass spectrometry 73
2.14 Myeloperoxidase (MPO) assay 74
2.15 Preparation of different murine tissues for flow cytometry 75
2.15.1 Blood analysis 75
2.15.2 Tissue analysis (Spleen, liver and lung) 76
2.15.3 Bone marrow analysis 76
2.16 Cell counting 77
2.16.1 Neubauer haemocytometer 77
2.16.2 Automated Cellometer 78
2.16.3 Countbright counting beads 78
2.17 CCRL2 KO mouse genotyping 79
2.17.1 Genomic DNA isolation 79
2.17.2 Polymerase chain reaction (PCR) 80
2.17.3 Agarose gel electrophoresis 81
2.18 Data analysis 82
3 Optimisation of the zymosan induced peritonitis model to probe the role of endogenous chemerin during sterile inflammation. 84

3.1 Introduction 84

3.1.1 Experimental Peritonitis 84

3.1.2 Zymosan induced peritonitis (ZIP) 88

3.1.3 Applications of the zymosan induced peritonitis model in innate immunity. . 89

3.2 Rationale for the experiments presented in this chapter 91

3.3 Aims 92

3.4 Results 93

3.4.1 Characterisation of the zymosan induced peritonitis model 93

3.4.2 CCR2 plays a non-redundant role in monocyte recruitment during ZIP 102

3.4.3 Use of 100μg ZIP to assess the efficacy of the CC chemokine binding protein 35K 105

3.5 Discussion 108

3.5.1 Characterisation of the 100μg zymosan induced peritonitis model. 108

3.5.2 Validation of the 100 μg ZIP model with CCR2 KO mice. 113

3.5.3 Use of 100 μg ZIP to assess the CC chemokine binding protein 35K 114

3.5.4 Limitations of the study 116

3.6 Summary 117

4 Chemerin modulates inflammation 118

4.1 Introduction 118

4.1.1 Chemerin expression and processing 118

4.1.2 Chemoattractant properties of Chemerin 118

4.1.3 Endogenous chemerin levels in health and disease 119

4.1.4 Anti-inflammatory effects of chemerin and chemerin derived peptides 120

4.2 Rationale for the experiments 121

4.3 Aims of this chapter 122

4.4 Results 123

4.4.1 Characterisation of the chemoattractant properties of chemerin and chemerin derived peptides *in vitro.* ... 123
4.4.2 Characterisation of cytoskeletal changes induced by chemerin and chemerin derived peptides *in vitro.* ... 127
4.4.3 Bioactivity of chemerin and chemerin peptides in inflammatory activation assays. ... 134
4.4.4 The effects of chemerin and C17 peptide pre-treatment on inflammation *in vivo.* ... 141
4.4.5 The Effects of chemerin and the C17 peptide intervention on inflammation *in vivo.* ... 142
4.4.6 Endogenous chemerin levels increase *in vivo* during inflammation ... 153
4.4.7 The effects of knockdown of endogenous chemerin *in vivo.* ... 158
4.5 Discussion ... 163
4.5.1 Characterisation of the chemoattractant properties of chemerin and chemerin derived peptides *in vitro.* ... 163
4.5.2 Bioactivity of chemerin and chemerin peptides in inflammatory activation assays. ... 167
4.5.3 The effects of chemerin and C17 peptide on inflammation *in vivo.* ... 170
4.5.4 Endogenous chemerin levels increase *in vivo* during inflammation ... 173
4.5.5 The effects of knockdown of endogenous chemerin *in vivo.* ... 176
4.5.6 Limitations of these studies ... 179
4.6 Summary ... 180
5 The role of the non-signalling chemerin receptor CCRL2 during inflammation. ... 182
5.1 Introduction ... 182
5.2 Rational for the experiments ... 183
5.3 Experimental aims. ... 184

5.4 Results 185

5.4.1 CCRL2 plays a role in chemerin-induced adhesion in the electrical impedance sensing platform but not in chemotaxis assays. 185

5.4.2 Phenotypic characterisation of naïve animals lacking the CCRL2 receptor .. 189

5.4.3 Characterisation of inflammatory responses of animals lacking the CCRL2 receptor following challenge with zymosan..... 194

5.4.4 Animals lacking CCRL2 display increased CXCL1 production in the peritoneum during 1-hour thioglycollate challenge. 201

5.4.5 Animals lacking CCRL2 display no difference in neutrophil recruitment to the lungs or liver during LPS induced endotoxemia..... 203

5.4.6 Animals lacking CCRL2 experience exaggerated weight loss and enlarged spleens in a model of Dextran sodium sulphate (DSS) induced colitis. 205

5.5 Discussion 208

5.5.1 CCRL2 plays a role in chemerin-induced adhesion of murine macrophages in the electrical impedance sensing platform but not in chemotaxis. 208

5.5.2 Phenotypic characterisation of naïve animals lacking the CCRL2 receptor .. 209

5.5.3 Characterisation of inflammatory responses of animals lacking the CCRL2 receptor following challenge with zymosan..... 211

5.5.4 Animals lacking CCRL2 display increased neutrophil recruitment to the peritoneum and increased CXCL1 production during 1-hour thioglycollate challenge..... 214

5.5.5 Animals lacking CCRL2 display no difference in neutrophil recruitment to the lungs or liver during LPS induced endotoxemia..... 215

5.5.6 Animals lacking CCRL2 experience exaggerated weight loss and enlarged spleens in a model of dextran sodium sulphate (DSS) induced colitis. 216

5.5.7 Limitations and potential future studies 218

5.6 Summary 219

6 Summary and Final Discussion 220

6.1 Key findings 220

6.2 Future directions 221

6.2.1 *In vivo* administration of chemerin administration during an ongoing inflammatory response. 221

6.2.2 Identifying chemerin bioactivity at different inflammatory sites 222

6.2.3 Targeting chemerin therapeutically 224

6.2.4 Elucidating the role of the CCRL2 chemerin receptor in innate immune cell recruitment to sites of inflammation 227

6.3 Final summary and conclusions 229

References 231

Appendix 1: Published work 250

List of Figures

Figure 1.1 The Leukocyte adhesion cascade. 3

Figure 1.2 Monocyte recruitment and plaque development during atherosclerosis. 10

Figure 1.3. Predicted structure of chemerin. 25

Figure 1.4 Putative signaling pathways induced by ChemR23 and GPR1 activation. 54

Figure 2.1 Cell adhesion as measured using the impedance platform. 68

Figure 2.2 Standard curve of chemerin ELISA used to interpolate chemerin levels 72

Figure 2.3 Representative flow cytometry plot of countbright counting beads and cells to quantify cell numbers. 79

Figure 2.4 Typical genotyping results from the CCRL2 KO, heterozygous and wild type animals. 82

Figure 3.1 Representative flow cytometry images of a naïve unchallenged peritoneal cavity. 94

Figure 3.2 Different doses of zymosan/mouse produce varying degrees of inflammation as measured by inflammatory cell recruitment. 95

Figure 3.3 Kinetics of zymosan induced peritonitis. 96

Figure 3.4 100µg of zymosan induces a self-resolving inflammatory response. 99

Figure 3.5 Zymosan challenge induces a range of inflammatory cytokines and chemokines. 100

Figure 3.6 Kinetics of inflammatory mediator production during zymosan induced peritonitis. 101

Figure 3.7 Gating strategy for flow cytometric analysis of peritoneum, blood and bone marrow 103

Figure 3.8 CCR2 plays a non-redundant role in monocyte recruitment to the peritoneum during zymosan induced peritonitis. 104

Figure 3.9 Hydrodynamic delivery of the broad-spectrum CC chemokine binding 35K mutant R89A significantly reduces inflammatory cell recruitment in zymosan induced peritonitis 107

Figure 4.1 Chemerin and chemerin peptides promote chemotaxis of primary murine macrophages. 125

Figure 4.2 A range of chemotactic proteins induce adhesion of Bio-gel elicited macrophages in electrical impedance real time adhesion assay. 126
Figure 4.3 Adhesion in the impedance platform is dependent on $G_{\alpha i}$ signalling and cytoskeletal rearrangements. 130
Figure 4.4 Pertussis toxin and cytochalasin D do not affect the viability of Bio-Gel elicited PECs. 131
Figure 4.5 Chemerin and chemerin peptides induce adhesion of primary murine macrophages in a ChemR23 dependent manner. 133
Figure 4.6 Bone marrow derived macrophages display variable anti-inflammatory responses to chemerin and C17 treatment. 136
Figure 4.7 Recombinant M-CSF vs L929 conditioned media does not affect ChemR23 expression or inflammatory responses to TLR agonists in bone marrow derived macrophages. 140
Figure 4.8 Pre-treatment model of zymsoan induced peritonitis 144
Figure 4.9 Interventional model of zymosan induced peritonitis. 145
Figure 4.10 Acetylated C17 peptide does not decrease monocyte or neutrophil recruitment in 6 hour ZIP. 148
Figure 4.11 Chemerin intervention decreases monocyte numbers in ZIP. 149
Figure 4.12 Chemerin intervention decreases local CCL4 levels. 151
Figure 4.13 Recombinant human neutrophil elastase and cathepsin-g cleave recombinant chemerin to shorter bioactive peptides *in vitro.* 152
Figure 4.14 Endogenous chemerin levels increase during inflammation. 155
Figure 4.15 Dexamethasone decreases systemic chemerin levels during homeostasis and during inflammation. 157
Figure 4.16 Knock down of chemerin expression *in vivo* has no effect on inflammatory cell recruitment during zymosan induced peritonitis. 160
Figure 4.17 Knock down of chemerin expression *in vivo* has no effect on inflammatory mediator production during zymosan induced peritonitis. 161

Figure 4.18 Knock down of chemerin expression *in vivo* increases neutrophil and Ly6C^{hi} monocyte numbers in the blood during zymosan induced peritonitis. 162
Figure 5.1 CCRL2 is required for optimal chemerin induced adhesion in the electrical impedance sensing platform. 187
Figure 5.2 CCRL2 does not play a role in chemerin-induced chemotaxis of primary murine macrophages. 188
Figure 5.3 Animals lacking CCRL2 display larger spleens and decreased CD4 splenic T cell content under resting conditions. 190
Figure 5.4 Animals lacking CCRL2 display no overt differences in circulating cells in the blood under resting conditions. 191
Figure 5.5 Animals lacking CCRL2 display no obvious differences in monocyte or neutrophil numbers in the bone marrow under resting conditions. 193
Figure 5.6 Animals lacking CCRL2 display exaggerated monocyte and neutrophil recruitment during zymosan induced peritonitis. 195
Figure 5.7 Cytokines and chemokines in the peritoneal cavity of CCRL2 KO animals and C57Bl/6J animals. 198
Figure 5.8 Animals lacking CCRL2 display no obvious differences in spleen weight or composition during 4-hour ZIP. 199
Figure 5.9 Animals lacking CCRL2 display increased neutrophil and Ly6-C^{hi} monocytes in the blood after 4-hour zymosan induced peritonitis. 200
Figure 5.10 Animals lacking CCRL2 display increased CXCL1 levels after 1-hour challenge with thioglycollate. 202
Figure 5.11 Animals lacking CCRL2 do not display an obvious difference in neutrophil recruitment to the liver or lungs following LPS challenge 204
Figure 5.12 Animals lacking CCRL2 display exaggerated weight loss and splenomegaly in DSS induced colitis. 207

List of Tables

Table 1.1 Proteolytic cleavage of human chemerin by different proteases. 31

Table 2.1 Antibodies used throughout this thesis. 60

Table 3.1 Stimuli used to elicit peritoneal inflammation in mice. 86

Table 4.1Variation between experiments using bone marrow derived macrophages and modification of different variables. 139

1 Introduction

1.1 Acute inflammation

Inflammation is the physiological response to infection or damage and functions to limit the spread of a pathogen or to alert the body of local damage. Acute inflammation is defined as an inflammatory response normally resolved in a matter of days. The optimal outcome of an acute inflammatory response is the return to tissue homeostasis and the clearance of the pathogen or chemical agent that caused the inflammatory insult [1]. Classically, inflammation is characterised by heat, redness, swelling, pain and loss of function, first described by Celsus [2]. In the initial phase of an inflammatory response, mediators such as prostaglandins, leukotrienes, histamine, cytokines and complement components are rapidly released by resident macrophages, mast cells and endothelial cells. This is followed by an increase in vascular permeability and the rapid influx of plasma proteins and neutrophils followed by inflammatory monocytes. Recruited monocytes subsequently differentiate into macrophages and phagocytose both the invading pathogen as well as apoptotic neutrophils. This process, called efferocytosis will usually trigger the resolution phase of acute inflammation and the return to homeostasis [1]. Initially, the recruited inflammatory macrophages are potent producers of inflammatory eicosanoids such as prostaglandin E_2, D_2 and leukotriene B_4 [3]. In order to coordinate a successful halt to the inflammatory process, these macrophages upon phagocytosing apoptotic neutrophils must switch to sythesising pro-resolving eicosanoids such as lipoxins, resolvins, protectins and maresins. These pro-resolving eicosanoids alongside other mediators such as transforming growth factor-β (TGF-β) promote

inflammation resolution [4]. Inflammation is a complex process involving different cell types and a wide range of mediators which I will now discuss [5].

1.1.1 Endothelial cells.

Among the first cells to become activated during an inflammatory response are the endothelial cells which line vessels. Upon activation, endothelial cells increase expression of adhesion molecules on their surface such as P- and E-selectin. While both P- and E-selectin are expressed on endothelial cells, L-selectin and P-selectin glycoprotein ligand-1 (PSGL-1) are expressed on leukocytes and mediate the initial capture and slow rolling of neutrophils [6, 7] (Figure. 1.1). During this rolling, neutrophils can interact with the endothelial surface and come into contact with chemokines bound to the surface. Endothelial cells can make chemokines (IL-8) and bind chemokines made by other cell types on their surface via heparin sulphate proteoglycans [8, 9]. While E- and P-selectins can transiently bind neutrophils, affinity for their ligands is low. Another set of adhesion molecules that are expressed upon activation are the integrins. Integrins such as VLA-4 and LFA-1 mediate tighter adhesion of leukocytes under flow upon binding their counter ligands (VCAM-1 and ICAM-1) on activated endothelial cells [10-12]. Integrins on the neutrophil surface are activated in response to selectin and chemokine binding, increasing their affinity for their corresponding integrin on the endothelium [12, 13]. Another aspect of activated endothelial cells is the loosening of tight-junctions between adjacent endothelial cells, allowing adherent leukocytes to migrate into the inflamed tissue. The increased permeability of the endothelium is also responsible for the increase in fluid into the tissue (oedema) [14].

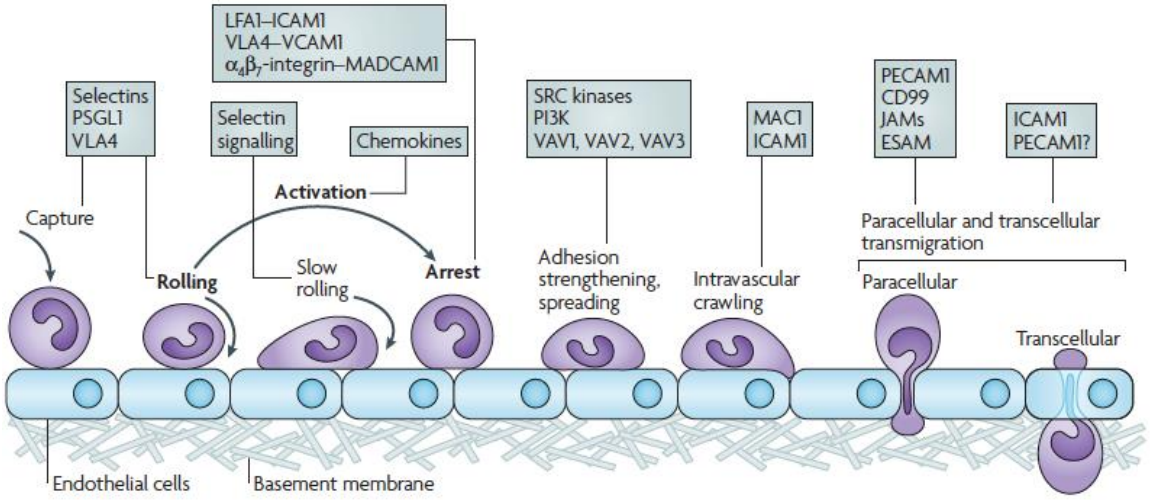


Figure 1.1 The Leukocyte adhesion cascade.

Adapted from Ley *et al.* [6]

1.1.2 Neutrophils

Neutrophils are the first cells recruited from the blood into an inflamed tissue [15]. One of the first signs of acute inflammation is a large number of neutrophils in a tissue. As mentioned earlier, interactions between neutrophils and endothelial cells are critical for rapid neutrophil entrance to sites of infection and inflammation. Under resting conditions, neutrophils are retained in the bone marrow, circulate in blood vessels and are found in spleen, liver and lung, although rarely in other healthy tissue [15-17]. Upon activation, local tissue resident macrophages and endothelial cells secrete chemokines such as IL-8, CXCL1 and CXCL2, which induce the mobilisation and recruitment of neutrophils to the site of inflammation. Upon E- and P- selectin (endothelial cells) binding L-selectin and PSGL-1 on neutrophils, integrins on the neutrophil surface (MAC-1) change into an active conformational state and this allows their migration into the inflamed tissue [6]. Neutrophils are capable of recognising a wide variety of pathogenic proteins. They

express pattern recognition receptors (PRRs) such as the Toll Like Receptors (TLRs), Nod-Like Receptors (NLRs) and opsonic receptors such as Fc receptors [18, 19]. Once a pathogen has been recognised and engulfed by a neutrophil into a phagosome, the phagosome fuses with the lysosome creating what is called the phagolysosome [20]. The neutrophil endeavors to destroy the pathogen by the production of reactive oxygen and reactive nitrogen species in a process known as the respiratory burst [21]. This is not the only mechanism by which neutrophils can destroy pathogens. Neutrophils have a number of potent anti-microbial peptides and enzymes stored in granules such as LL-37 and lysozyme, which can directly kill bacteria when the phagosome fuses with their granules [22]. Neutrophils are effective at clearing invading pathogens but they rapidly undergo apoptosis after phagocytosis and must be cleared by incoming macrophages to avoid undergoing necrosis and inducing further inflammation. NETosis is a recently described mechanism of neutrophil mediated pathogen clearance. Neutrophils secrete "extracellular traps" (composed of DNA, histones and intracellular proteins including antimicrobial proteins) to trap and kill bacteria in addition to eliciting further inflammatory signals and enhancing the recruitment of more leukocytes [23].

Another important function of neutrophils is the recruitment of inflammatory monocytes. Activated neutrophils rapidly undergo degranulation, releasing preformed mediators from their granules into the cellular milieu. The first granules to be released are the secretory granules, including azurocidin, which increases firm adherence of monocytes to the endothelium as well increasing oedema and plasma protein leakage into the tissue [24, 25]. Azurocidin is also capable of increasing CCL3 production from monocytes and macrophages, thus promoting further monocyte recruitment [26]. Both azurocidin and cathepsin-G (a neutrophil derived protease) have been reported to be directly chemotactic for monocytes and neutrophils [27]. Other proteases derived from

neutrophil granules such as proteinase-3 can induce further chemokine production from endothelial cells important for monocyte recruitment such as CCL2 [28]. Finally, neutrophils themselves also make a wide range of chemokines including IL-8, CCL3 and CCL4 [19, 29].

Neutrophils play important roles in directly clearing an invading pathogen but also in the recruitment of inflammatory monocytes to the site in order to begin resolution and return to tissue homeostasis.

1.1.3 Monocytes

Monocytes are circulating mononuclear myeloid cells that can traffic to sites of injury or infection and differentiate into macrophages or dendritic cells depending on specific growth factors. While it was thought that monocytes were primarily an intermediate differentiation state between bone marrow precursors and macrophages, it is now appreciated that they play important effector functions such as phagocytosis of pathogens and secretion of immunomodulators and chemokines [30, 31]. Monocytes are recruited to a site of inflammation by a range of classical chemokines (such as CCL2 and CCL3 [31]) as well as non-classical chemoattratants (galectins and chemerin [32, 33]). There are three distinct monocyte populations in humans and two in mice. In mice these two populations are classified as the $Gr1^{+}$/Ly6-c^{hi} and $Gr1^{-}$/Ly6-C^{lo} subsets and are functionally distinct. The $Gr1^{+}$/Ly6-c^{hi} monocytes are known as the "inflammatory" monocytes while the $Gr1^{-}$/Ly6-C^{lo} monocytes are thought to play a role in tissue repair and fibrosis [34]. Different monocyte subsets play important roles in inflammation. For example in myocardial infarction, $Gr1^{+}$/Ly6-c^{hi} monocytes accumulate at the site of injury and promote inflammation via the production of inflammatory mediators such as TNF-α. However, an

accumulation of $Gr1^{-}/Ly6\text{-}C^{lo}$ monocytes is also observed, they dominate at a later stage of post-infarction, which are associated with tissue repair, angiogenesis, collagen deposition and VEGF production [34, 35]. Wound healing in a cardiovascular injury model such as the aforementioned may depend on the fine balance between these two monocyte subsets. Novel therapies which shift this balance in favour of "tissue repair" $Gr1^{-}/Ly6\text{-}C^{lo}$ monocytes may be of clinical benefit. Humans have three monocyte subsets. The $CD14^{hi}$, $CD16^{-ve}$ subset correspond to the classical $Ly6C^{hi}$ monocytes in mice and also express CCR2. The $CD14^{+ve}$, $CD16^{hi}$ subset shares similar patrolling behavior to the $Ly6C^{lo}$ monocytes in mice and there is also a third intermediate subset, defined as $CD14^{hi}$, $CD16^{+ve}$ [31, 36].

Once monocytes have been recruited to inflamed tissue they can differentiate into macrophages. The characteristic most associated with macrophages is their capacity for phagocytosis and efferocytosis. One of the most important functions of newly recruited macrophages is the clearance of apoptotic neutrophils that have phagocytosed pathogens, and these cells will be discussed in detail in section 1.2.

1.1.4 Mast cells

Mast cells are resident within tissue and are rapid responders to inflammatory signals. Although these cells are classically thought of in the context of IgE/FcεRI mediated allergic inflammation and parasitic infections, it is now appreciated that mast cells respond to range of inflammatory stimuli [37]. For example, mast cells have been shown to express the receptors for the C3a and C5a complement components and readily respond to stimulation by complement cleavage products [38]. Complement components can induce both chemotaxis of mast cells as well as degranulation [39]. In addition, cytokines

such as IL-33 have been demonstrated to activate mast cells [40]. Mast cells have a large number of preformed inflammatory mediators stored within their granules such as histamine, proteases and TNF-α, which are secreted upon their activation. They can also produce other cytokines such as IL-6 and IL-8 as well as inflammatory prostanoids such as PGD_2 and LTB_4 [41]. Thus, mast cells rapidly respond to inflammatory cues and secrete a range of inflammatory mediators upon activation.

1.2 Macrophages; Sentinels of the immune system.

The classical phagocytic functions of macrophages and neutrophils were first recognised by Élie Metchnikoff over a century ago [42]. Resident macrophages populate most tissues of the body and act as the first line of defense against infection and tissue injury. In contrast to macrophages derived from inflammatory monocytes, resident macrophages exist in the tissue from birth and are derived from the yolk sac, rather then monocytic progenitors. They are heterogeneous depending on which tissue they are found in. Resident macrophages have been described in most tissues including the peritoneum, lungs, spleen, liver (Kuppfer cells), brain (microglia), lymph nodes, adipose tissue, bone, the gastrointestinal tract and the skin (Langerans cells) [43-45]. Studies have reported a common transcriptional profile of resident macrophages derived from the yolk sac in the liver, skin, brain, pancreas, lung, spleen and kidney, highlighting a common origin [44]. However, these cells are seeded in different tissues very early during development and recent studies have demonstrated that the tissue environment can exert a profound effect on the epigenetic profile of these populations [46, 47]. Interestingly, the enhancer landscape of resident macrophages from one tissue take on the epigenetic characteristics of another tissue they are implanted in, highlighting the plasticity of these cells as well as

the importance of the tissue in the context of macrophage phenotype [46]. For example, bone marrow derived macrophages transplanted into irradiated animals were found to have enhancers specific for each tissue and similar to the embryonic derived resident cells, highlighting the importance of the tissue microenvironment on macrophage enhancers [46].

The majority of tissue resident macrophage populations are now thought to self renew by local proliferation. One notable exception are the intestinal macrophages which are replenished by monocytes from the blood [48, 49]. Resident macrophages possess a large repertoire of pattern recognition receptors (PRRs) to detect invading pathogens including toll like receptors (TLRs), NOD like receptors (NLRs), Retinoic Acid Inducible Gene 1 (RIG-I) like receptors as well as scavenger receptors such as CD36 and SR-A [50]. TLRs recognise a range of conserved Pathogen Associated Molecular Patterns (PAMPs) such as components of bacterial cell walls (LPS by TLR4) to double stranded RNA derived from viruses (TLR3) [51]. The NLRs are a group of intracellular molecular sensors that detect both bacterial and viral PAMPs and activate the inflammasome, which is required for the secretion of the inflammatory cytokines IL-1β and IL-18 [52]. RIG-I like receptors are intracellular receptors that detect viral PAMPs and induce anti-viral responses [53]. Upon recognition of a pathogen, macrophages secrete a range of cytokines including TNF-α, IL-8, IL-6 and G-CSF. This initial response is important for the recruitment of both neutrophils as well as monocytes into a site of inflammation. The importance of resident macrophages in the initiation of inflammation has been demonstrated by the reduction in chemokine production and neutrophil recruitment after resident macrophages have been depleted using clodronate liposomes [54]. As well as secreting inflammatory chemokines, resident macrophages are thought to play important roles in antigen presentation to T cells in draining lymph nodes. Following zymosan

induced peritonitis in a mouse for example, labelled F4/80^{hi} resident macrophages disappear rapidly and have been observed in the draining lymph nodes. These macrophages were reported to be important for the contraction of lymph nodes during the resolution phase in these experiments [55].

As inflammation progresses, the majority of macrophages at the local site are monocyte derived inflammatory macrophages. However it has been demonstrated that tissue resident macrophages as well as recruited inflammatory macrophages undergo proliferation during inflammation, highlighting this as a potentially important mechanism of macrophage accumulation at a site of inflammation [56-58]. Another important function of macrophages, which will be discussed further is the clearance of apoptotic neutrophils and the initiation of tissue repair. Defective clearance of apoptotic neutrophils leads to secondary necrosis with the release of intracellular inflammatory mediators, thus prolonging the inflammatory response and delaying repair [59].

1.3 Atherosclerosis: An example of macrophage dominated chronic inflammation

As mentioned, acute inflammation is normally shut off in a matter of days and the return to tissue homeostasis begins. However, if the inciting stimulus is not removed or dead/dying neutrophils are not efficiently cleared, this acute inflammation can turn into chronic inflammation which is a different disease process rather then just a continuation of the acute response. I have chosen to use atherosclerosis as a relevant example of chronic inflammation (Figure 1.2). It was assumed for years that the formation of atherosclerotic lesions in artery walls was merely the result of cholesterol accumulation in the vessel walls. The development of plaques and particularly plaque rupture is now regarded as a non-resolving chronic inflammatory disease [60].

Cholesterol is transported in the blood by low-density lipoprotein (LDL) particles, which are composed of cholesterol, triglycerides and apolipoprotein B100 [61]. These particles accumulate in the intima of arteries where they become trapped and undergo oxidative modifications by enzymes (2/15-lipoxygenase and myeloperoxidase) as well as by reactive oxygen species [62]. These modified LDL particles activate the overlying endothelial cells, which in turn express adhesion molecules such as VCAM-1 and E-selectin [63, 64]. The activated endothelial cells also secrete chemokines such as CCL2, CCL5 and CX_3CL1, which recruit monocytes from the blood stream [65-67].

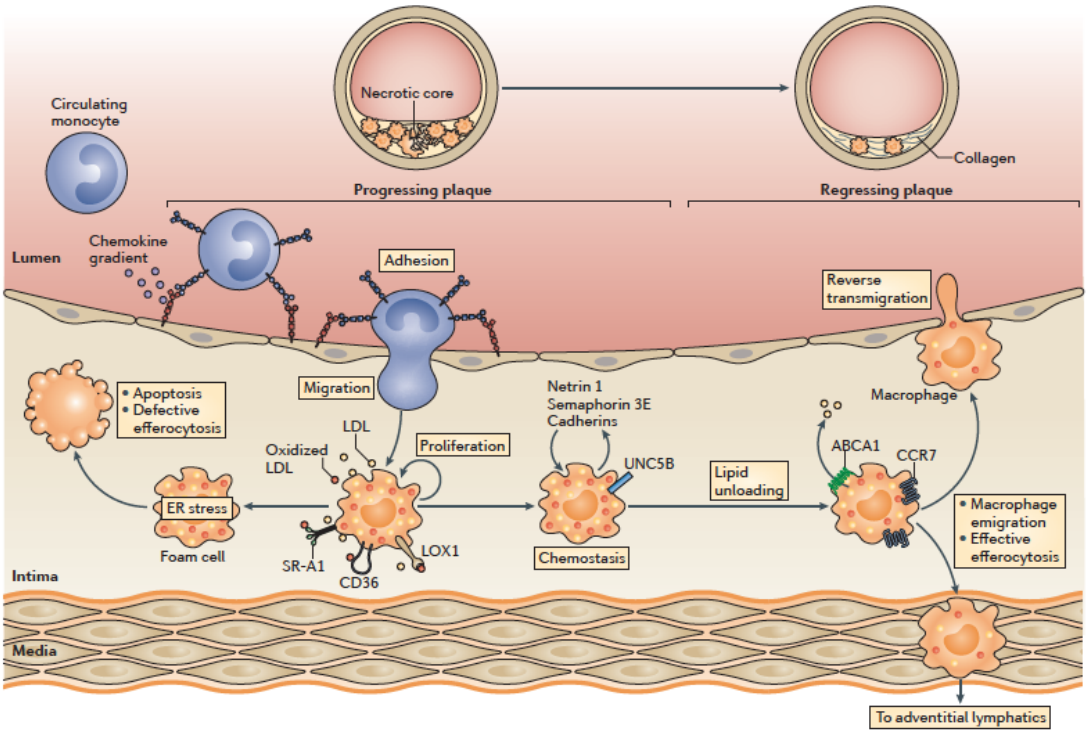


Figure 1.2 Monocyte recruitment and plaque development during atherosclerosis.

The sequence of events leading to plaque progression; endothelial cell activation, chemokine secretion and upregulation of surface adhesion molecules. This is followed by monocyte transmigration into the plaque where they differentiate into macrophages/foam cells and take up cholesterol leading to apoptosis and defective efferocytosis. This defective clearance leads to more inflammatory mediator production in the plaque setting up a positive feedback loop. Taken from Moore *et al.* [68].

Once monocytes have migrated into the subendothelial space (Tunica intima), they differentiate into inflammatory macrophages, a process driven by local production of M-CSF by activated endothelial cells [69, 70]. Upon differentiation, these inflammatory macrophages take up oxidised and other modified forms of LDL that has accumulated in the artery via scavenger receptors like CD36 and SR-A1 [71, 72] (Figure 1.2). There is no negative feedback mechanism for cholesterol uptake via scavenger receptors and as a result, the macrophages take up too much and cannot efficiently break down the oxidised lipid [73]. They become lipid laden foam cells, which are key drivers of atherogenesis. These foam cells themselves secrete a host of inflammatory cytokines and chemokines as well as matrix metalloproteases. However, when these cells undergo apoptosis they are not cleared and undergo secondary necrosis, releasing all of their intracellular contents into the artery wall thus perpetuating an inflammatory positive feedback loop [68]. The release of intracellular contents such as ATP and cholesterol crystals have been demonstrated to activate the NLRP3 inflammasome of surrounding cells resulting in IL-1β secretion [74]. This persistent cycle of recruitment and death of inflammatory foam cells creates a necrotic core within the plaque. This necrotic core weakens the fibrous cap on the luminal side of the plaque, thus making the plaque more vulnerable to rupture and subsequent thrombosis. It should be noted that it has recently become apparent that macrophage accumulation in atherosclerotic plaques is due to both monocyte recruitment as well as local macrophage proliferation within the plaque [75, 76]. Indeed, Tang *et al*. in a recent report demonstrated that inhibiting macrophage proliferation in the plaque using a nanoparticle approach significantly reduced plaque inflammation and progression using animals lacking the Apo E protein (APO E KO) [77]. These animals are widely used for atherosclerosis studies because they spontaneously develop atherosclerotic lesions on a

normal chow diet within 12 weeks of age due to resulting defects in cholesterol homeostasis and cholesterol accumulation in arteries [78].

This process continues over the course of years and in contrast to an acute inflammatory response, there is also an adaptive immune component to this pathology. CD4 T cells are actively recruited to the plaque at the same time as monocytes [79, 80]. Dendritic cells and macrophages that have migrated to the draining lymph nodes from the plaque have possibly activated these effector T cells while in the lymph node. Once in the plaque, they are again presented with oxidised LDL antigen by antigen presenting cells within the plaque and become activated to an inflammatory Th1 state [81]. These Th1 cells secrete inflammatory cytokines such as interferon-γ (IFN-γ), IL-12 and TNF-α (all of which further activates macrophages). The functional contribution of these T cells to disease progression has been demonstrated in studies using severe combined immunodeficient (SCID) animals lacking Apo E which spontaneously develop atherosclerotic plaques as mentioned previously. Interestingly, SCID animals (lacking functional T or B cells) that also had a deletion of the Apo E gene displayed reduced plaque burden [82]. Furthermore, adoptive transfer of functional CD4 T cells into these animals restored their plaque burden to a similar level as normal immunocompetent animals. Regulatory T cells (Tregs) have been postulated to play an important anti-inflammatory role in atherosclerosis, first reported by Mallet *et al*. The authors demonstrated that administration of Treg cells to APO E KO animals significantly reduced atherosclerotic lesion size as well as decreased interferon-γ and increased IL-10 production [83]. While Tregs have been documented to play a role in atherosclerosis development, further research is ongoing to establish the viability of Tregs as a therapeutic candidate for atherosclerosis [84, 85].

During this chronic inflammatory pathology of major arteries, both the innate and adaptive arms of the immune system are involved in the progression of tissue damage and inflammation. Although not discussed here, B cells, dendritic cells and mast cells have been observed in atherosclerotic plaques and may also play an important part in disease progression [86].

1.4 The resolution of inflammation

As mentioned previously, acute inflammation must be efficiently resolved in order to prevent a chronic inflammatory disease developing. Macrophages play a key part in the resolution phase of inflammation as well as in its initiation. Neutrophils are very short-lived cells and once they have phagocytosed an invading pathogen, they quickly undergo apoptosis and must be cleared in order for resolution to begin [59]. Apoptotic neutrophils release specific "find me" signals such as lysophosphatidylcholine, which are recognised by macrophages (via the G2A receptor) and "eat me" signals such as phosphatidylserine which induces their non-phlogistic phagocytosis [87, 88].

If apoptotic cells are not cleared, they undergo secondary necrosis. Necrosis is an alternate form of cell death that is characterised by cell swelling, organelle disruption and breakdown of the plasma membrane resulting in the intracellular contents being released into the extracellular miliu [89]. Release of intracellular cytokines and other molecules such as ATP induce local inflammation, thus hindering resolution [90].

Upon ingestion of apoptotic neutrophils, macrophages switch from an inflammatory (M1) to a resolving (M2 like) phenotype in order to promote return to tissue homeostasis. This phenotypic switch results in a number of changes including lipid

mediator class switching, release of pro-resolving cytokines as well as growth factors like vascular endothelial growth factor (VEGF), which will be discussed.

1.4.1 Pro-resolving eicosanoids

Upon apoptotic neutrophil uptake, there is a shift in eicosanoid synthesis from inflammatory to resolving lipids. Eicosanoids are produced from the metabolism of arachadonic acid and other polyunsaturated fatty acids (PUFAs) by cyclooxygenase, 5-lipoxygenase and Cytochrome P450 enzymes [91]. During the onset of inflammation, prostaglandins (Prostaglandin E_2 ($PGE_{2)}$ and prostaglandin D_2 (PGD_2)) and leukotrienes (Leukotriene B_4) are synthesised by macrophages and other cells in the inflamed tissue [92]. Prostaglandins exert pro-inflammatory effects by increasing vascular permeability as well as acting as chemoattractants for neutrophils [93]. PGE_2 in particular plays an important role in the induction of the classical hallmarks of inflammation such as swelling, redness and pain [94, 95]. Interestingly, under resting conditions, PGE_2 also has a range of important homeostatic functions including regulation of blood pressure, bone formation and gastrointestinal motility [94]. PGE_2 has also been demonstrated to exert anti-inflammatory effects and inhibits pro-inflammatory mediator production in certain settings, highlighting the complex biology of this molecule [96, 97]. Leukotriene B_4 is a potent neutrophil chemoattractant as well as inducer of their activation (degranulation and inflammatory mediator release) [98]. LTB_4 has also been demonstrated to increase IL-6 production by human monocytes, indicating that although the majority of the effects of this molecule are on neutrophils, it can also mediate pro-inflammatory effects on other cell types [99].

After initial production of these pro-inflammatory eicosanoids, leukocytes at the inflammatory site begin to switch to pro-resolving eicosanoid production. Prostaglandin and leukotriene signalling promotes this switch to pro-resolving mediator production and in the case of macrophages, ingestion of apoptotic neutrophils also triggers this switch [3, 100]. Lipoxins are synthesised by the same 5-lipoxygenase enzyme as leukotrienes but exert opposing effects. Lipoxins are synthesised from arachadonic acid via transcellular routes involving multiple cell types and enzymes including 15-lipoxygenase (epithelial cells and monocytes) and 5-lipoxygenase (neutrophils) [101, 102]. Lipoxin-A4 can also be synthesised using a pathway involving platelet and leukocyte interactions [103]. Aspirin triggered lipoxins (ATLs) are another set of lipoxin molecules that can be synthesised by cells that express the COX-2 enzyme in response to aspirin treatment [104] Lipoxin-A_4 has been demonstrated to effectively halt neutrophil chemotaxis and recruitment while promoting recruitment of monocytes which will in turn increase the clearance of dying neutrophils [105]. In contrast to the pro-inflammatory eicosanoids, lipoxins do not increase superoxide production in recruited monocytes and promote non-phlogistic phagocytosis of apoptotic neutrophils by macrophages [106]. The lipoxins mediate their effects predominantly through a GPCR called ALXR which is expressed on human neutrophils, monocytes, T cells, epithelial cells and fibroblasts [101, 107].

The resolvins are another class of pro-resolution eicosanoids. They were first identified in resolving exudates of murine dorsal air pouches and subsequently demonstrated to exert potent pro-resolution effects [108, 109]. These molecules are derived from omega-3 PUFAs. Resolvin E1 was the first mediator of its class to be characterised and has been demonstrated to inhibit neutrophil recruitment *in vivo* as well inhibiting IL-12 production by dendritic cells in response to a microbial antigen [109]. Using the zymosan induced peritonitis model, resolvins were demonstrated to promote

phagocytosis of apoptotic neutrophils by macrophages and increased IL-10 production by macrophages while decreasing IL-6 and interferon-γ production during this phagocytosis [110]. They also enhanced macrophage clearance from the site of inflammation via migration of zymosan containing macrophages to the lymph nodes [110]. An interesting aspect of resolvin biology is that resolvin E1 has been reported to exert its pro-resolution effects at least in part through the chemerin ChemR23 receptor, which will be discussed in more detail in section 1.7. The protectins are another class of pro-resolving lipid mediators that are produced from omega-3 PUFAs. Protectins are synthesised via the 5-lipoxygenase pathway and exert potent anti-inflammatory and pro-resolution effects [110, 111].

The most recent family of pro-resolution eicosanoids to be described are the maresins (macrophage mediators in resolving inflammation). These are a family of eicosanoids that are produced by macrophages and exert potent anti-inflammatory and pro-resolution effects directly on leukocytes. Maresins are derived from the PUFA docosahexaenoic acid and once generated inhibited neutrophil recruitment as well as increasing macrophage efferocytosis [112, 113].

1.4.2 Cytokines

While the anti-inflammatory and pro-resolution eicosanoids clearly play important roles in inflammation resolution they are by no means the only important mediators. IL-10 has long been recognised as an important anti-inflammatory cytokine, which is produced by a range of cell types including Treg cells, Th2 cells, dendritic cells and macrophages [114, 115]. IL-10 exerts potent anti-inflammatory effects on a wide range of cell types and was first discovered as a factor secreted from Th2 cells that was capable of suppressing inflammatory cytokine production by activated Th1 cells [116].

Another cytokine central to inflammation resolution is Transforming Growth Factor-β (TGF-β). TGF-β is released by macrophages upon ingestion of apoptotic neutrophils [117, 118]. TGF-β exerts important immunomodulatory effects on T and B cells [119, 120]. However, in the context of inflammation resolution, TGF-β also inhibits macrophage activation and promotes non-phlogistic clearance of apoptotic leukocytes [121]. TGF-β also promotes wound healing and collagen deposition [4].

1.4.3 Adenosine

During inflammation, adenosine is released from cells under hypoxic and metabolic stress. Extracellular adenosine can also be produced by degradation of extracellular ATP or ADP by the cell surface enzymes CD39 and CD73 [122]. The biology of adenosine is complicated by the fact its effects are dependent on which of the four-adenosine receptors is activated. However, broadly speaking, adenosine is capable of directly inhibiting neutrophil adhesion to activated endothelium by inhibiting both selectin and integrin mediated adhesion [123]. Adenosine also promotes a switch from the M1 inflammatory macrophage phenotype to the M2 like state, decreasing TNF-α, IL-6 and IL-12 production while increasing IL-10 production [124-126]. It is worth noting that the majority of pro-resolution effects of adenosine are thought to be dependent on the $A2_A$ receptor [127].

1.4.4 Annexin A1 and the annexin peptide Ac2-26

Annexin A1 is a 37 kDa protein that is induced after treatment with glucocorticoids and is thought to mediate at least some of the potent anti-inflammatory effects observed with steroid hormones [128, 129]. Annexin A1 is stored in the cytoplasm of neutrophils, monocytes and macrophages under resting conditions [130]. However, following cell

activation, annexin A1 is rapidly secreted into the extracellular space. For example, upon adhesion to the endothelium, annexin is released from activated neutrophils from gelatinase granules [131, 132]. Similarly, activated macrophages secrete the protein via the ATP-binding cassette transporter [133]. Once released, Annexin A1 halts neutrophil recruitment, increases neutrophil apoptosis and enhances macrophage phagocytosis of apoptotic neutrophils [134, 135]. The importance of this protein in inflammation resolution is exemplified by studies using transgenic animals. Animals lacking annexin A1 displayed increased neutrophil recruitment to the peritoneum after zymosan challenge as well as a decrease in macrophage numbers [136]. Interestingly, annexin A1 mediates its effects via the same ALXR receptor as lipoxin-A_4 highlighting the ability of some receptors to bind both peptide and lipid ligands [137].

The anti-inflammatory properties of this protein have been mapped to the N-terminus and a synthetic N-terminus annexin derived peptide called Ac2-26 was synthesised. This shorter annexin peptide has subsequently demonstrated potent anti-inflammatory effects in a wide range of *in vivo* inflammation models [138].

1.4.5 Return to tissue homeostasis

As has been discussed above, there is a large repertoire of anti-inflammatory and pro-resolution mediators required to initiate the resolution phase of an acute inflammatory response. These different mediators broadly speaking all inhibit further neutrophil recruitment and enhance non-phlogistic clearance of dead and dying cells. Once resolution has begun, the optimal outcome is a return to tissue homeostasis and this requires a number of events. Macrophages play a large role in the clearance of apoptotic cells at a site of inflammation and upon ingesting these cells they undergo a phenotypic switch to an M2 like resolving state secreting a number of pro-resolution mediators. It

should be noted that these resolving macrophages (rM) are neither M1 nor M2, expressing markers of both subsets [139]. They secrete pro-resolving mediators, display increased antigen processing capabilities and secrete B and T cell chemoattractants such as CXCL13 and XCL1 [139]. While macrophages exert important functions at a local site of inflammation, they must themselves leave the site to prevent local tissue damage and potential chronic granuloma formation. In addition, it has been demonstrated that during return to tissue homeostasis, the tissue must also be repopulated with cells of the adaptive immune system (T cells, B cells, NK cells) in order to respond to secondary infections [140]. However, this repopulation does not seem to be required for resolution itself as RAG KO animals lacking B and T cells displayed no overt differences in resolution [140]. Using the zymosan induced peritonitis model, it was subsequently demonstrated that during resolution, resolving macrophages migrated to draining lymph nodes and induced the expansion of FoxP3 regulatory T cells (Treg) as well as lymph node contraction [55]. Animals lacking CCR2 displayed impaired monocyte and macrophage recruitment to the peritoneum following zymsoan challenge but also impaired T cell (including Treg) and B cell numbers in the cavity during the resolution phase.

Clearly, the orchestration of inflammation resolution and return to tissue homeostasis is a complex process involving the coordination of multiple cell types and mediators both locally as well as systemically. It is now appreciated that resolution also involves both the innate and adaptive arms of the immune system and both aspects must be taken into account when contemplating novel treatments for chronic inflammatory diseases.

1.5 Leukocyte recruitment and chemotaxis in inflammation

1.5.1 Neutrophil mobilisation during inflammation

Between 5 and 10 $x10^{10}$ new neutrophils are made in the bone marrow every day [17]. The majority of these neutrophils reside in the bone marrow under homeostatic conditions with only about 2% being present in the blood [141]. During an inflammatory response, neutrophils are rapidly mobilised from the bone marrow into the blood stream in order to be available for recruitment to local sites of inflammation. Whether neutrophils are retained in the bone marrow or leave it is largely a matter of balance between CXCR4 and CXCR2 receptor signalling, both of which are expressed on neutrophils in the bone marrow [142]. The ligand for CXCR4 (CXCL12) is produced in the bone marrow stroma and functions to retain immature neutrophils there [142]. CXCR4 expression becomes decreased on mature neutrophils, leading to the idea that CXCR4 functions to retain immature neutrophils in the bone marrow while allowing mature neutrophils to leave [143]. The ligands for CXCR2 (CXCL1 and CXCL2) are also produced in the bone marrow. During inflammation, granulocyte colony stimulating factor (G-CSF) orchestrates neutrophil mobilisation by decreasing CXCL12 production in the bone marrow, thus tipping the balance towards neutrophil egress [141]. G-CSF which was first described as an important growth factor involved in increasing neutrophil production in the bone marrow, also contributes to increase neutrophil numbers during inflammation [144].

CXCL1, CXCL2 and other mediators produced in the periphery also induce neutrophil mobilisation from bone marrow. The importance of this mechanism was illustrated by the observations that neutralisation of CXCL1 and CXCL2 or G-CSF by intraperitoneal injection of antibodies abrogated neutrophil influx into the blood stream

following thioglycollate challenge [145]. Furthermore, intraperitoneal injection of either CXCL2 or G-CSF increased neutrophil mobilisation into the blood stream, highlighting the importance of locally produced chemoattractants in the context of neutrophil mobilisation during inflammation [145].

1.5.2 Monocyte mobilisation during inflammation

Monocytes are also mobilised from tissues such as bone marrow and spleen during an inflammatory response but there is also a pool of circulating monocytes in the blood under resting conditions [146]. As mentioned previously, the monocytes in the blood are broadly defined as non-classical patrolling monocytes and classical inflammatory monocytes. The patrolling monocytes continually inspect the vasculature for signs of damage or infection while classical inflammatory monocytes are rapidly recruited to sites of inflammation and secrete a host of inflammatory mediators. The inflammatory monocytes in mice are $Ly6C^{hi}$, $CCR2^{hi}$, CX_3CR1^{lo}, while non-classical monocytes are defined as $Ly6C^{lo}$, $CCR2^{lo}$, $CX3CR1^{hi}$ [147].

Monocytes are made in the bone marrow as immature progenitors and develop into $Ly6C^{hi}$ classical monocytes while there (which is dependent on macrophage colony stimulating factor (M-CSF))[148]. $Ly6C^{hi}$ monocytes are mobilised from the bone marrow in response to chemokine signals, particularly CCR2 ligands such as CCL2 and CCL7. It has been demonstrated that CCR2 is required for the mobilisation of $Ly6C^{hi}$ monocytes in response to infection by *Listeria monocytogenes*. Animals lacking CCR2 displayed impaired monocyte mobilisation into the bloodstream although $Ly6C^{hi}$ monocytes already in the blood were capable of migrating into inflamed tissues, indicating CCR2 is required for mobilisation into the circulation but not for local tissue

recruitment [149]. In a subsequent study, the same group demonstrated that CCL2 and CCL7 were the two chemokines required for Ly6C^{hi} monocyte egress from bone marrow during inflammation [150]. Using animals deficient in either CCL2 or CCL7, the authors report both CCL2 and CCL7 are required for maximal monocyte mobilisation and bacterial clearance in a model of *L. Monocytogenes* infection [150]. In addition to CCR2 signalling, TLR stimulated monopoesis also plays an important role in monocyte mobilisation during infection [151]. It has been demonstrated that non-classical monocytes in the bloodstream actually differentiate from classical Ly6C^{hi} monocytes in the blood [45]. These cells also seem to be generated in the bone marrow although the mechanisms of their development and their mobilisation remain unknown [45]. CX_3CL1 (fracktalkine) is largely responsible for non-classical monocyte recruitment to sites of inflammation [34]

In addition to the bone marrow, the spleen has been established as a reservoir for monocytes. In contrast to bone marrow, Ly6C^{hi} and Ly6C^{lo} monocyte subsets are present in the spleen in an equal ratio, rather than dominated by the Ly6C^{hi} subset [152]. As mentioned earlier, this has been suggested to play an important role following myocardial infarction where both monocyte subsets are recruited to the inflamed tissue. However, it remains unclear if a similar process occurs during infection [153].

1.5.3 Non-classical chemoattractants

In addition to classical chemokines and eicosanoids that have been discussed above, there remains a number of other mediators with important chemoattractant properties such as complement fragments, (C5a, C3a) bacterial components (N-formylmethionyl-leucyl-phenylalanine, fMLP) as well non-classical chemoattractants such as annexin and

chemerin. During an acute inflammatory response, the complement cascade is rapidly activated producing factors (such as C3b) that coat an invading pathogen to enhance phagocytosis by leukocytes (opsonisation) as well as factors that act as potent chemoattractants to recruit leukocytes to a site of infection (C3a, C5a) [154].

Bacterial products such as fMLP can themselves act as potent chemoattractants for leukocytes. fMLP derived from bacteria induces chemotaxis of neutrophils via the Formyl Peptide Receptor 1 (FPR1) receptor [155]. Interestingly, FPR1 also binds and mediates the anti-inflammatory effects of annexin-A1, highlighting the differential signalling that can be induced at the same receptor by different ligand binding [156].

1.5.4 Targeting chemokines for the treatment of inflammatory diseases.

From the literature it is clear that chemokines and chemoattractants play crucial roles in the recruitment of leukocytes to sites of inflammation as well as the progression of chronic inflammatory pathologies such as atherosclerosis, rheumatoid arthritis and inflammatory bowel disease. Despite a wealth of pre-clinical data using mouse models supporting a number of chemokines as therapeutic targets, results in clinical trials have been disappointing [157, 158]. The reasons for this are unclear. The so-called redundancy of the chemokine system has been blamed to a large extent, even if one receptor such as CCR2 is blocked its ligands can bind and mediate similar effects via other receptors to compensate . However, this theory ignores differences in binding affinities, receptor internalisation kinetics upon ligand binding as well differential signalling pathways induced by different ligands at the same receptor [158, 159]. Another possibility is that the issue has been due to inadequate dosing of the drugs *in vivo* [158]. Further work on dosing regimes, time of intervention and drug half lives could yield improved outcomes

as Schall *et al.* propose that over 90% of all the target receptors in the body must be blocked to achieve effective dosing, otherwise there is enough residual receptor activity to continue inflammatory cell recruitment [158]. Another approach is targeting multiple chemokines at once, an approach which our laboratory has explored using the 35K protein derived from the Vaccinia virus. This protein binds and scavenges CC chemokines and has demonstrated efficacy in monocyte recruitment *in vivo* [160, 161].

That said, there are a number drugs targeting chemokines and their receptors, which have shown promise in clinical trials such as drugs targeting CCR2 for example. An anti-CCR2 monoclonal antibody (MLN1202) generated by Millennium displayed efficacy in a small human trial [162]. These patients had increased levels of C-reactive protein (CRP) and increased risk of cardiovascular events. Patients that received the drug displayed decreased CRP levels as well as a 70% decrease in circulating monocyte levels. While promising, this trial did not provide information as to whether this treatment could decrease monocyte recruitment to atherosclerotic plaques [162].

There is a great deal of pre-clinical data suggesting targeting chemokines could be a beneficial strategy for the treatment of inflammatory diseases. There are currently a number of ongoing clinical trials investigating the therapeutic benefit of this approach including therapies targeting CCR2 and CCR9 amongst others, and with further research this strategy could yield a whole new class of drugs [158, 162, 163].

1.6 Chemerin

1.6.1 Historical overview and structure

Chemerin was first discovered in 1997 in skin and in psoriatic lesions of patients treated with the retinoid tazarotene. They called it tazarotene induced gene 2 (TIG2) and found it was induced by retinoic acid receptor specific agoinsts only. Agonists of retinoid X receptors or vitamin D receptors alone did not induce its expression [164]. In this initial description, the authors also reported TIG2 expression in a number of different tissues using northern blot (liver, pancreas, small intestine, ovary and prostate) [164]. TIG2 mRNA was also reported to be induced during osteoclast differentiation [165]. In particular, ST2 stromal cells were reported to express TIG2 when treated with a combination of vitamin D and dexamethasone [165].

The predicted secondary structure of chemerin indicates it may have a structure similar to chemokines but in a reversed orientation [166] (Figure 1.3). This predicted structure has a disordered carboxyl-terminus, an antiparallel β-pleated sheet and an amino-terminal α-helical domain [166]. Chemerin has three disulphide bonds stabilising its structure and is predicted to be structurally similar to cytstatin. Other proteins with similar overall 3D structures include defensins, cathelicidins and kininogens [166, 167].

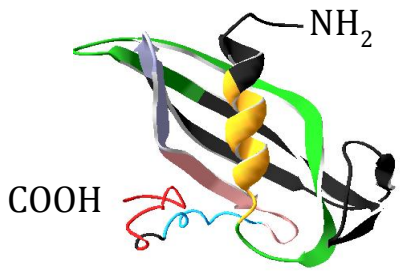


Figure 1.3. Predicted structure of chemerin.

Unplublished data, Dr. Fernando Martinez.

The first chemerin receptor to be identified was the ChemR23 receptor or CMKLR1. It was first cloned as an orphan G-protein coupled receptor that shared sequence homology with chemokine receptors [168]. The same receptor was also cloned by another group and renamed ChemR23 [169]. ChemR23/CMKLR1 was found to share homology with C5a, C3a and FPR receptors. Its expression was also reported on monocyte derived dendritic cells and macrophages [169].

Chemerin was first described as the natural ligand for the orphan receptor ChemR23 by two groups in 2003 [170, 171]. Wittamer *et al* using a ChemR23/Gαi transfected cell screening assay, identified bioactivity in HPLC purified fractions of inflammatory fluids such as ascites from ovarian tumours, synovial fluid from arthritic joints as well as from spleen extracts. The active product was purified and identified as chemerin by mass spectrometry [170]. Meder *et al.* took a similar approach screening human hemofiltrate against ChemR23 activity and identified chemerin as the active component after HPLC fractionation and mass spectrometry [171]. Furthermore, they demonstrated that synthesised chemerin exerted the same biological activity as the hemofiltrate in the same assay [171].

1.6.2 Regulation of chemerin expression by steroid hormones, metabolic cues and cytokines.

Chemerin has been reported to be expressed in a range of different tissues including liver, skin, lung, pituitary, ovary, kidney and white adipose tissue [170, 172]. Chemerin is thought to be produced predominantly in the liver and white adipose tissue, although platelets have also been reported to release pre-formed chemerin during activation [33]. Human chemerin is initially synthesised as a 163 amino acid pre-pro form with a 20 amino acid long N-terminal signal sequence [164]. Once the signal sequence is cleaved, pro-chemerin is secreted into the blood and circulates between the range of 90-200 ng/ml

total chemerin [173]. Under resting conditions, the majority of chemerin that is present in the blood is inactive pro-chemerin [174]. In order to become active, the carboxyl terminus of the protein is cleaved to generate active chemerin isoforms. The exact isoforms that are generated depend on which proteases are present [175, 176]. Is has been demonstrated that the majority of signalling and chemoattractant activity of chemerin is derived from the carboxyl terminus and bioactivity can be conserved using smaller peptides derived from the carboxyl terminus [177]. Wittamer *et al*. generated a number of different human chemerin peptides as well as introducing various different amino acid substitutions in order to investigate which residues are important for signalling at the ChemR23 receptor. They found that a 9 amino acid peptide (YFPGQFAFS) dubbed C9, was the smallest peptide that could still retain signalling function using ChemR23 transfected CHO-K1 cells [177].

Chemerin expression may be regulated by a number of factors including free fatty acids, insulin, steroid hormones and inflammatory cytokines (TNF-α, IL-1β, Interferon-γ). As mentioned earlier, the combination of dexamethasone and vitamin D was first found to induce expression of chemerin in human skin [164]. This is potentially due to PPAR-γ binding sites near the chemerin promoter region (from in silico analysis) [178]. There is also some evidence of retinoic acid receptor-β has a role in controlling chemerin expression during development of intestinal epithelial cells [179]. A recent study confirmed that retinoic acid (RA) induced the production and secretion of chemerin from murine endothelial cells. RA treatment increased bioactive chemerin expression and was capable of inducing transmigration of dendritic cells across the endothelial cell monolayer. This important study identified another potential source of bioactive chemerin production *in vivo* [180].

Chemerin expression seems to be regulated by metabolic factors. Using an *in vitro* system, free fatty acids (FFAs) induced chemerin expression in 3T3-L1 cells during adipocyte differentiation. FFAs were found to also increase the activity of sterol regulatory element-binding protein 2 (SREBP2). SREBP2 is activated during cholesterol shortage in a cell and migrates to the nucleus where it binds to sterol regulatory elements in promoter regions of certain genes to increase cholesterol synthesis [181]. Forced cholesterol depletion of the cells induced SREBP2 activation and an increase in chemerin levels. Interestingly, siRNA knockdown of SREBP2 in differentiating adipocytes ablated FFA induced chemerin expression [182]. These studies implicate SREBP2 as an important inducer of chemerin during adipocyte differentiation as well as a possible link between cholesterol levels and chemerin expression.

Chemerin has been reported to be increased in women suffering from polycystic ovary syndrome (PCOS) [183]. Interestingly, insulin treatment significantly increased chemerin levels in these patients while metformin (an anti-diabetic drug) significantly decreased its expression [183]. These data suggest that excess insulin may drive chemerin expression *in vivo.*

Lastly, pro-inflammatory cytokines are also capable of increasing chemerin expression. TNF-α treatment of 3T3-L1 adipocytes induced significant increases in chemerin production [184]. The same study found that TNF-α treatment increased chemerin levels in plasma of wild type mice and this effect was abrogated using animals lacking the TNF receptor [184]. Interestingly, TNF-α did not seem to increase chemerin expressin in the liver, suggesting that during inflammation, the majority of chemerin may be produced by white adipose tissue [184]. Banas *et al*. report similar findings in the skin, where IL-1β was capable of increasing chemerin expression while cytokines associated with psoriasis like IL-17 and IL-22 decreased chemerin expression [185]. In a similar set

of experiments using adipocytes, IL-1β increased chemerin expression by ~1.3 fold. However, these studies were not confirmed by *in vivo* experiments [186]. Interferon-γ and TNF-α both induced chemerin expression in fibroblast like synoviocytes from rheumatoid arthritis patients [187]. It should be noted however, that a recent study by Gonzalvo-Feo *et al.* observed no increase in chemerin expression in lymphatic or vascular murine endothelial cells in response to TNF-α, interferon-γ, IL-1β or LPS stimulation [180]. Surprisingly, another study using human tubular epithelial cells, reported that TNF-α and interferon-γ treatment actually decreased overall chemerin production [188].

Chemerin expression can seemingly be regulated by a number of different factors *in vivo* but the effects and mechanisms seem to vary depending on cell type and this requires further research. In addition, while transcriptional regulation of chemerin may be important, proteolytic regulation of chemerin bioactivity is equally important.

1.6.3 Chemerin bioactivity regulation by proteolytic cleavage

Chemerin is secreted into the bloodstream in an inactive pro-form, pro-chemerin, which requires proteolytic cleavage of the carboxyl terminus to generate active chemerin isoforms. During an inflammatory response a range of neutrophil and mast cell derived proteases including cathepsin-g, elastase, tryptase, mast cell chymase as well as coagulation factors can cleave the carboxyl terminus of chemerin to generate active chemerin isoforms [175, 189, 190]. Exactly which chemerin isoforms are generated at a site of inflammation are dependent on which proteases are present and where they cleave (Table 1.1). Interestingly, staphopain B, a cysteine protease derived from *Staphylococcus aureus* is also capable of generating active chemerin from prochemerin, indicating a potential role for chemerin in host defense as well tissue homeostasis [191].

The most active isoform that has been reported in human samples is chemerin^{157} although four others have also been reported; chemerin^{154}, chemerin^{155}, chemerin^{156} and chemerin^{158} [175, 189]. Chemerin^{156},chemerin^{157} and chemerin^{158} display activity at the ChemR23 receptor while chemerin^{154} and chemerin^{155} do not [177, 189, 192]. In one of the first descriptions of chemerin from biological samples, Wittamer *et al*. demonstrated that active chemerin from ascites fluid was predominantly the chemerin^{157} isoform [170]. The neutrophil derived proteases cathepsin G and elastase were subsequently demonstrated to generate the active chemerin isoforms chemerin^{156} and chemerin^{157} from pro-chemerin, respectively [175]. In contrast, the same group demonstrated that neutrophil derived proteinase-3 generated the inactive chemerin^{155} isoform from pro-chemerin [189]. In addition, it was reported that active chemerin^{157} and chemerin^{156} could be inactivated by mast cell chymase, which generated the inactive and chemerin^{154} isoform. Incubation with pro-chemerin however did not yield any other products [189]. This ability of active chemerin isoforms to undergo multiple rounds of proteolytic cleavage is further exemplified by the ability of caboxypeptidases B and N to cleave chemerin^{158} (relatively low activity) to chemerin^{157} (the most active isoform) [192]. In addition, mast cell tryptase and elastase are capable of cleaving chemerin at multiple cleavage sites [176]. Clearly, the regulation of chemerin activity by proteolytic processing is complex and which isoforms are generated *in vivo* will vary depending on which proteases are present in the microenvironment (a list of chemerin isoforms and their proteolytic products are shown in Table 1.1).

Protease	Cleavage substrate	Product	C-terminal sequence	Bioactivity	Reference
Elastase	Chemerin^{163}	Chemerin^{157} Chemerin^{155}	…PGQFAFS …PGQFA	High Inactive	[175]
Cathepsin-G	Chemerin^{163}	Chemerin^{156}	…PGQFAF	High	[175]
Proteinase-3	Chemerin^{163}	Chemerin^{155}	…PGQFA	Low	[189]
Mast cell chymase	Chemerin^{156} Chemerin^{157}	Chemerin^{154}	…PGQF	Inactive	[189]
Cathepsins K, L	Chemerin^{163}	Chemerin^{157}	…PGQFAFS	High	[190]
Mast cell tryptase	Chemerin^{163}	Chemerin^{158} Chemerin^{155}	…PGQFAFSK …PGQFA	Low Inactive	[176]
Plasmin	Chemerin^{163}	Chemerin^{158}	…PGQFAFSK	Low	[176]
Factors XIIa, VIIa	Unconfirmed	Unconfirmed	Unconfirmed	n/a	[176]
uPA, tPA	Unconfirmed	Unconfirmed	Unconfirmed	n/a	[176]

Table 1.1 Proteolytic cleavage of human chemerin by different proteases.

Different chemerin isoforms have been identified from different tissues including blood, cerebrospinal fluid, synovial fluid and ascites fluid. Zabel *et al.* reported pro-chemerin and chemerin^{155} to be the main isoforms present in the blood [176]. A subsequent study using ELISAs developed specifically against prochemerin, chemerin^{157} and chemerin^{158} reported the predominant chemerin species present in the blood to be pro-chemerin (~40ng/ml) with some chemerin^{158} (~10ng/ml) present [174].The predominant isoform present in inflammatory ascites fluid was chemerin^{157} and this was demonstrated to be highly active at the ChemR23 receptor. In contrast, chemerin^{158} was found to be the dominant chemerin isoform present in synovial fluid from patients with rheumatoid arthritis, osteoarthritis and psoriatic arthritis, with minimal levels of pro-chemerin and chemerin^{157} found [174]. When the same group examined cerebrospinal fluid from patients suffering from glioblastoma, similar results were found with chemerin^{158} being the predominant isoform present, although the trend was not as striking in these samples [174]. There is a need to develop specific reagents to quantify different specific chemerin isoforms in different tissues and in different pathologies. The development of isoform specific reagents would allow the proper interrogation of the biology of chemerin as well

as exploring the possibility of targeting chemerin isoforms in the context of different pathologies.

1.6.4 The role of chemerin in chemotaxis and recruitment of immune cells to sites of inflammation

Chemerin has been established to play a role in the recruitment and chemotaxis of leukocytes to local sites of inflammation. Chemerin is a potent chemoattractant for macrophages, immature dendritic cells (DCs), plasmacytoid dendritic cells (pDCs) and natural killer (NK) cells [33]. Wittamer *et al.* were the first to describe the chemotactic abilities of human chemerin on immature human dendritic cells using a modified Boyden chamber assay [170, 193]. The chemotaxis was confirmed to be ChemR23 and $G_{\alpha i}$ dependent by the use of a blocking antibody against ChemR23 and pertussis toxin respectively [170]. Zabel *et al.* subsequently demonstrated that the chemerin receptor ChemR23 was expressed on pDCs in the blood and that serum derived chemerin was capable of inducing chemotaxis of human pDCs using a transwell system coated with human umbilical vein endothelial cell (HUVEC) monolayers [194]. The transmigration was completely blocked by anti-ChemR23 antibodies. Extending these findings, chemerin induced transmigration of both myeloid DCs and pDCs across endothelial cell monolayers was subsequently observed using human cells and again this effect was blocked by anti-ChemR23 antibodies, confirming active ChemR23 expression on a number of human DC subsets, rather than on pDCs alone [195]. In agreement, a recent study demonstrated that chemerin produced by murine endothelial cells could induce the transmigration of myeloid dendritic cells as well as pDCs. This effect was seen using both vascular and lymphatic endothelial cells, indicating a role of chemerin in dendritic cell

transmigration *in vivo* [180]. The transmigration was completely blocked by anti-ChemR23 antibodies.

Chemerin was also demonstrated to be capable of inducing chemotaxis of human ChemR23 expressing NK cells using a transwell Boyden chamber system as well as in an endothelial cell transmigration system. CXCL8 was used as a control and in fact was a less potent inducer of chemotaxis with an EC_{50} value of 1nM compared to an EC_{50} value of 0.05nM for chemerin. However, chemerin induced a lower maximal chemotaxis (% of migrated cells) compared to CXCL8 [196]. Chemerin induced migration was blocked by pertussis toxin and as well as with an anti-ChemR23 blocking antibody [196]. A number of studies (including from this laboratory) extended these studies establishing that chemerin was also a potent chemoattractant for macrophages [197-199]. In particular, Hart *et al*. demonstrated that chemerin induced adhesion of murine macrophages to fibronectin and VCAM-1 via integrin clustering, highlighting another mechanism of chemerin induced recruitment [198].

The significance of these chemotactic and integrin activating effects of chemerin on different cells of the immune system has been highlighted by a number of studies identifying chemerin and ChemR23 expressing DCs and NK cells at sites of local inflammation as well as lymphoid organs. Vermi *et al.* examined human lymph nodes using immunohistochemistry and identified high levels of chemerin staining on the luminal side of high endothelial venules (HEVs), which colocalised with ChemR23 expressing DCs and pDCs. ChemR23 staining was also observed on sinus macrophages and germinal centre macrophages [195].

These immunohistochemistry studies and others have reported colocalisation of chemerin with dendritic cell subsets as well as NK cells in psoriatic skin lesions [195, 200-202]. Parolini *et al.* observed high levels of chemerin staining in dermal endothelium

of lesions from psoriasis patients. There were DC, pDC and NK cells all expressing the ChemR23 receptor present in these lesions leading the authors to suggest the chemerin/ChemR23 axis as a means of inflammatory cell recruitment during this disease [196]. In a subsequent study, Albensi *et al.* reported similar findings, observing chemerin staining in psoriatic lesions, which colocalised with ChemR23 expressing pDCs. The majority of chemerin was found on fibroblasts, endothelial cells and mast cells. The authors found that when primary fibroblasts from healthy donors and psoriasis patients were cultured, fibroblasts from the psoriasis group produced significantly more chemerin [200]. Interestingly, when fibroblasts were treated with different agonists such as TNF-α or interferon-γ, there was no effect on chemerin production. Even treatment with retinoic acid produced only a minimal increase in chemerin levels detected, highlighting again the importance of cell types involved when investigating regulation of chemerin production. The same study demonstrated that the chemerin produced by fibroblasts was active and capable of inducing chemotaxis of purified pDCs across endothelial monolayers in a transwell chemotaxis assay [200].

The Chemerin/ChemR23 system is also thought to play a role in inflammatory cell recruitment in a number of other inflammatory pathologies such as rheumatoid arthritis and lupus nephritis. Chemerin has been reported to be expressed on chondrocytes, endothelial cells and fibroblast like synoviocytes (FLSs) in joints of patients suffering from rheumatoid arthritis. In addition, ChemR23 expression was noted on macrophages, DCs and FLSs [187, 203]. These studies indicate again that chemerin may play a role in DC recruitment in this pathology.

Lupus nephritis is an autoimmune pathology characterised by pDC influx into the kidney. De Palma *et al.* observed no ChemR23 expressing cells or chemerin expression in normal renal tissue. However, when they examined tissue from patients suffering from

lupus nephritis, there was obvious ChemR23 expression on infiltrating myeloid DCs, pDCs as well as on endothelial cells. In addition, there was abundant chemerin expression, particularly concentrated on tubular epithelial cells (TECs) and lymphoid endothelial cells [188]. Chemerin production by TECs and lymphatic endothelial cells was confirmed by *ex vivo* culturing of these primary cells. In contrast to an earlier report indicating that TNF-α and interferon-γ treatment increased chemerin production in adipocytes and in plasma, these treatments actually decreased chemerin production by TECs [184, 188]. An interesting observation from these studies was that although there were high levels of chemerin produced from TECs, the chemerin they produced was not very active at inducing migration of DCs across a monolayer of endothelial cells. TNF-α treatment (despite decreasing overall levels) was required to induce chemoattractant chemerin release from these cells [188]. Similar results were observed with TNF-α treatment of 3T3-L1 adipocytes in that TNF-α treatment increased bioactive chemerin levels and this was demonstrated to be due to TNF-α induced protease production (elastase and tryptase) by the cells [204].

It seems clear from these studies reviewed in this section that the chemerin/ChemR23 system plays a role in the recruitment of DCs, pDCs and NK cells during inflammatory pathologies such as psoriasis, lupus nephritis and rheumatoid arthritis. The exact functional consequences of these observations remain ambiguous however, and require further study.

1.6.5 The role of endogenous chemerin in inflammatory diseases

Chemerin has long been implicated in a range of inflammatory diseases. For example, chemerin has been reported to play a role in the recruitment of pDCs, DCs and NK cells to psoriatic lesions [195, 205]. In line with these observations, chemerin levels were

increased in the blood of patients with psoriasis compared to healthy controls [206]. Patients suffering from psoriasis displayed reduced chemerin levels after treatment with the anti-TNF-α drug Inflixamab as well as decreased CRP and resistin [207].

Chemerin has also been implicated in inflammatory bowel disease (IBD), although the literature concerning chemerin in this pathology is contradictory. Patients suffering from IBD (ulcerative colitis and Crohns disease) in one study displayed higher circulating chemerin levels compared to healthy controls while in another there was no difference reported [208, 209]. In the study in which there was no difference in chemerin levels between healthy controls and IBD patients, corticosteroid treatment also had no effect on chemerin levels in the serum while effectively decreasing resistin and visfatin [209]. One important point to note however is that the first study which reported elevated serum chemerin levels in IBD patients recruited a cohort of 230 patients compared with a cohort of 24 patients in the second study which was underpowered in comparison.

There have also been two conflicting reports using murine models of IBD. The first study by Lin *et al*. reported elevated chemerin expression in the colon of animals during dextran sodium sulphate (DSS) induced colitis as well as elevated levels in colon biopsies from patients suffering from ulcerative colitis [210]. Animals that received chemerin during DSS experiments experienced increased colon inflammation as judged by histology as well as increased inflammatory cytokine production from cultured tissue explants. This increased pathology was reportedly due to a skewing of intestinal macrophages to a M1 inflammatory phenotype by chemerin treatment as chemerin treated animals displayed decreased levels of M2 macrophage markers such as Arginase 1, FIZZ 1 and IL-10. Extending these studies, the authors reported that neutralising endogenous chemerin with a polyclonal antibody significantly improved the observed disease severity,

highlighting chemerin as a possible novel therapeutic target in the context of inflammatory bowel disease [210].

In a subsequent study, Dranse *et al*. reported similar increases in chemerin expression in the colon of animals during DSS induced colitis. They reported a decrease in total chemerin levels in the serum of DSS treated animals but an increase in the ratio of bioactive chemerin to total chemerin. However, systemic levels of chemerin did not correlate with disease severity, leading the authors to suggest that at a site of inflammation, local chemerin levels rather then systemic levels are more important in determining disease severity [211]. However, in contrast to the study by Lin *et al*. they saw no difference in disease severity with chemerin treatment using the same dose, route of administration and genetic background. Further studies, using multiple *in vivo* models of inflammatory bowel disease and chemerin receptor KO mice will be required to address this discrepancy [211].

The role of chemerin in the pathology of rheumatoid arthritis is perhaps clearer. A number of studies have examined chemerin levels and functions in the context of rheumatoid arthritis and osteoarthritis. The first study investigating the role of chemerin in this context demonstrated that human chondrocytes expressed both chemerin and its receptor ChemR23. Treatment of isolated chondrocytes from patients with recombinant human chemerin^{157} induced a time dependent phosphorylation of Akt and ERK1/2. Chemerin treatment resulted in an increase in various inflammatory mediators including IL-6, IL-8, TNF-α, MMP-9 and IL-1-β [203]. Similar effects were observed in a subsequent study using fibroblast like synoviocytes (FLS) from rheumatoid arthritis patients. Both chemerin and ChemR23 were expressed in these isolated cells and chemerin treatment induced phosphorylation of Akt and ERK1/2. Chemerin treated FLSs produced increased IL-6 and CCL2 [187]. Eisinger *et al.* observed chemerin and

ChemR23 expression on synovial fibroblasts at the RNA and protein level, however they reported no increase in IL-6 or MMP-9 or phosphorylation of Akt. They did observe increased CCL2 production by chemerin treated synoviocytes [212].

Perhaps unsurprisingly in light of results with FLS culture sytstems, chemerin levels are also reported to be increased in the plasma of patients with rheumatoid arthritis [213]. Anti-TNF-α therapy decreased chemerin levels in serum and this decrease correlated with decreased disease severity as well as decreased serum IL-6 [214]. Given a previous report demonstrating TNF-α treatment of animals increased serum chemerin levels, it is tempting to link decreased chemerin levels as a novel mechanism by which anti-TNF-α therapy exerts some of its anti-inflammatory effects [184]. In accordance with this, a study by Makrilakis *et al*. found that treatment with the humanised anti-IL-6 monoclonal antibody significantly decreased serum chemerin levels in patients with rheumatoid arthritis [215]. These data imply a potential mechanism of chemerin induction *in vivo* involving both TNF-α and IL-6. Although given the complexity of chemerin regulation as discussed in section 1.6.2, this axis would probably be one of many factors.

Although there are relatively few studies addressing the role of chemerin in the context of cancer, it was recently reported that chemerin plays an important role in the recruitment of NK cells to tumors [216]. Chemerin levels were measured in a cohort of patients with a number of different cancers. Chemerin levels were decreased in patients with all cancers compared to healthy control samples and survival correlated with increased chemerin expression [216]. Using a murine tumor transplant model, Pachynski *et al*. reported elevated DC, T cell and NK cell infiltration into chemerin expressing tumors compared to tumors that did not express chemerin along with a concomitant decrease in tumor size [216]. Exogenous chemerin treatment also decreased tumor size compared to control. The importance of chemerin-induced recruitment of NK cells to the

tumors was confirmed by depleting NK cells and using RAG KO animals (which lack T and B cells). In these experiments RAG KO animals displayed the same responses to chemerin treatment as wild type animals but chemerin treatment had no effect on tumor growth when NK cells were depleted [216]. This study implicates chemerin or stabilised chemerin derived peptides as an attractive therapeutic strategy for the treatment of melanoma, possibly in conjuction with standard chemotherapeutic agents.

The last inflammatory pathology that will be discussed in this section is multiple sclerosis (MS). Although there are no definitive reports to date of an association between chemerin and MS in human patients, there have been two reports using murine models of MS (experimental autoimmune encephalomyelitis (EAE)) suggesting a possible role for chemerin and the ChemR23 receptor in leukocyte recruitment during this pathology. Graham *et al.* demonstrated that mice lacking the ChemR23 chemerin receptor experienced significantly reduced clinical signs of disease and pathology as judged by histology [217]. They go on to show that infiltrating DCs and macrophages to the central nervous system (CNS) during the experiment express ChemR23 as well as increased expression of chemerin within the CNS of animals experiencing EAE compared to naïve controls [217]. The same authors in a subsequent study identified a potent small molecule antagonist of the ChemR23 receptor, called α-NETA. They reported subcutaneous administration of α-NETA delayed disease onset in the same EAE model, decreased disease severity by histology and clinical disease scores. Antagonist treatment also decreased infiltration of T cells, B cells, DCs and macrophages to the CNS during disease as well as decreasing NK cell localisation to the spleen [218]. These data although not confirmed in humans, presents another inflammatory pathology in which targeting chemerin may be of clinical benefit. However, the pathology of MS in humans is more

complicated and effectively targeting chemerin with drugs with sufficient half-lives *in vivo* will no doubt be complicated.

Taken together, these data suggest chemerin is at the very least a biomarker for inflammation (if not a direct driver of inflammation) in the context of rheumatoid arthritis, psoriasis, lupus nephritis and potentially MS. Its expression is consistently increased during inflammatory diseases and in some cases is decreased by anti-inflammatory therapies. It remains to be conclusively proven however, if chemerin is directly driving inflammation in these pathologies or whether its expression is increased as a byproduct of inflammation. Potential chemerin agonists and antagonists against of the ChemR23 receptor will be of interest in clarifying this.

1.6.6 The function of chemerin as an adipokine and its role in metabolic disease

While the focus of this thesis is on chemerins' function during inflammation and inflammatory cell recruitment, chemerin has long been appreciated to have important functions as an adipokine. The first report of chemerin as an adipokine was from Goralski *et al.* who reported high levels of chemerin expression in white adipose tissue as well as expression and secretion by maturing adipocytes. The chemerin that was secreted was demonstrated to be active by the ability of supernatants of differentiating adipocytes to induce migration of ChemR23 transfected CHO-K1 cells in a transwell chemotaxis assay. Adipocyte differentiation was demonstrated to be dependent on chemerin expression by small hairpin RNA knockdown experiments [219]. Adipocytes also expressed ChemR23 and chemerin seems to function in an autocrine/paracrine manner during adipocyte differentiation, supported by the requirement for chemerin secretion in maturing 3T3-L1 adipocytes [219]. This work was closely followed by a number of papers reporting similar

findings. Bozaoglu *et al.* reported that chemerin was increased in adipose tissue of *P. Obesus* mice, which are obese and have type 2 diabetes. In the same study, plasma chemerin levels were measured in a cohort of human volunteers, half of which were from patients with type 2 diabetes. There was no significant difference in plasma chemerin levels between the two groups, although they did observe a correlation between chemerin and higher body mass index (BMI) and a metabolic syndrome phenotype [172]. Roh *et al.* also reported chemerin and ChemR23 expression in differentiating adipocytes and confirmed the importance of chemerin signalling during this process [220].

In contrast, chemerin has also been suggested to have a function in insulin sensitivity. Takahashi *et al.* reported that chemerin was capable of increasing insulin stimulated glucose uptake by adipocytes as well as increasing insulin stimulated signalling, suggesting a possible role for chemerin in obesity and diabetes [221]. A subsequent study reported chemerin impaired insulin signalling in skeletal smooth muscle cells, highlighting the different effects chemerin seems to exert depending on the cell types involved [222]. In the context of insulin sensitivity, Takahashi *et al.* reported that animals lacking chemerin displayed impaired insulin sensitivity. This was mainly due to increased glucose production by the liver and decreased insulin secretion [223]. These data in addition to their previous report (showing chemerin increased insulin stimulated glucose uptake by adipocytes) indicates chemerin may play an important role in glucose production as well as insulin stimulated glucose uptake. Confirming this hypothesis, the authors generated chemerin overexpressing mice and these animals displayed improved glucose uptake, higher insulin levels and increased insulin sensitivity compared to wild type animals [223]. These effects of chemerin seemed to be at least in part acting on the pancreatic β-cells which were demonstrated to express chemerin as well as both the ChemR23 and GPR1 chemerin receptors. Chemerin was also required for insulin

secretion from β-cells *in vitro* and *in vivo* [223]. Extending these findings, Wargent *et al.* reported that animals lacking the ChemR23 receptor displayed impaired glucose tolerance and that chemerin as well as the previously reported chemerin peptide C15 could induce glucose uptake by adipocytes in the presence of insulin but this was dependent on ChemR23 expression [224, 225]. A similar study by Rourke *et al.* reported animals lacking the GPR1 chemerin receptor also displayed glucose intolerance and decreased insulin sensitivity, indicating both ChemR23 and GPR1 may be important for the observed effects of chemerin on glucose homeostasis [226]. In contrast, Rouger *et al.* reported animals lacking ChemR23 displayed no differences in glucose tolerance or insulin sensitivity [227]. Hence, the exact role of chemerin and its receptors on glucose homeostasis remain unclear, with some studies proposing chemerin drives metabolic dysfunction while others support a protective function by increasing glucose update and insulin sensitivity.

In human studies, there have been numerous reports linking elevated chemerin levels in patients to metabolic disease and cardiovascular disease, although the exact function of chemerin in these studies remains unclear [222, 228-231]. One study reported a strong correlation between chemerin levels and inflammatory markers, body mass index and triglycerides [232]. Another study however, reported a correlation between chemerin levels and BMI but observed no link between chemerin and triglycerides. This same study also reported a correlation between chemerin levels and type 2 diabetes [229]. This was supported by a more recent report which found chemerin levels to be a weak predictor of diabetes risk [233]. Finally, by setting a chemerin concentration limit in the blood of 240μg/L, Stejskal *et al.* were able to diagnose metabolic syndrome with 75% accuracy [234].

There were clearly some discrepancies between these studies. One reason for this could be that the ELISA kit used in all these studies detects prochemerin as well as active chemerin isoforms. As Lehrke *et al.* discuss themselves; the lack of specific antibodies to differentiate inactive prochemerin from active chemerin makes it challenging to draw concrete conclusions from these kinds of studies [232]. In addition, the fact that a number of different active chemerin isoforms can be generated at a site of inflammation further complicates attempts to accurately quantify bioactivity of chemerin [175, 189, 190].

The exact function of chemerin and its receptors in the context of metabolic disease remains unclear as the majority of murine models indicate chemerin to play a protective role, increasing glucose tolerance and insulin sensitivity. However, the majority of studies in humans seem to indicate a correlation between increased chemerin levels, BMI, C-reactive protein levels and metabolic disease. The exact role played by chemerin in the setting of metabolic dysfunction remains unclear and convoluted. New reagents capable of recognising different chemerin isoforms or measuring only chemerin bioactivity in patients will be of benefit in addressing these issues further.

1.6.7 The role of chemerin in host defence

Chemerin is a potent chemoattractant for macrophages, DCs and NK cells [33]. The fact that chemerin is present in an inactive proform at multiple barrier sites and is activated by inflammatory stimuli points to a possible role in host defense. In addition, chemerin shares structural similarities with antimicrobial proteins such as cathelicidens and kininogens which also require proteolytic activation [166]. In addition, LL-37, a member of the catheliciden family, binds the FPR1 receptor, which shares homology with the chemerin ChemR23 receptor [166]. Indeed there have been two published studies

reporting direct antimicrobial functions of chemerin as well as unpublished data from our laboratory corroborating these findings. The first report by Kulig *et al.* demonstrated that prochemerin could be cleaved to the active chemerin^{157} isoform by cathepsin L and K. The authors demonstrated that both prochemerin and the active isoform chemerin^{157} could inhibit *E.coli*. growth, although chemerin^{157} was more potent then prochemerin. Similar results were observed with clinical isolates of *K. pneumoniae* [190]. The authors suggest that prochemerin was processed to shorter active forms during incubation by bacterial proteases. This study did not investigate the mechanism by which chemerin mediated these antibacterial effects. A subsequent study by Banas *et al.* extended these observations further [235]. They firstly identified chemerin to be present in keratinocytes of human skin biopsies using immunohistochemistry. Supernatants from 3D cultures of human keratinocytes exerted potent antibacterial activities against *E.coli* which were abrogated by anti-chemerin blocking antibodies. In order to identify which part of the protein was exerting these effects, the authors synthesised a range of chemerin derived peptides spanning the entire protein and tested them for antibacterial activity against *E.coli*. In contrast to the chemotactic effects of chemerin which are localised at the carboxyl terminus, the anti-bacterial properties of chemerin were localised to amino acids Valine^{66} to Proline^{85} localised in the middle of the protein [235]. Using a synthetic peptide of this sequence demonstrated potent antibacterial effects on a number of different bacteria including *Staphylococcus aureus*, *Pseudomonas aeruginosa* and *Candida albicans*. The peptide exerted comparable effects to the established antibacterial protein LL-37 [235]. Based on the highly positively charged nature of this chemerin peptide, the authors postulated it could mediate its antibacterial effects via direct lysis of the negatively charged bacterial membrane. Using a β-galactosidase reporter *E.coli* strain, the authors proved that this peptide could indeed directly lyse *E.coli*. In agreement with a

role for chemerin in host defence, it has also been demonstrated that staphopain B, a protease derived from *Staphylococcus aureus*, is capable of cleaving prochemerin to active chemerin^{157} [191]. In agreement with the above studies, a recent report found chemerin expression in the skin to be increased in response to bacteria such as *Staphtylococcus aureus* and *E.coli* both *in vitro* and *in vivo.* The importance of chemerin for host defence was further highlighted by use of chemerin deficient animals, which exhibited decreased bacterial killing and clearance *in vivo* after ectopic administration of *Staphtylococcus aureus* [185].

The above data therefore support yet another function of chemerin *in vivo*: acting as sensor of bacterial infection as well as a potent anti-microbial defence mechanism. Present in numerous sites in the inactive pro-form, including skin, chemerin can be rapidly cleaved (by host and bacterial proteases) to generate active isoforms. These isoforms are capable of both recruiting cells of the innate immune system such as macrophages, DCs and NK cells to a site of infection as well as directly lysing the invading bacteria, keeping the infection in check until the immune system can be sufficiently mobilised.

1.6.8 Anti-inflammatory effects of chemerin

Despite the evidence in section 1.6.5 implicating a pro-inflammatory role for chemerin in certain pathologies, there is also a body of evidence suggesting chemerin can exert anti-inflammatory effects. The first report of an anti-inflammatory effect of chemerin was from our laboratory. Cash *et al*. demonstrated that murine chemerin (corresponding to the active chemerin^{157} isoform in humans) could effectively decrease inflammatory responses of murine macrophages (Bio-Gel elicited) to LPS and interferon-γ challenge *in vitro* and

these effects were dependent on cysteine proteases, indicating possible further cleavage of the protein to shorter peptides. A range of synthetic chemerin derived peptides were synthesised and screened for anti-inflammatory effects and the C15 peptide was identified. This peptide did not induce chemotaxis of macrophages but did exert potent anti-inflammatory effects in a zymosan induced peritonitis model at picomolar concentrations. These effects were ablated in animals lacking the ChemR23 receptor. Cash *et al.* also demonstrated that blocking endogenous chemerin with a polyclonal antibody resulted in increased inflammation in the same model [225]. In a follow up study, the same authors investigated the mechanism of action of C15 further. C15 promoted phagocytosis of labelled zymosan particles *in vivo* while full-length active chemerin did not. Similar effects were observed using *in vitro* apoptotic cell phagocytosis assays except in these experiments, full-length chemerin also promoted phagocytosis of apoptotic cells (these effects were lost when in the presence of a serine and cysteine protease inhibitor). Again, these effects were reported to be ChemR23 dependent [236]. Thus, the mechanism of C15 action was postulated to be through increasing non-phlogistic phagocytosis of apoptotic cells at inflammatory sites.

In contrast, a study by Bondue *et al*. reported no anti-inflammatory activity of chemerin using similar macrophage activation experiments. When murine macrophages (Bio-Gel and thioglycollate elicited) were challenged with LPS and interferon-γ, pre-treatment with chemerin at any concentration tested had no effect on inflammatory responses [237]. They performed experiments using human macrophages with similar results. One point to note is that Bondue *et al*. used animals on a C57Bl/6J background throughout their study while Cash *et al*. used animals on a SV129 genetic background for experiments with animals lacking ChemR23. However, C57Bl/6J animals were used for the majority of their other experiments so the reason for this discrepancy remains unclear.

Since these reports, there have been two more published reports by Cash *et al*. describing potent anti-inflammatory effects of C15. The first of these found the C15 peptide could inhibit human neutrophil adhesion to TNF-α treated HUVECs under flow. Similar effects were found pre-treating mice with C15 followed by TNF-α challenge. Intravital microscopy of the mesentery was used to monitor leukocyte/endothelial cell interactions. In addition, using a murine model of myocardial infarction, C15 was capable of decreasing neutrophil infiltration in the heart and decreased troponin-1 expression (a measure of myocardial damage). The effects of C15 were ChemR23 dependent and reported to occur through inhibition of integrin activation and clustering [238]. The most recent study by Cash *et al.* reports wound healing properties of C15. The peptide decreased macrophage and neutrophil recruitment to sites of dermal injury. C15 also accelerated wound closure, decreased wound area and reduced scarring. In contrast to a recent study reporting chemerin polarised intestinal macrophages to an M1 phenotype, Cash *et al*. in this study report the C15 peptide polarises macrophages to an M2 phenotype, increasing expression of arginase-1 and decreasing expression of M2 markers like iNOS and TNF-α [210, 239]. A recent study by Chang *et al*. report similar effects of C15 in an ischemia reperfusion injury model. C15 treatment decreased infarct size as well as troponin-1 levels indicating decreased cardiac damage. C15 treatment also decreased neutrophil recruitment (measured by myeloperoxidase activity) and increased M2 markers suggesting a possible increase in M2 macrophages [240].

One important point regarding the C15 peptide is that although it seems to exert potent anti-inflammatory effects at picomolar levels that are dependent on the ChemR23 receptor, there have never been any reports of C15 inducing direct signalling of this receptor (my own studies confirm this). Therefore, the exact mechanism of action of this peptide has proven difficult to dissect [33, 237, 241].

In addition to the C15 peptide, full-length active chemerin also seems to exert anti-inflammatory effects. The first of these reports was from Luangsay *et al*. Animals were administered PBS, LPS (1μg), murine chemerin (5μg) (Chemerin^{157} in humans) or LPS and chemerin via intratracheal instillation and inflammatory responses in the lungs were assessed. LPS treatment resulted in marked increase of neutrophils into the lungs and bronchiolar lavage (BAL) fluid as well as an increase in inflammatory mediators in the BAL fluid such as CXCL1, IL-6, TNF-α and IL-1β. Chemerin treatment dramatically reduced neutrophil numbers both in the lungs and in the BAL fluid. In addition, chemerin decreased all the above cytokines in the BAL fluid. These anti-inflammatory effects were dependent on ChemR23 as chemerin treatment of animals lacking this receptor no longer exerted any appreciable anti-inflammatory effects. Furthermore, ChemR23 KO animals also displayed increased neutrophil recruitment to the lungs after challenge with LPS alone compared to wild type animals, indicating a possible role for endogenous chemerin in the regulation of inflammatory responses in the lung [241]. In contrast, chemerin treatment increased macrophage numbers in the BAL fluid but not in the lung compared to LPS treatment alone. The authors postulate chemerin plays a role in resolution by recruiting alveolar macrophages, which have previously been reported to exert immunosuppressive effects, in order to hasten resolution. Whether this is the case is unclear however. ChemR23 KO animals challenged with LPS alone also displayed increased macrophage recruitment to the lungs, which presumably was not due to chemerin signalling, although this observation could also be a result of increased inflammatory mediator production by the recruited macrophages in ChemR23 KO animals [241].

Similar results were observed in the lungs of mice lacking the ChemR23 receptor in a model of viral pneumonia [242]. ChemR23 KO animals displayed increased

neutrophil recruitment to the lungs and increased inflammatory mediator production. These animals also exhibited impaired pDC recruitment, decreased type 1 interferon production and delayed viral clearance. There was an increase in macrophage recruitment in animals lacking ChemR23 in agreement with the previous study by Luangsay *et al*. Through adoptive transfer experiments, Bondue *et al*. established that the anti-inflammatory role of the chemerin/ChemR23 system in this inflammatory model was acting on non-leukocyte populations [242]. As a possible explanation for this, ChemR23 was reported to be expressed on human endothelial cells and to exert anti-inflammatory effects by Yamawaki *et al* [243]. It is tempting therefore to attribute some of chemerins anti-inflammatory effects in these lung models to direct effects on the lung endothelium rather than on leukocytes [243]. However, these effects were not reproduced by a recent study by Neves *et al.* who reported that chemerin could exert pro-inflammatory effects directly on human microvascular endothelial cells. Chemerin treatment of human microvascular endothelial cells (HMECs) increased mRNA expression of CCL2, TNF-α and VCAM-1 as well as increased the adhesion of THP-1 monocytes [244].

Extending the role of chemerin in airway inflammation, chemerin has been reported to play an anti-inflammatory role in the context of allergic airway inflammation. Zhao *et al.* used an allergic ovalbumin (OVA) induced airway inflammation model to assess chemerin treatment in this context [245]. Chemerin was administered intranasally (200ng/mouse). The authors observed chemerin treatment abrogated CD4 T cell, eosinophil and inflammatory DC recruitment to the lungs during OVA challenge. Chemerin also decreased Th2 cytokine production in the lungs including IL4, IL-13 as well as T cell chemoattractants CCL17 and CCL22. The mechanism by which chemerin treatment decreased inflammatory DC recruitment was demonstrated to be through reducing CCL2 production by activated epithelial cells in the lungs, highlighting a novel

mechanism by which chemerin may exert its anti-inflammatory actions in the context of allergic airway inflammation [245].

A further demonstration of the potential of chemerin to exert anti-inflammatory actions in the context of allergic airway inflammation was reported by Doyle *et al*. who developed lipidated analogues of the 9 amino acid C9 peptide (YFPGQFAFS) first reported by Wittamer *et al*. (in order to overcome the short half lives of short chemerin peptides *in vivo*) [177, 246]. This lipidated C9 peptide displayed anti-inflammatory effects in the same OVA induced allergic airway inflammation model used by Zhao *et al*. [245, 247]. These above reports highlight a potential utility of chemerin or stabilised chemerin peptides in the treatment of allergic asthma and lung inflammation. These stabilised peptides would also be interesting to investigate in other pathologies where chemerin treatments has shown beneficial effects such as certain inflammatory pathologies and melanoma for example [216, 242].

1.7 Chemerin receptors

1.7.1 ChemR23

ChemR23 is a $G_{\alpha i}$-protein coupled receptor sharing sequence homology with the C5a , C3a and FPRL1 receptors [248]. ChemR23 is expressed on a range of cell types including DCs, pDCs, NK cells, macrophages, microglial cells, adipocytes, chondrocytes, endothelial cells and epithelial cells [33, 173]. Its expression in the mouse is decreased by inflammatory stimuli such as LPS, interferon-γ and other TLR ligands but increased by TGF-β [197, 198]. ChemR23 is thought to mediate chemotactic effects of chemerin and its activation has been reported to lead to rapid downstream signalling cascades. These

include release of intracellular calcium, inhibition of cAMP, phosphorylation of ERK1/2 and cytoskeletal rearrangements dependent on P38, phosphatidylinositol 3-kinase (PI3K) and Akt [33, 197, 198]. Recent work using reporter cell lines by Rourke *et al.* demonstrated ChemR23 activation also induces activation of the transcription factor serum related factor (SRF) and was RhoA and rho-associated protein kinase (ROCK)-dependent [249]. ChemR23 activation induced MAP kinase and ERK 1/2 signalling which converged with the RhoA and ROCK pathway at the activation of SRF. Chemerin induced chemotaxis was also dependent on RhoA/ROCK, MEK 1/2 and P38, which agrees with a previous report by Hart *et al.*using primary murine macrophages [198, 249] (Figure. 1.4).

A recent study by Herova *et al*. examined ChemR23 expression on human monocytes and macrophages. Firstly, they found ChemR23 to be expressed both on human monocytes and macrophages, although at a higher level on macrophages. They also report that in contrast to the previous murine studies, pro-inflammatory signals like interferon-γ and LPS increased surface expression of ChemR23 while TGF-β had no effect [197, 198, 250]. The Th2 cytokines IL-4 and IL-13 actually decreased ChemR23 expression. LPS polarised M1 macrophages and naïve macrophages chemotaxed towards chemerin while IL-4 and IL-13 M2 polarised macrophages did not, suggesting alternatively activated human macrophages do not respond to chemerin. In agreement, Banas *et al*. reported similar findings in human skin, demonstrating that Il-1β increased ChemR23 expression [185]. This is an important observation as it highlights a possible difference in the regulation of ChemR23 between mice and humans, which has important implications for future studies between species [250].

ChemR23 has been reported to be one of the receptors for the pro-resolving eicosanoid resolvin E1 [109]. Resolvin E1 was identified in pro-resolving exudate and has

demonstrated potent pro-resolving and anti-inflammatory effects in a range of *in vivo* models [251]. Using a luciferase reporter assay, Arita *et al*. demonstrated ChemR23 was one of the receptors responsible for these effects and this has been corroborated by ligand binding experiments using radiolabelled resolvin E1 as well as subsequent studies [109, 251]. Resolvin E1 binding to ChemR23 is capable of inducing downstream signalling including phosphorylation of P42 MAP kinase, Akt and ribosomal protein S6. The phosphorylation of ribosomal protein S6 was reported to be dependent on PI3K and ERK but not on P38. These studies were carried out using ChemR23 transfected CHO-K1 cells, HL60 cells and primary human macrophages. These signalling cascades led to increased phagocytosis of FITC labelled zymosan by human macrophages [252]. The leukotriene B_4 receptor can also bind resolvin E1 and acts as an antagonist for leukotriene B_4 on human neutrophils [253].

1.7.2 GPR1

GPR1 is G-protein coupled receptor that shares sequence homology with ChemR23 [33]. It was first recognised as a receptor for chemerin by Barnea *et al*. through the development of a screening assay to identify novel ligands for orphan G-protein coupled receptors [254]. They found that both full-length chemerin and the C9 chemerin peptide could activate GPR1 (as judged by β-arrestin recruitment to the receptor) with EC_{50} values of 240 pM and 1 nM respectively. The authors also demonstrated the ability of chemerin to induce calcium mobilisation in GPR1 transfected cells, although to a lesser degree then at ChemR23. It should also be noted that all signalling studies on GPR1 have so far not been on primary cells.

GPR1 is expressed in mice in white adipose tissue, skin, muscle and in the central nervous system [33, 185, 226]. The physiological role of this receptor remains unclear, however animals lacking GPR1 have been reported to exhibit glucose intolerance and decreased insulin secretion in response to glucose, implicating GPR1 in glucose homeostasis [226]. GPR1 may also play a role in host defence, as GPR1 mRNA expression is increased in response to IL-1β and bacteria such as *Staphtylococcus aureus* and *E.coli.,* although the importance of this receptor in this context requires further investigation [185].

Relatively little is known about GPR1 signalling but the report by Rourke *et al*. using transfected reporter cell lines, demonstrated GPR1 mediated signalling involving activation the transcription factor SRF which was RhoA and ROCK dependent, similarly to their findings with ChemR23 [249]. This study investigated downstream signalling from both murine and human GPR1 and found important differences between the murine and human receptors. Chemerin activation of human GPR1 for example activated the SRF reporter but was not dependent on ERK 1/2 or P38. In contrast, chemerin activation of murine GPR1 also activated the SRF reporter but was dependent on both ERK 1/2 and P38 [249]. This study emphasises the complexity of the signalling cascades downstream of this receptor as well as important species specific differences, which merit further study.

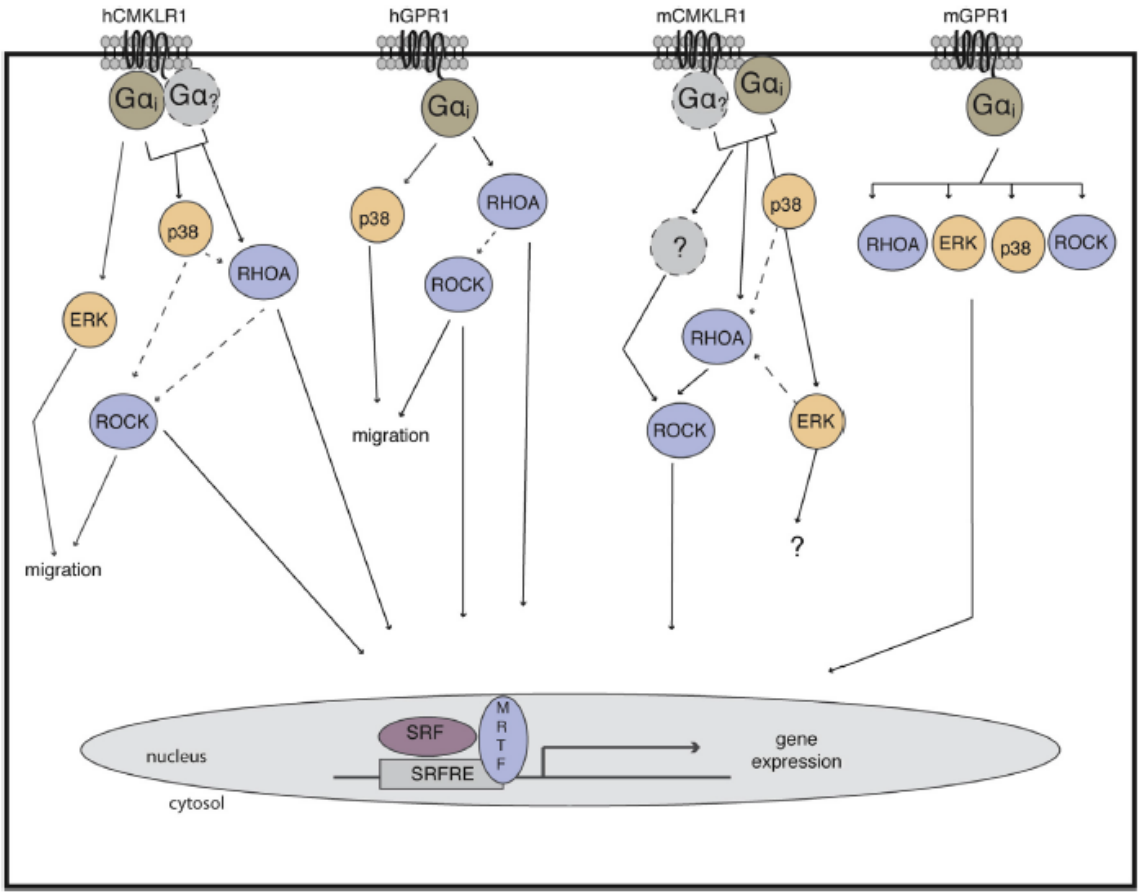


Figure 1.4 Putative signaling pathways induced by ChemR23 and GPR1 activation.

Proposed signalling cascades induced from human ChemR23 (hCMKLR1), murine ChemR23 (mCMKLR1), human GPR1 (hGPR1) and murine GPR1 (mGPR1) based on experiments using reporter cell lines. Chemerin signalling via mChemR23 also induces calcium flux and inhibition of cAMP (not shown here) [170]. Taken from Rourke *et al.* [249].

1.7.3 CCRL2

CCRL2 was first identified in 1998 as a gene that was upregulated in murine macrophages after LPS stimulation [255]. CCRL2 has only been identified on murine immune cells, including DCs, mast cells and activated macrophages [256-259]. It was not reported to be expressed on eosinophils ,T cells, B cells, bone marrow neutrophils or resident peritoneal macrophages [258, 259]. CCRL2 expression was also reported in other murine cell types following challenge with inflammatory stimuli including glial cells, epithelial cells and endothelial cells [257, 259, 260]. CCRL2 shares sequence homology

and many structural similarities to classical CC chemokine receptors such as CCR5 [255]. However, similar to the atypical chemokine receptors, D6 and DARC, CCRL2 lacks the DRYLAIV motif required for chemotactic responses [255]. CCRL2 has been reported to display a differential expression pattern in humans, being expressed on nearly all hematopoietic cells including monocytes, macrophages, dendritic cells, neutrophils, T cells, B cells and NK cells. Its expression was also increased following stimulation with pro-inflammatory or activating ligands such as LPS,interferon-γ or CD40 ligand [261-264].

Despite the large number of cell types expressing CCRL2 and the fact that its expression is increased during inflammation, relatively little is known about the function of this receptor in inflammation. CCRL2 has been reported to bind chemerin with high affinity but does not seem to internalise its ligand like classical decoy receptors such as D6 [259, 265]. The first paper to report the generation of a CCRL2 KO mouse used a model of 2,4-Dinitrophenol (DNP) specific IgE mediated cutaneous inflammation. Zabel *et al.* demonstrated that animals lacking CCRL2 displayed decreased dermal inflammation at a low dose of DNP- specific sensitisation followed by DNP challenge, although this was a modest difference. The exact mechanism by which CCRL2 modulated these responses was not clear. However, cells expressing CCRL2 were shown to bind and concentrate local chemerin and when incubated with ChemR23 transfected cells could induce calcium flux [259].

CCRL2 was subsequently reported to play a role in ovalbumin (OVA)-induced lung inflammation. Specifically, Otero *et al.* demonstrated that CCRL2 KO animals challenged with OVA had reduced numbers of leukocytes recruited to the bronchiolar lavage (BAL) fluid (eosinophils and lymphocytes) as well as lower levels of Th2 cytokines in the BAL fluid [258]. Antigen loaded DCs in CCRL2 KO animals displayed

impaired trafficking to draining lymph nodes in response to OVA challenge and levels of Th2 cytokines such as IL-5 and IL-13 were reduced in lymph nodes challenged with antigen *ex vivo* in CCLR2 KO animals. However, DC trafficking to the lungs remained unaffected [258].

In addition, animals lacking CCLR2 have been reported to display reduced ChemR23 expressing NK cell recruitment to the lungs of animals challenged with LPS [260]. CCRL2 KO animals displayed increased chemerin levels in the blood both under naïve conditions and after LPS challenge. CCRL2 protein expression was increased in the liver after LPS treatment but there was no increase in lungs, which had constitutively high expression. The authors postulated that CCRL2 functions to concentrate chemerin locally and present it to ChemR23 expressing cells as they did in their previous report [259]. CCRL2 may also be important in other pathologies such as ischemic brain injury. Douglas *et al.* demonstrated that animals lacking CCRL2 displayed decreased cell death and smaller infarct volumes compared to wild type animals [266]. CCRL2 was rapidly induced in brain slices from wild type animals after ischemia but the mechanism by which CCRL2 exerts these effects are unclear [266].

There have been reports of increased CCRL2 expression both in glioblastoma and liver carcinoma. Yin *et al.* found increased CCRL2 in patients suffering from glioblastoma and using CCRL2 transfected glioma cell lines demonstrated that CCRL2 promoted glioma cell migration in a transwell invasion assay, although the mechanism was not identified [267].

1.8 Original hypotheses for this thesis

1. Full-length active chemerin promotes chemotaxis and recruitment of macrophages to sites of inflammation. However, during an inflammatory response, chemerin can be further cleaved to shorter chemerin peptides, which may exert anti-inflammatory effects.
2. CCRL2 plays a non-redundant role in dampening neutrophil and monocyte mobilisation to sites of inflammation.

1.9 Experimental Aims.

At this start of my graduate studies in 2011, I set myself the following experimental aims:

- To characterise and optimise the zymosan induced peritonitis model of sterile inflammation.
- To demonstrate the chemotactic and pro-adhesion effects of chemerin and chemerin derived peptides on murine macrophages.
- To investigate the anti-inflammatory effects of chemerin and chemerin derived peptides *in vivo.*
- To characterise endogenous chemerin levels during in vivo inflammation models and assess the effect of knocking down endogenous chemerin levels *in vivo.*
- To investigate the effects of deleting the CCRL2 receptor in the context of inflammatory cell recruitment.

2 Materials and Methods

2.1 Materials

2.1.1 Proteins and peptides used

Recombinant murine and human chemerin: R&D systems Ltd.

Chemerin peptides: Mouse C17 (AGEDPHGYFLPGQFAFS), Mouse C9 (FLPGQFAFS), Mouse mutant C17 (AGEDPHGYALPGQFAAS) were ordered from Peptide Protein Research Ltd.

CCL2, CCL5, CXCL12, fMLP, M-CSF, interferon-γ: Chemokines, fMLP, M-CSF and interferon-γ were obtained from Peprotech Inc.

Anti-sense oligonucleotides (ASO): ASOs were a kind gift from ISIS Pharmaceuticals.

CCX417: The CCR2 antagonist CCX417 was a kind gift from ChemoCentryx (MountainView, CA.)

2.2 *In vivo* procedures

All animal studies were conducted with approval from the Dunn School of Pathology Local Ethical Review Committee and in accordance with the UK Home Office regulations (Guidance on the Operation of Animals, Scientific Procedures Act, 1986). Experiments on animals were performed under the PPL 30/3035. I received training and was signed off on all procedures by Professor David R. Greaves and Dr. Asif J. Iqbal. All animal experiments were planned with consideration of the 3Rs ie. Replacement, Reduction and Refinement. For instance when planning *in vivo* experiments, statistical

power calculations were performed to ensure that all experiments used the minimum number of animals required to obtain a statistically significant result. Animals were fed a standard laboratory chow diet and water *ad libitum*. Animals were housed on a standard 12 hour light cycle followed by a 12 hour dark cycle under pathogen-free conditions.

C57Bl/6J mice- Male 8-12 week old-Harlan (Blackthorn, U.K.). Average of 24g in weight.

C57Bl/6J mice –Male or female 8-12 week old animals bred in the Pathology Support Building were used as wild type controls for the CCRL2 KO animals.

CCRL2 KO mice-Jackson laboratory, backcrossed onto a C57Bl/6J genetic background for 12 generations (original genetic background SV129). Bred in the Pathology Support Building.

Littermate controls-Age matched littermate controls were generated by crossing heterozygous CCRL2 KO animals with wild type C57Bl/6J animals and the resulting progeny were in the expected Mendelian ratios.

ChemR23 KO mice- Paradigm Pharmaceuticals. 8-12 week old mice on a Sv129 genetic background bred in the Pathology Support Building.

SV129 mice-Male 8-12 weeks old. Bred in the Pathology Support Building.

2.3 Antibodies

Specificity	Supplier	Clone	Isotype	Format	Concenration
F4/80	Abd Serotec	CI:A3-1	Rat IgG2b	Alexa fluor 647	10 µg/ml
LY-6B.2	Abd Serotec	7/4	Rat IgG2a	FITC	1 µg/ml
LY-6B.2	Abd Serotec	7/4	Rat IgG2a	APC	1 µg/ml
Ly6-C	Biolegend	HK1.4	Rat IgG2c	FITC	5 µg/ml
CD45	BD Biosciences	30-F11	Rat IgG2b	APC-CY7	2 µg/ml
Ly6-G	BD Biosciences	1A8	Rat IgG2a	PE	2 µg/ml
LY6-G	Biolegend	1A8	Rat IgG2a	Pacific Blue	2 µg/ml
CD3	Biolegend	17A2	Rat IgG2b	PE	2 µg/ml
CD4	Biolegend	RM4-5	Rat IgG2a	Brilliant violet 421	0.5 µg/ml
CD8	BD Biosciences	53-6.7	Rat IgG2a	FITC	5 µg/ml
B220	eBioscience	RA3-6B2	Rat IgG2a	PE	2 µg/ml
CD19	Biolegend	6D5	Rat IgG2a	Brilliant Violet 421	2 µg/ml
CD11c	BD Biosciences	HL3	Armenian hamster IgG1	FITC	5 µg/ml
CD11b	Biolegend	M1/70	Rat IgG2b	PerCP	2 µg/ml
ChemR23	eBioscience	BZ194	Rat IgG2a	PE	2 µg/ml
CD115	Biolegend	AFS98	Rat IgG2a	PE	2 µg/ml
MHC-II	Biolegend	M5/114.15.2	Rat IgG2b	PE	2 µg/ml
Siglic-F	BDBiosciences	E50-2440	Rat IgG2a	Alexa Fluor 647	2 µg/ml
CD16/CD32	Abd Serotec	FCR4G8	Rat IgG2b	-	10 µg/ml
Mouse gamma globulin	Jackson	-	Mouse	-	50 µg/ml

Table 2.1 Antibodies used throughout this thesis.

2.4 In vivo models

2.4.1 Zymosan induced peritonitis

10 mg of Zymosan A (Sigma-Aldrich) was weighed out and dissolved in 50 ml of sterile PBS. This suspension was vortexed thoroughly and the Falcon tube was inverted repeatedly between each injection to ensure a uniform suspension was injected [268]. 0.5 ml of this suspension was injected intraperitoneally (i.p.). Chemerin, chemerin peptides or dexamethasone were diluted to the required concentrations with ice cold sterile PBS or in the case of dexamethasone, 2% ethanol. Animals were injected i.p. using a 0.5 ml insulin syringe (BD). Animals were administered these treatments either 45 minutes before zymosan injection or 2 hours after zymosan. Mice were sacrificed at stated time intervals after zymosan injection by CO_2 euthanasia followed by cervical dislocation for confirmation. A small incision was made along the abdomen and the skin was pulled back to expose the peritoneum. Ice cold PBS supplemented with 2mM EDTA (5 ml) was injected into the peritoneal cavity using a 5 ml syringe and a 25G needle. The cavity was massaged firmly but gently with the side of a 19G needle. The same needle attached to a 5 ml syringe was carefully inserted into the abdomen avoiding internal organs and blood vessels. The contents were gently mixed and the peritoneal exudate fluid was slowly removed and lavage fluid was immediately transferred to 15 ml falcon tubes on ice.

450 µl of lavage fluid was transferred to polypropylene tubes for flow cytometry analysis. These were centrifuged at 250 G at 4°C for 5 minutes and resuspended in 50 µl blocking buffer which is FACS buffer (PBS with 2% FCS, 5mM EDTA and 25mM HEPES) supplemented with10 µg/ml anti-CD16/CD32 (Abd Serotec) and 50 µg/ml mouse gamma globulin (Jackson). Cells were blocked for 15 minutes on ice. Following blocking, an equal volume of 2 X antibody mastermix was added and cells were incubated with indicated antibodies for 30 minutes on ice in the dark. FACS buffer was

added and tubes were centrifuged at 250 G for 5 minutes at 4°C. Cells were resuspended in 1% formalin in PBS. Cells were stored at 4°C until analysed using a CyAn ADP flow cytometer (Beckman Coulter). The remainder of the lavage fluid was centrifuged at 250 G at 4°C for 5 minutes and supernatant was stored at -80°C for ELISA and Luminex assays.

Cell counts per ml were multiplied by the volume of lavage fluid used (5 ml) in order to calculate total cell counts. The percentage of different cell types recruited to the cavity was quantified using flow cytometry and this was multiplied by the total peritoneal cell counts to obtain the total number of each cell type in the cavity.

2.4.2 Thioglycollate induced peritonitis

A 4% solution of brewers thioglycollate yeast was made in sterile PBS and allowed to mature in the dark for 4 weeks before being aliquoted into 50 ml falcon tubes and stored at -20°C. This maturation process is important as it increases the yield of inflammatory cells recruited to the peritoneum due to the generation of advanced glycation end products [269]. 8-12 week old male mice were injected i.p. with 1ml of 4% thioglycollate broth using a 26G needle [270]. Animals were sacrificed 1 hour later by CO_2 euthanasia followed by cervical dislocation for confirmation. A small incision was made along the abdomen and the skin was pulled back to expose the peritoneum. 5 ml of ice cold PBS supplemented with 2 mM EDTA was injected into the peritoneal cavity using a 5 ml syringe and a 25G needle. The cavity was massaged gently but firmly with the side of a 19G needle. The same needle attached to the 5 ml syringe was carefully inserted into the abdomen avoiding internal organs and obvious blood vessels. The contents was gently mixed and the peritoneal exudate fluid was slowly removed. Lavage fluid was immediately transferred to 15 ml falcon tubes on ice. 450 µl of lavage fluid was

transferred to polypropylene tubes and prepared for flow cytometric analysis as previously described. Lavage fluid was centrifuged at 250 G at 4°C for 5 minutes and supernatant was stored at -80°C for ELISA and Luminex assays.

2.4.3 LPS endotoxemia

Mice were weighed and LPS (Serotype 0127: B8, Sigma-Aldrich) was diluted to a concentration corresponding to a final dose of 1 mg/kg in sterile PBS. Animals were injected i.p. with 0.2 ml sterile PBS or 0.2 ml LPS (1 mg/kg final) using a 29G insulin syringe (BD) [271]. 2 hours later, animals were sacrificed by CO_2 euthanasia followed by cervical dislocation for confirmation. A small incision was made in the abdominal cavity and the skin was pulled back. The abdomen was opened to expose to the hepatic portal vein. A 1 ml syringe and 23G needle were carefully inserted into the hepatic portal vein, blood was slowly withdrawn, transferred to Eppendorf tubes and left on ice (the blood was allowed to clot for a minimum of 3 hours at 4 °C in order to obtain serum). Once blood had been allowed to clot at 4°C for 3 hours, it was centrifuged at 2000 G for 10 minutes at 4°C. Serum was carefully removed and stored as aliquots at -80°C for subsequent analysis.

Animals were perfused with PBS and one lobe of lung and one lobe of liver were transferred to ice cold PBS for analysis by flow cytometry as detailed in section 1.10.2.

2.4.4 Dextran Sodium Sulphate (DSS) induced colitis.

Female mice (10-12 week old) were co-housed for 2 weeks prior to beginning the experiments. This was to minimise differences due to microbiota variation. A 2% solution

of dextran sodium sulphate (MP Biologicals) was made up using drinking water supplied in the Pathology Support Building. On day 0, animal weights were recorded and drinking water was replaced water with 2% DSS [272]. Animals were weighed at the same time every day and mice were evaluated for clinical signs of disease. Cages were checked for loose faeces and animals were checked for rectal bleeding and inflammation of the anus. Weight loss was monitored and if any animals lost more then 20% of their initial body weight, they would have been humanly sacrificed in line with animal welfare protocols set out in the project license. Drinking water was replaced with fresh DSS every 2 days. On day 7, DSS was replaced with normal drinking water and animals were sacrificed on day 10 by cervical dislocation. A small incision was made in the abdomen and skin was pulled back to reveal the peritoneum. The peritoneum was cut to reveal the internal organs. The spleen was removed and weighed. The entire colon was removed and colon length was measured as readout for inflammation. The mid and distal colon, as well as the caecum were collected into 10% formalin (in PBS) for histology. The mid and distal colon were cut into sections using a microtome (~10μm sections) and stained with Haemotoxylin and Eosin (H&E) by the histology facility at the Sir William Dunn School of Pathology, Oxford. A piece of tissue (~1 mm) from the distal colon was snap frozen in liquid nitrogen and stored at -80°C for myeloperoxidase (MPO) activity analysis. After colon sections were H&E stained, disease severity and inflammation of the colon was assessed by an established disease scoring system using a light microscope [273].

2.5 Biogel-elicited peritoneal exudate cell isolation.

Bio-gel P100 polyacrylamaide beads have been used to elicit large numbers of macrophages from animals [274]. Injected i.p. these 45-90 μm beads induce a robust

inflammatory response characterised by an initial wave of neutrophils followed by large numbers of monocytes, which differentiate into macrophages. Macrophages endeavor to phagocytose the beads but the beads are too large, leading to a frustrated phagocytosis and a positive feedback loop and more macrophage recruitment.

A 2% solution of Bio-Gel P100 beads was made in sterile PBS and autoclaved before being used *in vivo.* 1 ml of this 2% w/v solution of Bio-gel P100 polyacrylamide beads were injected into the peritoneal cavities of 8-12 week old male C57Bl/6J mice, CCRL2 KO mice, ChemR23 KO mice or Sv129 mice using a 1 ml syringe and a 26G needle. Animals were sacrificed 4 days later, with CO_2 followed by cervical dislocation for confirmation. A small incision was made in the abdomen and the skin was pulled back to reveal the peritoneum. Peritoneal cavities were injected with 10 ml of ice cold PBS supplemented with 2 mM EDTA using a 25G needle. The cavity was massaged with the side of a 19G needle before lavage fluid was collected using the same needle. Lavage fluid was kept on ice until needed. Cells were centrifuged at 4 °C for 5 mins at 250 G, resuspended in 1 ml of chemotaxis buffer (Rosswell Park Memorial Institute (RPMI) 1640 medium (Sigma-Aldrich) supplemented with 0.5% BSA (Sigma-Aldrich), 25mM HEPES (Life technologies), 50 U/ml penicillin and 50µg/ml streptomycin) and counted for use in experiments.

2.6 Bone marrow derived macrophage isolation

Male C57Bl/6J mice (8-12 week old) were euthanised by CO_2 followed by cervical dislocation. Femurs and tibia were isolated and excess muscle and tissue were cut away to reveal the bones. Bones were washed with 70% w/v ethanol and placed in PBS on ice. The exposed bones were cut at the knee joint and flushed with 20mls of sterile PBS using

a 25G needle. Clumps of cells were broken up by repeatedly pipetting up and down using a pasteur pipette. The cell suspension was passed through a 70 μm cell strainer and centrifuged at 250 G for 5 minutes at room temperature. Cell pellets were resuspended in 10 ml macrophage growth medium (Dulbeccos Modified Eagle Medium (DMEM) supplemented with 15% supernatant from L929 cells (as a source of M-CSF and IL-3), 10% fetal bovine serum (FBS), 50 U/ml penicillin and and 50μg/ml streptomycin) [275]. 1.5 ml of this cell suspension was added to 8.5 ml growth media in non-tissue culture treated petri dishes with a further 5 ml of growth medium added on day 4. Media was removed on day 7 and cells were washed with PBS. 5 ml of ice cold 10 mM EDTA was added per dish, and cells were gently dislodged using a pasteur pipette. Cells were centrifuged at 250 G for 5 minutes and resuspended in DMEM supplemented with 10% FBS, 50 U/ml penicillin and and 50 μg/ml streptomycin. Cells were counted using a haemocytometer and resuspended to the desired concentration. Where indicated, recombinant murine M-CSF 10 ng/ml (Peprotech) was used instead of L929 conditioned media. Cells were not re-fed during these experiments.

2.7 Electrical impedance sensing assays

The ACEA Biosciences RTCA-SP instrument was used to analyse differences in cell adhesion and spreading of primary Bio-Gel elicited macrophages [160, 276]. This system uses 96 well plates, coated with gold electrodes on the bottom of the wells. An electrical current is passed through the plate and differences in cell adhesion and spreading can be detected by increases in impedance of the current, measured as cell index (CI). The CI increases as more cells adhere to the plate or as cells adhere more tightly and spread out. Bio-Gel elicited PECs were obtained as described in section 1.2. Cells were resuspended

in 2 ml of chemotaxis buffer and counted using a haemocytometer. Cells were diluted to a concentration of 1.08 x 10^6 cells/ml. 50 µl of chemotaxis buffer was added to each well and a background reading was taken as a baseline. 50 µl of cells was then added to give a final concentration of 54,000 cells/well. Cells were allowed to adhere for ~ 3 hours with impedance being read every 15 minutes until no further increases in CI were observed (typically 2-4 hours) (Figure. 2.1). This was to ensure that responses to agonist challenge would not be masked by cells settling down on the plate under resting conditions At this point, cells had reached maximum basal adherence. Agonists or inhibitors were made up in 96 well polypropylene plates at 11X the final concentration. The number of reads was then increased to every 5 seconds to ensure that rapid responses induced by chemokines were captured. 10 µl of 11 X stock of agonists were added to each well and cell responses were monitored for up to 2 hours. Responses were analysed using the ACEA SP software. Max-min values of the curves after agonist addition were compared to vehicle treated samples.

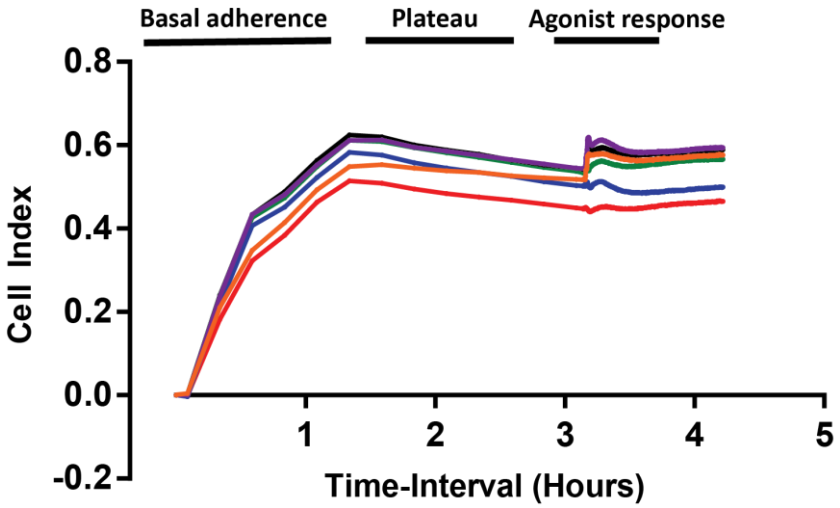


Figure 2.1 Cell adhesion as measured using the impedance platform.

The trace shows a Cell index (CI) as a function of time with 54,000 Bio-Gel elicited PECs per well plotted at t=0 and challenged with a GPCR agonist after 3 hours. The trace is broken up into the initial basal adherence, the plateau (maximal basel adherence) and the responses to agonist challenge.

2.8 Real time chemotaxis assay

The ACEA DP platform was used to measure chemotaxis of Bio-Gel elicited PECs. I and others in the laboratory have used a range of cell types in this system but for the experiments in the subsequent chapters, only Bio-Gel PECs were used [199]. This system uses the same principle as the impedance platform to detect cell adhesion, except it utilises trans well plates. The filters have 8 μm pores to allow the macrophages to squeeze through in response to a chemoattractant gradient. The underside of the filter is coated with gold electrodes and as cells migrate through the pores, they adhere to the underside of the filter, increasing the CI. Male C57Bl/6J, CCRL2 KO, ChemR23 KO or Sv129 mice (8-12 week old) were injected i.p. with 1 ml 2% Bio-Gel and peritoneal exudate cells were isolated as before 4 days later. Cells were kept on ice while chemokine solutions were made up. Chemerin, chemerin peptides or CCL5 were diluted to the required concentration in chemotaxis buffer and 160 μl of chemokine was added to the bottom

chamber of the trans well plate, avoiding the introduction of bubbles. The top chamber was attached and 50 µl of chemotaxis media was added to allow a chemotactic gradient to form for 30 minutes. Cells were centrifuged at 250 G for 5 minutes at 4°C, resuspended in 2 ml chemotaxis buffer and counted using a haemocytometer. Cells were diluted to a concentration of 8 x 10^6 cells/ml in pre-warmed (37°C) chemotaxis buffer. After a gradient had formed, a baseline reading of impedance was taken, followed by 50 µl of cell suspension (400,000 cells/well). CI was measured every 5 seconds for ~3 hours. Chemotactic responses were assessed by quantifying the slope of the curve in the first 40 minutes and by the Max-Min values of the curve over the entire experiment (data analysed using RTCA software, ACEA Biosciences, see Figure. 4.1).

2.9 ChemR23 β-arrestin recruitment assays.

The Pathunter eXpress kit was obtained from DiscoveRX corporation (Birmingham, U.K.) and manufacturers instructions were followed. The principle behind the assay is as follows. CHO-K1 cells were stably transfected with a version of the ChemR23 receptor tagged intracellularly with half a β-galactosidase fragment, while a complementary fragment was attached to β-arrestin 1. Upon receptor activation, β-arrestin is recruited to the receptor to produce a functional β-galactosidase enzyme. This functional enzyme is now capable of hydrolising the provided substrate to produce a chemiluminescent signal that can be quantified using a luminometer [277]. Briefly, CHO-K1 cells were thawed and resuspended in CP reagent supplied. Cell suspension (50 µl) was added per well of a 96 well half-area plate (83,000 cells/well). Cells were incubated at 37°C, 5% CO_2 for 48 hours. If inhibitors or antagonists were used, 11 X solution was made in CP reagent and 5 µl was added per well for 30 minutes at 37°C, 5% CO_2. Agonists were prepared in CP

reagent at 11 X the final required concentration. Agonists (5 µl) were then added per well. Plates were incubated for 90 minutes at 37°C, 5% CO_2. During this time, detection reagent was prepared following the manufacturers protocol and plates were read using a luminescence plate reader (PHERAstar FS, BMG Labtech) and data was analysed using GraphPad Prism 6.

2.10 Macrophage activation assays

Bone marrow derived macrophages were cultured as described earlier. Macrophages were resuspended in Optimem medium (Gibco,Life technologies) supplemented with 50 U/ml penicillin and 50 µg/ml streptomycin and 0.2% BSA to a concentration of 1 x 10^6 cells/ml. 1000 µl of this cell suspension was added to 12 well tissue culture treated plates and allowed to adhere for ~3 hours. 10 µl of a 100 X stock of chemerin, chemerin peptides or dexamethasone was added as a 40 minute pre-treatment. Following this, 10 µl of 10 µg/ml stock of LPS (serotype 0127 B8, Sigma) and 1 µl of 10 µg/ml of interferon-γ (Peprotech) was added per well to give a final concentration of 100 ng/ml LPS and 10 ng/ml interferon-γ for 16 hours at 37°C, 5 % CO_2. Cell supernatant was transferred into sterile 1.5 ml Eppendorf tubes and centrifuged at 250 G for 5 minutes at 4°C in order to remove any cell debris. Supernatant was transferred into fresh Eppendorf tubes, aliquoted and kept at -80°C for future analysis of cytokine production by ELISA.

2.11 ELISA assays.

Sandwich ELISAs for CCL2, CXCL1, IL-6 and chemerin (R&D systems) were performed according to manufacturers guidelines. 96 well high binding plates (Nunc)

were coated with 100 µl capture antibody diluted to required working concentration in PBS over night at room temperature. The next day, plates were washed 3 times with 300 µl ELISA wash buffer per well (PBS supplemented with 0.05% Tween). Non-specific binding was blocked with 300 µl 1% BSA per well for a minimum of 1 hour. During this blocking step, 7 point standard curves were prepared in Eppendorf tubes in 1% BSA (in PBS) and samples were diluted to ensure they were within the linear part of the standard curve. After blocking, plates were washed 3 times, and 100 µl of standards or samples were added to the plate and incubated for 2 hours at room temperature. Plates were washed again and 100 µl biotinylated detection antibody diluted to working concentration (as per manufactures instructions) in 1% BSA (in PBS) was added per well and incubated for 2 hours. Plates were washed 3 times and 100 µl of Streptavidin-HRP diluted 1 in 200 in 1% BSA (in PBS) was added per well for 20 minutes. Plates were washed 3 times and 50 µl of one-step Ultra TMB (Thermo Fisher) was added. The reaction was stopped with 50 µl 3N H_2SO_4 20 minutes later or when the standard curve had changed colour. Plates were read at 450 nm and at 630 nm using a PHERAstar FS plate reader (BMG Labtech). Absorbance at 630 nm was subtracted to correct for optical imperfections in the plate. Unknown values were interpolated using a 4-point linear regression analysis in Graphpad Prism 6 (Figure. 2.2).

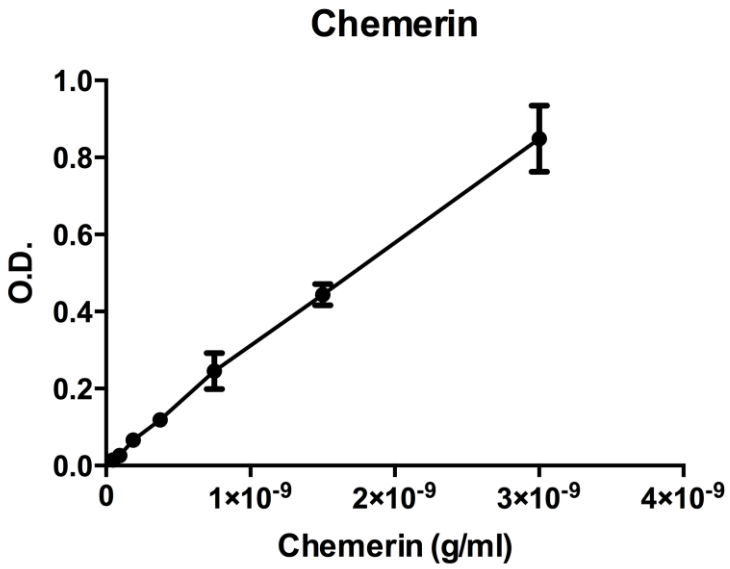


Figure 2.2 Standard curve of chemerin ELISA used to interpolate chemerin levels

4-point linear regression analysis was performed on a standard curve of known concentrations to interpolate concentrations of unknown samples.

2.12 Luminex assays

The principle of Luminex assays is very similar to ELISA except that it uses colour coded beads coated with antibodies specific for each analyte to be tested. Biotinylated detection antibodies specific for each analyte are added followed by Phycoerythrin (PE)-conjugated streptavidin. Samples are read using a laser detection system, which quantifies the amount of PE present for each analyte [278]. Custom multiplex polyacrylamide bead assays were purchased from R&D systems to determine levels of CCL2, CCL4, CXCL1, CXCL2, CXCL10, IL-10, IL-6 and MMP-9. The 96 well plate was wet with 100 µl assay buffer and removed using a vacuum filtration manifold system (Millipore). A 3 fold standard curve was made up as directed in calibrator diluent. All samples were diluted 1:2. 50 µl of reconstituted microparticle bead cocktail and 50 µl of standards or pre-diluted samples were added per well. The plate was sealed and incubated on an orbital shaker set to 500

rpm for 2 hours at room temperature. After this, unbound sample was removed using the vacuum manifold. 100 µl wash buffer was added per well and then removed using the vacuum manifold. This was repeated a total of three times. 50 µl of diluted biotin antibody cocktail was added to all wells. The plate was sealed with a new foil plate sealer and incubated for 1 hour on an orbital shaker set to 500 rpm at room temperature. The washing step was repeated 3 times as before. 50µls of diluted Strepavidin-PE was added to all wells. The plate was recovered with a new foil plate sealer and incubated for 30 mins at room temperature on an orbital shaker set to 500 rpm. The plate was washed three times. The microparticles were resuspended in 100 µl wash buffer and incubated for 2 minutes on an orbital shaker set to 500 rpm. The plate was then read on a Bio-Rad bioanalyser and Bio-Plex Manager software.

2.13 Mass spectrometry

Samples for mass spectrometry were desalted using a C18 reverse-phase column (Sigma-Aldrich) packed in a pipette tip. Briefly, the column was prepared as follows: 20 µl 100% Acetyl nitrile (ACN) was added to the column and centrifuged at 200 G for 5 minutes. 20 µl 0.1% trifluoroacetic acid (TFA) was added and column was centrifuged at 200G for 5 minutes. Up to 80 µl of sample was then added and centrifuged at 200 G for 5 minutes. Next, 40 µl 0.1% TFA was added to desalt the sample and centrifuged at 200 G for 5 minutes. The column and sample were transferred to new Eppendorfs and 40 ul 50% ACN/0.1% TFA were added and centrifuged at 200 G for 5 minutes to elute sample. Flow through containing sample was transferred to glass vials and concentrated using a vacuum centrifuge (Thermo Fisher). Samples were run on a LC-MS/MS QExactive mass spectrometer (Thermo) coupled to a RSLCnano HPLC system (Dionex). Mass

spectrometry experiments were performed in collaboration with the central proteomics facility at the Sir William Dunn School of Pathology, University of Oxford. Data were analysed using Mascot and searched against the Uniprot Mus reference proteome, with the precursor mass tolerance set at +/- 20 ppm, fragment tolerance +/-0.02 Da with no enzyme specificity defined.

2.14 Myeloperoxidase (MPO) assay

MPO is an enzyme found predominantly in granules of neutrophils and was used as a measure of neutrophil recruitment to tissue [279]. Tissue from the colon of DSS treated animals was homogenised in 50 mM sodium phosphate buffer (+ 0.5% hexadecyltrimethylammonium bromide) using glass beads (Marenfeld Superior) and a tissue homogensier (FastPrep-25, MP Biologicals) set at 6.5 m/s for 40 seconds. The tissue was then centrifuged at 4000 G for 20 minutes and supernatant was collected and used for measurement of MPO activity. 20 µl of samples were incubated with 160µl of 3,3',5,5'-tetramethylbenzidine (TMB) and 20 µl of H_20_2 in 80 mM sodium phosphate buffer pH=5.4 (Final of 0.3% H_20_2) (Sigma-Aldrich). This was carried out in 96 well plates and MPO standards (R&D systems) were run in duplicate. Plates were incubated at room temperature for 5 minutes and absorbance at 630nm was read using the PHERAstar platform. MPO levels were calculated by interpolating concentrations of unknown samples from the standards. Results were normalised to protein content and were expressed as MPO U/ mg of tissue.

2.15 Preparation of different murine tissues for flow cytometry

2.15.1 Blood analysis

Animals were euthanised with CO_2 followed by cervical dislocation for confirmation. The skin covering the peritoneum was removed and an incision was made to reveal the hepatic portal vein. A 23G needle attached to an EDTA coated 1ml syringe was gently inserted into the hepatic portal vein (being careful not to pierce the vein) and blood was slowly withdrawn. Blood was immediately transferred to an EDTA-coated vacutainer (Cole-Palmer, London, U.K.) and mixed by agitation. Whole blood (50 µl) was transferred to polyproplylene tubes, 2 ml of FACS buffer (PBS supplemented with 2% FCS, 5 mM EDTA and 25 mM HEPES) was added and centrifuged at 250 G at 4°C for 5 minutes. Blood was resuspended in 50 µl blocking buffer (FACS buffer supplemented with10 µg/ml anti-CD16/CD32 and 50 µg/ml mouse gamma globulin) for 15 minutes on ice. An equal volume of 2 X antibody mastermix was then added and cells were incubated with indicated antibodies for 30 minutes on ice in the dark. After antibody staining, 3 ml of 1X BD FACS Lysing Solution (Buffered solution with <15% formaldehyde and <50% diethylene glycol) diluted in distilled H_2O, was added and each tube was vortexed. Samples were incubated at room temperature for 5 minutes, occasionally vortexing. FACS buffer was then added and tubes were centrifuged at 250 G for 5 minutes at 4°C. Supernatant was discarded and cells were washed with 3 mls FACS buffer. Cells were centrifuged a second time and subsequently resuspended in 1% formalin in PBS. Cells were stored in the dark at 4°C until analysed using a CyAn ADP flow cytometer (Beckman Coulter). During this time, the remainder of blood not used for flow cytometry or counting was centrifuged at 2000 G for 10 minutes at 4°C to obtain plasma. The

supernatant was aliquoted and frozen at -80°C for use in ELISA and Luminex assays. Plasma was collected within 30 minutes of blood collection.

2.15.2 Tissue analysis (Spleen, liver and lung)

Spleen, liver and lung were removed and transferred to 1 ml of ice cold PBS in a 12 well plate. All three organs were transferred to HBSS supplemented with 1 mg/ml collagenase D (Roche) and cut up into smaller pieces and incubated at 37°C for 1 hour. Spleens, livers and lungs were passed through a 70 μm strainer (Corning) attached to a 50ml Falcon tube and washed through with 10mls of FACS buffer. Cells were centrifuged at 250 G for 5 minutes at 4°C. Cell pellet was resuspended in 1 ml FACS buffer and 200 μl was transferred to 1ml ACK red blood cell lysing reagent (ammonium chloride, potassium bicarbonate and EDTA) (ThermoFisher) for 5 minutes. 2 ml of FACS buffer was added and cells were centrifuged as before. Cell pellet was resuspended in 1 ml FACS buffer. 100 μl of this cell suspension was transferred to polypropylene tubes, centrifuged at 250 G for 5 minutes and resuspended in 50 μl blocking buffer for 15 minutes on ice. An equal volume of antibody mix was added and cells were stained on ice in the dark for 30 minutes. FACS buffer (2 ml) was added and cells were centrifuged at 250 G at 4 °C for 5 minutes. Cell pellets were resuspended in 1% formalin and stored in the dark at 4 °C until analysed using a CyAn ADP flow cytometer (Beckman Coulter).

2.15.3 Bone marrow analysis

Animals were sacrificed as before and femurs and tibia were isolated. Once excess skin and muscle had been removed, the bones were flushed with 20 ml of sterile PBS using a

25G needle. Clumps were broken up by repeatedly pipetting up and down using a pasteur pipette. The cell suspension was passed through a 70 μm cell strainer (Corning) and centrifuged at 250 G for 5 minutes at room temperature. The cell pellet was resuspended in 10 ml of ACK Lysing Buffer (Thermo Fisher) for 5 minutes and centrifuged again. Cell pellet was resuspended in 1 ml FACS buffer and 50 μl of this cell suspension was transferred to polypropylene tubes, centrifuged at 250 G for 5 minutes and resuspended in 50 μl blocking buffer. Cells were prepared for analytical flow cytometry as described above.

2.16 Cell counting

Cell suspensions were counted using a Neubauer haemocytometer, an automated cellometer (Nexcelom) or countbright counting beads (Invivogen). Counting beads were used to quantify cell numbers in blood and bone marrow because these were more accurate methods of quantifying such large numbers of cells. Automated cellometer was used to quantify total cell counts in the peritoneal cavity following inflammatory insult. Neubauer haemocytometer was used to count Bio-Gel PECs as the polyacrylamide beads caused difficulties for the automated cellometer. Counts per ml were equivalent between haemocytometer and automated cellometer.

2.16.1 Neubauer haemocytometer

Cells were diluted 1:10 in 0.4% trypan blue solution (Sigma-Aldrich) and 10 μl was loaded onto the counting chamber and viewed under a light microscope using a 10 X magnification on an AE2000 inverted microscope. Four quadrants were counted and

viable cells (differentiated by uptake of trypan blue) were quantified by eye. The mean of these four counts was calculated and total cells per ml were calculated using the formula:

Average cell count per square X dilution factor X 10^4 = Cell counts/ml.

2.16.2 Automated Cellometer

Cells were diluted 1:10 in 0.4% trypan blue solution (Sigma-Aldrich) and 20 µl was loaded onto the provided counting chamber slides. Slides were inserted into the Cellometer Auto 4X Cell Counter (Nexcelom) and viable cells were quantified. Cells that the software counted as viable were routinely checked by eye.

2.16.3 Countbright counting beads

Up to 300 µl of cells were added to a polypropylene tube. Countbright beads (Thermofisher) were vortexed and 50 µl were added per tube. For absolute counts, a specific volume of beads is added to a specific volume of sample (hence the ratio of sample volume to bead volume is known). The volume of sample analysed is calculated from the number of bead events. This is used with cell events to determine cell concentration [280]. Cells were run immediately on a DacoCyan flow cytometer. Gates were drawn on the beads and at least 1500 bead events were collected per sample (Figure 2.3). Cell concentration was calculated using the following formula:

$$\frac{Number\ of\ cell\ events}{Number\ of\ bead\ events} \text{ X } \frac{Assigned\ bead\ count\ per\ 50\ \mu l}{Volume\ of\ sample}$$

In the case of blood, a red blood lysis step was necessary before counting bead addition otherwise beads were not detected by the flow cytometer (Figure 2.3).

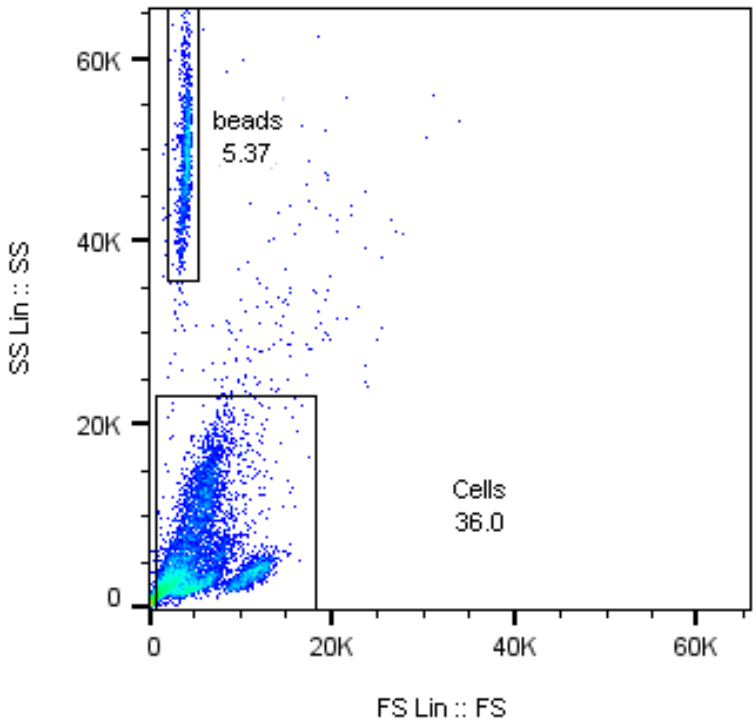


Figure 2.3 Representative flow cytometry plot of countbright counting beads and cells to quantify cell numbers.

2.17 CCRL2 KO mouse genotyping

2.17.1 Genomic DNA isolation

DirectPCR lysis reagent (Viagen) was used to digest ear clips. This lysis buffer was supplemented with proteinase K (0.4 mg/ml) (Sigma-Aldrich). 170 µl was added to each Eppendorf containing an ear clip. Eppendorfs were vortexed and incubated at 65°C overnight. The next morning, Eppendorf tubes were vortexed and incubated at 85 °C for

45 minutes to inactivate the proteinase K. Crude DNA was frozen at -20 °C for future analysis.

2.17.2 Polymerase chain reaction (PCR)

PCR reactions were made up in PCR tubes (Thermo Fisher Scientific) on ice that contained 12.5 µl 2X Biomix Red mastermix (Bioline), 0.13 µl (500 nM) forward primer, 0.13 µl (500 nM) reverse primer and 12.3 µl nuclease free water (25 µl total reaction volume). The primers used were as follows: CCRL2 forward (5' GGCAAAGAGAGCGCAGTAGCCATGG 3'), Neomycin forward (5'GGGCCAGCTCATTCCTCCCACTCAT 3') and common (5' GCCTCCGATGGATAACTACACAGTG 3'). A mastermix of these components was made up and 23.5 µl of this was added to each tube containing1.5 µl of crude DNA. Mastermix without crude DNA was used as the negative control.

The PCR conditions used were as follows:

1. 95 °C for 3 minutes (denature)
2. 94 °C for 30 seconds (denature)
3. 60 °C for 45 seconds (annealing step)
4. 72 °C for 3 minutes (elongation step)
5. 72 °C 3 minutes
6. 10 °C hold.

Steps 2-4 were repeated 32 times. PCR reactions were amplified using a PTC 100 Programmable Thermal Controller. Primer sequences were provided by the Jackson

Laboratory. The wild type forward primer and common primer amplified the wild type CCRL2 gene and the mutant primer and common primer amplified the neomycin cassette that was introduced in order to disrupt the CCRL2 gene.

2.17.3 Agarose gel electrophoresis

A 1.5% agarose gel was made containing 1 X TBE and 1:1000 final dilution of Safeview (NBS Biologicals). Hyperladder-50bp (7 μl) (Bioline) was loaded to estimate DNA product size and 10 μl of each reaction mixture was loaded per well. The gel was run at 130 volts for 40 minutes in 1 X TBE buffer with a 1:1000 dilution of Safeview using a Wide Mini-Sub Cell GT electrophoresis cell (Bio-Rad, Hemel Hempstead, U.K.). Bands were visualised using a UV light Gel Doc 2000 (Bio-Rad). Wild type animals displayed the 512 bp CCRL2 band. CCRL2 KO animals displayed the 314 bp neomycin cassette band. Heterozygous animals displayed both the 512 bp band and the 314 bp band (Figure 2.4).

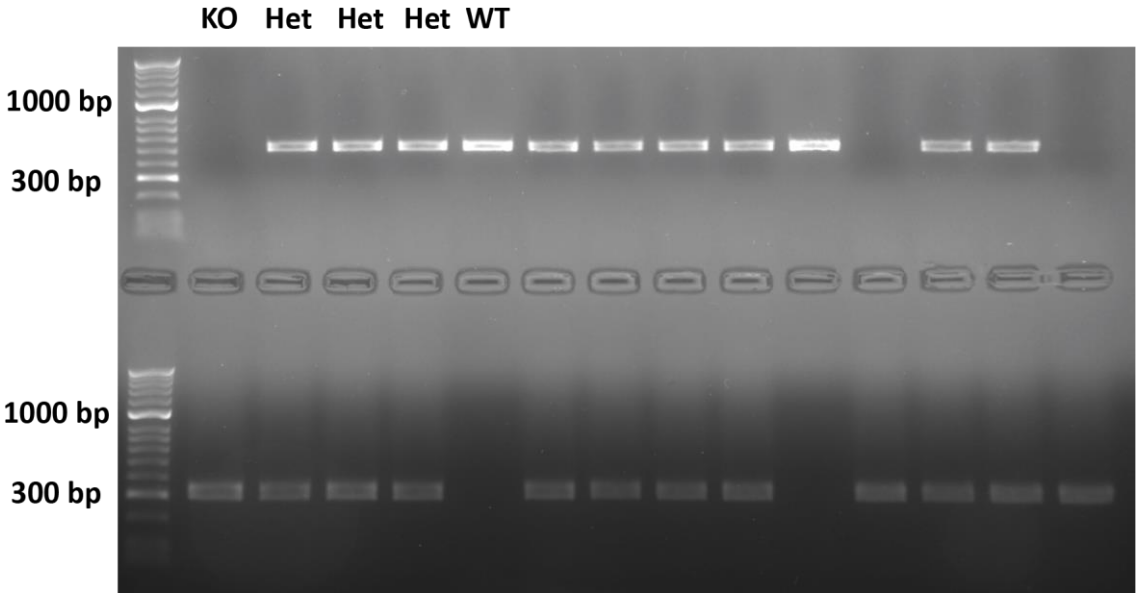


Figure 2.4 Typical genotyping results from the CCRL2 KO, heterozygous and wild type animals.

PCR products run on a 1.5% agarose gel.Wild type (WT) animals displayed a band at 314bp. CCRL2 KO animals (KO) animals displayed a band at 512bp. Heterozygous (Het) animals displayed both bands.

2.18 Data analysis

Chemotaxis data and impedance data were analysed using RTCA software. Flow cytometry data was collected using Summit (Beckman Coulter) and analysed using FlowJo (Tree Star Inc, OR, USA). Luminex data was collected using Bio-Plex Manager. ELISA data was collected using the PHERAstar plate reader and software (BMG Labtech). All remaining data and graphs were generated using GraphPad Prism 6. Software (La Jolla, CA, USA.). All data were tested for normal distribution using GraphPad Prism. Statistical significance was assessed using one-way ANOVA followed by Dunnett's or Bonferroni post hoc test. In some cases a two-way ANOVA was used followed by Sidak's multiple comparisons test. Where there were only two variables analysed, a students unpaired t-test was used. P value ≤ 0.05 was considered significant. Error bars of data are either standard deviation (S.D.) or standard error of the mean (S.E.M.) depending on the experiment. S.D. quantifies the scatter of the data while

S.E.M. quantifies how accurately your mean represents the true mean of a population. S.E.M. is calculated by dividing the S.D. by the square root of the number of data points. S.E.M was used in all *in vivo* experiments because it gives a measure of the true mean of the biological population. For *in vitro* experiments, if only one experiment was performed, error bars represent the S.D. of technical replicates. If more then one experiment was performed, the mean was calculated from technical replicates from each individual experiment, these means were pooled and error bars represent the S.E.M. of the pooled data.

3 Optimisation of the zymosan induced peritonitis model to probe the role of endogenous chemerin during sterile inflammation.

3.1 Introduction

Inflammation is the bodys response to tissue injury or infection. Usually, once the insulting stimulus or infection is cleared, inflammation resolves and tissue homeostasis is restored. However, in some cases inflammation does not resolve and develops into what is known as chronic inflammation, which is characterised by continuous recruitment of mononuclear leukocytes and irreversible tissue damage. Failure to resolve inflammation plays an important role in many disease pathologies including inflammatory bowel disease, atherosclerosis, tuberculosis, rheumatoid arthritis and cancer [5]. In order to better understand this process, animal models that can recapitulate what happens during a self-limited inflammatory response are essential. There are many different animal models of acute and chronic inflammation and the kinetics and cell types involved can vary substantially depending on the details of the model, the gender and mouse strain [281].

3.1.1 Experimental Peritonitis

The peritoneum is a membrane that lines the abdominal cavity. The cavity is well vascularised. Blood is supplied by the mesenteric and coeliac arteries, which drain into the portal vein. The peritoneum is also connected to the lymphatic system and drains via the mesenteric lymph node. The induction of peritonitis in rodents has proven an invaluable tool for studying the basic biology and pathology of inflammation. A variety of inflammatory stimuli have been used to elicit leukocyte recruitment to the peritoneum,

including IL-1β, brewer's thioglycollate broth, zymosan and even necrotic cells (Table 3.1) [282-285].

Inflammagen	Immediate cell types recruited	Predominant chemokines/cytokines involved	References
Zymosan (0.01-10mg)	Neutrophils, Monocytes, Macrophages	CCL2,CXCL1, CCL3, IL-1β, IL-6,	[55, 283, 286, 287]
Thioglycollate broth (2% solution)	Neutrophils, Monocytes, Macrophages, Eosinophils	CCL2, CXCL1, Eotaxin, IL-5, IL-9	[288-292]
LPS (1mg/kg)	Neutrophils	IL-1β, CXCL1, TNF-α	[293, 294]
Necrotic cells	Neutrophils Monocytes Macrophages	IL-1α, IL-1β, TNF-α, IL-6	[295, 296]
MSU crystals	Neutrophils Monocytes Macrophages	IL-1β, TNF-α, IL-6, CCL2.	[285, 295]
IL-1β (0.5-50ng)	Neutrophils Monocytes Macrophages	CCL2, CXCL1	[284, 297, 298]
Carrageenan (75µg/mouse)	Neutrophils Mast cells	TNF-α, IL-1β	[299]

Table 3.1 Stimuli used to elicit peritoneal inflammation in mice.

Thioglycollate broth has been used in this model to probe whether T cells and B cells can modulate neutrophil and monocyte recruitment. Several studies have compared mice lacking RAG-1 (no B or T cells), NUDE mice (no T cells) and μMT KO mice (no B cells) in this model. From these studies, it has been demonstrated that lymphocytes can indeed modulate neutrophil and monocyte trafficking to the peritoneum. T cells seem to dampen inflammatory cell recruitment while B cells seem to increase it [289]. More recently, Michaud *et al* used the thioglycollate model of murine peritonitis to probe the role of sphingosine 1-phosphate receptor 2 in macrophage chemotaxis [300]. Sphingosine 1-phosphate (S1P) exerts a variety of different effects on recruitment of immune cells depending on the receptor involved [301]. There are 5 receptors through which S1P can signal, some of which can promote cell migration (sphingosine 1-phosphate receptor 1) while others inhibit migration (sphingosine 1-phosphate receptor 2) [300, 302]. Michaud *et al.* report that mice lacking sphingosine 1-phosphate receptor 2 displayed decreased macrophage recruitment to the peritoneal cavity 5 days post thioglycollate challenge. This decreased macrophage recruitment appeared to be due to decreased chemoattractant induced Akt phosphorylation as well as increased cAMP production.

The cell types recruited to the peritoneal cavity vary depending on the inflammagen used. Injection of recombinant IL-1β, for example, results in a heavy bias towards neutrophil recruitment to the cavity [297]. Another interesting use of this model is the intraperitoneal injection of necrotic cells, which elicited a robust recruitment of neutrophils. This was dependent on the IL-1 receptor and IL-1α. Monocytes were also recruited. However their recruitment was not dependent on the IL-1 receptor, indicating a different mechanism [296]. Subsequently, it was reported that when injected intraperitoneally, danger signals released by necrotic cells were recognised via the activation of the NLRP3 inflammasome, which in turn, induced IL-1β production [90].

This work utilising the peritonitis model of inflammation led to important insights into the pathology of sterile injury induced inflammation that were previously unrecognised.

3.1.2 Zymosan induced peritonitis (ZIP)

Zymosan is a polysaccharide component of the cell wall of the yeast *Saccharomyces cerevisiae*. Doherty *et al.* were the first group to report its actions as an inflammatory stimulus [268]. They reported that injection of zymosan (1mg) induced the classical signs of inflammation including pain, leukocyte recruitment as well as prostaglandin production. Since then, the ZIP model of sterile inflammation has been used extensively for the study of various aspects of inflammation. Injection of zymosan results in an initial wave of neutrophils, followed by monocytes, which, in turn, differentiate into inflammatory macrophages. At later time points, T cells and B cells also repopulate the cavity [140, 303]. Zymosan itself is recognised by resident peritoneal macrophages and mast cells via TLR2 and TLR6 heterodimers as well as the β-glucan receptor dectin-1 [304, 305]. Downstream signalling via these receptors results in macrophage activation. Activated peritoneal macrophages produce a range of inflammatory mediators including arachadonic acid metabolites such as leukotrienes and prostaglandins as well as pro-inflammatory proteins such as C5/C5a and cytokines [268, 283].

Resident mast cells also play an important role in the production of inflammatory mediators in this model, as demonstrated by Ajuebor *et al.* When mast cells were depleted using compound 48/80, there was significantly less CCL2 and CXCL1 produced as well as a concomitant decrease in neutrophil influx [306]. ZIP is a very dynamic system and the extent of inflammation is heavily influenced by cell types already present in the cavity including stromal cells, endothelial cells, mast cells as well as resident tissue

macrophages [306]. There is also a resident population of dendritic cells in the cavity. However, they constitute a very small percentage of total cells (~1% in rats and ~2% in my experiments, Figure 3.1) [307]. The ZIP model has provided many insights into the mediators and cell types that are important for the initiation as well as the resolution of inflammation, discussed below.

3.1.3 Applications of the zymosan induced peritonitis model in innate immunity.

The ZIP model has been used to test the importance of different mediators and cell types in sterile inflammation. A number of studies have demonstrated the importance of the CCR2 receptor in monocyte mobilisation from the bone marrow and recruitment to sites of inflammation. The first study of animals lacking the CCR2 receptor reported impaired macrophage recruitment in a model of thioglycollate peritonitis as well as decreased granuloma size when challenged with beads coated with protein isolated from *Mycobacterium bovis* [308]. There was a number of similar studies carried out highlighting the importance of this receptor and its ligand in monocyte recruitment [309, 310]. Ajuebor *et al* addressed the role of the CCL2/CCR2 axis in monocyte trafficking to local sites of inflammation using the ZIP model [311]. The authors reported local increases in CCL2 levels in the peritoneum after injection of zymosan followed by neutrophil and monocyte/macrophage influx. The monocyte/macrophage recruitment was inhibited by pre-treatment with an anti-CCL2 polyclonal antibody. Injection of CCL2 alone also selectively recruited monocytes, thus confirming the ability of this chemokine to induce monocyte recruitment *in vivo.*

Another important mediator of inflammation and the selective recruitment of neutrophils is the cytokine IL-1β. Using the ZIP model, Perretti *et al* reported the increase

of endogenous IL-1β activity in the peritoneum after zymosan challenge with concomitant neutrophil recruitment. IL-1β activity and neutrophil influx increased maximally between 2 and 4 hours post 1 mg zymosan challenge (5.1 to 19.1 units/hour IL-1 activity respectively and 3.8 $x10^6$ and 9.6 $x10^6$ neutrophils/hour respectively). Neutrophil recruitment was in turn, abrogated by pre-treatment with a polyclonal antibody against IL-1β. Polyclonal antibodies against IL-1α had no effect in this system and levels of prostaglandin E2 and mononuclear cell influx remained unaffected by either treatment [312]. Identification of IL-1β as a key inflammatory mediator informed the development of monoclonal antibodies against IL-1β such as Canakinumab as a potential therapy for a range of inflammatory diseases, including rheumatoid arthritis [313, 314]. Canakinumab is currently a recommended treatment for patients with inflammatory diseases such as Cryopyrin-Associated Periodic Syndromes including familial cold auto inflammatory syndrome, Muckle-Wells Syndrome and juvenile arthritis [315].

Lipid mediators are another important class of molecules that modulate inflammation. A number of lipid mediators have been isolated and described using the ZIP model. The pro-inflammatory prostaglandins and leukotrienes have been described in some detail, including PGE2, PGI2, LTB4, LTC4, LTD4 and LTE4 [283, 316]. Relatively recently, anti-inflammatory eicosanoid derivatives have been described and tested using a number of models, including the ZIP model. Lipoxins, resolvins, protectins and maresins have all been validated using this model, highlighting its value as a platform for the testing of novel anti-inflammatory drugs [112, 286, 317-319]. For example, the ZIP model was used to demonstrate the pro-resolution effects of a stable analogue of lipoxin-A4 [320]. In this study, stable analogues of the endogenous lipid decreased neutrophil recruitment in mice that were injected intraperitoneally with 1mg of zymosan. These biological effects were confirmed using another model of IL-1β induced peritonitis [321].

Similarly, the 1 mg ZIP model was used to demonstrate the pro-resolution effects of a resolvin-E1 analogue [322] .

Another interesting mediator that has been investigated using the ZIP model is annexin-A1 and the annexin derived peptide Ac2-26. This protein is induced by treatment with corticosteroids and has been reported to have potent anti-inflammatory effects in a number of models including ZIP. In these studies, the glucocorticoid dexamethasone was demonstrated to exert potent anti-inflammatory effects in ZIP using 1 mg of zymosan A. However, these effects were abrogated when animals were pre-treated with sera against endogenous annexin-A1 or the N-terminus derived annexin peptide Ac2-26. Although it is well appreciated that glucocorticoids induce expression of annexin-A1, the mechanism by which they can regulate its expression remains unknown [323]. The receptors responsible for mediating the effects of annexin-A1 were also identified using ZIP [321, 324]. Perretti *et al*. using the ZIP model identified FPR2 as a receptor for annexin-A1 and annexin peptides. The inhibition of neutrophil migration into the cavity by annexin-A1 and annexin peptides was reduced in mice lacking the FPR2 receptor, although not completely abolished [321].

3.2 Rationale for the experiments presented in this chapter

The ZIP model has been characterised to varying degrees by different groups. However, as stated earlier, this is a complex and dynamic model whose kinetics can vary depending on a number of factors, including the dose of zymosan used and the strain and gender of mouse [325]. Previous work in our laboratory utilised a 10 µg dose of zymosan [225, 236]. I began my studies with this model. However I found this dose to be too low to yield consistent numbers of neutrophils and monocytes. Hence, I tested a range of doses

before I fixed the dose at 100 µg zymosan intraperitoneally per mouse. I have characterised the cell types recruited to the cavity at different time points until resolution of inflammation as well as the different mediators produced. In September 2014, Newson *et al.* reported an apparent second wave of cell recruitment at later stages during the resolution phase of the ZIP model, which I also investigated in this chapter. This report was however published after the majority of experiments for this chapter were completed [55].

3.3 Aims

The aims of this chapter were as follows:

- To compare different doses of zymosan in order to establish a robust platform for the interrogation of novel inflammatory mediators.
- To characterise the kinetics of inflammatory cell recruitment across a range of time points.
- To characterise the kinetics of local inflammatory mediators produced in the peritoneum following zymosan challenge.
- To validate this model using animals lacking the CCR2 receptor as well as using a broad spectrum CC chemokine blockade approach.

3.4 Results

3.4.1 Characterisation of the zymosan induced peritonitis model

I began my studies by characterising the naïve cavity of male C57Bl/6J mice. There is a large population of F4/80^{hi} resident macrophages (~55%). There is a population of B220, CD19^{+ve} B2 cells (~8%) as well as a population of CD19^{+ve}, B220^{-ve} B1 cells (~7%) (Figure 3.1). There was a very small population of resident dendritic cells (~2%) and a population of resident CD3^{+ve} T cells (~5%) including both CD4 and CD8 T cells (Figure 3.1).

When beginning the studies with zymosan, different doses were compared as well as different time points to optimise the model to monitor monocyte recruitment. Initially I compared 4 hours post zymosan challenge using 10 µg/mouse as used previously in our laboratory and others (Figure 2A, B) [57, 303]. The anti-inflammatory glucocorticoid dexamethasone (1 mg/kg) was used to validate our model. Dexamethasone administered intraperitoneally (i.p.) at this dose significantly decreased both monocyte and neutrophil recruitment when animals were challenged with either the 10 µg or 100 µg dose of zymosan (Figure. 3.2). However, I found the 10 µg dose resulted in more variable numbers of cells recruited to the cavity. For example a 10 µg dose at 4 hours resulted in 0.66 x10^6 ± 0.11 x 10^6 monocytes. In comparison, a dose of 100 µg at 16 hours resulted in 3.31 x 10^6 ± 0.14 x 10^6 monocytes. Total neutrophils at 4 hours post 10 µg were 1.56 x 10^6 ± 0.20 x 10^6 compared with 7.29 x 10^6 ± 0.74 x 10^6 at 16 hours post 100 µg. The number of recruited leukocytes with the 100 µg dose was very reproducible and exhibit less variance. Hence, the dose was fixed on 100 µg and a range of time points were examined to investigate the dynamics of leukocyte recruitment to the cavity (Figure 3.4A-C)

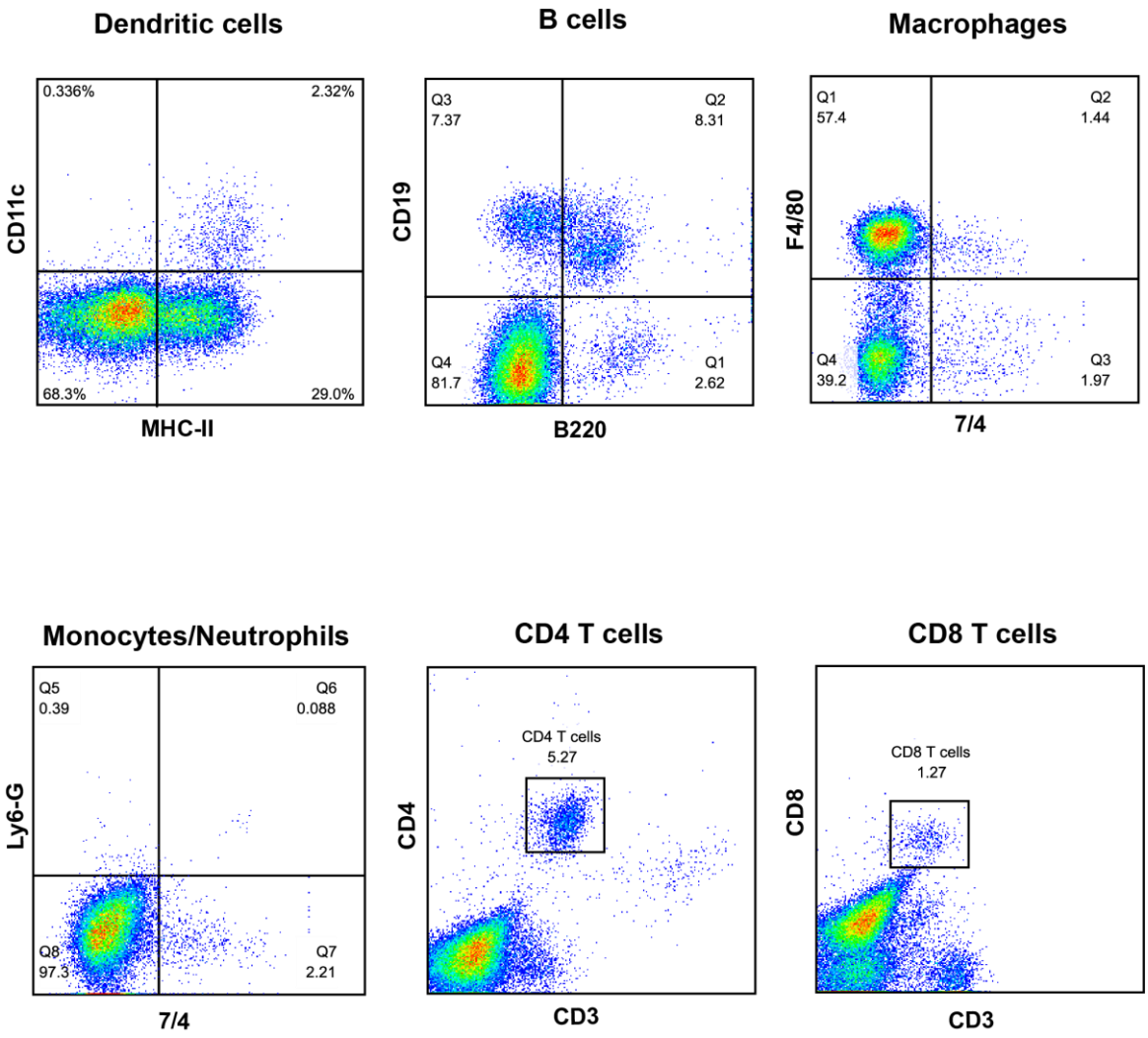


Figure 3.1 Representative flow cytometry images of a naïve unchallenged peritoneal cavity.

The peritoneal cavities of naïve male C57Bl/6J mice were lavaged with ice-cold PBS supplemented with 2mM EDTA. Myeloid dendritic cells were identified as $CD11c^{hi}$, $MHC\text{-}II^{hi}$. B cells were identified as $B220^{hi}$, $CD19^{hi}$, $CD3^{-ve}$. Monocytes were identified as $7/4^{hi}$ and $Ly6\text{-}G^{-ve}$**. N**eutrophils were identified as $7/4^{hi}$ and $Ly6\text{-}G^{hi}$. Macrophages were identified as $F4/80^{hi}$, $7/4^{-ve}$. Representative flow cytometry plots from an individual animal are shown.

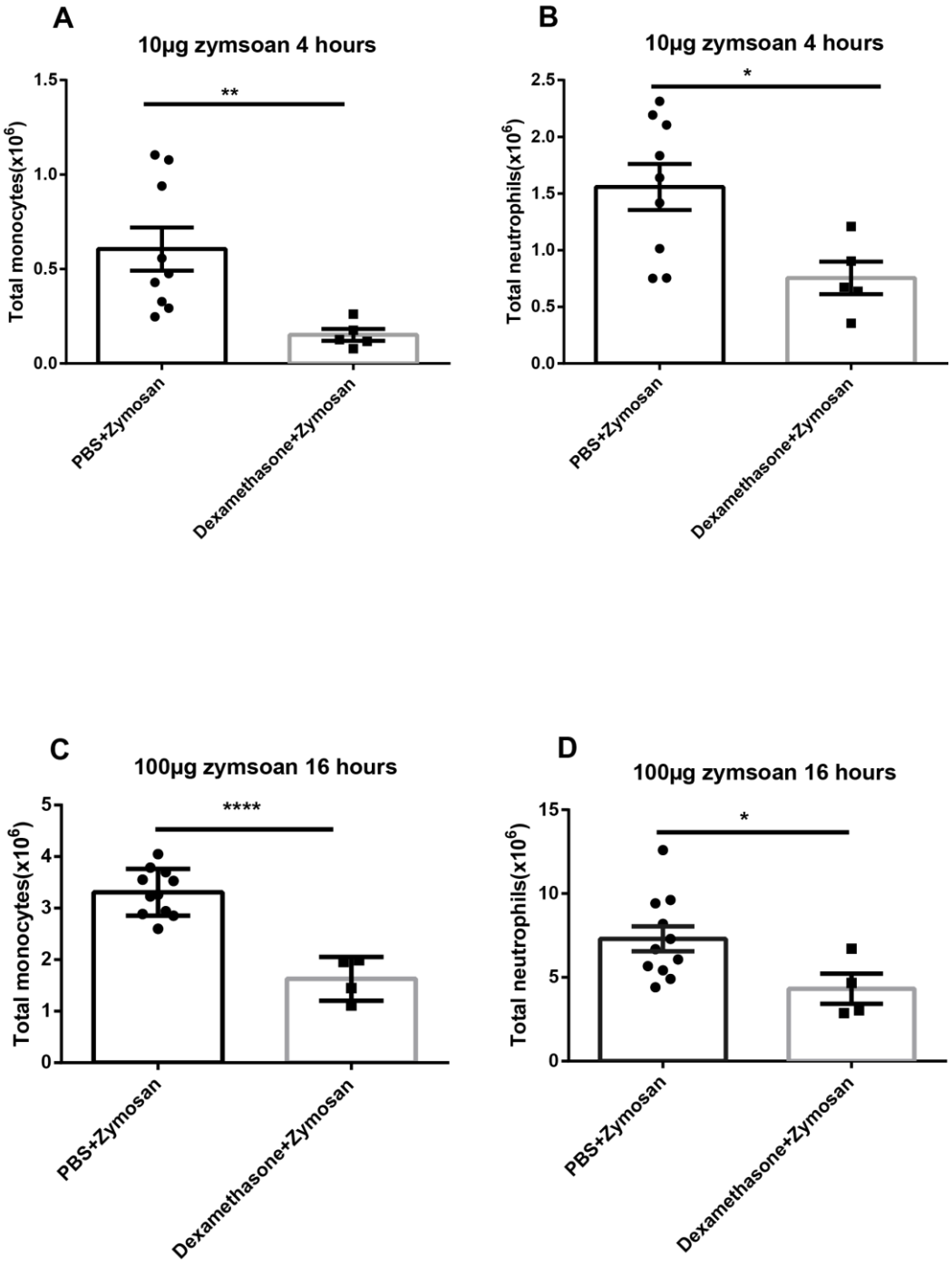


Figure 3.2 Different doses of zymosan/mouse produce varying degrees of inflammation as measured by inflammatory cell recruitment.

Male C57Bl/6J mice were given PBS or Dexamethasone (1mg/kg) via i.p. injection 45 minutes prior to a second injection of 10 µg (**A**. and **B**.) or 100 µg (**C.** and **D.**) zymosan. Mice were subsequently sacrificed 4 (**A.** and **B.**) or 16 hours (**C.** and **D.**) later and peritoneal exudate cells were collected by cold peritoneal lavage using PBS supplemented with 2mM EDTA. Total cells were counted using a haemocytometer and different cell populations were quantified using flow cytometry. Monocytes were identified as $7/4^{hi}$ and Ly6-G^{lo}. Neutrophils were identified as $7/4^{hi}$ and Ly6-G^{hi}. Error bars represent S.E.M of 2 separate experiments, 4-12 animals per group. Significance was assessed with a student's unpaired t-test. . * $P \leq 0.05$. ** $P \leq 0.01$. *** $P \leq 0.001$

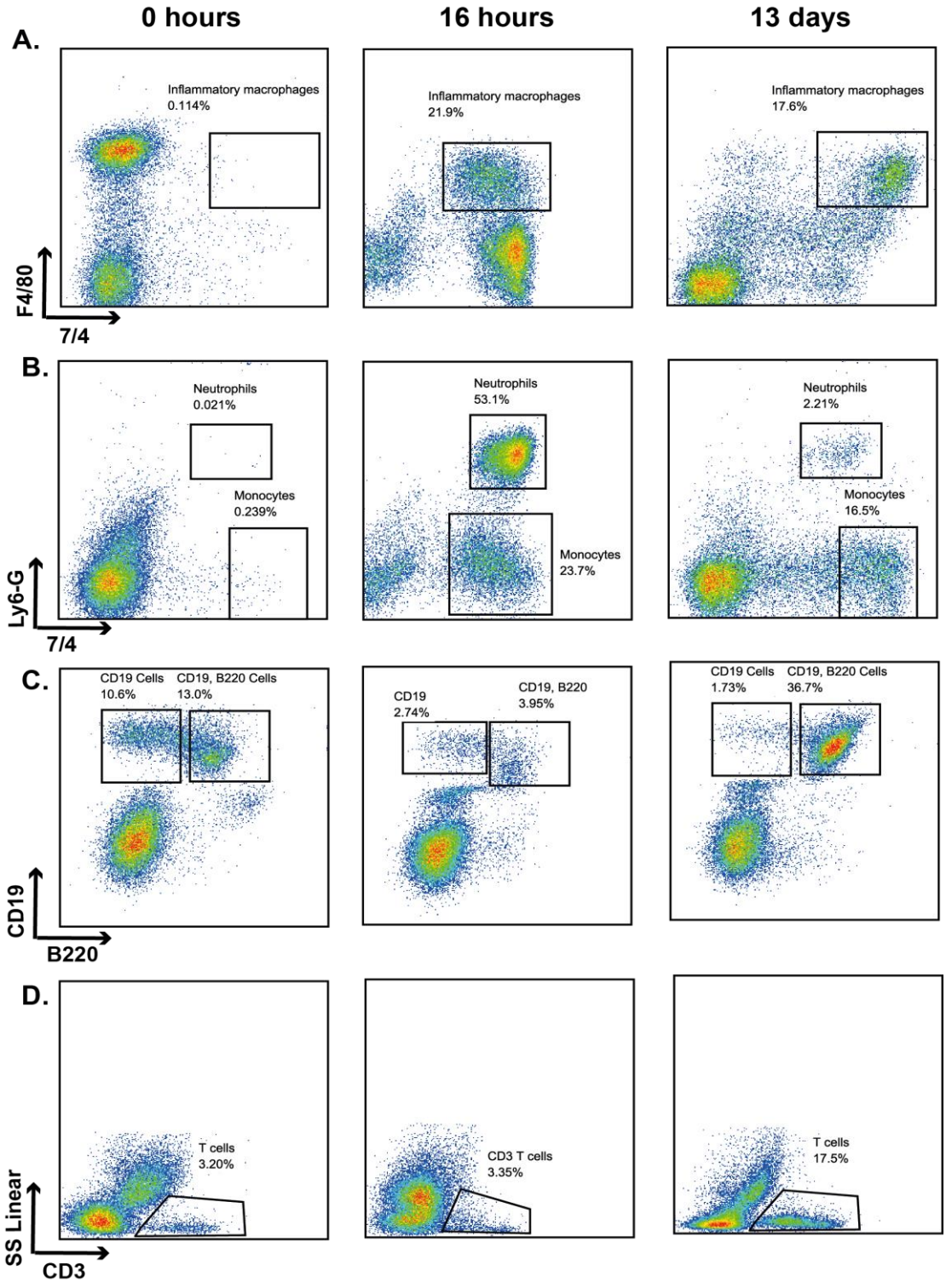


Figure 3.3 Kinetics of zymosan induced peritonitis.

C57Bl/6J male mice were injected i.p. with 100 µg zymosan. Animals were sacrificed at indicated time points and peritoneal cavites were lavaged with ice cold PBS supplemented with 2mM EDTA. Flow cytometry plots of indicated time points. **A.** Inflammatory macrophages were identified as F4/80hi, 7/4hi. **B.**Monocytes were identified as 7/4hi, Ly6-Glo. Neutrophils were identified as $7/4^{hi}$, Ly6-G^{hi}. **C**. B1 cells were identified as $CD19^{hi}$, $B220^{lo}$. B2 cells were identified as $CD19^{hi}$, $B220^{hi}$. **D.** T cells were identified as $CD3^{hi}$.Total cells recruited to cavity.

After zymosan challenge, peak neutrophils were observed at 4 hours while monocytes/macrophages peaked at 8 hours and remained high at 16 hours post zymosan challenge (Figure 3.4B). The 100 μg dose of zymosan was very robust in terms of eliciting reproducible levels of monocyte recruitment and it was self-resolving by 96 hours (as judged by neutrophil numbers). However, when the time course was extended out to 9 and 13 days post zymosan challenge a second wave of cell recruitment was observed in line with what Newson *et al.* reported in November 2014 after the bulk of experiments in this chapter had been completed [55]. Total cell numbers in the cavity increased (from $7.8 \times 10^6 \pm 0.59 \times 10^6$ at day 4 to $13 \times 10^6 \pm 1.03 \times 10^6$ at day 13), as did monocyte/inflammatory macrophage numbers ($1.14 \times 10^6 \pm 0.14$ at day 4 compared to $2.30 \times 10^6 \pm 0.44 \times 10^6$ at day 13) (Figure 3.4A). Neutrophil numbers remained low at later time points ($0.11 \times 10^6 \pm 0.17 \times 10^6$ at day 4 compared to $0.33 \times 10^6 \pm 0.03 \times 10^6$ at day 13) (Figure 3.4B). There was a large increase in T cell numbers by day 13 compared to naïve cavity ($0.18 \times 10^6 \pm 0.08 \times 10^6$ compared to $1.96 \times 10^6 \pm 0.22 \times 10^6$) (Figure 3.4C). Interestingly, the population of B cells that repopulated the cavity were almost exclusively $CD19^{+ve}$ and $B220^{+ve}$ (B2 cells) while there were very few $CD19^{+ve}$, $B220^{-ve}$ cells (B1 cells) (Figure 3.3C). The number of B2 cells increased from $0.28 \times 10^6 \pm 0.16 \times 10^6$ in the naïve cavity to $4.23 \times 10^6 \pm 0.57 \times 10^6$ at day 13 post zymosan (Figure 3.4C).

In order to gain a better understanding of the mediators produced in the peritoneal cavity, I used an R&D proteome profiler kit to characterise endogenous mediator expression at 4 hours post zymosan challenge. I chose this time point based on previous experiments in which I found that CCL2 levels peak at 4 hours but are ~10% of peak levels by 16 hours (Figure. 3.6.A). Animals treated with either 100 μg zymosan or PBS were compared. Peritoneal exudate was pooled from 3 separate animals for each treatment. A number of mediators were induced including CCL2, IL-6, CXCL10, CCL4,

CCL9, CD54, GM-CSF and IL-1β (Figure 3.5A-C). There was also a large number of mediators that were not detectable in this assay (listed in Figure 3.5D) including IL-4, IL-10, CCL5, CCL3, CXCL12 and IL-12p70. This technique is similar to a western blot; hence it is not very quantifiable. Densitometry can be used to generate a rough measurement, however ELISA or Luminex are more accurate. The kinetics of a number of different mediators in the inflammatory exudate using the proteome profiler kits were subsequently investigated by ELISA and Luminex at a range of time points. The majority of mediators including CCL2, CXCL1, CCL4, CXCL10 and IL-6 all reached peak levels by 4 hours post zymosan and were no longer detectable by 24 hours (Figure 3.6A-E).

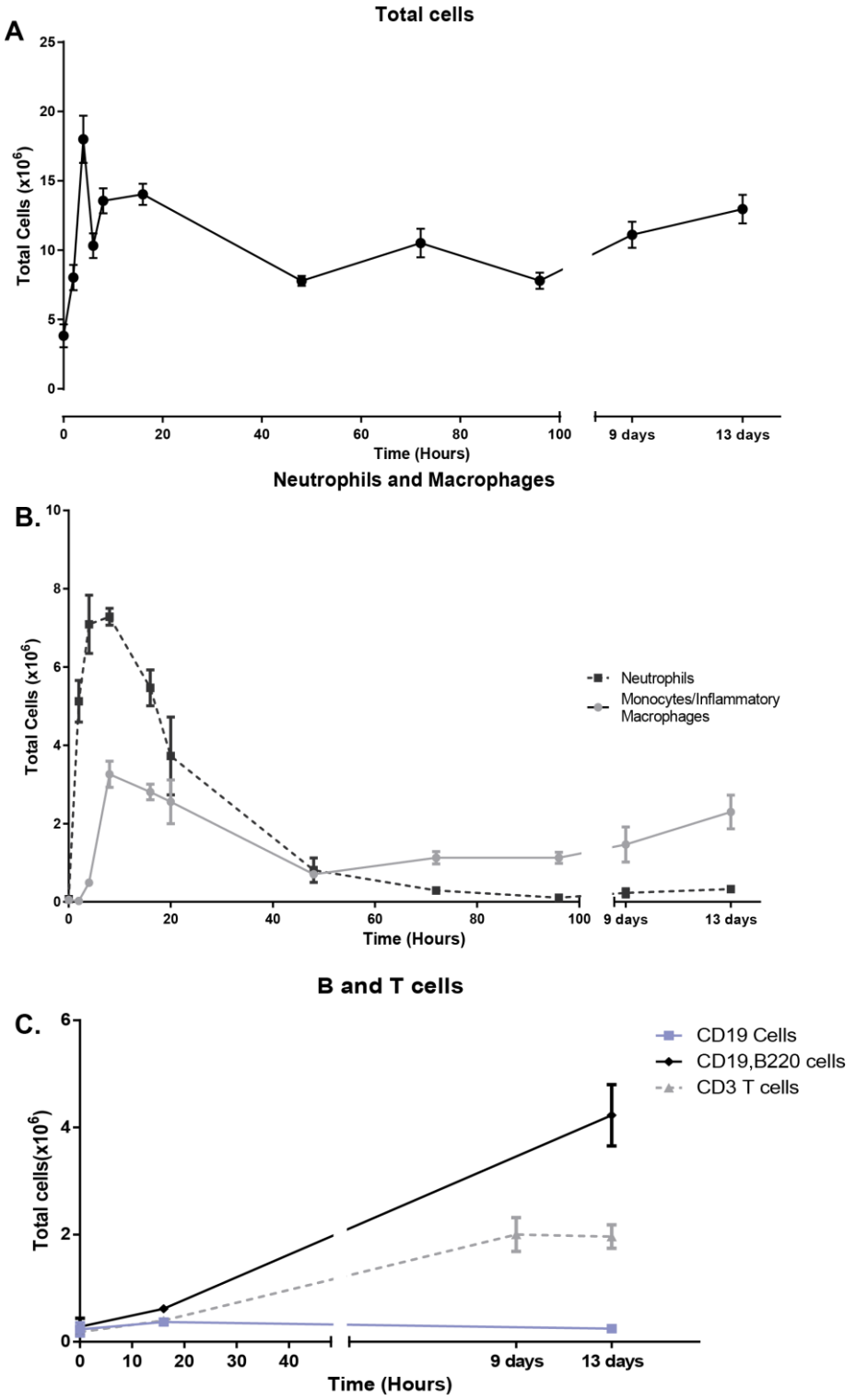
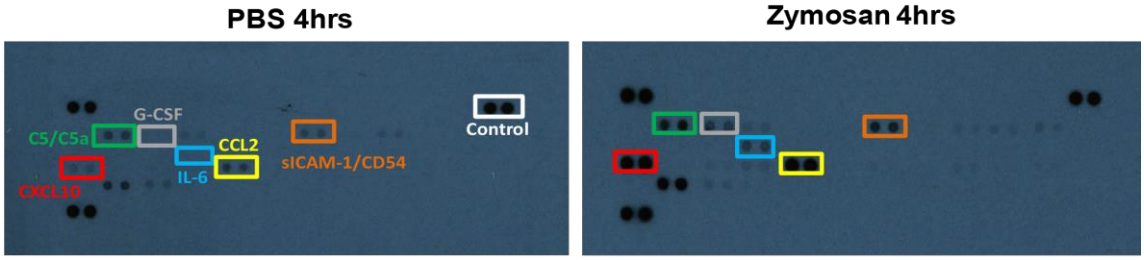


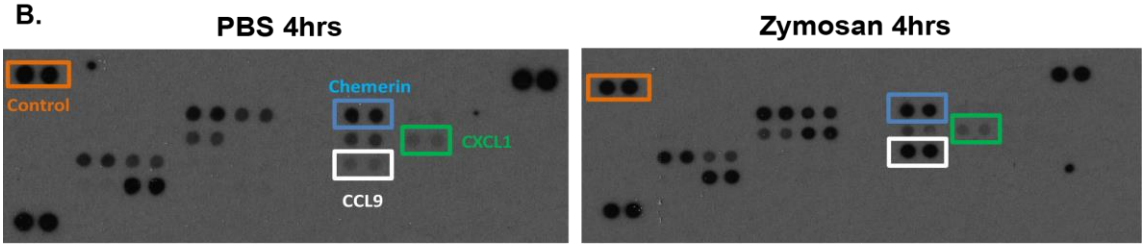
Figure 3.4 100µg of zymosan induces a self-resolving inflammatory response.

C57Bl/6J male mice were injected i.p. with 100 µg zymosan. Animals were sacrificed at indicated time points and peritoneal cavities were lavaged with ice cold PBS supplemented with 2mM EDTA. **A.**Total cell numbers at indicated time points. **B.** Total neutrophils (black broken line) and inflammatory monocytes/macrophages (grey line) at indicated time points. **C.** Total $CD19^{hi}B220^{lo}$ cells (B1 cells) (blue line), Total $CD19^{hi}$, $B220^{hi}$ (B2 cells) (black line). Total CD3 T cells (grey broken line). Error bars represent S.E.M. n=4-15 animals/time point.

A.



B.



C.

<2 Fold increase	>2 Fold increase	>10 fold increase	>100 fold increase
CXCL13/BLC	GM-CSF	IFN-γ	G-CSF
C5/C5a	CCL11/Eotaxin	IL-7	IL-1α
IL-5	sICAM-1/CD54	M-CSF	IL-1β
CCL17/TARC	IL-3	CCL3/MIP-1a	IL-1ra
TIMP-1	CXCL10/IP-10	TREM-1	IL-2
TNF-α	CXCL1/KC		IL-6
CCL6	CCL2/JE		CXCL9/MIG
Chemerin	CXCL1		CCL4/MIP-β
IL-16			CCL9
CCL2			
MCP-2/CCL8			
MCP-5/CCL12			

D.

Mediators not detectable by proteome profiler;

I-309/CCL1, Eotaxin/CCL11, IL-2, IL-3, IL-4, IL-5, IL-7, IL-10, IL-13, IL-12p70, IL-16, IL-17, IL-23, IL-27, MCP-5/CXCL12,MIP-1a/CCL3, RANTES/CCL5, SDF-1/CXCL12, CCL21, CXCL13, CCL28, CCL27, CXCL16, CX3CL1,CXCL5,CCL22, CXCL9, CXCL2, CXCL11.

Figure 3.5 Zymosan challenge induces a range of inflammatory cytokines and chemokines.

8 week old male C57Bl/6J mice were challenged with 100 µg zymosan i.p. Four hours later animals were sacrificed and the peritoneal cavity was lavaged with ice-cold PBS supplemented with 2mM EDTA. Cell free supernatant from 3 separate animals were pooled for each treatment and screened for inflammatory mediators using the proteome profiler kit. **A.** Raw blots of the cytokine assay. **B.** Raw blots of the chemokine array. **C.** Results of densitometric analysis. Results are fold increases of zymosan treated samples compared to PBS treated samples. **D.** List of mediators not detectable by the kit.

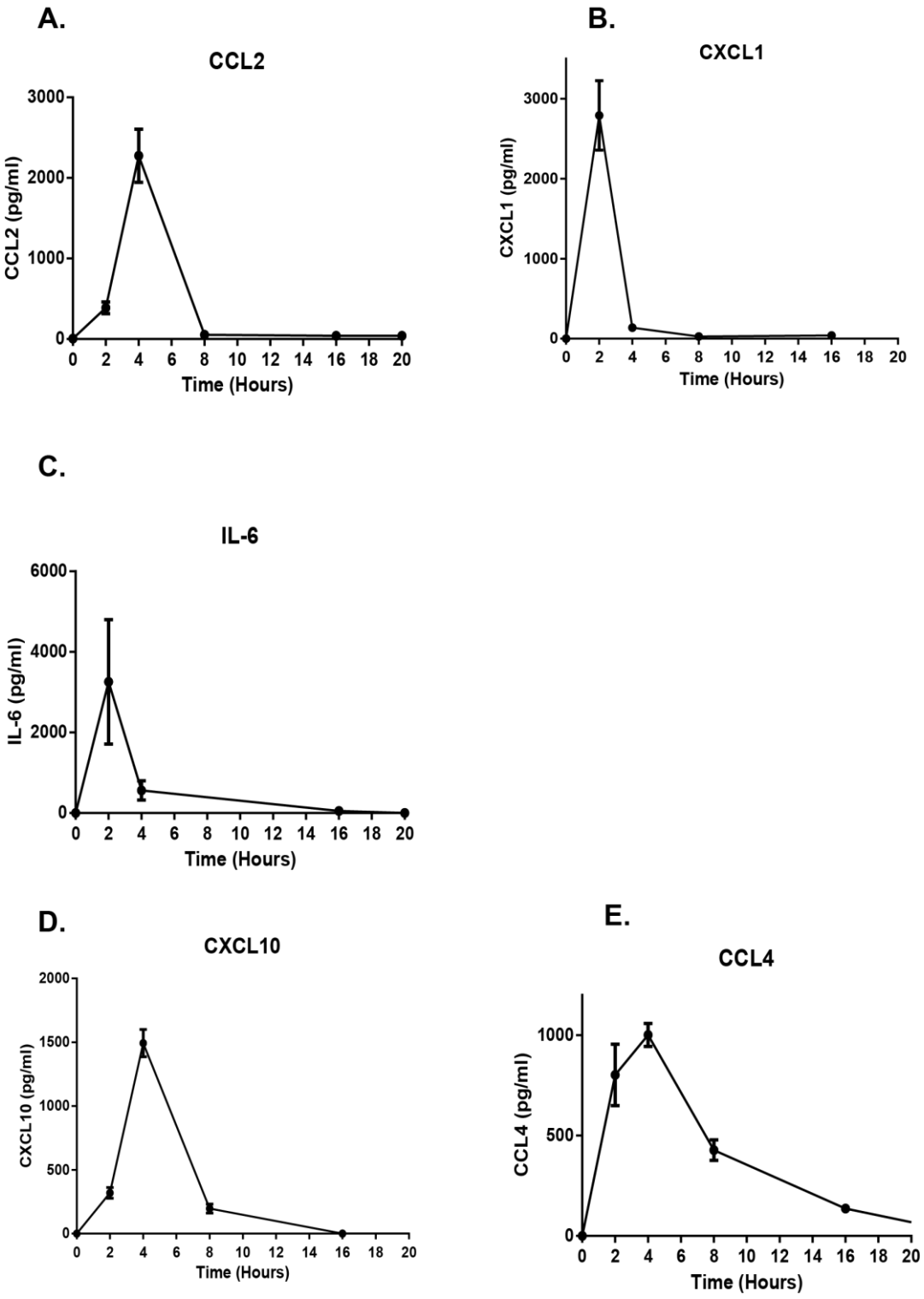


Figure 3.6 Kinetics of inflammatory mediator production during zymosan induced peritonitis.

8-10 week old male C57Bl/6J mice were injected i.p. with 100 μg zymosan and sacrificed at indicated time points. Peritoneal cavities were lavaged with ice cold PBS supplemented with 2mM EDTA and lavage fluid was analysed for mediator levels by ELISA (**A**.-**C**.) or Luminex (**D.** and **E.**). Error bars represent mean ± S.E.M. of 2-7 animals per time point.

3.4.2 CCR2 plays a non-redundant role in monocyte recruitment during ZIP.

CCR2 has been reported previously to play an important role in monocyte mobilisation from the bone marrow to sites of inflammation [66, 149, 308, 309]. One of these studies used a model of peritoneal bacterial infection while another used zymosan. As a validation of the ZIP model with the 100 μg dose, monocyte and neutrophil populations were investigated in bone marrow, blood and peritoneum of wild type and CCR2 KO animals in ZIP (gating strategy for flow cytometry shown in Figure. 3.7.) As expected, animals lacking CCR2 displayed almost complete absence of monocyte recruitment to the peritoneum at 16 hours post zymosan ($2.83 \times 10^6 \pm 0.23 \times 10^6$ monocytes in WT animals compared to $0.33 \times 10^6 \pm 0.034 \times 10^6$ in CCR2 KO animals) (Figure 3.8B). There was a significant decrease in total cell recruitment as well ($11 \times 10^6 \pm 0.49 \times 10^6$ in WT compared to $7.77 \times 10^6 \pm 1.2 \times 10^6$ in CCR2 KO animals) (Figure 3.8A). Monocyte and neutrophil numbers in bone marrow and blood were quantified from these animals during inflammatory responses. No significant differences in monocyte or neutrophil numbers were observed in the bone marrow between WT and CCR2 KO animals during zymosan challenge or under resting conditions (Figure 3.8 G-H). Naïve animals lacking CCR2 displayed lower numbers of circulating Ly6-C^{hi} and Ly6-C^{lo} monocytes but higher numbers of neutrophils in the blood compared to wild type animals. However, after zymosan challenge no significant differences were observed between the groups (Figure 3.8D-F). It should be noted that due to low animal numbers in the naïve WT and CCR2 KO groups, it is difficult to draw conclusions from the statistical tests and further animals will be required to add statistical power to these groups.

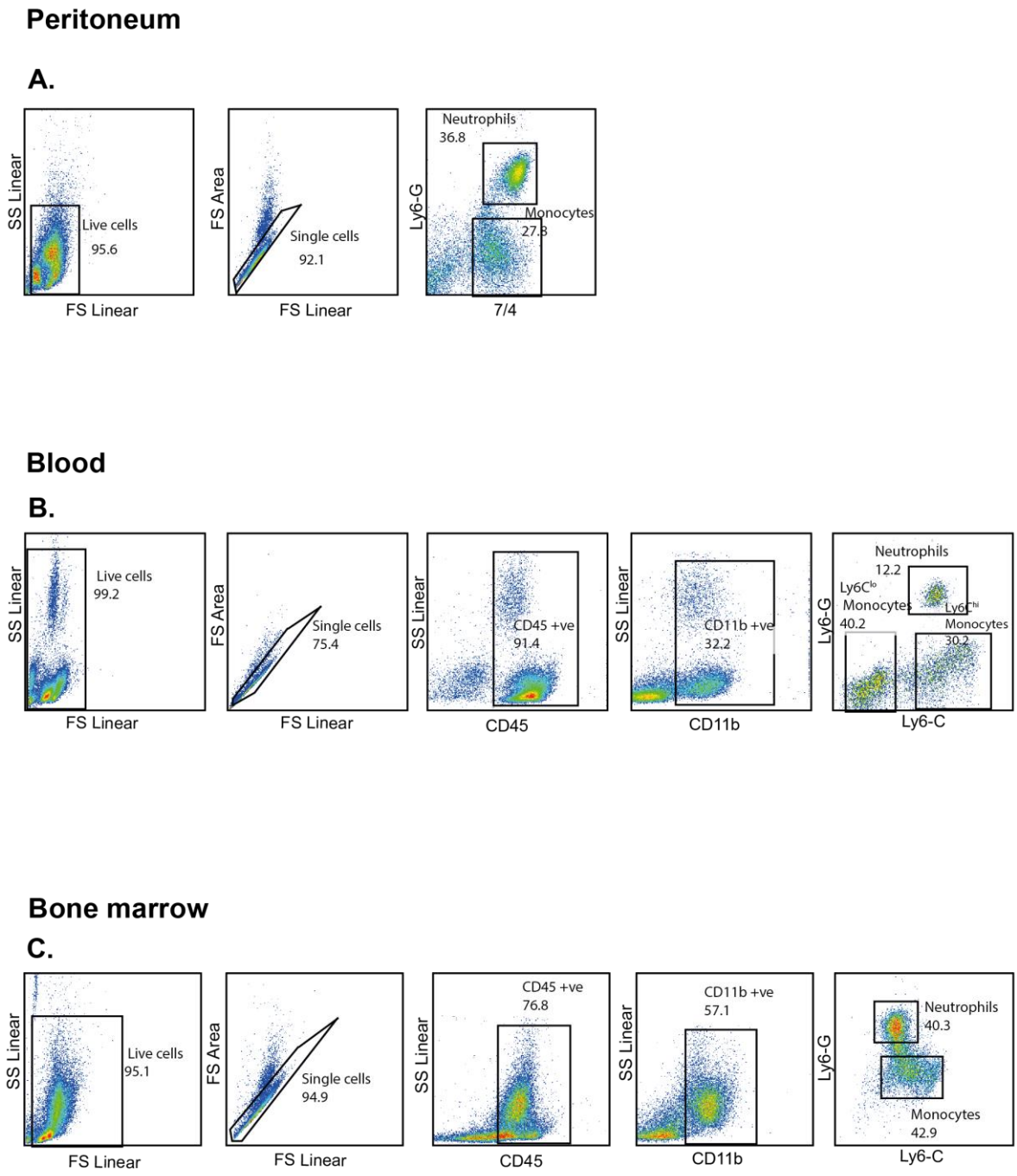


Figure 3.7 Gating strategy for flow cytometric analysis of peritoneum, blood and bone marrow.

8-10 week old male C57Bl/6J mice were injected i.p. with 100 µg zymosan. Animals were sacrificed at 16 hours post zymosan and tissues were isolated. **A.** Peritoneal cavities were lavaged with ice cold PBS supplemented with 2mM EDTA. Cells were counted using counting beads and stained for indicated cell types. **B.** Venous blood was collected into EDTA coated vacutainers for quantification of blood monocytes and neutrophils. **C.** Femurs and tibia from the same animals were flushed with PBS and bone marrow cells were stained to distinguish monocytes and neutrophils.

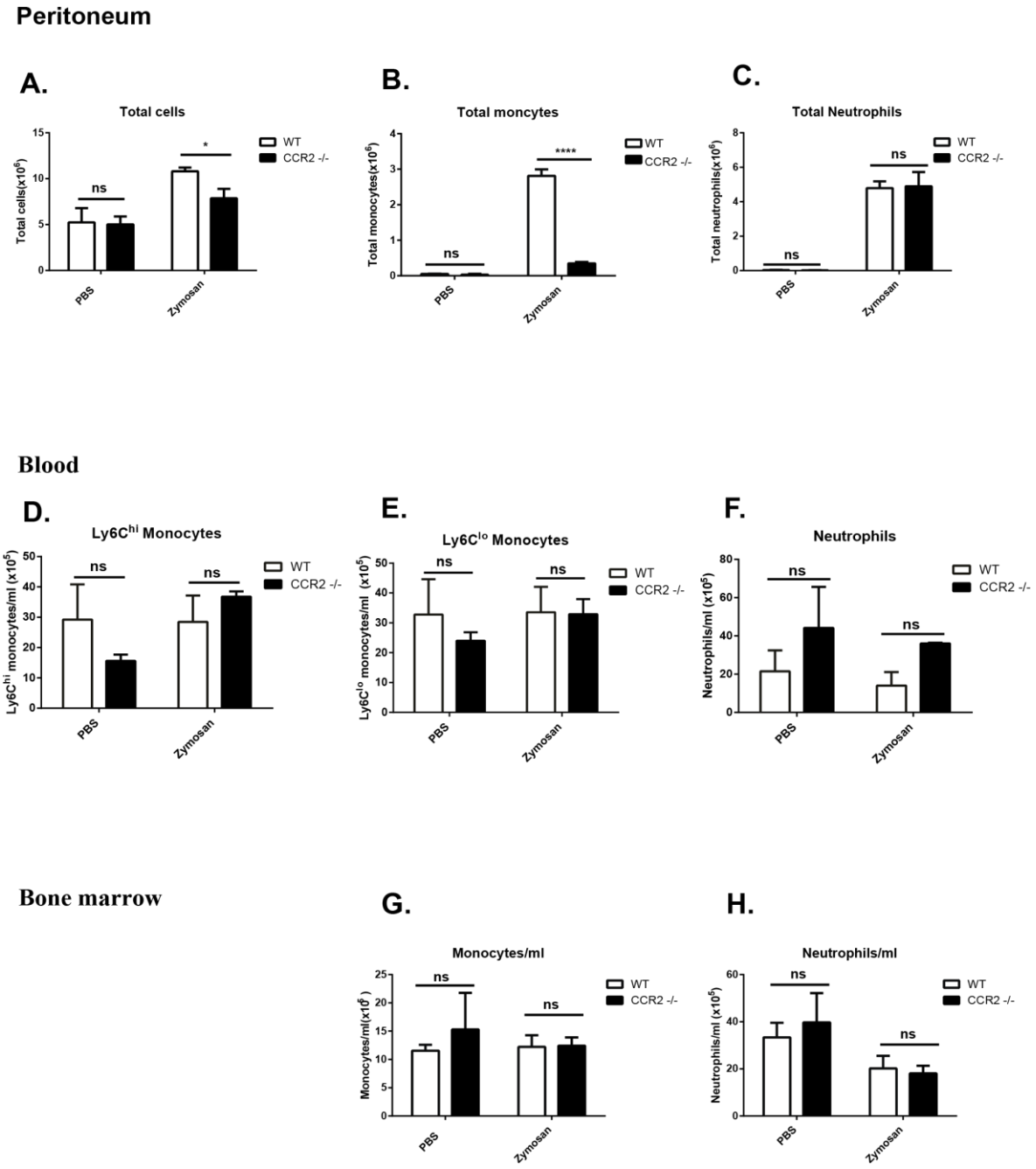


Figure 3.8 CCR2 plays a non-redundant role in monocyte recruitment to the peritoneum during zymosan induced peritonitis.

8-10 week old male C57Bl/6J wild type (WT) mice or mice lacking CCR2 backcrossed onto a C57Bl/6J background for 10 generations were injected i.p. with 100 µg zymosan. 16 hours later animals were sacrificed. Peritoneal cavities were lavaged with PBS supplemented with 2mM ice cold EDTA and total recruited cells were quantified (**A.-C.**). Venous blood was collected into EDTA coated vacutainers for quantification of blood monocytes and neutrophils (**D.-F.**). Bone marrow was isolated from tibia and femur from the same animals and stained for monocytes and neutrophils (**G.-H.**). Error bars represent S.E.M of 2-9 animals per group. Significance was assessed with a 2-way ANOVA followed by Sidaks post-hoc test. * $P \leq 0.05$. ** $P \leq 0.01$, *** $P \leq 0.001$, **** $P \leq 0.0001$.

3.4.3 Use of 100µg ZIP to assess the efficacy of the CC chemokine binding protein 35K

From the literature and my experiments with CCR2 KO animals, it is clear that CC chemokines play an important role in the recruitment of immune cells to sites of inflammation. As a proof of concept that modulation of CC chemokines can alter monocyte recruitment in this model, I took advantage of the 35K protein derived from vaccinia virus. This protein binds a broad range of CC chemokines with high affinity and is one of the mechanisms by which poxviruses have evolved to evade the immune system [326]. Previous studies have demonstrated the ability of the 35K protein to decrease inflammation in a number of disease models including atherosclerosis, fibrosis and arthritis [326, 327]. Gemma White from our laboratory, in collaboration with the Channon laboratory, designed a range of 35K mutants, one of which (named R89A) displayed higher chemokine binding affinity than the wild type protein [160]. Expression of the R89A mutant protein was induced systemically in C57Bl/6J male mice via hydrodynamic tail vein delivery of the plasmid (performed by Eileen McNeill). Protein expression in plasma was confirmed using ELISA. This method is a well-validated tool for *in vivo* delivery and transgene expression in mice and rats [328, 329]. Animals injected with a GFP vector plasmid instead of the mutant were used as a control. We observed that when injected with 100 µg zymosan, animals expressing R89A had significantly decreased total cell ($18 \times 10^6 \pm 1.4 \times 10^6$ and $12.5 \times 10^6 \pm 0.6 \times 10^6$ respectively), total monocyte ($4.68 \times 10^6 \pm 0.53 \times 10^6$ and $3.16 \times 10^6 \pm 0.25 \times 10^6$ respectively) and total neutrophil ($8.93 \times 10^6 \pm 0.75 \times 10^6$ and $5.96 \times 10^6 \pm 0.53 \times 10^6$ respectively) recruitment to the peritoneum 16 hours post zymosan challenge compared to control animals (Figure 3.9A-C). These results are in line with previously published

results from our laboratory using purified 35K-Fc protein [160]. This blunting of inflammatory cell recruitment by broad spectrum CC chemokine blockade highlights the potential for therapeutic intervention in the early stages of an inflammatory response when inflammatory mediator production peaks (Figure. 3. 5).

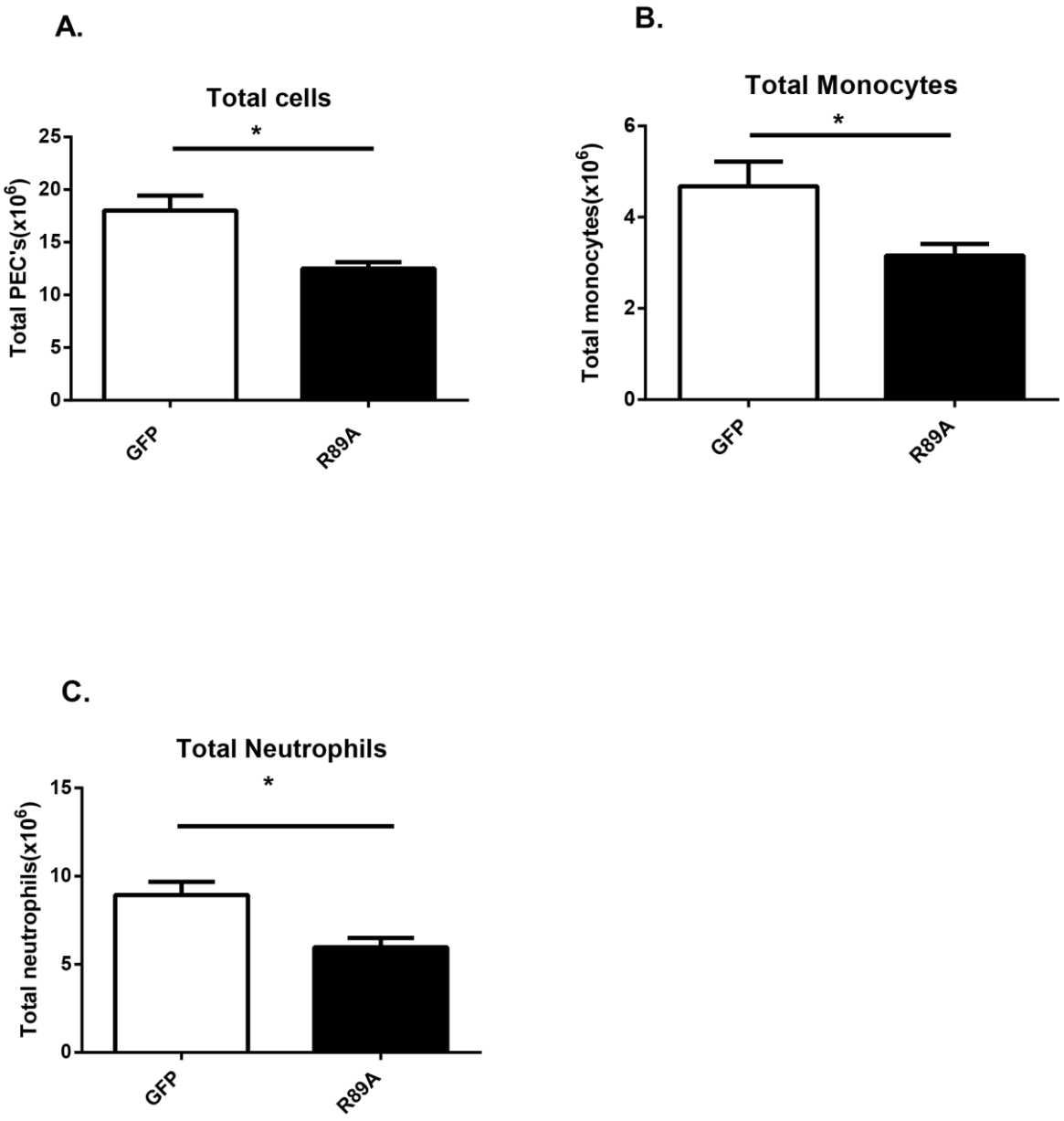


Figure 3.9 Hydrodynamic delivery of the broad-spectrum CC chemokine binding 35K mutant R89A significantly reduces inflammatory cell recruitment in zymosan induced peritonitis.

8-10 week old male C57Bl/6J mice were injected with indicated plasmids via a 2.5 ml injection through the tail vein. Animals were allowed to recover for 5 days before undergoing any other procedure. Animals were subsequently injected with 100 µg of zymosan i.p. and sacrificed 16 hours later. Total cells **A.** total monocytes **B.** and total neutrophils **C.** were quantified as stated previously. Error bars represent S.E.M of n=4 animals/group. Students unpaired t-test. * $P \leq 0.05$.

3.5 Discussion

3.5.1 Characterisation of the 100µg zymosan induced peritonitis model.

In the beginning of this chapter, I set out to characterise the zymosan induced peritonitis model of sterile inflammation. I began by looking at what cell types were present in a naïve peritoneal cavity. I found that the predominant cell types were resident F4/80^{hi} macrophages and CD19^{+ve} B cells. Within the CD19^{+ve} cell population, ~50% were B220^{+ve} (Figure 3.1). These cells are most likely B1 cells. B1 cells are almost exclusively found in the peritoneal and plural cavities of mice and are characterised by CD19 and B220 staining. These cells differ from conventional B cells in that they secrete large amounts of IgM and are much less specific in terms of antigen recognition [330]. Furthermore, there are two subtypes of B1 cells (B1a and B1b), which are differentiated on the basis of CD5 staining. However I did not investigate these populations further as this was beyond the scope of my studies.

The resident macrophage population I observed in the naïve cavity seems to perform a sentinel role in that after zymosan challenge this population disappears (Figure. 3.3A). The majority of macrophages that repopulate the cavity retain 7/4 expression, which the resident population does not. This is also in line with what Newson *et al* have reported [55]. Ly6-C is used instead of 7/4 as a myeloid marker in their study. However the expression patterns of these two markers are identical [331]. Given the published literature, it seems likely that these cells migrate to the draining lymph nodes and spleen soon after the onset of inflammation and are replaced by both the differentiation of infiltrating Ly6-C^{hi} monocytes and the proliferation of the resident population [55, 57, 58]. Newson *et al.* performed studies using a cell tracker dye in which they labelled cells

in the naïve cavity with the dye to monitor whether labelled or unlabelled cells repopulated the cavity. They found that by day 3 post zymosan challenge ~30% of F4/80^{hi} macrophages were labelled with the dye while ~70% were not, consistent with a large proportion of these macrophages being derived from blood monocytes while the rest are from local proliferation, as has been previously been reported by Davies *et al.* [55, 57]. Newson *et al.* confirmed that the unlabelled macrophages were blood monocyte derived by using animals lacking the CCR2 receptor in these experiments. These animals did not display an unlabelled F4/80^{hi} macrophage population at any point investigated. Our laboratory recently described a novel CD68-GFP reporter mouse which will allow us to repeat and extend these experiments with genetically tagged F4/80^{hi} macrophages which would overcome potential problems with cell tracker dye leakage *in vivo* [332, 333].

The ZIP model has been widely used in the past by our group and others to study inflammation. However, I was interested in investigating the kinetics of inflammatory cell recruitment to different doses of zymosan as well as undertaking a detailed analysis of which mediators are produced in the peritoneal cavity. This was beneficial in terms of having a broader idea of what to expect after the onset of inflammation when I began therapeutic intervention studies chapter 4. I began my studies with the lower 10 μg dose of zymosan, as this was used in previous studies in our laboratory. However, this dose was very variable in terms of cell recruitment due to the low overall numbers of recruited cells [225, 303]. Higher doses of zymosan were therefore investigated. In Figure 3.2 for example, the coefficient of variation of total cell recruitment with the 10 μg dose of zymosan was 36.48% whereas the coefficient of variation of total cell recruitment with the 100 μg dose was 21.07%. There was much less variance observed with the higher dose of zymosan and the overall numbers recruited were far more reproducible. Additionally, I was interested in screening for novel anti-inflammatory compounds and

given that the lower dose of zymosan is such a mild inflammatory insult, the higher dose was chosen as a more robust inflammatory stimulus.

The glucocorticoids, including dexamethasone, have been widely used in research and in clinics for inflammatory diseases. The exact mechanisms of action of dexamethasone are still not fully understood. There is a host of transcriptional effects such as repression of inflammatory gene expression by inhibition of NF_KB and AP-1 nuclear translocation. This inhibition results in a decrease in a wide range of inflammatory cytokines, chemokines, adhesion molecules and enzymes involved in prostaglandin synthesis amongst others [334, 335]. In addition, glucocorticoid treatment upregulates expression of anti-inflammatory genes such as IL-10 and IL-1-receptor antagonist [336]. More recently, it has been discovered that dexamethasone induces the production of the anti-inflammatory protein annexin-A1 [337-339]. Annexin-A1 itself exerts anti-inflammatory effects directly on various immune cells (neutrophils, monocytes, macrophages) as well as on endothelial cells [323, 340]. Given that glucocorticoids have been used extensively for the treatment of inflammatory diseases and have been reported to decrease recruitment of cell types we see in the inflamed peritoneum, dexamethasone was chosen as an anti-inflammatory control in many of the initial experiments. As expected, dexamethasone at 1mg/kg given either as a pre-treatment or an intervention significantly decreased both total cell recruitment and total monocyte recruitment (Figure 3.2). There was no significant effect on neutrophil recruitment to the cavity. This may be due to the 16-hour time point chosen for these studies given that at 16 hours neutrophil numbers are quite low at this dose of zymosan (possibly from neutrophil death).

During characterisation of cytokines in ZIP, both R&D proteome profiler kits and Luminex assays were used to investigate which mediators are produced in the cavity

during inflammation. The proteome profiler kit is similar to a western blot but able to measure up to 40 analytes at once. However like a western blot, this kit is not very quantitative. Luminex allows quantification of mediators but fewer analytes in each kit. Using these techniques and ELISA, a range of mediators which were expected were identified including CCL2, CXCL1, IL-6 amongst others, but also some less obvious ones such as CXCL10, TIMP-1, CCL4, CCL9 and GM-CSF (Figure 3.5). A number of these were monitored over the entire time course. Most of the inflammatory mediators observed reached peak levels by 4 hours post zymosan challenge except for CXCL1which peaked at 2 hours (Figure 3.6B). These kinetics were not surprising given that neutrophil numbers recruited to the cavity peak at 4 hours and that CXCL1 is a key driver of neutrophil recruitment. Similarly, CCL2, CCL4 and CXCL10 levels peaked at 4 hours while monocyte numbers peaked at 8 hours (Figure 3.6A, E and D respectively). The choice of mediators monitored over the time course and in the intervention studies was based on results from the proteome profiler array as well as the literature. Both CCL2 and CCL4 are known to play important roles in monocyte recruitment. CCL2 binds and signals predominantly via the CCR2 receptor while CCL4 signals via the CCR5 receptor [157]. CXCL1 is a potent neutrophil chemoattractant and very quickly produced in the cavity in our model (Figure 3.6B) [297, 311]. IL-1β is another potent neutrophil chemoattractant [312]. This was detectable in the peritoneum after 100 μg zymosan using the proteome profiler kit (Figure 3.5C) but not by ELISA or Luminex.

The kinetics of cell recruitment in our model are in line with what others have seen at similar doses of zymosan [55, 57, 341]. In the paper mentioned earlier, Newson *et al*. using the ZIP model extended the time course of zymosan challenge up to 17 days with both 100 μg and 10 mg of zymosan per mouse. Interestingly, they reported a second wave of cell recruitment beginning 9 days following zymosan challenge and peaking at

day 13 when mice were challenged with the lower 100 μg dose. During this second wave one population of cells that seemed to persist throughout resolution were postulated to be myeloid derived suppressor cells based on their ability to suppress T cell proliferation and surface markers of activation. Although I did not specifically look for these cells in my experiments I did observe similar increases in total cell recruitment at days 9 and 13. In the same study it was reported that during resolution there are two populations of macrophages that repopulate the cavity. The resident population exhibit pro-resolving properties such as efficient phagocytosis of apoptotic neutrophils, expression of pro-resolving genes (TGF-β, IL-10 and Alox15) and the ability to supress T cell proliferation *ex vivo* in an iNOS dependant manner. The other population is derived from $Ly6C^{hi}$ monocytes. This population displays less pro-resolving properties and does not seem to play a role in neutrophil clearance. Interestingly, when co-cultured with CD4 T cells, both the resident and monocyte derived populations of macrophages skewed CD4 T cells towards FoxP3 positive Treg phenotypes [55].

Using differential labelling, Newson *et al.* demonstrated that both the monocyte derived macrophages and resident macrophages migrated to the mesenteric lymph nodes and spleen during resolution and play roles in the onset and resolution of inflammation respectively [55]. It would be interesting to extend these studies to interrogate differences in these cell populations and their trafficking to secondary lymphoid organs when well validated anti-inflammatory compounds such as corticosteroids are used in this system. Adoptive transfer studies using cells from donor CD68-GFP reporter mice into wild type mice would be an elegant way to address this [332].

3.5.2 Validation of the 100 µg ZIP model with CCR2 KO mice.

It has been well documented that the CCR2 receptor plays a key role in monocyte mobilisation from the bone marrow and recruitment into inflamed tissue [66, 149, 310]. Given the importance of this receptor in monocyte recruitment, I took advantage of mice lacking CCR2 as a validation of our model for the investigation of novel phenotypes involved in monocyte recruitment. In agreement with previously published results, when challenged with zymosan, animals lacking CCR2 displayed a near complete ablation of monocyte recruitment into the peritoneum compared to wild type controls (Figure 3.8B). However, there were no significant differences in monocyte numbers in either the bone marrow or the blood between the groups after zymosan challenge (Figure 3.8D-H). It is possible that this was due to the time point analysed, since this was 16 hours following zymosan challenge, the majority of monocytes were likely already mobilised and recruited to the peritoneum. There was a trend towards increased monocytes in the bone marrow of naïve CCR2 KO animals as well as decreased circulating monocytes in the blood. Although we might have expected to see a difference in blood and bone marrow counts in naïve CCR2 KO animals, our results are in line with what Boring *et al.* reported. In naïve animals, they found no differences in circulating peripheral blood cells (including monocytes) between KO and wild type animals [308].

Although not investigated in these studies, from the literature one might expect to see differences in cell numbers in spleen and lymph nodes between wild type and CCR2 KO animals as well as differences in other cell types recruited to the peritoneum at later time points. These effects were postulated to be a result of depletion of both monocyte derived dendritic cells and monocyte derived macrophages at later stages of inflammation (days 9 and 13) [55]. Although Boring *et al* did not report any differences in neutrophil or lymphocyte recruitment to the peritoneum during injection of thioglycollate, this may

reflect the different time point investigated as well as the different inflammagen [308]. Boring *et al*. investigated the acute phase of the inflammatory response while Newson *et al.* only observed these differences during the second wave of cell recruitment during resolution. However, Boring *et al.* did report defects in interferon-γ production from lymph nodes in response to antigen challenge.

3.5.3 Use of 100 µg ZIP to assess the CC chemokine binding protein 35K

It is clear from the literature and my data that CC chemokines play an important role in the pathology of a number of inflammatory diseases including atherosclerosis, rheumatoid arthritis and nephritis amongst others [66, 310, 327, 342]. The poxvirus derived 35K protein can potently bind a broad range of CC chemokines with high affinity including CCL2, CCL3, CCL4 and CCL5 [343]. Our laboratory has previously demonstrated the efficacy of broad spectrum chemokine blockade by 35K both *in vitro* and *in vivo* [344, 345]. In one study, animals lacking apolipoprotein E (which are very susceptible to atherosclerosis) were put on a high fat western diet to induce atherosclerosis. At a later point, these animals were given adenovirus with either 35K protein or GFP control via tail vein injection and the extent of plaque formation and macrophage recruitment to the plaques was quantified. Lesions were smaller in animals that had received 35K. Macrophage content and lipid deposition was also reduced in these animals compared to animals that received control GFP vector [345]. This study highlighted the potential utility of broad spectrum chemokine blockade in the treatment of chronic inflammatory diseases.

Viral delivery of 35K has drawbacks however, including difficulty in accurately administering a consistent dose as well as a short window of expression of the protein *in*

vivo [346]. In a subsequent study, an Fc fusion protein of 35K was generated in our laboratory. The addition of an Fc domain can substantially increase the half-life of proteins *in vivo* [347]. To further increase the efficacy of this protein, site directed mutagenesis was performed and mutants were screened for CC chemokine binding affinity. One mutant, designated R89A, displayed higher binding affinity than 35K towards CC chemokines [160]. This Fc fusion protein significantly decreased monocyte recruitment in a low dose (10μg) zymosan induced peritonitis model.

As this protein was so effective in these models, I wanted to validate my model with the R89A 35K mutant protein. At the time of writing, our laboratory was no longer producing Fc fusion 35K protein. As discussed in the results section, expression of the R89A mutant protein was instead induced systemically via hydrodynamic tail vein delivery. The results I saw in Figure 3.9 were similar to published results with the 35K fusion proteins. However, in these previous reports, there was no effect on neutrophil recruitment to the peritoneum during the low dose zymosan challenge. In my experiments I did see a significant decrease in neutrophil recruitment compared to the GFP control expressing animals (Figure 3.9 A-C). There could be a number of reasons for this difference. We might not in fact expect a difference in neutrophil numbers given that their recruitment is dependent on a number of mediators including non-CC chemokines such as CXCL1, CXCL2 and C5a. However, there have been reports that monocytes can themselves produce neutrophil chemoattractants such as CXCL8 so the decrease in monocyte recruitment could exert an indirect effect on neutrophil recruitment [348]. Another point to consider is the concentrations of R89A in the animals administered R89A fusion protein locally via intraperitoneal injection compared to systemic expression of the protein via hydrodynamic delivery. Concentrations of the protein were not measured systemically in this study. Given the route of administration and duration of this

study (6 hours) it seems likely that the proteins effects are predominantly local rather than systemic. In our studies, R89A expression was induced systemically; hence there may have been a greater effect on mobilisation of cells from bone marrow and spleen.

3.5.4 Limitations of the study

The greatest limitation of this model is that cell recruitment and inflammatory mediators can only be measured at a single point in time. Therefore, in order to get an idea of the dynamics and kinetics of the inflammatory response, it is necessary to measure multiple time points. Even then, there will be variability between experiments given it will be different animals being examined at different time points rather than the same animal. However, this is a difficult issue to overcome without using transgenic animals that have differentially labelled immune cells and *in vivo* live imaging of the animals throughout the entire experiment.

Another limitation of these studies is the detection of soluble mediators. The mediators that can be detected are limited by which ones have good antibodies against them for use in assays like ELISA and Luminex. Using peritoneal exudate fluid in a bioassay, such as chemotaxis assays is another approach to assess overall mediator production but would not be capable of measuring differences in any specific mediators. Lipid mediators were not investigated in these studies but could also be measured using liquid chromatography-tandem mass spectrometry.

Additionally, none of these approaches give any information about which cells make different mediators. Given the complexity of the microenvironment during an inflammatory response it could prove beneficial to further interrogate this. One could isolate specific cell populations using FACS and measure mediator levels at the mRNA level, but this is not always a reliable indication of protein expression. Alternatively a

FACS sort of different cell populations could be employed and cytokine production *ex vivo* in supernatants could be measured.

Other investigators have extended analysis of cell recruitment by histology and immunohistochemistry of intraperitoneal fat deposits and the inner lining of the peritoneum. Such studies could provide additional qualitative data to the quantitative analysis presented in this chapter [349].

3.6 Summary

In this chapter I have set up and characterised the 100 µg ZIP model. I have used proteome profilers, ELISA and Luminex to characterise the relative levels of mediators produced in the peritoneum after zymosan challenge. I have followed the time course of inflammatory mediator production as well as the different cell types recruited. I have validated the ZIP model using corticosteroids, broad spectrum CC chemokine blockade as well as CCR2 KO animals. This characterisation was informative in relation to my studies on the role played by chemerin and chemerin peptides during ongoing inflammation reported in chapter 4.

4 Chemerin modulates inflammation

4.1 Introduction

4.1.1 Chemerin expression and processing

Chemerin is produced initially as an inactive precursor called pro-chemerin and secreted into the blood. Chemerin was originally identified in ascites fluid from patients with ovarian and liver carcinomas as well as from arthritic joints [170]. Chemerin is expressed in a number of tissues with highest expression in liver, lymph nodes, spleen and pancreas [170, 194]. Chemerin is synthesised initially as an inactive precursor. However, during an inflammatory response a range of neutrophil and mast cell derived proteases including cathepsin-g, elastase, tryptase, mast cell chymase as well as coagulation factors can cleave the carboxyl terminus of chemerin to generate active chemerin isoforms [175, 189, 190]. The most active isoform that has been reported in human samples is chemerin^{157} although three others have also been reported; chemerin^{154}, chemerin^{155} and chemerin^{156} [175, 189]. Chemerin^{156} and chemerin^{157} display activity at the ChemR23 receptor while chemerin^{154} and chemerin^{155} do not [177, 189]. The mouse equivalent of chemerin^{157} is chemerin^{156} and it is this protein, which I have used in my murine studies and will be referring to as chemerin from now on.

4.1.2 Chemoattractant properties of Chemerin

Ex vivo and *in vitro* studies suggest that the chemerin/ChemR23 axis plays an important role in the recruitment of DCs, NK cells and macrophages to sites of injury and inflammation. *In vitro* studies have demonstrated that chemerin acts as a chemoattractant

for immature DCs, plasmacytoid DCs (pDCs) and macrophages [195, 205]. Chemerin was shown to colocalise on the luminal side of high endothelial venules along with ChemR23 expressing pDCs in human lymph nodes. Similarly, chemerin was found to colocalise with ChemR23 expressing pDCs as well as NK cells in psoriatic lesions from patients [205]. Finally, chemerin was shown to induce migration of immature DCs, pDCs and macrophages using *in vitro* systems in a number of studies including work from our laboratory [195, 198, 199, 205].

It has been demonstrated that the majority of signalling and chemoattractant activity of chemerin is derived from the carboxyl terminus and bioactivity can be conserved using smaller peptides derived from the carboxyl terminus. Wittamer *et al*. generated a number of different human chemerin peptides and found that a 9 amino acid peptide derived from the carboxyl terminus (YFPGQFAFS) called C9, was the smallest peptide that could still retain signalling function using ChemR23 transfected CHO-K1 cells [177].

4.1.3 Endogenous chemerin levels in health and disease

The role of endogenous chemerin has been the subject of debate since its first description. There have been a number of reports of increased chemerin levels in patients with metabolic and inflammatory diseases although the implications of these studies remain unclear [222, 228-231].

As mentioned earlier, chemerin plays a role in the recruitment of pDCs, DCs and NK cells to psoriatic lesions [195, 205]. In line with these observations, chemerin levels were increased in the blood of patients with psoriasis compared to healthy controls [206]. Additionally, patients suffering from psoriasis displayed reduced chemerin levels after

treatment with the anti-TNF-α drug Inflixamab as well as decreased levels of CRP and resistin [207].

4.1.4 Anti-inflammatory effects of chemerin and chemerin derived peptides

In contrast to the above studies, chemerin has also been reported to exert anti-inflammatory effects in a number of murine inflammation models.

Using a murine model of LPS induced lung inflammation; Luangsay *et al.* reported potent anti-inflammatory effects of full-length murine chemerin. Animals that received both chemerin and LPS displayed significantly less neutrophil recruitment to the lungs as well as decreased IL-6, TNF-α, IL-1β and CXCL1 levels in bronchiolar lavage (BAL) fluid. In our laboratory, we have demonstrated using plasma surface resonance that chemerin is capable of binding the lipid A component of LPS (data not shown) which could be a confounding factor in this kind of experiment. However, the authors confirmed that these effects were ChemR23 dependent, which suggests that the observed anti-inflammatory effects were independent of the LPS binding properties of chemerin. In addition, animals lacking the ChemR23 receptor displayed much higher neutrophil and macrophage numbers both in the BAL fluid and lungs as well as increased inflammatory mediator production [241].

In a similar manner to its chemotactic effects, it seems that the anti-inflammatory effects of full-length active chemerin can be recapitulated by short C-terminal derived peptides. The first report of a chemerin-derived peptide exerting anti-inflammatory effects was from our laboratory. The C15 peptide decreased monocyte and neutrophil recruitment in a zymosan induced peritonitis model as well as decreased inflammatory mediators [225]. This peptide also promoted efferocytosis of apoptotic neutrophils in a subsequent study [236]. The exact mechanism of this peptide remains elusive but Cash *et*

al. demonstrated direct anti-inflammatory effects of chemerin on Bio-gel elicited peritoneal macrophages in response to challenge with LPS and these effects were dependent on proteases [225].

In contrast, Bondue *et al*, reported no anti-inflammatory effect of chemerin on peritoneal Bio-gel elicited macrophages when challenged with LPS [237]. The reason for this discrepancy remains unclear and requires further investigation.

A more recent study developed a stabilised C9 peptide and demonstrated its efficacy in an allergic airway inflammation model similar to the model used by Zhao *et al.* [245, 247]. These studies highlight the complex biology of the chemerin/ChemR23 axis as well as the need for further investigation using specific chemerin isoforms and peptides.

4.2 Rationale for the experiments

As discussed above, the literature surrounding chemerin is difficult to interpret due to conflicting reports of pro- and anti-inflammatory effects of chemerin in different disease settings and different pre-clinical models. There is a growing body of evidence that chemerin levels correlate with increased BMI and systemic markers of inflammation in patients with metabolic and inflammatory diseases [172, 213, 230, 233, 350]. Similarly chemerin levels are increased in patients with rheumatoid arthritis and chemerin seems to directly increase inflammatory mediator production in this context [187, 203, 212, 213]. Conversely, a number of studies have reported anti-inflammatory effects of chemerin and chemerin derived peptides in a number of murine models of inflammation [225, 236, 238, 241, 245, 247]. Given the exact function of chemerin during inflammation remains

uncertain, the rationale for this chapter was to endeavor to clarify these contrasting reports in the literature.

4.3 Aims of this chapter

The aims of this chapter were to;

- Characterise the bioactivity and anti-inflammatory effects of full-length chemerin and a number of chemerin derived peptides on murine primary cell populations.
- Characterise endogenous chemerin levels and bioactivity in our murine models of inflammation.
- Investigate the effects on inflammation of modulating endogenous chemerin levels *in vivo*.
- Investigate the therapeutic potential of both full-length active chemerin as well as a previously unpublished chemerin derived peptide C17, in the context of primary macrophage inflammation assays and *in vivo* inflammation models.

4.4 Results

4.4.1 Characterisation of the chemoattractant properties of chemerin and chemerin derived peptides *in vitro.*

The cells used in the majority of *in vitro* experiments in this chapter are Bio-gel elicited peritoneal macrophages. This cell population was chosen based on my initial optimisation of the ACEA xCELLigence real time chemotaxis system in which we compared Bio-gel elicited macrophages, bone marrow derived macrophages, thioglycollate elicited macrophages and resident peritoneal macrophages. Bio-gel elicited macrophages were selected because they displayed the most robust chemotaxis towards classical chemoattractants and their production was relatively efficient [199]. In addition, they provided a relatively low level of background. I began by characterising the purity of this population 4 days after intraperitoneal injection of 2% Bio-gel. Despite previous reports in which the macrophage yield in peritoneal exudate cells (PECs) has been higher, I and others, in the laboratory observed ~30% macrophages by F4/80 and 7/4 staining [292, 351, 352] (Figure 4.1A). In addition, there was also a large population of neutrophils (~40%) (Figure 4.1A). However, neutrophils are not detected in the real time chemotaxis system, nor do they express the ChemR23 receptor so their contribution to the detected signal should be minimal [351] (Figure 4.1C). The F4/80^{hi} macrophages however do express the ChemR23 receptor (Figure 4.1B). Full-length active chemerin has been well documented to induce chemotaxis of both macrophages and immature dendritic cells by our group and others [198, 225]. However, I wanted to explore how potent peptides derived from the carboxyl terminus would be at inducing chemotaxis in this system. I used the murine version of the previously published C9 peptide (FLPGQFAFS), an unpublished peptide that we called C17 (AGEDPHGYFLPGQFAFS) and a C17 mutant

peptide in which two alananines were substituted in place of phenylalanines (AGEDPHGYALPGQFAAS). In this system I used the slope of the curve (in the first 40 minutes) as a measure of initial acceleration of cells and the max-min as a measure of both initial chemotaxis and adhesion of the cells to the underside of the filter [199].

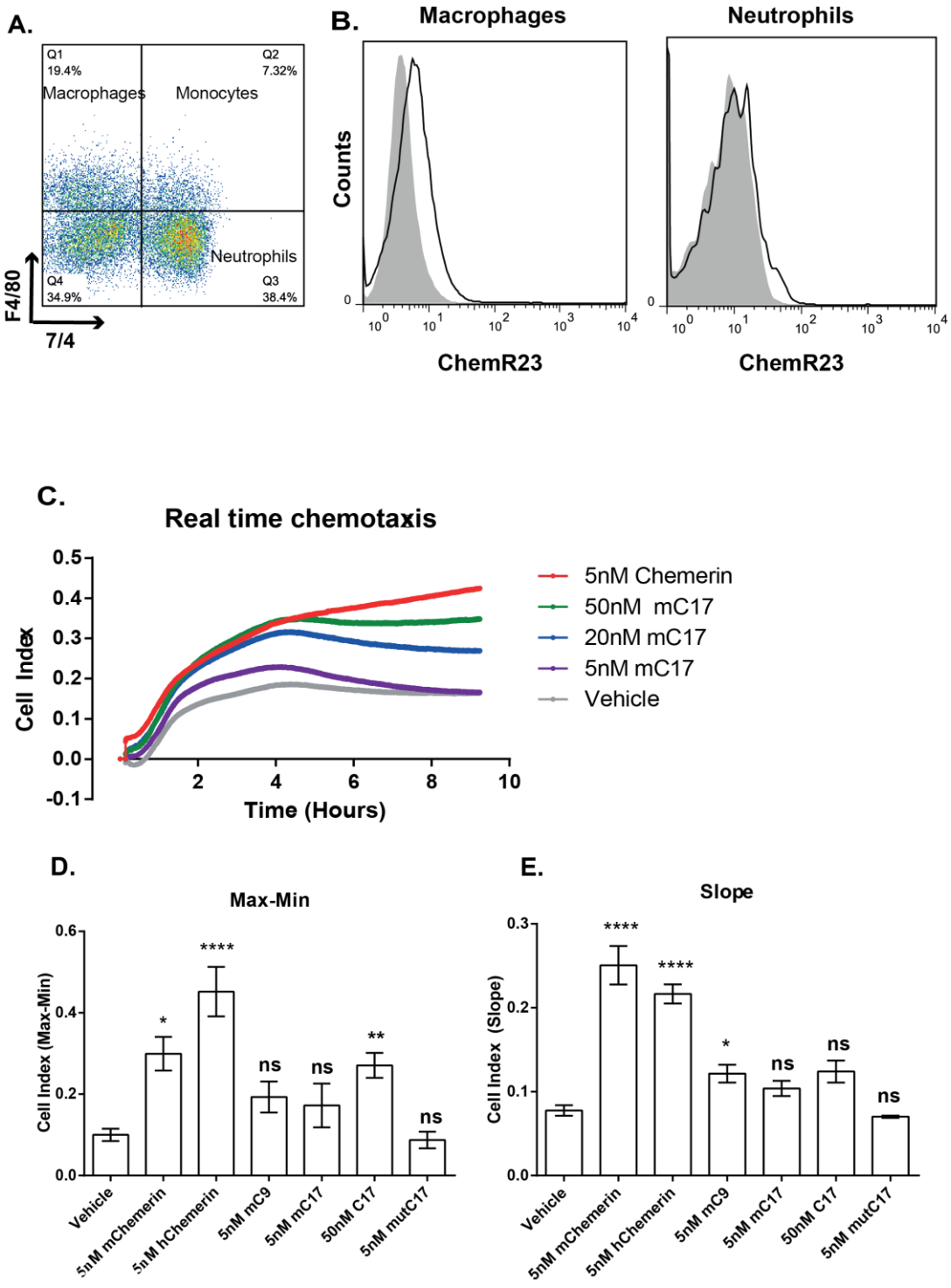


Figure 4.1 Chemerin and chemerin peptides promote chemotaxis of primary murine macrophages.

8-10 week old male C57Bl/6J mice were injected i.p. with 2% Bio-gel and sacrificed 4 days later. Peritoneal cavities were lavaged with ice-cold PBS supplemented with 2mM EDTA **A.** Representative flow cytometry plot of peritoneal exudate cells 4 days after Bio-gel injection. **B.** Representative plot of ChemR23 expression on F4/80^{+ve}, 7/4^{-ve} macrophages and F4/80^{-ve}, 7/4^{+ve}, Ly6-G^{+ve} neutrophils. Grey filled histogram is isotype control. Black line is positive staining.**C**.Representative trace. **D.** 4x10^{6} macrophages were allowed to migrate towards a gradient of indicated chemoattractants. Responses were measured in terms max-min (**D**) and initial slope (0-50 mins) (**E.**).Error bars represent S.E.M of at least 2 independent experiments. Statistical significance was assessed using One-Way ANOVA with Dunnets post-hoc test. .* $P \leq 0.05$. **$P \leq 0.01$. *** $P \leq 0.001$.

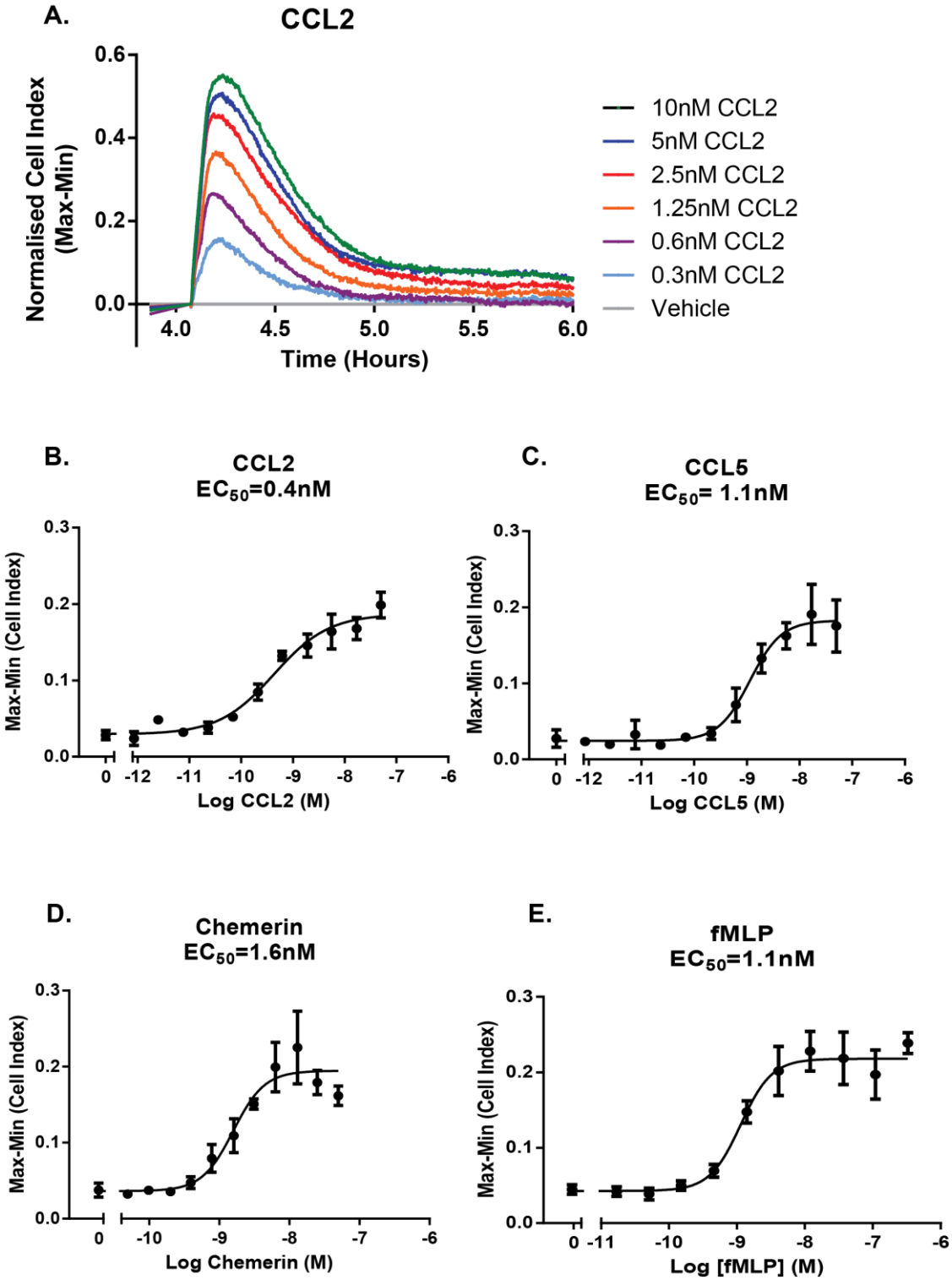


Figure 4.2 A range of chemotactic proteins induce adhesion of Bio-gel elicited macrophages in electrical impedance real time adhesion assay.

8-10 week old male C57Bl/6J mice were injected i.p. with 2% Bio-gel and sacrificed 4 days later. Peritoneal cavities were lavaged with ice-cold PBS supplemented with 2mM EDTA. PECs (5.4 x10^4) were allowed to adhere for 3 hours until no further increases in CI were observed. Cells were then challenged with indicated agonists (**B**-**E**). **A.** Raw trace of normalised CI responses of Bio-gel macrophages to CCL2. Responses were quantified using max-min values (**B**.-**E.**). Error bars represent S.E.M of at least 2 separate experiments. EC_{50} values for each agonist are quantified.

Both murine and human chemerin induced significant chemotaxis at low nanomolar levels. 5 nM murine chemerin induced a slope of 0.25 ± 0.034 Cell Index (CI) and max-min CI of 0.30 ± 0.07 while 5 nM human chemerin induced a slope CI of 0.22 ± 0.02 and a max-min CI of 0.45 ± 0.09 (Figure. 4.1. D-E). At equivalent doses the C9 peptide did not induce significant chemotaxis by max-min (0.19 ± 0.10) but did induce a significant increase in CI by slope (0.12 ± 0.03). The C17 peptide did not induce chemotaxis at the 5 nM dose and required 10-fold higher concentrations to induce chemotaxis in this system (max-min CI of 0.27 ± 0.07) (Figure. 4.1E). As expected, the mutant C17 peptide, which has two alanines, substituted in the place of two phenylalanines displayed no chemotactic effects (Figure 4.1 D-E). These substitutions were based on a previous study by Wittamer *et al.*, who demonstrated these aromatic phenylalanine amino acids at the C-terminus of chemerin were required for signalling at the chemerin receptor [177].

From these studies I demonstrated that Bio-gel elicited macrophages express a functional ChemR23 receptor and that both murine and human full-length chemerin are potent chemoattractants. Neither the C9 or C17 peptide were efficient at inducing chemotaxis at the equipotent concentrations. 10-fold higher doses of C17 compared to full-length chemerin were required to observe significant chemotaxis (Figure 4.1D-E).

4.4.2 Characterisation of cytoskeletal changes induced by chemerin and chemerin derived peptides *in vitro.*

Full-length chemerin has previously been shown to induce adhesion of Bio-gel-elicited macrophages to VCAM-1 and fibronectin [198]. I used the ACEA xCELLigence SP system (an electrical impedance based platform) to investigate whether these chemerin peptides could also induce similar effects to the full-length protein. I began by validating

the system using a number of well-characterised chemoattractants including CCL2, CCL5, fMLP as well as murine chemerin. All 4 of these proteins induced adhesion of Bio-gel elicited macrophages with EC_{50} values ranging between 0.4nM (CCL2) and 1.6nM (Chemerin) (Figure 4.2B-E).

In order to validate this system, I investigated the effects of pre-treating cells with cytochalasin D (a potent inhibitor of actin polymerisation) to demonstrate that this system is indeed dependent on cytoskeletal rearrangements [353]. Pre-treatment of cells with cytochalasin D completely ablated responses to both CCL2 and chemerin in this system with an IC_{50} value of 102 nM in cells challenged with CCL2 and an IC_{50} value of 56 nM in cells challenged with chemerin (Figure 4.3A-B).

The majority of chemokine receptors are $G_{i/o}$ coupled GPCRs and signalling downstream of both the $G_{\alpha i}$ and $G_{\beta\gamma}$ is required for chemotaxis and adhesion. Chemotactic responses are pertussis toxin sensitive; via blocking the exchange of GTP for GDP on the G_{α} subunit [354]. Pertussis toxin efficiently blocked signalling to both CCL2 and chemerin in this system with IC_{50} values of 12.6 nM and 7.4 nM respectively (Figure 4.3C-D). The ablation of signalling with cytochalsin D and pertussis toxin treatments were not due to cell death, as cell viability assays measuring ATP production showed no differences in viability between different treatments (data not shown).

I next used a CCR2 antagonist obtained from ChemoCentryx (CCX417), which has previously been used in a murine model of diabetes [355]. Using CHO-K1 cells transfected with a tagged CCR2 receptor I was able to show that this antagonist efficiently blocked CCR2 mediated β-arrestin recruitment to the receptor in these cells (IC_{50}= 10nM) as well as CCL2 mediated adhesion (IC_{50}= 2nM) in the electrical impedance system (Figure 4.3E-F). I also used this compound on primary Bio-gel macrophages in this system but did not see significant inhibition of signal (data not

shown). This may be due to the overexpression of CCR2 in transfected cells or due to redundancy in the CCL2 signalling via CCR4 on primary cells [157].

I proceeded to investigate the bioactivity of chemerin and the chemerin peptides (Figure 4.5A). In contrast to the chemotaxis system, chemerin peptides were just as effective at increasing in CI as full-length chemerin (Figure 4.5B.). Full-length murine chemerin induced a max-min CI of 0.068 ± 0.01 compared to 0.08 ± 0.03 for 5 nM C17 and 0.1 ± 0.02 for 5 nM C9. In contrast to the chemotaxis system, a 10-fold higher dose of C17 did not induce significantly higher adhesion in these experiments (CI of 0.1 ± 0.01). Full-length 5 nM human chemerin induced the highest adhesion with a max-min CI of 0.11 ± 0.02 while the mutant C17 peptide did not induce any increase in signal compared to vehicle (0.02 ± 0.01 and 0.03 ± 0.01 respectively).

These increases in adhesion were completely blocked by pre-treatment with pertussis toxin indicating that these effects were indeed $G_{\alpha i}$ coupled (Figure 4.5C). 50 nM murine chemerin induced a max-min CI of 0.1 ± 0.011 which was decreased to 0.03 ± 0.01 with pertussis treatment. Similarly, 50 nM C17 induced a max-min CI of 0.14 ± 0.02 which was decreased to 0.02 ± 0.01 with pertussis treatment and 50nM C9 induced a max-min CI of 0.2 ± 0.04 which decreased to 0.05 ± 0.01 with pertussis treatment.

The requirement for the ChemR23 receptor to induce these responses was confirmed using Bio-gel elicited macrophages from mice lacking the ChemR23 receptor. These cells did not display any CI change in response to chemerin but did respond to CCL5 illustrating that these cells were capable of adhesion in response to other ligands (Figure. 4.5D).

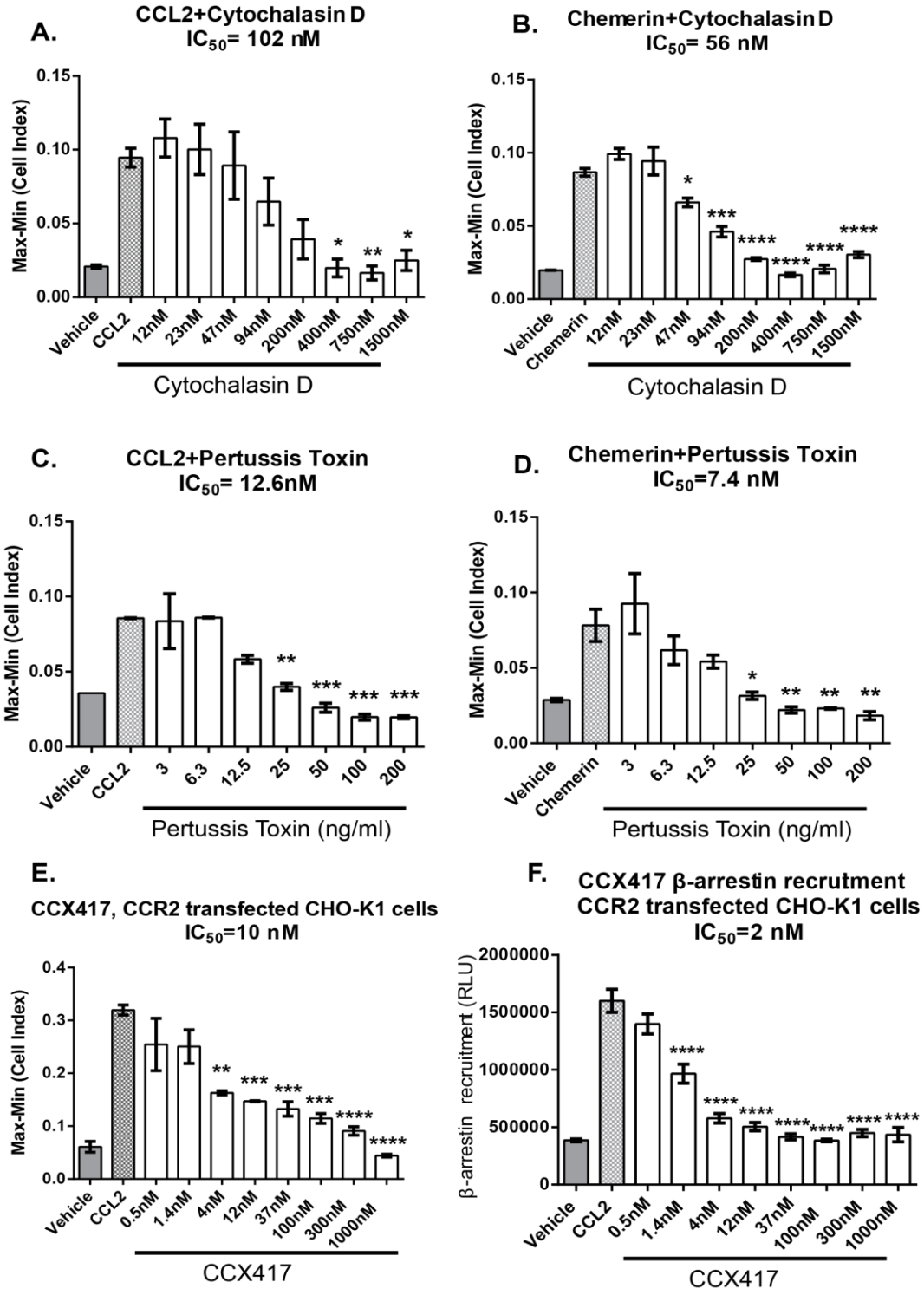


Figure 4.3 Adhesion in the impedance platform is dependent on $G_{\alpha i}$ signalling and cytoskeletal rearrangements.

A-D. $5.4x10^4$ PECs were allowed to adhere for 3 hours. Cells were pre-treated with indicated concentrations of cytochalasin D (**A**+**B**) or pertussis toxin (**C**+**D**) for 90 mins before challenge with 5nM of indicated agonists. Max-Min CI was measured for ~4 hours and IC_{50} values were calculated. **E.** CCR2 transfected CHO-K1 cells were allowed to adhere for~48 hours. Cells were pre-treated with CCX417 at indicated concentrations for 90 mins before challenge with 5nM CCL2. Adhesion (**E.**) and β-arrestin recruitment was measured in the same cells (**F.**) Error bars represent S.E.M of the mean of at least 2 separate experiments (consisting of technical duplicates). Significance was assessed using One-Way ANOVA followed by Dunnets post-hoc test.* $P \leq 0.05$. **$P \leq 0.01$. *** $P \leq 0.001$, ****$P \leq 0.0001$.

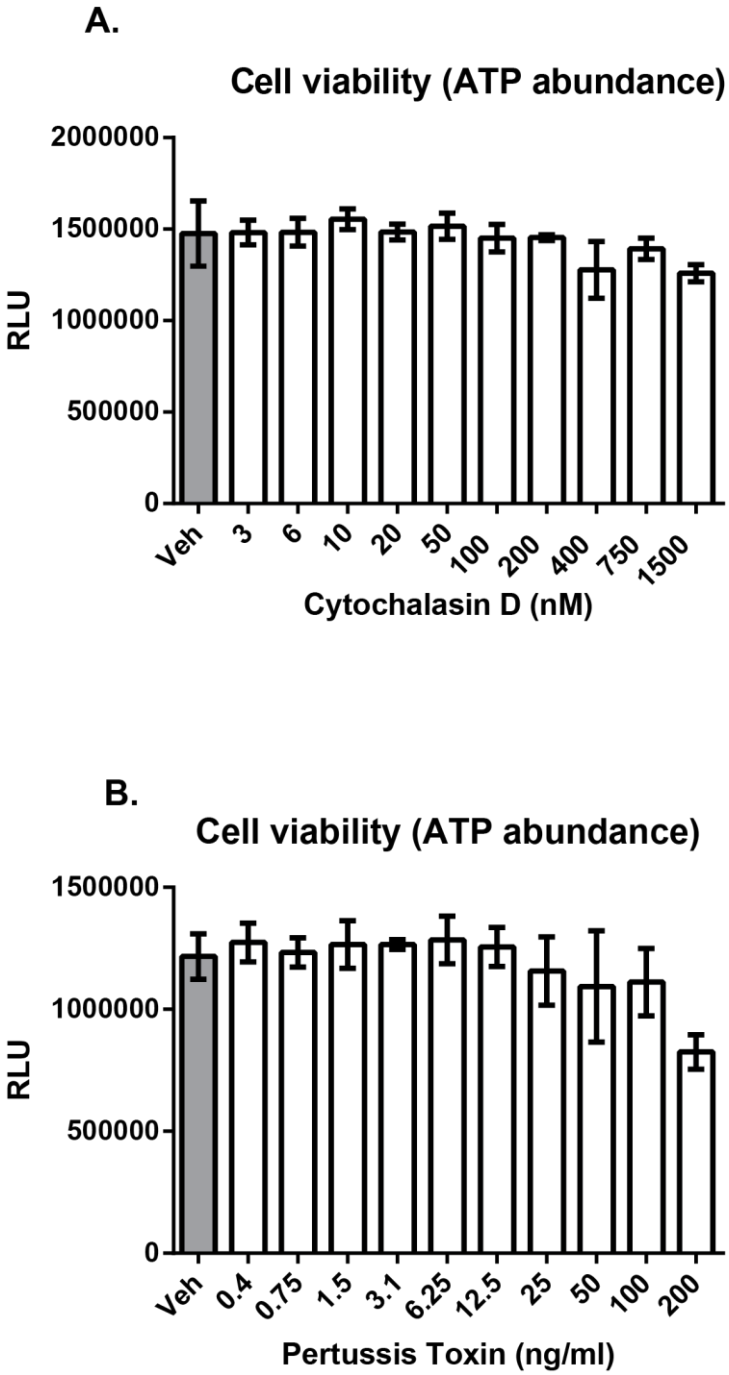


Figure 4.4 Pertussis toxin and cytochalasin D do not affect the viability of Bio-Gel elicited PECs.

5.4 x 10^4 PECs were allowed to adhere for 3 hours. Cells were pre-treated with indicated concentrations of cytochalasin D (**A**) or pertussis toxin (**B**) for 90 mins. 50µls Cell Titre Glow reagent was added per well and plates were placed on an orbital shaker for 10 minutes. Luminescnce was read using a Pherastar plate reader. RLU=Relative light units. Luminescnce is a measure of ATP. Error bars represent S.D. of 3 technical replicates.

I next investigated if there were differences in β-arrestin recruitment to the ChemR23 receptor between chemerin peptides and full-length murine chemerin. Using ChemR23 transfected CHO-K1 cells, I observed that both the C9 and C17 peptides were less potent activators of the receptor compared to the full-length protein (Figure 4.5E). Full-length chemerin activated the receptor with an EC_{50} of 1.1nM while C17 and C9 displayed EC_{50} values of 6.8 nM and 11.4 nM respectively. However, both peptides acted as full agonists of ChemR23, although higher concentrations were required when compared to full-length chemerin.

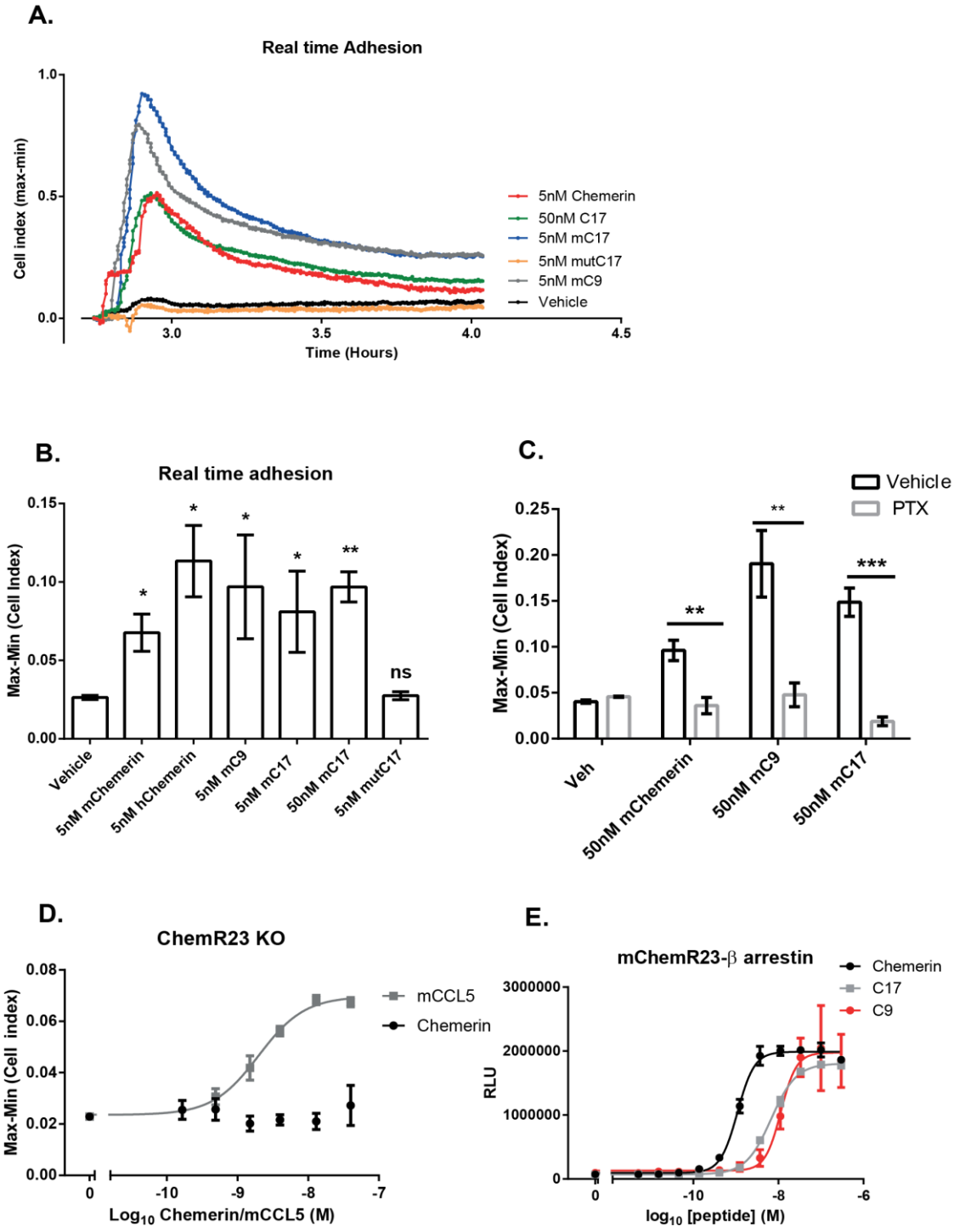


Figure 4.5 Chemerin and chemerin peptides induce adhesion of primary murine macrophages in a ChemR23 dependent manner.

A. Raw trace of impedance assay. $5.4x10^4$ Bio-gel PECs were allowed to adhere for 3 hours until no further increases in adhesion were observed. Cells were challenged with indicated agonists. **B.** Responses were quantified using max-min values. **C.** Cells were pre-treated with vehicle or 200 ng/ml pertussis toxin (PTX) for 90 minutes before challenge with indicated agonists. **D.** Responses of cells from animals lacking ChemR23 were evaluated. **E.** β-arrestin recruitment to the ChemR23 receptor was measured in ChemR23 transfected CHO-K1 cells. Error bars represent S.E.M of the mean of 2 technical replicates of at least 2 separate experiments. Significance was assessed using One-Way ANOVA followed by Dunnets post-hoc test in **B** and **C**. and two Way ANOVA was used in **E.*** $P \leq 0.05$. **$P \leq 0.01$. *** $P \leq 0.001$.

4.4.3 Bioactivity of chemerin and chemerin peptides in inflammatory activation assays.

As stated previously, there has been a number of reports on anti-inflammatory effects of both chemerin and chemerin derived peptides [225, 236, 238, 239, 245, 247]. In order to probe the mechanism of these effects in cell-based assays, I set up a macrophage activation assay using bone marrow derived macrophages. The reason for switching from Bio-gel elicited macrophages to bone marrow derived macrophages was the purity of the macrophage population obtained. In my initial experiments there was a relatively small F4/80^{hi}, 7/4^{-ve} population from Bio-gel preparations (Figure 4.1A). However, using 7 day differentiated bone marrow derived macrophages (cultured in L929 conditioned media) there was ~85% F4/8^{hi}, 7/4^{-ve} macrophages by flow cytometry (Figure 4.7 A).

Using 100 ng/ml LPS and 10 ng/ml interferon-γ as activation signals I observed 30-40 ng/ml TNF-α production after 16 hours of stimulation (Figure 4.6E). However, results I obtained following chemerin and chemerin peptide treatment were variable. In a number of experiments I observed near complete ablation of TNF-α production in cells that had been pre-treated with varying concentrations of C17 (Figure. 4.6A). However in other experiments I observed no difference in cells that had been pre-treated with C17 peptide compared to vehicle (Figure 4.6B). Similar results were observed for full-length chemerin (Figure 4.6C-D). When the data was pooled, LPS/Interferon-γ alone induced 41.5 ± 7.8 ng/ml TNF- α production. Dexamethasone, which was used as a positive control, decreased TNF-α levels to 23.4 ± 8.7 ng/ml but this was not significant due to the high degree of variability in this system (Figure 4.6E). The reasons for this variability remain unclear. I altered a number of parameters to investigate the source of this variability (tabulated in table 4.1). However none of these variables seems to have had a

reproducible effect. When I examined ChemR23 expression on the surface of these cells, they expressed the receptor at low levels and there may have been variation between different preparations, which may account for some variability in responses (Figure 4.7A).

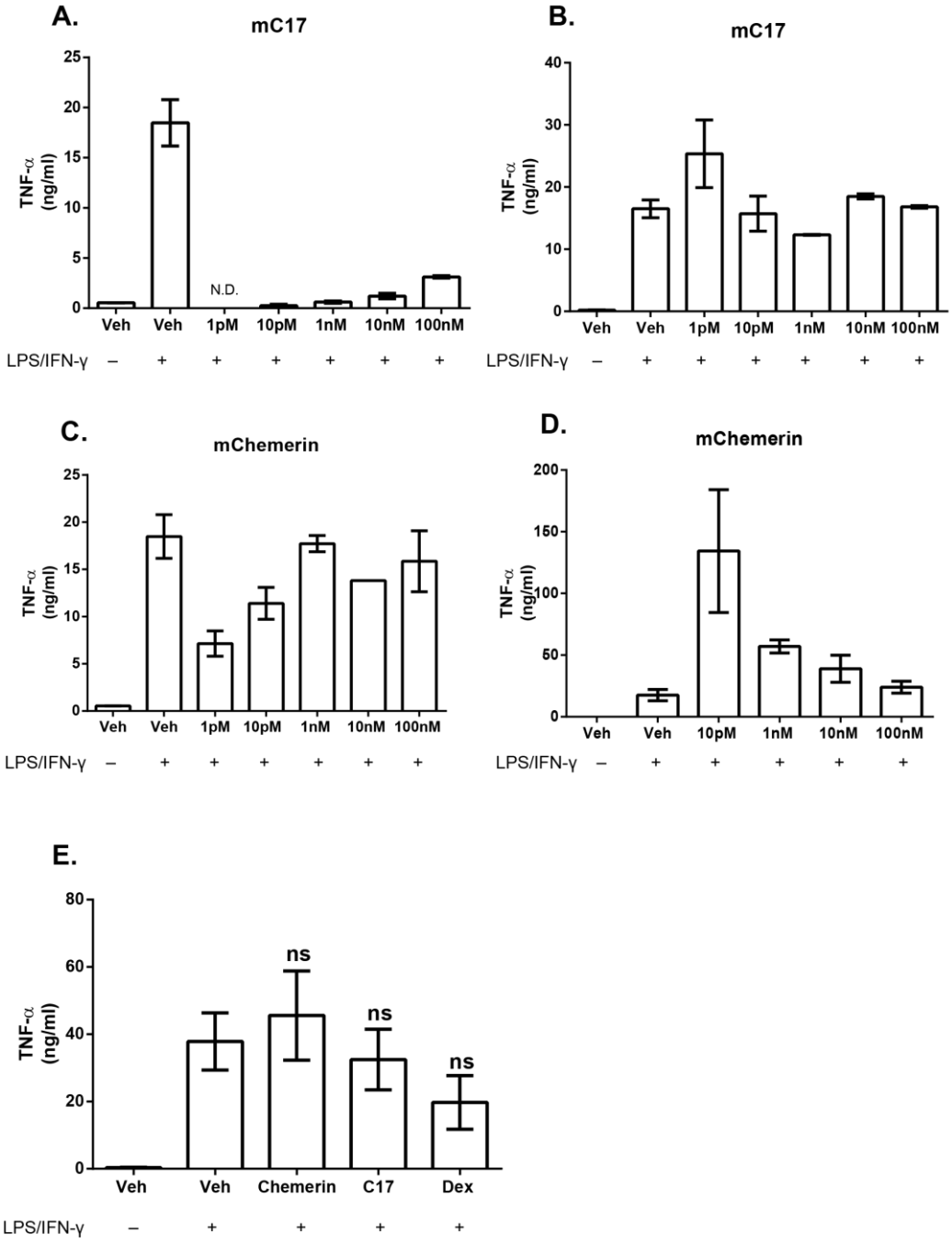


Figure 4.6 Bone marrow derived macrophages display variable anti-inflammatory responses to chemerin and C17 treatment.

Bone marrow derived macrophages were cultured in DMEM supplemented with 10% FCS, 15% L929 conditioned media for 7 days and extra media was added on day 3. Macrophages were harvested on day 7, plated out into tissue culture treated plates in optimum and allowed to adhere for ~4 hours in the absence of serum before challenge. Cells were pre-treated with indicated concentrations of agonists (**A-D**) or 1nM chemerin or C17 (**E.**) for 45 minutes prior to challenge with 100 ng/ml LPS and 10 ng/ml IFN-γ.for 16 hours. Supernatants were collected and assayed for TNF-α production by ELISA. TNF-α levels from 4 separate experiments (**A-D)** are shown here Error bars represent S.D. of one experiment with 2-3 technical replicates. **E.** Pooled data from 11 separate experiments. Error bars represent S.E.M of means from technical replicates from 11 indiviual experiments. Statistical significance was assessed by One-way ANOVA followed by Dunnetts post-hoc test.

Another variable I assessed was the growth medium used to differentiate the bone marrow derived cells into macrophages [356]. In the experiments discussed so far, L929 conditioned media was used as a source of M-CSF. There are also a large number of other growth factors and cytokines present in this medium, which are difficult to control for and it is possible macrophages derived by this method are more activated [357]. Hence, I explored using DMEM supplemented with recombinant murine M-CSF instead [358]. Using recombinant murine M-CSF (10ng/ml) I obtained a pure population of bone marrow derived macrophages, very similar in F4/80 and 7/4 expression as L929 cultured macrophages (Figure 4.7A). ChemR23 was also expressed at a similarly low level (Figure 4.7B).

Given the variability of TNF-α expression seen in previous experiments using LPS and interferon-γ, I switched to Polyinosinic:polycytidylic acid (Poly I:C) (a TLR3 agonist) in my activation assays. Another reason for this choice was the ChemR23 receptor expression pattern. ChemR23 is highly expressed on a number of cell types, which are important for anti-viral responses such as pDCs, NK cells and macrophages [194, 195, 241]. In addition, there have been reports of the ChemR23 receptor playing an important role in murine models of viral infection [242]. Using this TLR ligand, I saw similar variability with chemerin and C17 pre-treatment in macrophages stimulated with 10 μg/ml poly I:C as I did with LPS/interferon-γ challenge. Full-length chemerin actually trended towards increasing TNF-α production compared to poly I:C alone (2.9 ± 0.9 ng/ml and 1.7 ± 0.3 ng/ml respectively). However this did not reach significance (Figure 4.7C). C17 on the other hand trended towards decreased TNF-α production but again this was not significant (1.2 ± 0.8 ng/ml). Dexamethasone was used as a control in these experiments and decreased TNF-α production from 1.7 ± 0.3 to 0.13 ± 0.1 ng/ml.

Inflammatory responses to poly I:C were compared in macrophages generated with L929 and macrophages generated using recombinant M-CSF. Overall TNF-α production in response to poly I:C did not seem to differ between these different preparations. L929 generated macrophages produced 1.1 ± 0.1 ng/ml TNF-α compared to 1.3 ± 0.5 ng/ml in M-CSF generated macrophages (Figure 4.7D). This experiment was not repeated. Given the variability I observed in these two different cell based assays it was difficult to draw many conclusions about the pro- or anti-inflammatory properties of chemerin and C17 from these experiments and as a result turned to an *in vivo* model of inflammation.

Experiment number	**1**	**2**	**3**	**4**	**5**	**6**	**7**	**8**	**9**	**10**	**11**	**12**	**13**
Peptide batch	1st	1st	1st	1st	1st	2nd	2nd	2nd	2nd	2nd	2nd	2nd	2nd
Serum starved 24hrs prior to LPS	Yes	Yes	Yes	No	No	No	No	No	No	No	No	No	No
Vehicle (TNF-α levels, pg/ml)			1,035	500		196	ND	3700	ND	200	ND	ND	ND
Vehicle CCL2 levels, pg/ml)	1345	600	116	1,029	980								
LPS (TNF-α levels, pg/ml)			2,353	18,000		16,500	25,500	12,500	17,600	1,600	31,000	62,000	7,300
LPS (CCL2 levels, pg/ml)	15,000	6,300	257	19,968	9,154								
10nM C17 (TNF-α levels, pg/ml)			1,600	1,200		18,500	900	27,350	5,800	8,400	29,700	34,200	6,860
10nM C17 (CCL2 levels, pg/ml)	435	616	149	3,843	1,374								
C17 induced %decrease in CCL2	97.10	90.20	42	80.8	84.9								
C17 induced %decrease in TNF-α			32	93		+12.1	96.47	+55	67.04	+80	4.19	44.8	6.02

Table 4.1Variation between experiments using bone marrow derived macrophages and modification of different variables.

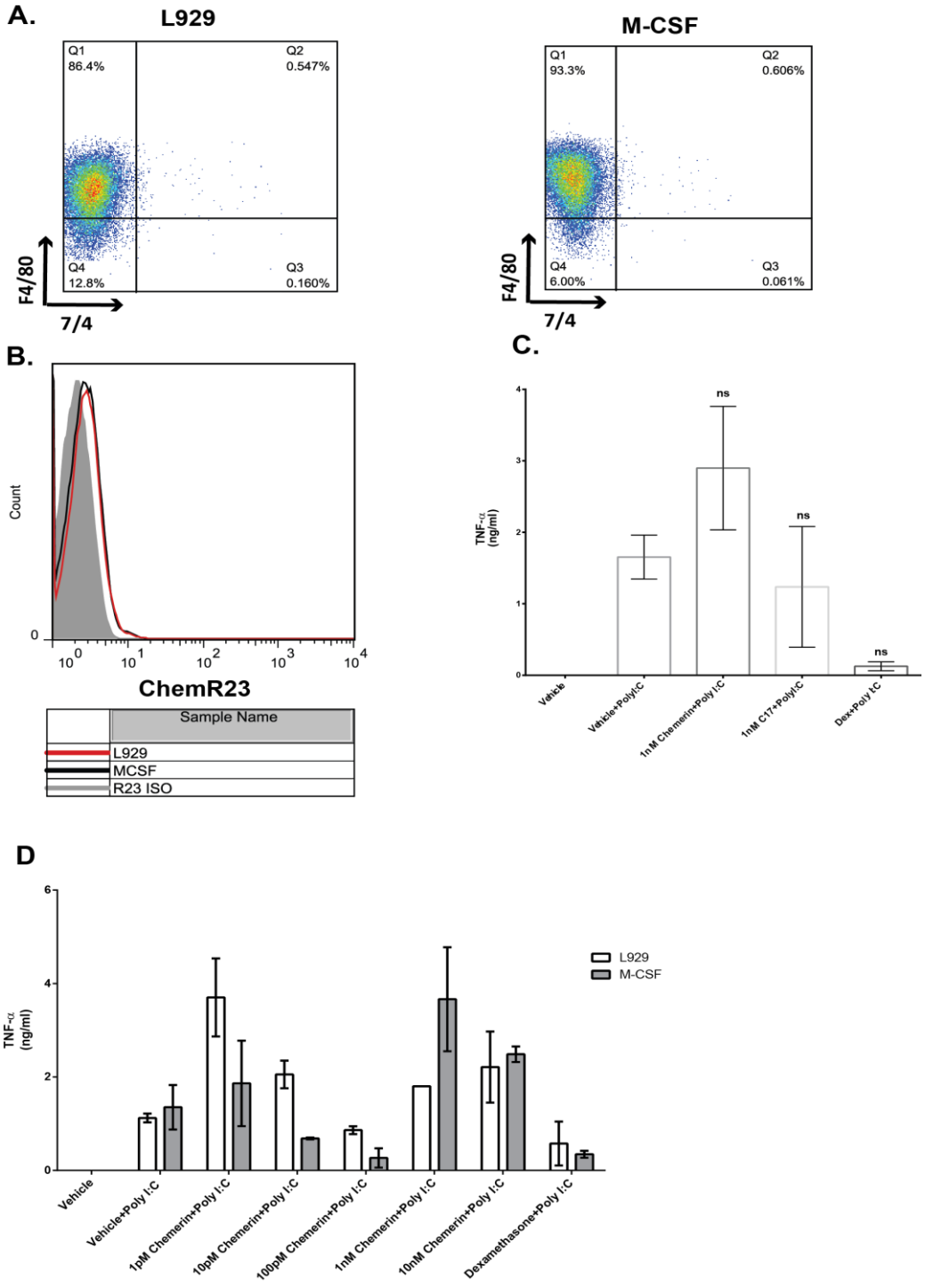


Figure 4.7 Recombinant M-CSF vs L929 conditioned media does not affect ChemR23 expression or inflammatory responses to TLR agonists in bone marrow derived macrophages.

BMDMs were cultured as before in DMEM supplemented with L929 conditioned media or in DMEM supplemented with 10ng/ml recombinant murine M-CSF. **A.**Macrophage purity was assessed by F4/80 and 7/4 staining. **B.** ChemR23 expression in the two populations. Grey filled area is isotype control. **C.**L929 generated macrophages were allowed to adhere for ~4 hours before a 45 minute pretreatment with indicated treatments. Cells were challenged with 10 µg Poly I:C for 16 hours and TNF-α levels were measured by ELISA. Error bars represent S.E.M of 7 separate experiments. Statistical significance was assessed by One-way ANOVA and Dunnetts post hoc test. **D.** Responses of both L929 and M-CSF cultured macrophages were compared. Cells were treated as above and TNF-α levels measured by ELISA. Error bars represent S.D. of 2 technical replicates.

4.4.4 The effects of chemerin and C17 peptide pre-treatment on inflammation *in vivo.*

The results from the *in vitro* inflammation assays did not yield a clear answer as to the pro- or anti-inflammatory properties of chemerin and chemerin derived peptides. I therefore took advantage of the zymosan induced peritonitis (ZIP) model I characterised in chapter 3 to investigate chemerin and chemerin derived peptides *in vivo*. From previous experiments, I had shown that after16 hours zymosan challenge there were ~3 $x10^6$ monocytes and ~8 $x10^6$ neutrophils recruited to the peritoneum (Figure 3.2 C-D). Using dexamethasone pre-treatment as an anti-inflammatory positive control, this time point resulted in sufficient cell recruitment to see reductions in total monocytes and neutrophils (Figure 3.2 C-D). Therefore, I began by using a pre-treatment model in which full-length chemerin, C17, dexamethasone (dex) or PBS were given intraperitoneally (i.p.) for 45 minutes prior to zymosan challenge for 16 hours. Dexamethasone pre-treatment significantly decreased monocyte numbers compared to PBS from 3.1 ± 0.12 $x10^6$ to 1.9 ± 0.1 $x10^6$ (Figure 4.8B). Dexamethasone, however, did not have any effect on neutrophil numbers compared to vehicle treated animals (5.8 ± 0.5 $x10^6$ and 6.6 ± 0.4 $x10^6$ respectively) (Figure 4.8 C). Chemerin pre-treatment did not affect monocyte recruitment. Mice that received a pre-treatment of 500 ng of murine chemerin, had 3.2 ± 0.2 $x10^6$ monocytes in the cavity compared to 3.1 ± 0.12 $x10^6$ in vehicle treated animals (Figure 4.8 B). However, chemerin treated animals had significantly more neutrophils ($P \leq 0.05$) recruited to the cavity compared to vehicle treated (9.1 ± 0.8 $x10^6$ and 6.6 ± 0.4 x 10^6 respectively) (Figure. 4.8 C). This result is interesting because there have been mixed reports regarding ChemR23 expression on murine neutrophils [198, 238]. It is possible that increased neutrophil influx is not a result of chemerin signalling directly on neutrophils but rather chemerin could be

modulating chemokine production by other ChemR23 expressing cells such as endothelial cells [243, 359].

I also investigated the C17 peptide in this model. I used a range of different doses ranging from 30 ng to 1000 ng per mouse. Pre-treatment with 50 ng C17 induced a modest but significant ($P \leq 0.05$) decrease in monocyte recruitment ($2.5 \pm 0.2 \times 10^6$ monocytes in C17 treated animals compared to $3.1 \pm 0.12 \times 10^6$ monocytes in vehicle treated). However, no other dose of this peptide affected monocyte numbers (Figure 4.8 E). Similarly, no concentration of C17 had any effect on neutrophil numbers (Figure 4.8 F).

4.4.5 The Effects of chemerin and the C17 peptide intervention on inflammation *in vivo.*

Although I did not see any significant anti-inflammatory effect of full-length chemerin in the pre-treatment model, I did observe a significant decrease in monocyte recruitment with the C17 peptide (Figure 4.8). Chemerin is well documented to be susceptible to proteolytic regulation; active chemerin is generated from inactive pro-chemerin by cleavage of the carboxyl terminus by inflammatory proteases [175, 176, 189]. I hypothesised that at a site of inflammation, active chemerin, once generated, could be further cleaved to generate shorter bioactive peptides. To test this hypothesis I switched from the pre-treatment model to an interventional model in which zymosan was injected first and 2 hours later indicated treatments were given. The reason behind this strategy was that neutrophil derived proteases are known to cleave pro-chemerin so I chose a time point in which there would be a large population of activated neutrophils present. At 2 hours post zymosan I observed a large influx of neutrophils but very few if any monocytes (Figure 3.4B).

Dexamethasone was used as a positive control in these experiments. Dexamethasone intervention significantly ($P \leq 0.05$) decreased total cell recruitment compared to vehicle ($8.5 \pm 1.4 \times 10^6$ and $13.3 \pm 0.7 \times 10^6$ respectively) as well as monocyte recruitment ($1.6 \pm 0.2 \times 10^6$ monocytes in dexamethasone treated animals and $3.4 \pm 0.1 \times 10^6$ in vehicle) (Figure 4.9A-C). Again, dexamethasone had no effect on neutrophil recruitment (Figure 4.9D). I tested a range of doses of chemerin in these experiments. Intervention with 500 ng chemerin resulted in significant decreases in total cells ($P \leq 0.05$) and total monocytes ($P \leq 0.001$) recruited to the cavity (Figure 4.9B and C). Chemerin treated animals had $10.3 \pm 0.6 \times 10^6$ total cells compared to $13.3 \pm 0.7 \times 10^6$ total cells in animals that received zymosan and PBS. Similarly, chemerin treatment resulted in a 27% decrease in monocytes ($2.5 \pm 0.1 \times 10^6$ monocytes in chemerin treated animals compared to $3.4 \pm 0.1 \times 10^6$ monocytes in PBS treated animals). Higher doses of chemerin did not display any obvious effects on cell recruitment in these experiments. In contrast to the pre-treatment experiments (Figure.4.8), no concentration of chemerin had any effect on neutrophil recruitment (Figure 4.9 D).

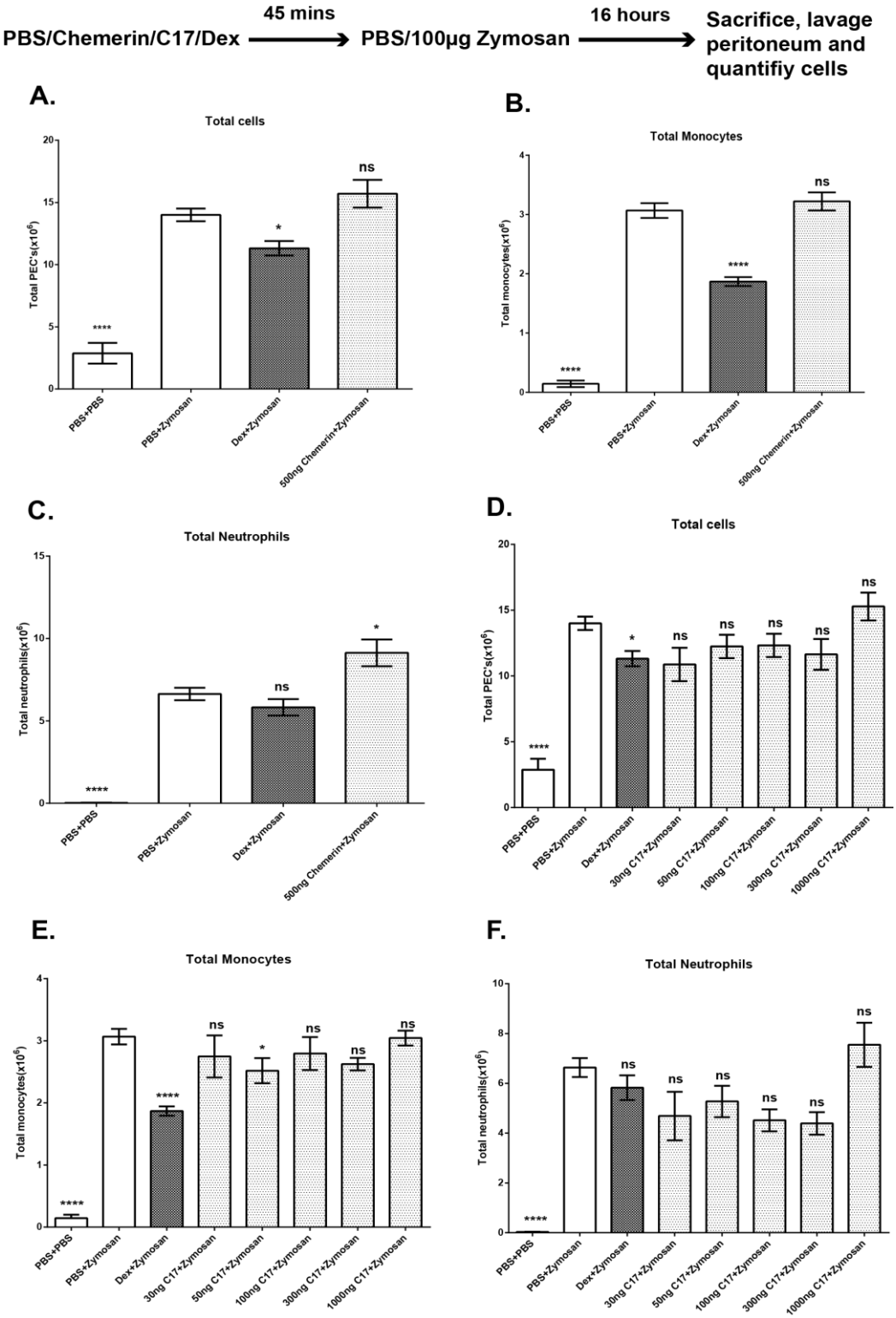


Figure 4.8 Pre-treatment model of zymsoan induced peritonitis

8-12 week old male C57Bl/6J mice were injected i.p. with PBS, Dexamethasone (1mg/kg) or chemerin (500 ng/mouse) (**A.-C**.) or indicated concentrations of C17 peptide 45 minutes before a second injection of PBS or 100µg zymosan (**D.-F**.)16 hours later animals were sacrificed. Peritoneal cavities were lavaged with ice cold PBS supplemented with 2mM EDTA. Cell populations were quantified using flow cytometry (Monocytes were $7/4^{hi}$, $Ly6G^{lo}$, neutrophils were $7/4^{hi}$, $Ly6G^{hi}$). Error bars represent S.E.M. 5-20 animals/group. Statistical significance was assessed by One-way ANOVA and Dunnetts post hoc test. * $P \leq 0.05$. ** $P \leq 0.01$. *** $P \leq 0.001$.

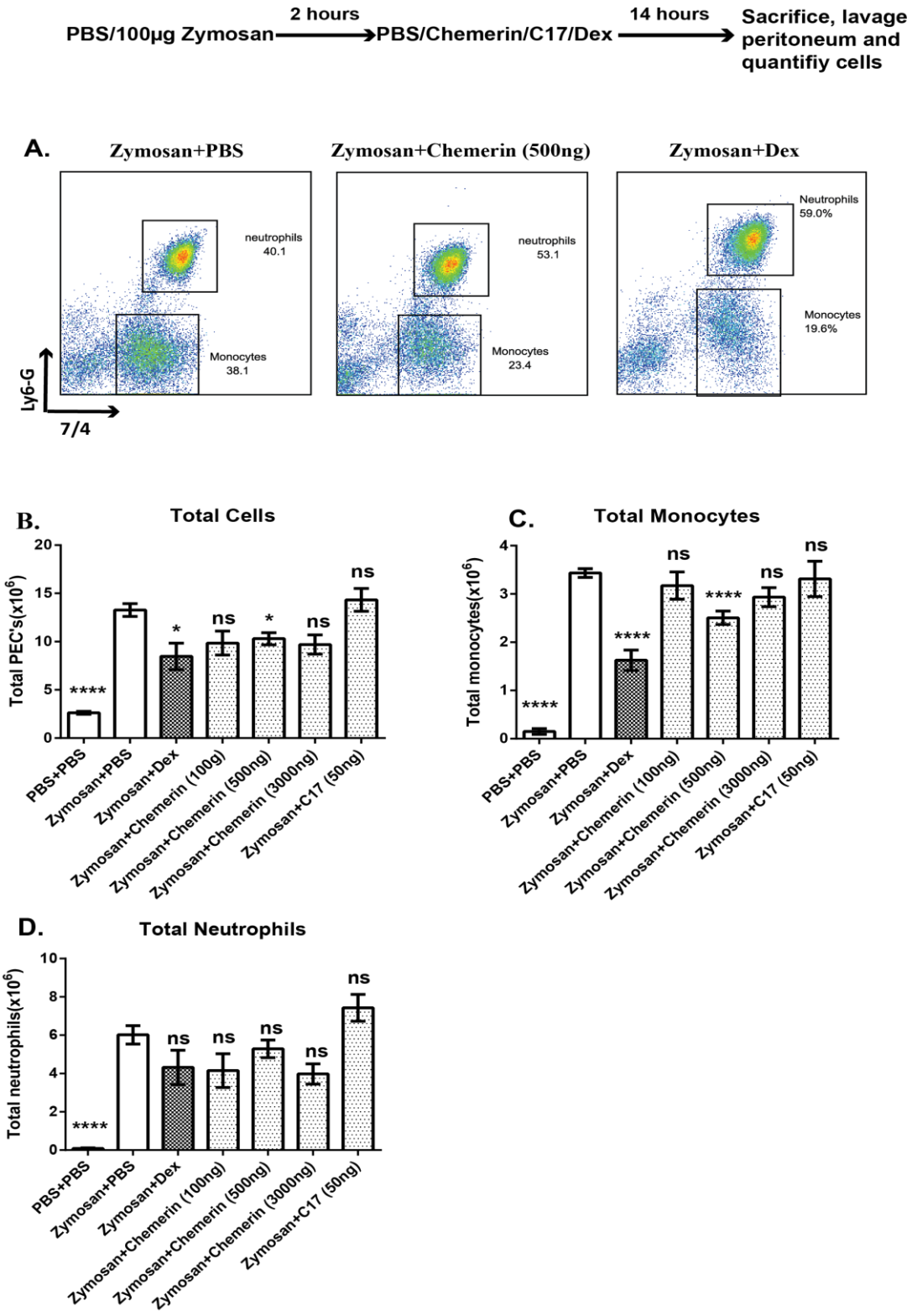


Figure 4.9 Interventional model of zymosan induced peritonitis.

8-12 week old male C57Bl/6J mice were injected i.p. with 100 µg zymosan or PBS and 2 hours later mice were injected with dexamethasone (1mg/kg), C17 peptide (50ng) or indicated doses of Chemerin. 14 hours later animals were sacrificed. Peritoneal cavities were lavaged with ice cold PBS supplemented with 2mM EDTA. Cell populations were quantified using flow cytometry. **A.** Flow cytometry plots of indicated treatments. Total cells **B.** total monocytes **C.** and total neutrophils **D.** recruited to peritoneum. Error bars represent S.E.M. 5-20 animals/group. Statistical significance was assessed by One-way ANOVA and Dunnetts post hoc test.* $P \leq 0.05$. **$P \leq 0.01$. *** $P \leq 0.001$, **** $P \leq 0.0001$.

I investigated possible effects of C17 in these experiments given that this peptide is active at the ChemR23 receptor and I observed a significant reduction in monocytes in the pre-treatment experiments using the 50 ng dose (Figure. 4.8E). In these interventional studies however, C17 had no effect on neutrophil or monocyte recruitment (Figure. 4.9 B-D). The reason for this could be due to instability of the peptide. It is possible that the peptide was rapidly degraded in the inflammatory environment before it could exert any significant effects.

Acetylation and PEGylation are established strategies for the stabilisation of peptides for *in vivo* delivery [360]. I explored acetylating the N-terminus of the C17 peptide. Using the ChemR23 transfected CHO-K1 cell system, I saw no functional difference in potency between the acetylated and non-acetylated C17 peptide in β-arrestin recruitment (Figure 4.10D). When the acetylated C17 peptide was administered in interventional ZIP experiments, there was a modest but significant decrease in total cell recruitment at the tested dose but no significant differences in total monocytes or neutrophils (Figure. 4.9A-C). It is possible that higher doses of the peptide are required to be effective. Alternatively, acetylation at the N-terminus alone may not be sufficient to stabilise the peptide. Using Expasy peptide cutter software (http://web.expasy.org/cgi-bin/peptide_cutter/peptidecutter.pl), neutrophil derived elastase and chymotrypsin are predicted to cleave further nearer the C-terminus end of the peptide, not only at the N-terminus. Hence, further stabilisation may be required, although modifications nearer the C-terminus could in turn affect the affinity of the peptide for the ChemR23 receptor.

Given the anti-inflammatory effects of full-length chemerin in these interventional studies at 16 hours, I extended these studies by performing interventional experiments at different time points and using the 500 ng dose of chemerin (Figure. 4.11). At 4 hours, I observed no differences in cell recruitment in chemerin treated

animals compared to vehicle treated animals (Figure. 4.11A-C). The anti-inflammatory effects only seem to manifest at later time points. I did observe significant decreases in monocyte numbers at 48 hours post zymosan challenge similar to what I observed at 16 hours (Figure. 4.11B). At 48 hours, chemerin treated animals had ~49% less monocytes/macrophages compared to vehicle treated animals ($272 \pm 0.4 \times 10^5$ monocytes in chemerin treated animals compared to $532 \pm 0.5 \times 10^5$ monocytes in vehicle treated animals) (Figure 4.11B). There was no difference in neutrophil numbers at any time point during these experiments.

In order to investigate whether chemerin intervention was decreasing local chemokine and cytokine production I measured a number of mediators in the peritoneal exudate fluid from 4-hour interventional experiments using Luminex and ELISA. I chose this time point because from my characterisation of this model in the previous chapter I observed that most mediators peak at 4 hours or before (Figure. 3.6). Chemerin intervention significantly ($P \leq 0.05$) reduced CCL4 levels in the cavity from $1,396 \pm 108$ pg/ml in vehicle treated animals to 983 ± 110 pg/ml in chemerin treated animals (Figure 4.12C). However chemerin treatment did not significantly affect any other mediator measured. There was a possible trend towards decreased IL-10 and MMP-9 levels in chemerin treated animals compared to vehicle treated although this was not significant (Figure 4.12D). CCL4 is a well-established monocyte chemoattractant, which signals via the CCR5 receptor [361-363]. There is also a large amount of CCL4 generated in the peritoneum post zymosan challenge (Figure. 3.6E). Although this decrease in local CCL4 levels probably contributes to the decrease in monocyte numbers in chemerin treated animals it seems likely that there may also be other contributing factors.

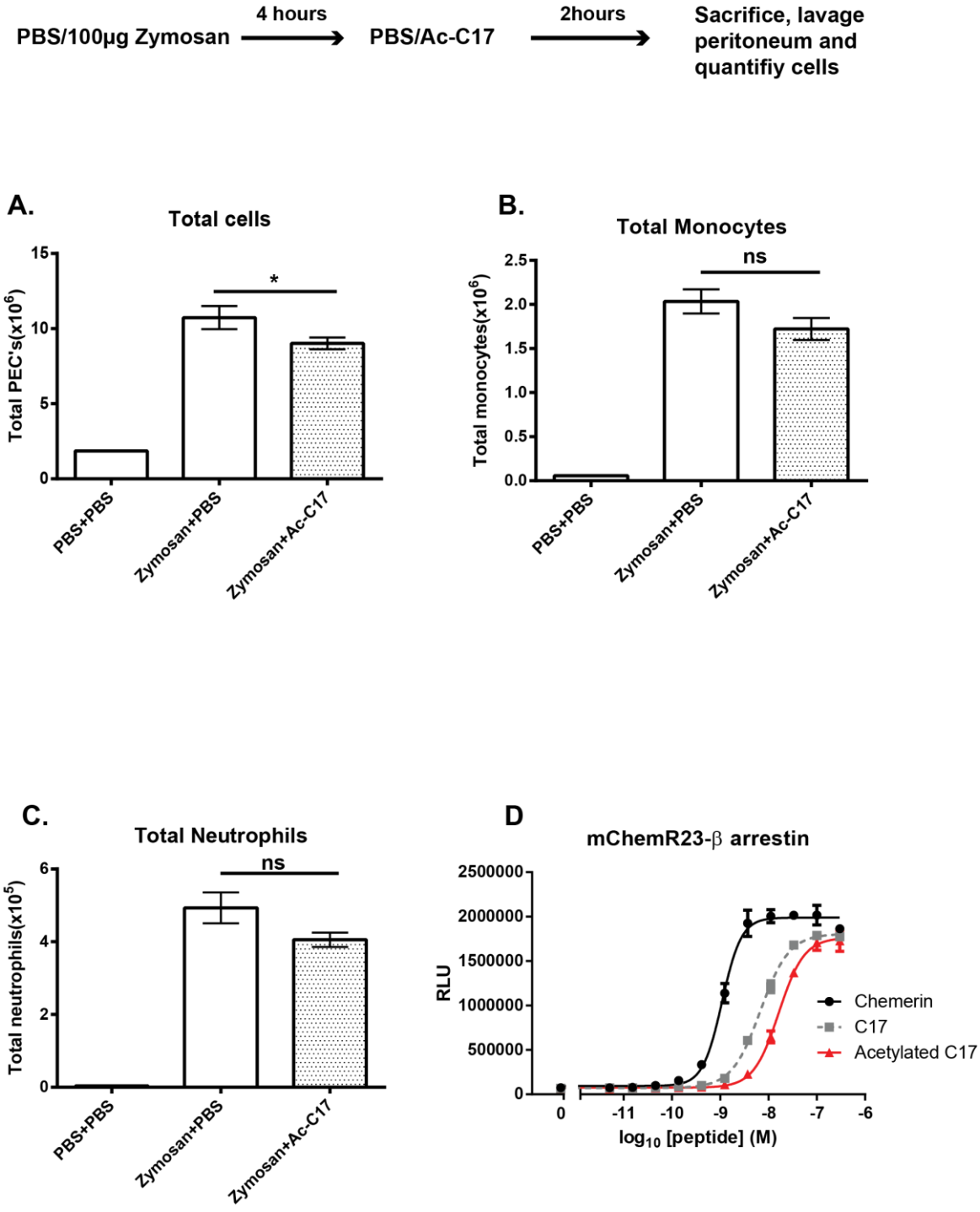


Figure 4.10 Acetylated C17 peptide does not decrease monocyte or neutrophil recruitment in 6 hour ZIP.

A.-C. 8-12 week old male C57Bl/6J mice were injected i.p. with 100 µg zymosan and 4 hours later with a second injection of PBS or 3µg Ac-C17 for a further 2 hours. Animals were sacrificed. Peritoneal cavities were lavaged with ice cold PBS supplemented with 2mM EDTA. Cell populations were quantified using flow cytometry.**A**. Total cells. **B.** Total monocytes. **C.** Total Neutrophils. Error bars represent S.E.M of 1-13 animals/group and 2 separate experiments. Significance was assessed using a students unpaired T-test. * $P \leq 0.05$. **D.** β-arrestin recruitment to the ChemR23 receptor was measured in ChemR23 transfected CHO-K1 cells. Error bars represent S.D 2 technical replicates

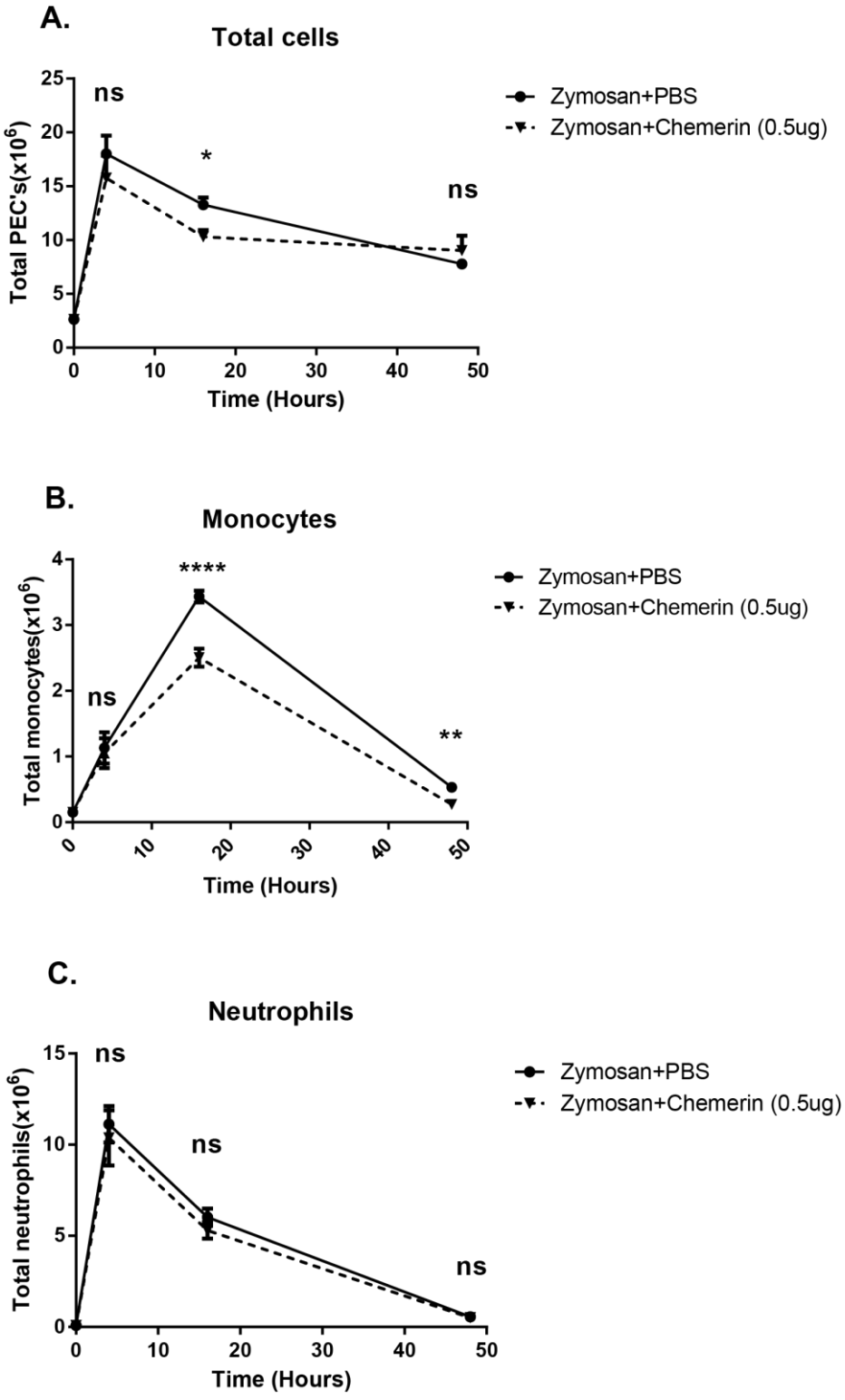


Figure 4.11 Chemerin intervention decreases monocyte numbers in ZIP.

8-12 week old male C57Bl/6J mice were injected i.p. with 100 µg zymosan or PBS and 2 hours later mice were injected with chemerin (500ng) or PBS. Mice were sacrificed at 4, 16 and 48 hours after initial zymosan injection. Peritoneal cavities were lavaged with ice cold PBS supplemented with 2mM EDTA. Cell populations were quantified using flow cytometry. **A.** Total cells **B.** Total monocytes **C.** Total neutrophils recruited to peritoneum. Error bars represent S.E.M. 5-20 animals/group. Statistical significance was assessed by One-way ANOVA and Dunnetts post hoc test. * $P \leq 0.05$. **$P \leq 0.01$. *** $P \leq 0.001$.

In order to confirm that chemerin was indeed being proteolysed to shorter peptides during these interventional ZIP experiments, I used mass spectrometry to attempt to identify these peptides from the *in vivo* peritoneal exudate fluid. Unfortunately, due to the large amount of proteins produced in the peritoneal cavity during peritonitis, the dynamic range of these samples was too large to allow detection of any chemerin peptides or even endogenous chemerin. I tried a number of different workflows to purify the samples but this strategy proved challenging. Instead, I switched to an *in vitro* system to address this question.

I incubated recombinant murine chemerin, which I had been injecting in our interventional studies with recombinant neutrophil derived elastase and cathepsin-g (both of which have been reported to process inactive pro-chemerin to active chemerin) [175, 176]. I incubated these samples for different times at 37°C. Samples were desalted using a C18 column and run on a LC-MS/MS QExactive mass spectrometer. Results were analysed using Mascot software. After incubation with neutrophil derived proteases, a number of peptides were identified as quickly as 1-hour after incubation (Figure 4.13A). Some of these peptides were from the middle and N-terminus of the protein. These regions are not thought to induce signalling at any of the chemerin receptors. However, there were a number of C-terminus derived peptides detected, including a 13 amino acid peptide called C13 which is also active at the ChemR23 receptor with similar potencies to the C17 peptide. Interestingly it was this C13 peptide that was the most abundant during these experiments (Figure. 4.13B).

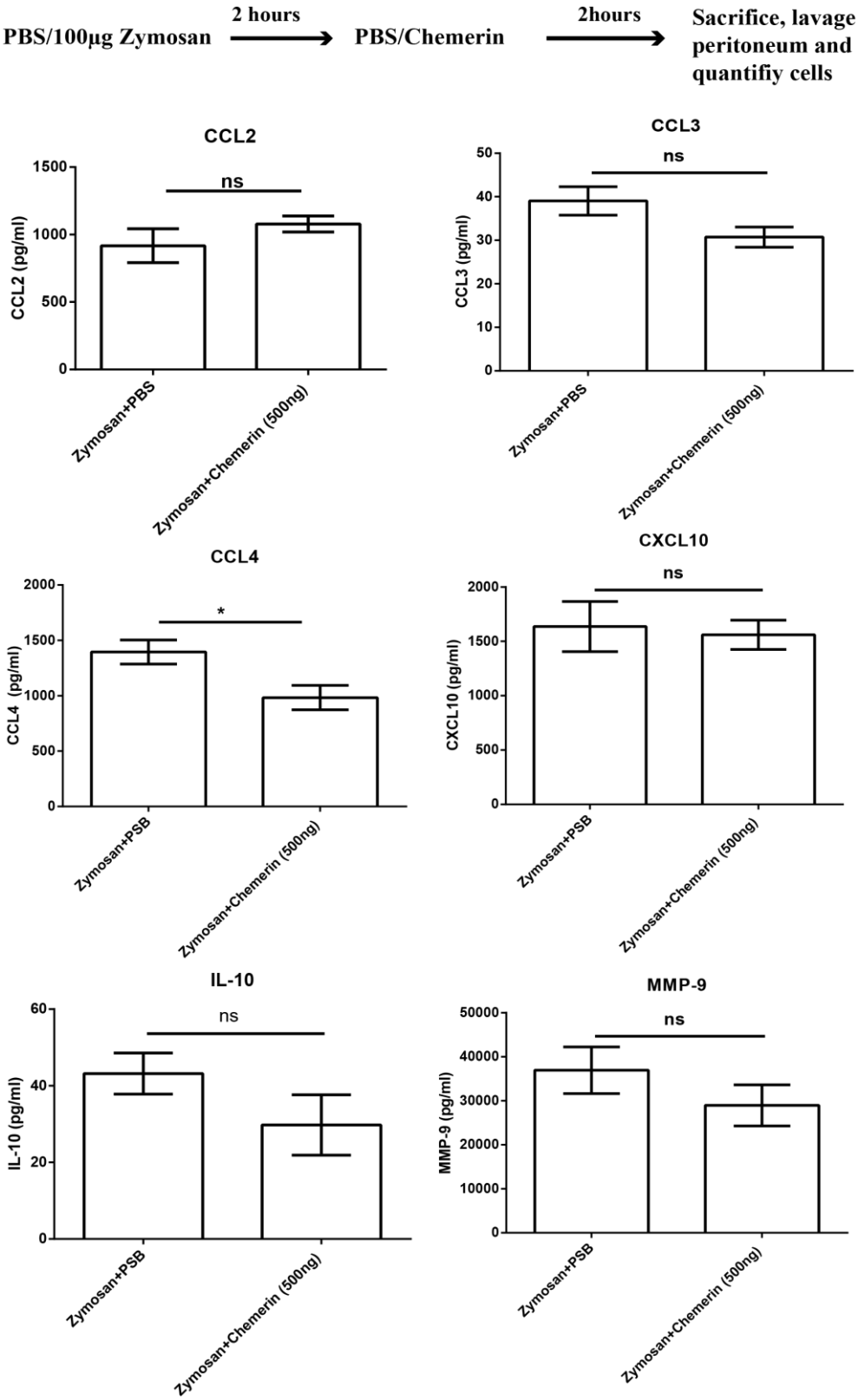


Figure 4.12 Chemerin intervention decreases local CCL4 levels.

8-12 week old male C57Bl/6J mice were injected i.p. with 100 µg zymosan or PBS and 2 hours later mice were injected with chemerin (500ng) or PBS. Mice were sacrificed at 4 hours. Peritoneal cavities were lavaged with ice cold PBS supplemented with 2mM EDTA. Peritoneal exudate fluid was collected and indicated mediators were measured using ELISA (**A.**) or Luminex (**B.-F**.). Error bars represent S.E.M. 7-9 animals/group. Statistical significance was assessed using a students unpaired T-test. * $P \leq 0.05$.

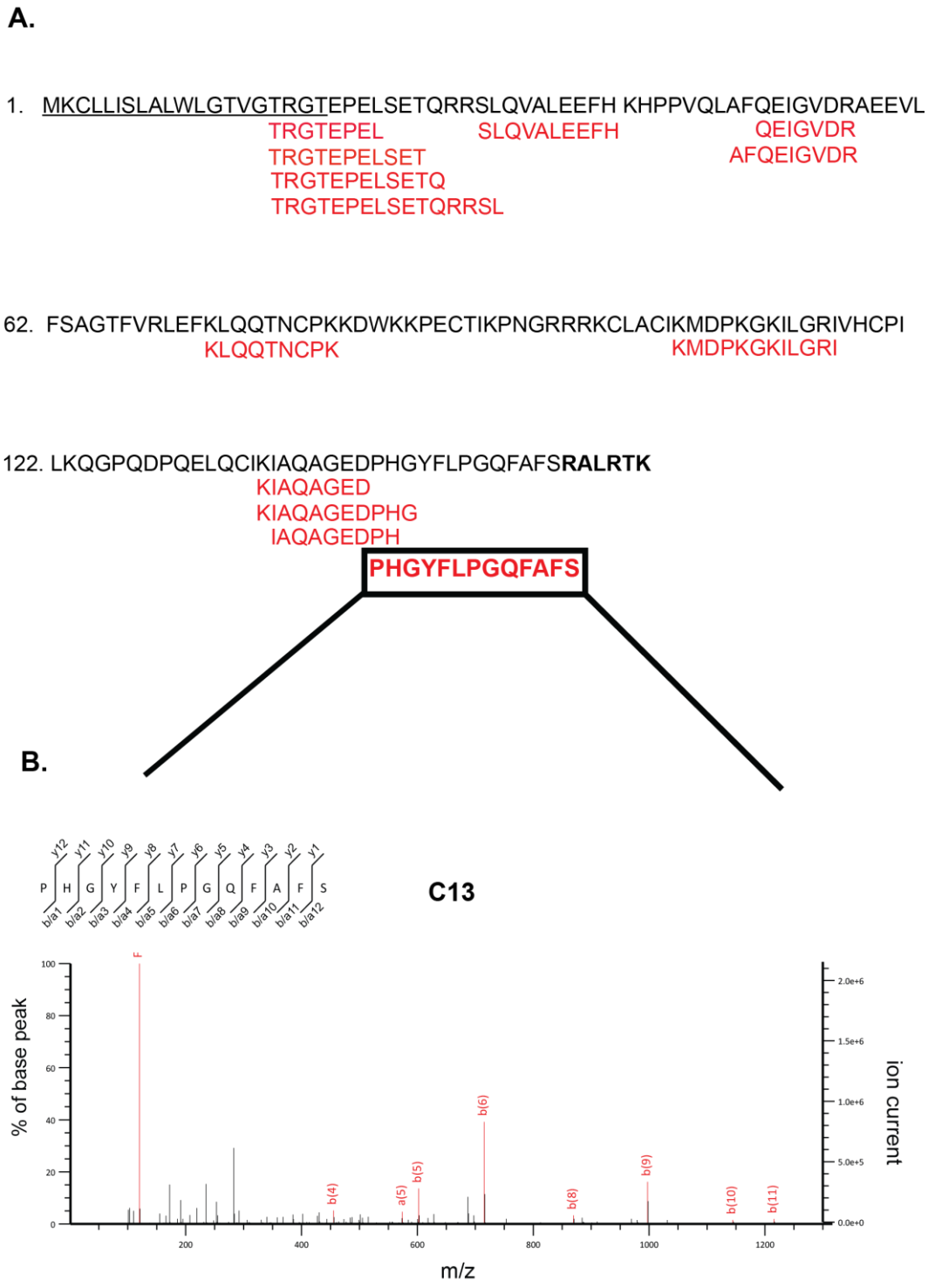


Figure 4.13 Recombinant human neutrophil elastase and cathepsin-g cleave recombinant chemerin to shorter bioactive peptides *in vitro.*

A. 500 ng murine chemerin was incubated in HBSS at 37°C for 1 hour in the presence of 500 µunits recombinant human elastase and 1.3 munits of human cathepsin-g. Samples were desalted using a C18 reverse-phase tip packed in a pipette tip and then run on a LC-MS/MS QExactive mass spectrometer (Thermo) coupled to a RSLCnano HPLC system (Dionex). Data were analysed using Mascot and searched against the Uniprot Mus reference proteome, with the precursor mass tolerance set at +/- 20ppm, fragment tolerance +/-0.02 Da with no enzyme specificity defined. **A.** Chemerin FASTA sequence is in black. Signal sequence is underlined. Inactive sequence of pro-chemerin denoted in **bold**. Identified peptides are denoted in red. **B.** Chromatogram of the detected C13 peptide.

4.4.6 Endogenous chemerin levels increase *in vivo* during inflammation.

The experiments presented in this chapter have addressed the effects of exogenous chemerin and chemerin peptide treatment *in vivo* and on isolated macrophages. An important question that remained to be addressed was what happened to endogenous chemerin levels during inflammation. I began by measuring endogenous chemerin levels in the peritoneum during ZIP. I used the chemerin ELISA from R&D during these experiments. Unlike other mediators I measured in the peritoneum during ZIP, there were detectable levels of chemerin (1.2 ± 0.4 ng/ml) in the naïve cavity under basal conditions (Figure. 4.14A). Two hours after the onset of inflammation, chemerin levels increased to 3.6 ± 0.7 ng/ml (Figure. 4.14A). Chemerin levels then dropped back near basal levels by 4 hours and remained relatively stable. It should be noted that this ELISA kit can detect inactive pro-chemerin as well as active chemerin which makes accurate quantification of bioactive chemerin more challenging. In addition, this ELISA does not detect shorter bioactive chemerin derived peptides.

Because of these limitations, I developed a bioassay to measure activation of the ChemR23 receptor. Using CHO-K1 cells stably transfected with tagged ChemR23 and β-arrestin (the same system used in Figure. 4.4E.), I investigated chemerin bioactivity of the peritoneal exudate fluid. Using this system, chemerin bioactivity increased after the onset of inflammation and remained high until 96 hours at which point it returned to baseline (Figure. 4.13B). While this is not a very quantitative measure of chemerin levels, given there are currently no commercially available reagents that can specifically measure active chemerin, this method does provide an estimate of active chemerin and chemerin peptide abundance *in vivo*.

Chemerin is known to circulate in the bloodstream at relatively high levels [172, 233]. Therefore, I also measured chemerin levels by ELISA in plasma of mice from the

ZIP studies. Chemerin levels in plasma were 67.5 ± 2.8 ng/ml (Figure. 4.13C). This increased to 73.9 ± 4 ng/ml by 4 hours and then decreased back to baseline. I did not observe statistically significant changes in chemerin levels in plasma during zymosan challenge.

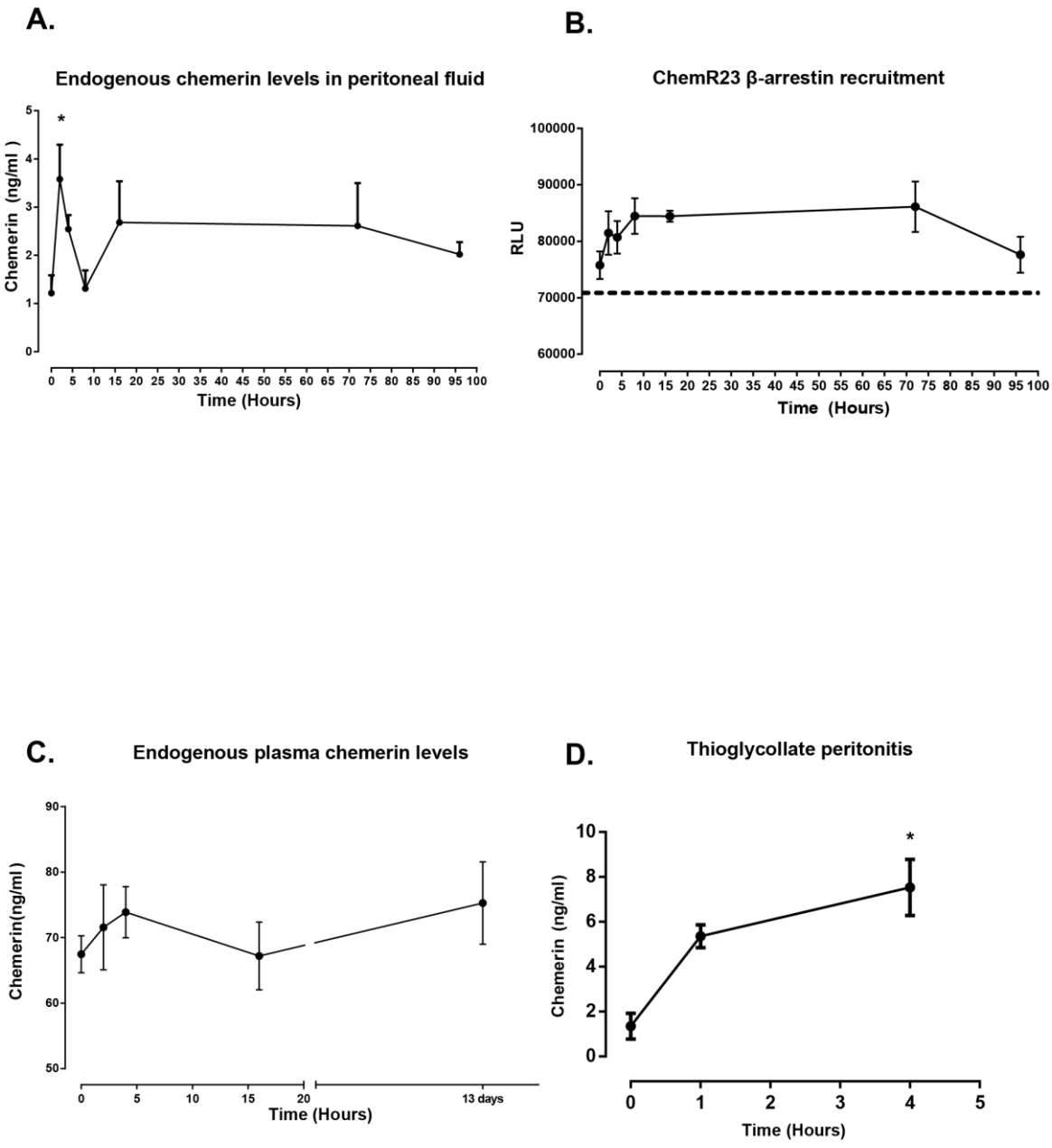


Figure 4.14 Endogenous chemerin levels increase during inflammation.

8-12 week old Male C57Bl/6J mice were injected with 100 µg zymosan. Animals were sacrificed at indicated time points. Peritoneal cavities were lavaged with ice cold PBS supplemented with 2mM EDTA. **A.** Peritoneal exudate fluid was collected and chemerin levels were measured by ELISA. **B.** β-arrestin recruitment in ChemR23 transfected CHO-K1 cells was measured in supernatant as a measure of chemerin bioactivity. Bioactivity was measured as relative light units (RLU). Dashed line indicates background**.** Whole blood was collected into EDTA coated vacutaners and plasma was collected after centrifugation. **C.**Plasma chemerin levels were measured by chemerin quantikine kit. **D.** Animals were injected with 4% thioglycollate. PEC fluid was collected and chemerin levels were measured at indicated time points. Error bars represent S.E.M of at least 2 separate experiments. **A.**10-13 animals/time point. **B.** 4 animals/time point. **C.** 6-11 animals/time point. **D.** 5-9 animals/time point. Statistical significance was assessed using one-way ANOVA with Dunnetts post hoc test.* $P \leq 0.05$.

In order to assess whether chemerin levels increase in a similar manner in response to other inflammatory stimuli, I measured chemerin levels in the peritoneal cavities of animals that received 4% thioglycollate i.p. over a time course. Thioglycollate is a well-established inflammatory agent that results in robust neutrophil recruitment by 4 hours followed by a large macrophage population at later time points (typically 4-5 days) [291, 292]. Similarly to previous experiments, naïve animals had ~1.3 ± 0.6 ng/ml chemerin in the peritoneum before challenge. After thioglycollate injection, chemerin levels increased rapidly to 7.5 ± 1.3 ng/ml by 4 hours (Figure. 4.14 D).

From these studies, I have shown that endogenous chemerin levels in the peritoneum are already present (presumably pro-chemerin) at nanogram quantities and during an inflammatory insult chemerin levels rapidly increase 4-7 fold depending on the inflammatory stimulus (Figure 4.14 A and D). These increases seem to be less dramatic systemically during ZIP, which may reflect non-specific detection reagents as discussed earlier. Alternatively, 100 μg zymosan may not induce large systemic changes as compared to more severe insults such as higher doses of zymosan, thioglycollate or LPS [291, 341, 364].

As shown, chemerin levels increase in the peritoneal cavity and in the blood during ZIP (Figure 4.14 A-C). Dexamethasone is the anti-inflammatory control I have used throughout these experiments. Because this is an established anti-inflammatory drug, I decided to investigate what effects dexamethasone might have on endogenous chemerin levels. Initially I injected dexamethasone or vehicle alone for 24 hours to observe what effect these treatments might have on resting chemerin levels in the peritoneum and in the plasma. Interestingly, dexamethasone

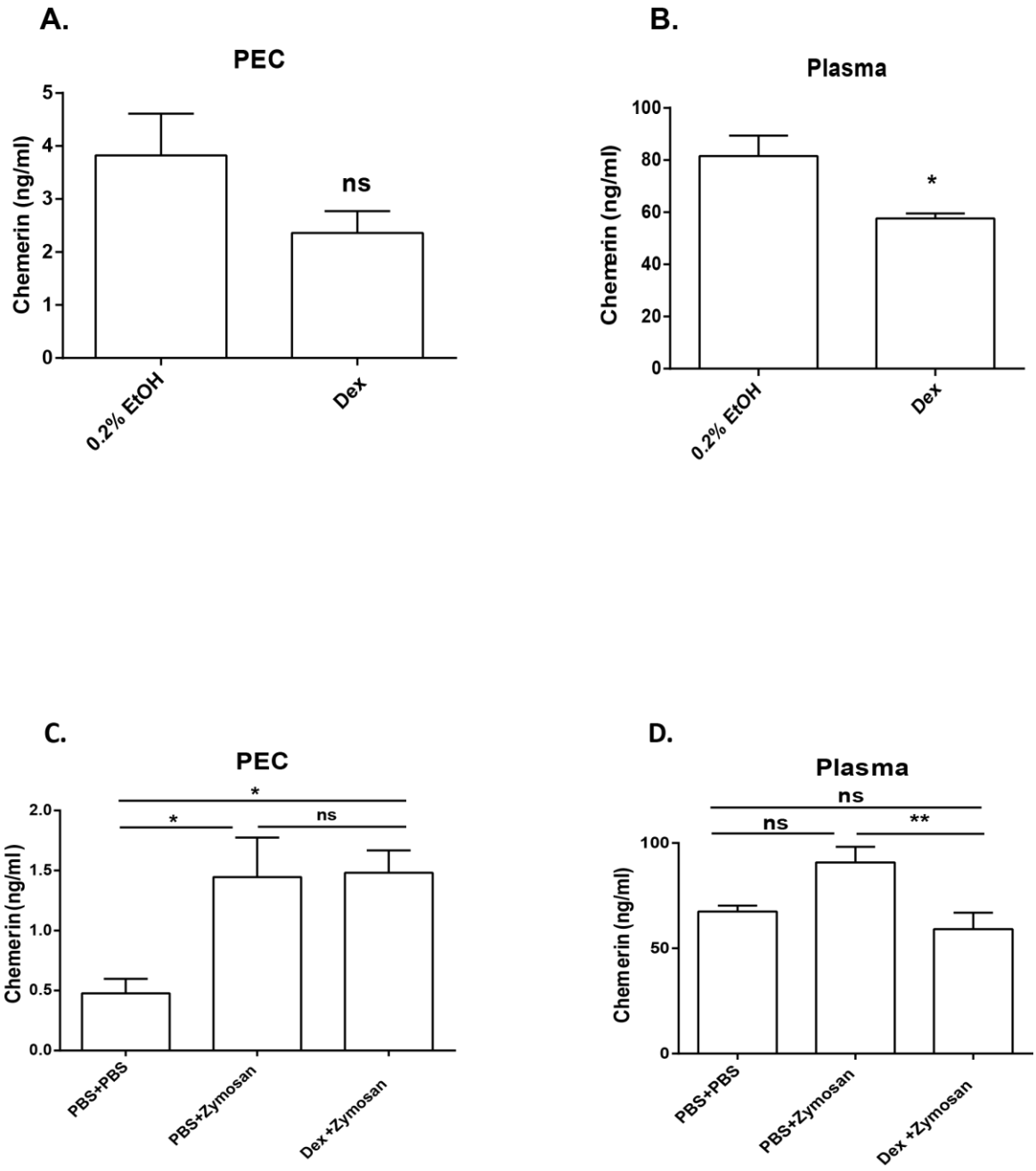


Figure 4.15 Dexamethasone decreases systemic chemerin levels during homeostasis and during inflammation.

8-12 week old male C57Bl/6J mice were injected with vehicle (0.2% ethanol) or dexamethasone at 1mg/kg for 24 hours. Peritoneal cavities were lavaged with ice cold PBS supplemented with 2mM EDTA and blood was collected into EDTA coated vacutainers. Blood was centrifuged and plasma was collected as before. Chemerin levels were measured in peritoneal exudate fluid using ELISA **A.** and in plasma using quantikine ELISA **B.** C57Bl/6J mice were injected with PBS or dexamethasone and 45 minutes later mice were injected i.p. with 100 μg zymosan or PBS. 16 hours later, animals were sacrificed. Peritoneal exudate fluid and plasma was isolated as before. Chemerin levels were measured in peritoneal exudate fluid by ELISA **C.** and in plasma by quantikine ELISA **D.** Error bars represent S.E.M. 5 animals/group. Statistical significance was assessed by a students unpaired T-test (**A** and **B**) or One-way ANOVA and Dunnetts post hoc test. * $P \leq 0.05$. ** $P \leq 0.01$.

treatment significantly ($P \leq 0.05$) decreased chemerin levels in plasma (from 81.6 ± 7.8 ng/ml in vehicle treated animals to 57.6 ± 4.8 ng/ml in dexamethasone treated animals) (Figure 4.15B). There was a similar trend in peritoneal levels, although this did not reach significance (P value = 0.1126) (Figure 4.15A).

I also investigated effects of dexamethasone treatment on chemerin levels during inflammation. Zymosan challenge increased chemerin levels in the peritoneum (Figure 4.15 C). Pre-treatment of dexamethasone did not alter local chemerin levels. Zymosan challenge also increased chemerin levels in plasma from 67.5 ± 2.8 ng/ml to 90.8 ± 7.4 ng/ml and pre-treatment with dexamethasone significantly decreased these levels to 59.1 ± 7.8 ng/ml (Figure 4.15 C).

The fact that dexamethasone decreases systemic chemerin levels is an interesting and previously unreported observation. Particularly as chemerin increases during the onset of inflammation and has been reported to play pro-inflammatory roles in a number of pathologies, this may hint at a novel mechanism by which dexamethasone reduces inflammation [206, 214, 233].

4.4.7 The effects of knockdown of endogenous chemerin *in vivo.*

As shown, chemerin levels increase in the peritoneum during the onset of inflammation as well as in the blood. The glucocorticoid dexamethasone decreases chemerin levels. Following on from these observations, I was interested in knocking down chemerin expression *in vivo* to investigate what effect this might have on the inflammatory responses we have observed so far. At the time of writing, there were no chemerin KO animals commercially available. As an alternative, I collaborated with ISIS pharmaceuticals. They kindly supplied me with a number of anti-sense oligonucleotides

(ASO) against chemerin as well as control oligonucleotides. In order to decrease chemerin levels systemically I used a 4-week dosing regime of one subcutaneous injection of anti-chemerin or control ASO once a week. At the end of this treatment, I performed a 4-hour challenge with 100 μg zymosan and measured chemerin levels as well as inflammatory cell recruitment to the peritoneum and to the blood.

When I quantified cell recruitment to the peritoneum, there were no significant differences between control ASO treated animals and chemerin ASO treated animals at 4 hours post zymosan. Control ASO animals had $0.45 \pm 0.1 \times 10^6$ monocytes compared to $0.40 \pm 0.1 \times 10^6$ monocytes in chemerin ASO animals (Figure 4.16). Similarly, control ASO animals had $5.0 \pm 0.7 \times 10^6$ neutrophils while chemerin ASO treated animals had $5.5 \pm 0.5 \times 10^6$ neutrophils. I ran a Luminex assay to measure a number of inflammatory cytokines and chemokines in the peritoneal exudate from these animals but observed no obvious differences between the two groups (Figure 4.17). Given that I did not observe any differences in cell recruitment to the cavity, this was not surprising. When I measured chemerin levels in the cavity of these animals, the chemerin ASO did not completely inhibit chemerin expression, although it did significantly decrease it ($P \leq 0.001$) (Figure 4.16 B). Chemerin ASO decreased chemerin levels in the peritoneum from 3.4 ± 0.3 ng/ml in control ASO animals to 1.0 ± 0.1 ng/ml in chemerin ASO treated animals. Hence, there is the possibility that although decreased, there was enough chemerin in the cavity to at least partially perform its function.

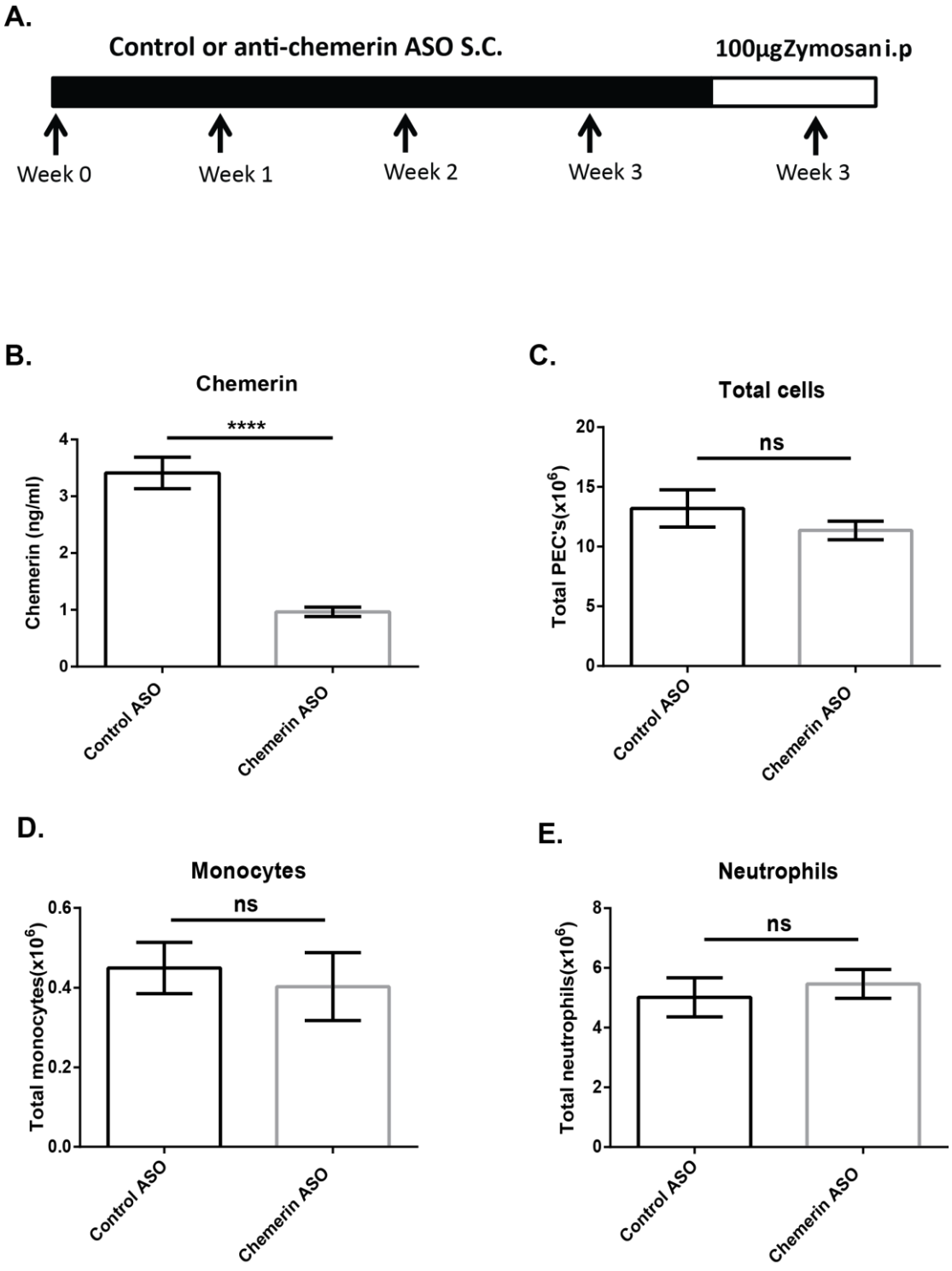


Figure 4.16 Knock down of chemerin expression *in vivo* has no effect on inflammatory cell recruitment during zymosan induced peritonitis.

A. Dosing regime used for anti-sense oligonucleotide (ASO) treatments. 8 week-old male C57Bl/6J mice were dosed subcutaneously once a week with 25mg/kg of either control ASO or anti-chemerin ASO for 4 weeks. After the fourth week, animals were injected i.p. with 100 µg zymosan and 4 hours later animals were sacrificed. Peritoneal cavitIes were lavaged with ice cold PBS supplemented with 2mM EDTA. **B.** Chemerin levels were measured by ELISA in the PEC fluid. **C.** Total cells were quantified using an automated cellometer. **D**. Total monocytes were quantified using flow cytometry. **E.** Total neutrophils were quantified using flow cytometry. Error bars represent S.E.M of 8 animals/group. Statistical significance was assessed by a students unpaired t test. **** $P \leq 0.0001$.

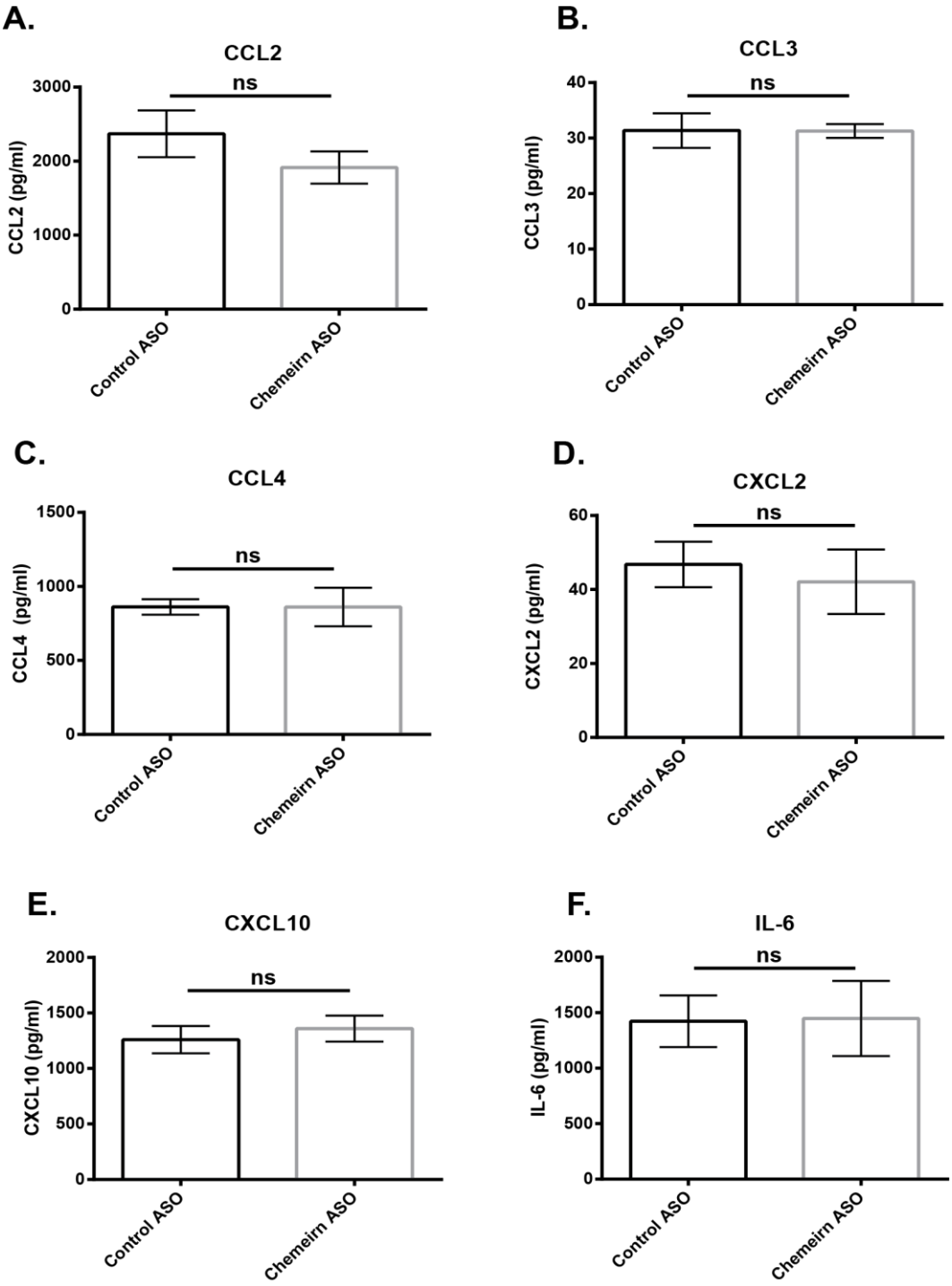


Figure 4.17 Knock down of chemerin expression *in vivo* has no effect on inflammatory mediator production during zymosan induced peritonitis.

8 week-old male C57Bl/6J mice were dosed subcutaneously once a week with 25mg/kg of either control ASO or anti-chemerin ASO for 4 weeks. After the fourth week, animals were injected i.p. with 100 µg zymosan and 4 hours later animals were sacrificed. Peritoneal cavites were lavaged with ice cold PBS supplemented with 2mM EDTA. Indicated mediators were measured using a Luminex assay. Error bars represent S.E.M of 8 animals/group. Statistical significance was assessed by a students unpaired t-test.

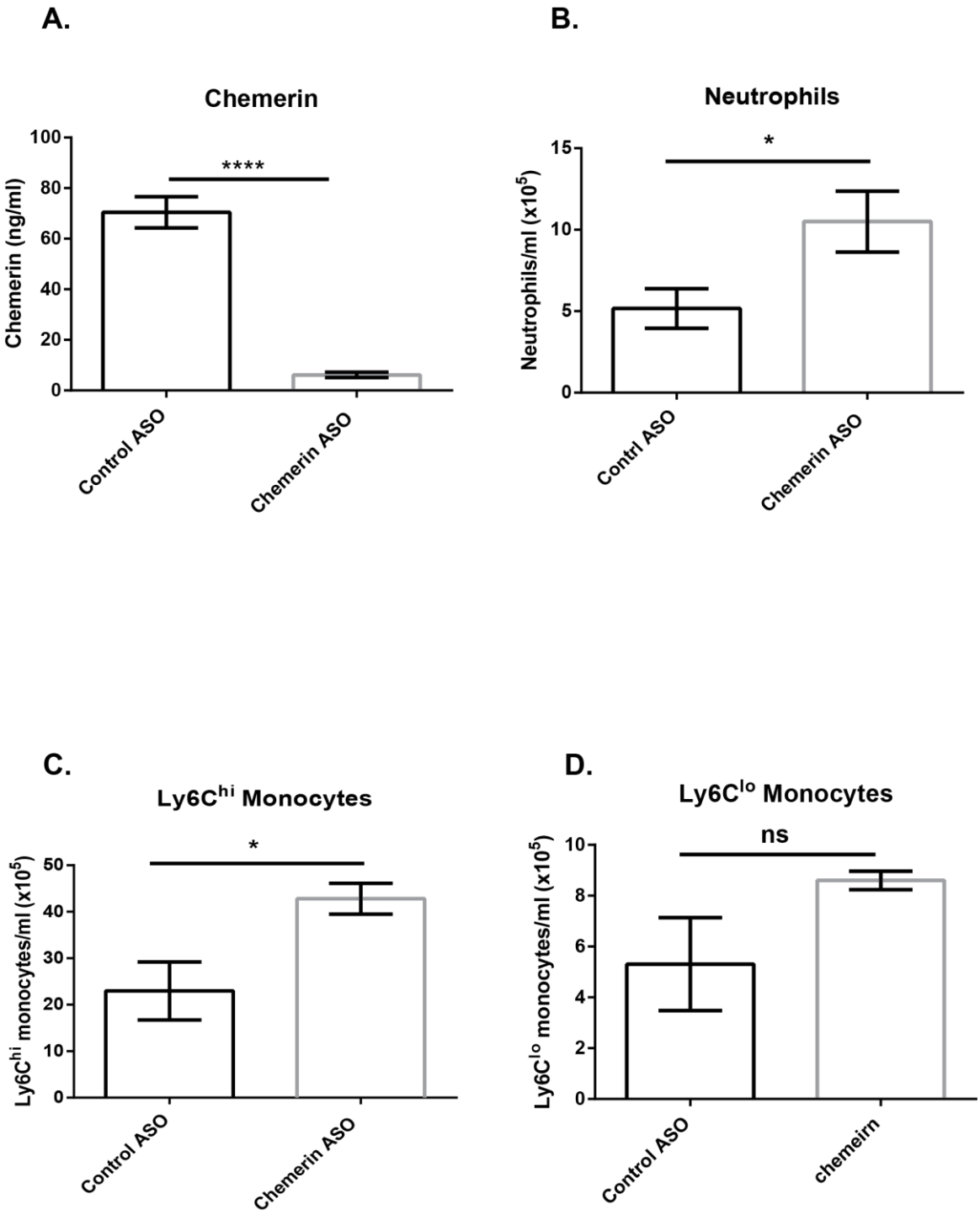


Figure 4.18 Knock down of chemerin expression *in vivo* increases neutrophil and Ly6C^{hi} monocyte numbers in the blood during zymosan induced peritonitis.

8 week-old male C57Bl/6J mice were dosed subcutaneously once a week with 25mg/kg of either control ASO or anti-chemerin ASO for 4 weeks. After the fourth week, animals were injected i.p. with 100 µg zymosan and 4 hours later animals were sacrificed. Blood was collected into EDTA coated vacutainers. Cells were counted using counting beads and cell populations were quantified by flow cytometry. Error bars represent S.E.M of 8 animals/group. Statistical significance was assessed by a students unpaired t-test.

In contrast, there were evident changes in cell numbers in the blood of these animals. Firstly, chemerin levels were reduced from 70.5 ± 6.2 ng/ml in control ASO treated animals to 6.2 ± 1 ng/ml in chemerin ASO treated animals (Figure 4.18A). When chemerin expression was reduced systemically, I observed significantly higher numbers of neutrophils in the blood of chemerin ASO treated animals compared to control ASO treated ($P \leq 0.05$). Control ASO animals had $4.3 \pm 1.0 \times 10^5$ neutrophils/ml compared to $9.6 \pm 1.4 \times 10^5$ neutrophils/ml in chemerin ASO treated animals (Figure 4.18 B). There was also a significant increase ($P \leq 0.05$) in $Ly6C^{hi}$ inflammatory monocytes with control ASO animals having $23.0 \pm 6.2 \times 10^5$ monocytes/ml compared to $41.3 \pm 3.5 \times 10^5$ monocytes/ml (Figure 4.18C). This was a 45% increase. There was no difference in the $Ly6C^{lo}$ monocyte subset between groups (Figure 4.18D).

4.5 Discussion

4.5.1 Characterisation of the chemoattractant properties of chemerin and chemerin derived peptides *in vitro.*

The overall aim of the first part of this chapter was to investigate the biological properties of chemerin and C-terminal derived chemerin peptides on macrophages. I began by analysing the composition of our Bio-gel elicited peritoneal exudate cells. By flow cytometry, percentages of macrophages were lower than expected and there was a large population of neutrophils (by F4/80 and 7/4 staining) (Figure 4.1A). However, neutrophils do not express the ChemR23 chemerin receptor (Figure 4.1B), nor do they score in the real time chemotaxis system while Bio-gel elicited macrophages did express the ChemR23 receptor (Figure 4.1B) [199, 351]. I investigated using other sources of primary murine macrophages, however Bio-gel elicited macrophages were the most

appropriate. Thioglycollate elicited macrophages did not migrate efficiently probably due to their activated state [292]. Bone marrow derived macrophages did migrate but there was a very high background. Resident peritoneal macrophages migrated to a similar degree to Bio-gel macrophages. However, the numbers of resident macrophages obtained per mouse (~1.5 x 10^6) was prohibitive for use in these experiments [199].

Bio-gel macrophages migrated efficiently to both murine and human full-length chemerin. Human chemerin actually induced higher migration than murine chemerin in terms of overall max-min migration. At equivalent doses both C9 and C17 induced very little if any migration in this system. These results are not surprising given previously published reports by Wittamer *et al.* which first characterised the C9 peptide. Using an aequorin based calcium release assay in ChemR23 transfected cells, they reported the shorter chemerin derived peptides induced calcium release but required higher concentrations than the full-length protein [177].

Chemerin has previously been reported to induce potent adhesion of murine macrophages as has the chemerin peptide C9. However, the effects of other chemerin derived peptides on macrophage adhesion have not been investigated [177, 198]. Furthermore, the study by Wittamer *et al.* used transfected cell lines rather then primary cells [177]. In order to investigate whether the C9 and C17 peptides induced similar effects on primary murine macrophages I validated and optimised the ACEA SP system. This is a platform that detects electrical impedance of current through a 96 well plate. The more cells that adhere to the plate or the more surface area covered by cells, the greater the signal. I validated the system using a range of known chemoattractants including CCL2, CCL5, chemerin and fMLP [157]. The advantage of this system over static adhesion microscopy assays is that it allowed me to monitor responses of primary

unlabelled cells to different agonists in real time, which yields more information and higher throughput than older methods.

The utility of this system as a platform for the screening for novel receptor antagonists is highlighted by the use of CCR2 transfected CHO-K1 cells and a CCR2 antagonist (CCX417) kindly provided by ChemoCyntryx. CCR2 has been reported to play a key role in the recruitment of monocytes to atherosclerotic plaques and CCR2 antagonists (including CCX417) have shown very promising results in a number of pre-clinical disease models as well as in clinical trials [162, 355, 365]. Given the importance of this receptor as a therapeutic target and the published literature using antagonists, it was an obvious receptor to use as a proof of concept in this system. Although this 96 well platform does not qualify as high throughput from an industrial point of view, it does allow for the screening of a large number of potential active compounds per plate. CCX417 did not inhibit primary Bio-gel macrophage responses to CCL2 in this system. This was surprising given previously published results showing the efficacy of this antagonist *in vivo* [355]. One explanation for this discrepancy could be the higher expression levels of CCR2 in transfected CHO-K1 cells compared to primary Bio-gel macrophages or expression of other CCL2 receptors such as CCR4.

Having characterised and validated this electrical impedance-sensing platform, the aim was to use this technology to interrogate the biology of the C-terminus derived chemerin peptides C9 and C17. In contrast to the observed responses in the real time chemotaxis system, both C9 and C17 induced higher increases in impedance compared to full-length murine chemerin (Figure 4.5B). This was interesting given that these peptides induced less chemotaxis and less β-arrestin recruitment compared to the full-length murine protein (Figure 4.1D-E and 4.5E). This differential signalling between the full-length protein and shorter peptides are reminiscent of annexin-a1 and the shorter

annexin peptide Ac2-26. While both the full-length protein and the Ac2-26 peptide induced anti-inflammatory effects *in vivo,* the Ac2-26 peptide induced potent migration of human neutrophils while the full length protein did not (due to Ac2-26 being capable of activating FRP1 receptor) [366].

This observation with chemerin and chemerin peptides was reproducible and implies a potential difference or biased agonism in the induced signalling downstream of the ChemR23 receptor. It has been reported previously that the C9 peptide is a more potent inducer of adhesion of ChemR23 transfected CHO-K1 cells to fibronectin (although it did not seem to be a full agonist compared to the full-length protein) [198]. In my experiments using the same source of primary murine macrophages, I observed that at the doses tested both C9 and C17 induced greater adhesion compared to full-length chemerin (Figure 4.5 B-C). In the previous study, macrophage adhesion to fibonectin and VCAM-1 was reported to be due to integrin clustering and inhibition of cytoskeletal rearrangements had no effect on chemerin-stimulated adhesion. These results contrasted with what I have seen using the electrical impedance system. However there are a number of probable reasons for the discrepancies. Firstly, I did not coat the plate with fibronectin or VCAM-1 in these experiments. Adhesion of macrophages to gold electrodes and plastic rather than biological substrates may change their phenotype and the downstream signalling pathways induced [367, 368].

In addition, the assays themselves differed in what they were addressing. The previously reported assay incubated macrophages with chemerin and chemerin peptides before adding the cells to a pre-coated 96 well plate for 1 minute. The plate was then washed and adherent cells measured by a cell viability assay. In the electrical impedance assay, cells were allowed to adhere in a 96 well impedance plate until there were no further increases in impedance (indicating maximum adherence was reached). After this

time, cells were then challenged with chemerin or chemerin peptides and further increases in impedance were measured every 5 seconds over a period of at least 1 hour. Cytochalasin D had no effect in the adhesion assay used previously but completely inhibited responses of the same cells in the impedance assay. Therefore, it seems that the initial adhesion of macrophages to fibronectin and VCAM-1 does not require cytoskeleletal rearrangements but once adhered, further tight adhesion does [6, 198]. Further experiments using blocking antibodies against integrin subunits would be required to confirm this. This is in line with published literature that integrins and selectins are sufficient for initial rolling of leukocytes on inflamed endothelium but further tight adhesion generally requires cytoskeletal rearrangements [6]. One other difference between my experiments and this previous report is the purity of the macrophage populations obtained by Bio-gel injection. In the initial characterisation using polyacrylamide beads as an eliciting agent for macrophages, Fauve *et al.* reported ~60% macrophages recovery [352]. From previous studies in our laboratory, Hart *et al.* and Taylor *et al.* obtained ~30-40% monocyte/macrophages which was in line with my observations [198, 351]. While I did observe ~40% neutrophils in Bio-gel PECs, neutrophils do not seem to express surface ChemR23 so it seems unlikely they contributed a significant signal in these assays [198].

4.5.2 Bioactivity of chemerin and chemerin peptides in inflammatory activation assays.

Another important aspect to the biology of chemerin and chemerin peptides is their potential anti-inflammatory properties. Having examined the ability of both chemerin and chemerin-derived peptides to induce chemotaxis and adhesion of primary murine macrophages I next examined their anti-inflammatory effects on macrophages. I used

bone marrow derived macrophages for inflammatory activation assays in which the percentage of F4/80^{hi} macrophages was consistently above 85% (Figure. 4.6A).

There have been a number of conflicting reports regarding the effects of chemerin and chemerin derived peptides on macrophage activation [225, 237]. From my experiments, I observed equally unclear results. In a number of experiments the C17 peptide completely ablated TNF-α production in response to LPS and interferon-γ while in others it had no effect whatsoever (Figure. 4.6A-B and Table 4.1). Similarly, full-length chemerin at picomolar concentrations decreased TNF-α production in a number of experiments but not in others. The reasons for these contrasting results remain unclear. I investigated a number of sources for possible variation in the system such as initial seeding density during culture. There was a previous report that different initial seeding densities could alter the macrophage phenotype at day 7 of culture. The authors found that lower seeding densities produced purer populations of mature macrophages while higher initial seeding densities produced higher percentages of Ly6-C^{+ve} immature cells [369]. The higher seeding density cells also produced less inflammatory mediators in response to LPS challenge. I therefore tested the same seeding densities to investigate if this was affecting my results. However, I did not observe significant changes in macrophage phenotype by flow cytometry or inflammatory responses. I therefore ruled this out as a source of variation in these assays.

Another variable, which was difficult to control for, was ChemR23 expression. ChemR23 expression was generally lower on these cells compared to Bio-gel elicited macrophages (Figure 4.7B). Variation in ChemR23 expression between different bone marrow macrophage preparations may account for differences in responses to chemerin and C17. I also tested different solvents for the C17 peptide as well as tested different batches of peptide, neither of which made the anti-inflammatory effects observed with

C17 any more reproducible. The last variable I investigated was the growth factors I was using to differentiate the macrophages. I was using growth media supplemented with 15% supernatant from L929 cells as a source for M-CSF [292, 358]. This is a well-established protocol for the maturation of bone marrow precursors to macrophages. However, because there are a large amount of other growth factors present, it is possible there is some variability between different preparations. Early reports using this method demonstrated distinct populations formed during culture rather then one homogenous population, which could also be a source of variability [370]. However, using recombinant M-CSF did not seem to change the purity of the macrophage populations obtained. Nor did it change ChemR23 expression (Figure 4.5A-B). The overall yield was much lower using recombinant M-CSF rather than L929 supernatant as a source of growth factors for macrophage differentiation. It is possible that the amount of recombinant M-CSF used was insufficient or perhaps other growth factors such as IL-3 are required for optimal bone marrow macrophage proliferation [371].

I subsequently decided to change the stimulus from LPS and interferon-γ to the TLR 3 agonist poly I:C which mimics a viral infection. This decision was due to the expression pattern of ChemR23 specifically on cells that are involved in host anti-viral responses, as mentioned earlier [197, 205, 241]. In addition, previous literature suggests the chemerin/ChemR23 axis plays important anti-inflammatory roles in murine models of viral infections [241, 242]. Initial comparison of responses to poly I:C from macrophages cultured in L929 or M-CSF indicated there to be little difference in TNF-α production between the two different macrophage preparations (Figure 4.7D). Using 10 μg/ml poly I:C, I observed the same variability in the system using C17 as previously.

I concluded that this system was too variable to accurately interrogate anti- or pro-inflammatory properties of chemerin and chemerin peptides. There has been a

number of conflicting reports using different macrophage populations to interrogate chemerin and chemerin peptide effects on inflammation and the variability I have observed in my experiments may be a factor in that [210, 225, 237]. However, if chemerin does modulate inflammation, it seems likely that the effects *in vivo* would be through multiple cell types and their subsequent interactions. One likely candidate are endothelial cells, which have been reported to express ChemR23 and respond to chemerin [187, 243, 359, 372].

4.5.3 The effects of chemerin and C17 peptide on inflammation *in vivo.*

Using *in vitro* assays in order to interrogate the biology of chemerin proved useful in terms of characterisation of the effects that both chemerin and chemerin peptides have on cell migration and adhesion of macrophages. However, inflammatory activation assays using bone marrow derived macrophages did not clarify the effects they may exert on inflammatory responses [225, 237]. Chemerin and chemeirn peptides could also modulate inflammatory responses by signalling via other cell types, therefore I switched to the *in vivo* ZIP model of sterile inflammation. Given the high expression of ChemR23 on resident peritoneal macrophages, dendritic cells as well as on endothelial cells, I hypothesised that pre-treatment of animals with either chemerin or the C17 peptide may modulate the subsequent responses to inflammation [197, 241]. At the time of these experiments, there was evidence to suggest that chemerin could promote anti-inflammatory responses in endothelial cells [243]. Chemerin pre-treatment did not affect monocyte numbers but did increase neutrophil numbers, suggesting chemerin may play a role in the recruitment of neutrophils to sites of inflammation either directly or indirectly (Figure.4.8A-C) [238]. At the time of writing, Lin *et al.* reported that

chemerin administration during dextran sodium sulphate (DSS) induced colitis polarised resident macrophages in the colon towards an M1 phenotype and increased local inflammation [210]. It seems plausible that, similarly to this study, chemerin treatment in our experiments may have synergised with zymosan to promote an M1 phenotype of resident macrophages, which would in turn produce inflammatory mediators. Injection of chemerin alone did not recruit monocyte or neutrophils in my experiments (data not shown and Rosie Hart, D.Phil thesis, 2010). In support of this hypothesis, I did not observe ChemR23 surface expression on circulating nor on recruited neutrophils, and this agrees with previously published reports [198]. It is possible that due to high levels of circulating chemerin in the blood that ChemR23 is present intracellularly and is rapidly internalised.

C17 did not have a large effect on recruitment in these experiments, except for a modest decrease in monocytes at the 50 ng/mouse dose (Figure 4.8E). The fact that I saw different results with a chemerin-derived peptide compared to the full-length protein is similar to the earlier *in vitro* results. These differing results probably stem from different pharmacology and receptor binding. In the context of *in vivo* administration, the amount of available C17 peptide present in the peritoneal cavity may differ from the full-length protein. The chemerin decoy receptor CCRL2 (whose expression is upregulated on endothelial cells and macrophages during inflammation) can bind full-length chemerin at its N-terminus and concentrate it locally whereas the C17 peptide presumably will not be bound by CCRL2 as it lacks this sequence [259, 260]. It is possible that during inflammation, chemerin will be bound and concentrated at a local site of inflammation by CCRL2, while shorter chemerin derived peptides will not.

Given previous reports of anti-inflammatory properties of chemerin derived peptides and the susceptibility of chemerin to proteolytic cleavage (potentially to shorter bioactive peptides), I switched from a pre-treatment to an interventional model. Administration of chemerin at a time point at which there were large numbers of activated neutrophils and proteases in the cavity resulted in significant decreases in monocyte numbers (Figure 4.9B). Furthermore, these effects were observed even at later time points (48 hours) (Figure 4.11B). Looking at local inflammatory mediator production, it was interesting that CCL2 levels remained unchanged, given that the main effects I observed were on monocytes (Figure 4.12A). In fact, the only mediator tested that was significantly different between the two treatment groups was CCL4. CCL4 is a CC chemokine capable of inducing monocyte recruitment and signals predominantly through the CCR5 receptor [373]. CCR5 has been reported to be expressed on circulating murine monocytes [374]. It can also bind to the CCR1 receptor but its binding seems to function to antagonize other ligand binding rather then induce chemotaxis [375]. There is a large body of evidence supporting the importance of synergy between different chemokine receptors and heterodimerisation of receptors in the context of chemotaxis [376, 377]. Furthermore, there have been previous reports of CCR5 and CCR2 heterodimersaition and synergism, indicating that maximal monocyte recruitment may require the synergistic effects of a number of chemokines [378]. Thus, synergy between CCL2 and CCL4 during monocyte chemotaxis is a plausible explanation as to how a reduction in CCL4 levels alone resulted in a 27% reduction in monocyte recruitment in my experiments [361, 362]. A further experiment which might clarify this would be to use an anti-CCL4 blocking antibody in ZIP to investigate whether I observe similar reductions in monocyte numbers as I did with chemerin treatment.

Intervention with the C17 peptide had no effect on cell recruitment. As discussed earlier, it is possible that higher concentrations of the peptide are required *in vivo* compared to full-length chemerin. The peptide may have been too unstable in the inflammatory environment. In addition, the fact that it is not capable of binding to the CCRL2 receptor may mean it cannot accumulate locally at high enough levels. By way of circumventing the stability issue, I acetylated the N-terminus of the peptide. This modification did not affect the ability of the peptide to activate the ChemR23 receptor (Figure 4.10D), nor did it seem to modulate inflammatory responses *in vivo* (Figure. 4.10A-C).

There have been a number of reports of modified chemerin derived peptides as well as one report of a lipidated C9 peptide exerting anti-inflammatory effects in a murine model of allergic airway inflammation [246, 247]. It is therefore conceivable that chemerin peptides may need numerous modifications in order to be sufficiently stabilised for use *in vivo.* It is also possible that chemerin exerts its most profound effects in the context of allergic Th2 type responses rather then classical Th1 type inflammation. It would be interesting to test the acetylated C17 peptide in an allergic airway inflammation model or in BALB/c mice.

4.5.4 Endogenous chemerin levels increase *in vivo* during inflammation.

As discussed earlier, there have been a number of reports of elevated chemerin levels in patients with metabolic and inflammatory diseases [172, 208, 233, 350]. Endogenous chemerin levels have not been characterised during ZIP to date and so I investigated endogenous levels both locally and systemically during ZIP. An interesting observation was that there are high levels of chemerin detected by ELISA in a naïve peritoneal

cavity (~1 ng/ml) whereas other mediators tested were not detectable (Figure 3.6 and 4.13A). The majority of this is likely pro-chemerin as the ELISA does not differentiate between pro and active chemerin. The fact that chemerin is present in the tissue under homeostatic conditions, coupled with the very high expression levels of the chemerin receptor ChemR23 on resident macrophages, highlights a possible role for chemerin as an alarmin and in host defense, which agrees with the current views in the literature [190, 191, 235]. Another potential role of chemerin in this system is modulation of resident macrophage function such as antigen presentation, cytokine production and migration to draining lymph nodes [43, 197, 379]. After onset of inflammation, chemerin levels in the peritoneum increased rapidly followed by a decrease back to baseline but never below detection (Figure 4.13A). Interestingly, the kinetics of the bioactivity at the ChemR23 receptor differed. The bioactivity peaked at 16 hours and remained high until 96 hours. I know from my own experiments that the commercial ELISA kit does not detect shorter chemerin peptides such as C17 and C9. It therefore seems likely that shorter bioactive peptides were being generated which were not detectable by ELISA. While one group have developed in house ELISAs for the detection of 3 different human chemerin isoforms, these are not commercially available and this study along with my own experiments highlights the importance of measuring bioactivity of chemerin in patients rather then overall protein levels [174]. Using these ELISAs the same group report that in healthy human volunteers, circulating chemerin in plasma is predominantly the inactive pro-chemerin. However, when they investigated synovial fluid from patients with rheumatoid arthritis, osteoarthritis and psoriatic arthritis they found that the active chemerin^{158} isoform was by far the most abundant isoform in all three groups [174].

The observation that in an inflammatory setting, there are large amounts of active chemerin locally and very little inactive chemerin again highlights the importance of local chemerin production during inflammatory diseases. When I measured plasma levels of chemerin during my ZIP experiments, total chemerin levels seemed to increase but not significantly and as discussed in the results, bioactivity could not be accurately measured.

Thioglycollate challenge also increased chemerin levels in the peritoneum, (Figure. 4.13D). The fact that chemerin levels peak later with thioglycollate compared to zymosan is not surprising given it elicits a larger inflammatory response, resulting in a larger influx of inflammatory cells and delayed resolution [380].

In contrast to inflammatory stimuli increasing endogenous chemerin levels, the corticosteroid dexamethasone decreased both peritoneal and plasma chemerin levels. Chemerin expression has been reported to be induced by retinoic acids such as tazarotene and rosaglitazone, as well as by pro-inflammatory cytokines such as IL-1β [178, 186, 381]. Corticosteroids to the best of my knowledge have not previously been reported to modulate chemerin expression *in vivo.* One study in 1999 reported that a combination of dexamethasone and vitamin D could induce chemerin expression after two days of treatment in ST2 stromal cells *in vitro* [165]. However, there was no description of treatment with dexamethasone alone and given the first description of chemerin expression in human skin reported no induction of expression using vitamin D alone, further investigation is needed [164]. Dexamethasone is thought to exert its anti-inflammatory properties via transcriptional down regulation of a number of pro-inflammatory genes as well as up regulating anti-inflammatory genes such as annexin-a1, as discussed in chapter 3 [321, 339, 382]. Chemerin expression has not been reported to be induced by NF_KB activation but it is induced by peroxisome proliferator activated

receptor gamma (PPARγ) agonists [178]. The glucocorticoid receptor itself has been reported to interact with both PPARγ and retinoid X receptors [383]. In fact, there is evidence that dexamethasone is capable of counteracting signalling of the PPARγ agonist thiazolidinedione in osteoblasts [384]. Therefore, dexamethasone may decrease chemerin expression *in vivo* by inhibiting PPARγ activity. Mice lacking PPARγ would be required to confirm if this is indeed the mechanism by which dexamethasone decreased chemerin expression.

4.5.5 The effects of knockdown of endogenous chemerin *in vivo.*

To the best of my knowledge, there have been limited studies to date, which have investigated blocking chemerin activity *in vivo* in the context of inflammatory responses. As stated earlier, there are currently no commercially available transgenic animals lacking the chemerin gene, although there is one report of this mouse by Takahashi *et al*. These animals were reported to have impaired glucose tolerance and insulin secretion compared to wild type animals [223]. As a further proof that chemerin is involved in glucose tolerance in this system, Takahashi *et al*. also generated transgenic mice over expressing chemerin and reported these mice had improved glucose tolerance and insulin secretion compared to wild type animals. Unfortunately, this report did not explore inflammatory responses of these animals in great detail. They examined macrophage infiltration of adipose tissue and found that under resting conditions, chemerin KO animals exhibited decreased macrophage infiltration compared to wild type controls. However, as their interest was in the metabolic phenotype, they did not pursue this any further [223].

For this reason, I explored knocking down chemerin expression *in vivo* using anti-sense oligonucleotides (ASO) kindly provided by ISIS Pharmaceuticals. ASO technology has been used to inhibit expression of target genes for a number of years. There are numerous ASOs currently in clinical trials across a range of diseases [385, 386].

There have been two studies, which investigated blocking chemerin activity *in vivo*. The first is a previous study from our laboratory by Cash *et al.* in which an anti-chemerin polyclonal antibody was administered intraperitoneally prior to challenge with zymosan [225]. They observed increased monocyte and neutrophil recruitment to the peritoneum in animals that received the anti-chemerin treatment compared to isotype control but did not investigate other tissues. It was difficult to confirm *in vivo* blockade of chemerin however, since chemerin is still detectable by ELISA with or without anti-chemerin polyclonal treatment given the antibody binds multiple epitopes. In contrast, a study by Lin *et al*. blocked endogenous chemerin using the same neutralising antibody in the context of DSS induced colitis and observed decreased local inflammation in the colon [210]. These studies highlight the different roles chemerin seems to play in inflammation depending on the type of inflammatory model used.

While I am not aware of any other studies directly targeting chemerin, a study by Graham *et al*. demonstrated the efficacy of a small molecule ChemR23 antagonist in the context of CNS inflammation using the experimental autoimmune encephalomyelitis (EAE) model [218]. Blocking of the ChemR23 receptor in this disease model resulted in significant decreases in clinical disease scores as well decreased T cell, B cell, DC and macrophage infiltration into the CNS.

Given the efficacy of the ASO technology at reducing protein levels *in vivo* and the fact that protein knockdown could be confirmed by ELISA, I chose to investigate the

effects of modulating chemerin expression on inflammation using the 100 μg ZIP model. In contrast to the study by Cash *et al*, I did not observe any differences in monocyte or neutrophil recruitment to the peritoneum. One possible explanation for this discrepancy is that the ASO treatment did not completely ablate chemerin expression in the peritoneum. Although chemerin expression was dramatically decreased compared to control ASO treated animals, it is possible that there was enough protein still being synthesised to mask any local effects on cellular recruitment. I did however see an increase in neutrophil numbers in the blood as well as increased $Ly6C^{hi}$ monocytes in chemerin ASO treated animals. These results indicate that chemerin may play a role in dampening monocyte and neutrophil mobilisation from the bone marrow, although further experiments will be required to assess this.

These results present an interesting dichotomy. Chemerin levels seem to increase in a number of human pathologies as well as in experiments I have presented in this chapter [174, 212, 387]. In addition, anti-inflammatory treatments such as anti-TNF therapy have been reported to decrease chemerin levels in patients with inflammatory diseases [207, 214]. As I have shown in this chapter, the anti-inflammatory glucocorticoid dexamethasone decreases chemerin levels both in the peritoneum and blood of mice. Given the literature, one might have expected decreased inflammatory cell recruitment when chemerin expression was decreased, rather then the increase in blood neutrophils and monocytes I observed. One explanation (aside from incomplete knockdown of chemerin expression in the peritoneum) could be the short term model used (4-hour ZIP) compared to long-term chronic inflammation which would have lasted for months to years in the patient cohorts. The fact that Cash *et al* observed an increase in monocyte and neutrophil recruitment in their zymosan peritonitis experiments following anti-chemerin treatment suggests the effect to be model specific.

It would be interesting to use these ASOs in longer-term models of inflammation such as K/BxN arthritis or EAE models to assess what effect if any this might have in these chronic inflammatory models. In future, it would also be beneficial to use a longer dosing regime or a higher dose of ASO to ensure complete knockdown of protein expression.

4.5.6 Limitations of these studies

There was a number of limitations to these studies. The first limitation was the purity of Bio-gel elicited macrophages used in the real time chemotaxis and real time adhesion experiments. The reason for the decrease in F4/80^{hi} macrophages obtained from Bio-gel injection remains unclear. Thioglycollate elicited macrophages did not migrate very efficiently and bone marrow derived macrophages did not express high levels of ChemR23. However, another eliciting agent such as proteose peptone could be tested as an alternative to produce high numbers of macrophages [292].

Another limitation was the lack of reagents that can specifically measure pro-chemerin, active chemerin isoforms as well as shorter chemerin peptides. As discussed earlier, the commercially available antibodies only allow the quantification of total chemerin levels (including pro-chemerin and active chemerin), which is not an accurate representation of chemerin bioactivity. Until such reagents become widely available, I would suggest that a bioassay such as the ChemR23 transfected CHO-K1 cells/tagged β-arrestin system used in this chapter is a more useful measurement of chemerin levels and activity *in vivo*. In future, a standard curve of active recombinant chemerin combined with samples of interest in this system will produce the most accurate measurement of chemerin activity present in biological samples.

During the interventional ZIP studies, I was relying on endogenous protease activity to cleave chemerin to shorter active peptides in each animal, in each experiment. While I did observe significant effects with chemerin in these studies, clearly this is source of variation that should be avoided if possible. Due to the large amount of other proteins produced in the peritoneum during the ZIP, it was not possible to characterise what chemerin cleavage products were produced in these experiments and this remains uncertain. From the *in vitro* experiments incubating recombinant proteases with chemerin I demonstrated elastase and cathepsin-g produced a range of shorter peptides. It seems very likely therefore that a similar process occurs in the inflamed cavity, but there would be a large number of other proteases produced in the cavity as well which might also cleave chemerin such as mast cell chymase [189, 388].

4.6 Summary

There were two main aims of this chapter. The first was to characterise the effects of chemerin and the chemerin peptides C17 and C9 on macrophage migratory and inflammatory responses. To this end, using the real-time chemotaxis system, I demonstrated that both C9 and C17 could induce chemotaxis of primary murine macrophages but were less potent than full-length chemerin. Interestingly, the peptides proved more efficient at inducing adhesion compared to full-length protein.

The effects of chemerin and chemerin peptides on macrophage inflammatory responses were difficult to discern due to lack of reproducibility between experiments. Unfortunately, the published literature is equally contradictory [225, 237].

The second part of this chapter focused on the role that chemerin and chemerin peptides play during inflammation *in vivo.* I observed a significant increase in neutrophil recruitment to the peritoneum when mice were pre-treated with chemerin but no effect

on monocytes. The C17 peptide induced a modest but significant decrease in monocyte recruitment. When administered into an inflamed peritoneal cavity, I observed very different results. Full-length chemerin significantly decreased monocyte numbers while not affecting neutrophils. The C17 peptide did not have any effects in these experiments. Acetylation of the C17 peptide in an effort to stabilise it did not affect its ability to signal through the ChemR23 receptor but I did not observe significant differences in monocytes or neutrophils *in vivo*.

I characterised endogenous chemerin levels both in plasma and in the peritoneum during ZIP and found that total chemerin levels as well as chemerin activity increase during inflammation. Furthermore, treatment with the corticosteroid dexamethasone decreased chemerin expression in plasma and in the peritoneum. This may hint at a novel mechanism by which corticosteroids exert anti-inflammatory effects, given that chemerin is a known chemoattractant for a number of immune cells and is increased in a number of disease pathologies as well as in our experimental systems.

5 The role of the non-signalling chemerin receptor CCRL2 during inflammation.

5.1 Introduction

CCRL2 was first identified as a gene whose expression was rapidly increased in murine macrophages upon stimulation with LPS [255]. As discussed in section 1.7.3, CCRL2 is expressed on nearly all hematopoietic cells in humans. In mice, it is expressed in DCs, mast cells, activated macrophages, epithelial cells and endothelial cells. Its expression is upregulated in response to inflammatory stimuli [255, 258, 259, 389]. CCRL2 has been demonstrated to bind chemerin with high affinity but does not internalise it nor does chemerin binding induce any detectable downstream signalling events [259].

Relatively little is known regarding the function of CCRL2 during inflammation. The prevailing theory in the literature is that it functions to concentrate chemerin on the surface of cells in order to more efficiently present chemerin to ChemR23 expressing cells [180, 259, 260]. Monnier *et al.* have shown that CCRL2 expressed on endothelial cells can bind chemerin and promote adhesion of ChemR23 expressing L1.2 lymphoid cells [260]. This was dependent on α4β1 integrins, in line with chemerin stimulated integrin clustering reported by Hart *et al* [198].

A number of studies have reported differences in animals lacking CCRL2 in different models of inflammation, particularly allergic inflammation. For example, animals lacking CCRL2 displayed impaired inflammatory responses in a dermal mast cell dependent hypersensitivity model [259]. Animals were sensitised with anti-DNP IgE antibodies to the ear and then challenged with 2,4-DNP-conjugated human serum albumin (DNP-HSA) intravenously. Mice lacking CCRL2 displayed decreased dermal inflammation in the ear and decreased leukocyte recruitment compared to wild type

animals. These results were dependent on CCRL2 expressed on mast cells as demonstrated by engraftment of with wild type or CCRL2 KO mast cells to mast cell deficient animals. However, the mechanism by which CCRL2 exerted these effects was unclear [259]. CCRL2 was also reported to play a role in ovalbumin induced lung inflammation. Animals lacking CCRL2 displayed decreased antigen loaded DC trafficking to draining lymph nodes, decreased leukocyte numbers in the bronchiolar lavage (BAL) fluid of the lungs, as well as decreased Th2 cytokines in the BAL fluid [258].

In an LPS induced lung injury model, animals lacking CCRL2 displayed less NK cell recruitment to the lungs following LPS challenge and this was proposed to be the result of decreased presentation of chemerin to ChemR23 expressing NK cells by CCRL2 [260]. The same report demonstrated that animals lacking CCRL2 displayed increased plasma chemerin levels after challenge with LPS, although the significance of this was not addressed.

5.2 Rational for the experiments

From critical reading of the literature, it was clear that relatively little is known about the function of CCRL2 *in vivo* in the context of inflammation. CCRL2 seems to bind chemerin with relatively high affinity. However it does not internalise chemerin, nor does the binding induce any detectable downstream signalling [259]. There have been a number of interesting observations on the biology of CCRL2, including the fact that its expression is upregulated by inflammatory stimuli, it is expressed on a range of cell types, it binds chemerin at the N-terminus and is thought to concentrate chemerin locally [259, 260, 390]. These observations prompted me to examine what effects deleting this

receptor *in vivo* might have during inflammation and homeostasis. Importantly, CCRL2 KO mice were obtained from Jackson Laboratories on C57Bl/6J background (backcrossed for 5 generations from an SV129 background) and backcrossed onto a C57Bl/6J background for a total of 12 generations before experiments were performed.

5.3 Experimental aims.

The aims of this chapter were to:

- Investigate what role, if any, CCRL2 plays in chemerin induced signalling in primary murine macrophages.
- Characterise any differences between wild type littermate controls and CCRL2 KO animals under normal physiological conditions.
- Investigate whether deletion of CCRL2 has any effect on different models of inflammation *in vivo* and to use these models to interrogate the non-redundant functions of the CCRL2 receptor.

5.4 Results

5.4.1 CCRL2 plays a role in chemerin-induced adhesion in the electrical impedance sensing platform but not in chemotaxis assays.

In the previous chapter, I characterised the action of chemerin and chemerin derived peptides to induce adhesion of primary murine macrophages in the impedance system. Although the majority of chemerin activity is thought to be through the ChemR23 receptor, CCRL2 is also expressed on macrophages and binds chemerin [257]. One possible function of CCRL2 is to bind and concentrate local chemerin to increase the amount of chemerin available to bind ChemR23 expressing cells [260]. To test this hypothesis, we obtained animals lacking the CCRL2 receptor (CCRL2 KO) from Jackson Laboratories, which had been backcrossed onto a C57Bl/6J background for 7 generations (originally SV129 background). Before conducting experiments with them, these animals were crossed onto a C57Bl/6J background for a further 5 generations for a total of 12 generations. Wild type littermates or WT C57Bl/6J bred within our animal unit were used as wild type (WT) controls in all experiments described in this chapter.

I used Bio-Gel elicited peritoneal macrophages from WT or CCRL2 KO animals in the impedance platform and measured responses to both chemerin as well as the CC chemokine, CCL5. I measured responses of these cells over a range of doses and observed that cells lacking CCRL2 displayed significantly ($P \leq 0.05$) less signalling in response to chemerin compared to WT cells. During a dose response of chemerin, the peak Cell Index (CI) observed in WT cells reached 0.15 ± 0.02 while the peak CI observed for CCRL2 KO cells was 0.11 ± 0.01 (Figure 5.1). In contrast, there was no difference in responses to CCL5, with WT cells reaching peak responses of 0.13 ± 0.02 CI and CCRL2 KO cells having a peak CI of 0.12 ± 0.02. The reason for this modest

defect in chemerin-mediated adhesion at higher chemerin concentrations is not immediately obvious. However, it is conceivable that chemerin binding by CCRL2 results in higher concentrations of chemerin being available for presentation to ChemR23, since CCRL2 binds chemerin at the non-signalling N-terminus, which is a model that has been proposed previously [259].

As I have shown, macrophage adhesion in response to chemerin is impaired in CCRL2 KO animals. Since the real time chemotaxis system used in the previous chapter measures both chemotaxis of cells as well as adhesion of migrated cells to the underside of the filter, it seemed logical there might be a similar trend in this assay. When challenged with 5 nM chemerin and 5 nM CCL5 however, I did not observe any differences between WT and CCRL2 KO cells in this system either by Max-Min or slope analysis (Figure 5.2A-C). When allowed to migrate to chemerin, WT macrophages had a Max-Min CI of 0.39 ± 0.03 and CCRL2 KO macrophages had a Max-Min CI of 0.32 ± 0.06 (Figure 5.2C). Similarly, WT cells had a slope CI of 0.2 ± 0.08 and CCRL2 KO cells had a slope CI of 0.2 ± 0.045. Responses to 5 nM CCL5 were unaffected by deletion of CCRL2 (Figure 5.2C). Given that the macrophages were chemotaxing in a gradient rather then adhering to a surface, it is possible that chemerin binding to CCRL2 does not exert as much of an effect in this system but may play a role in an *in vivo* setting where cells might be adhering to activated vascular or lymphatic tissue.

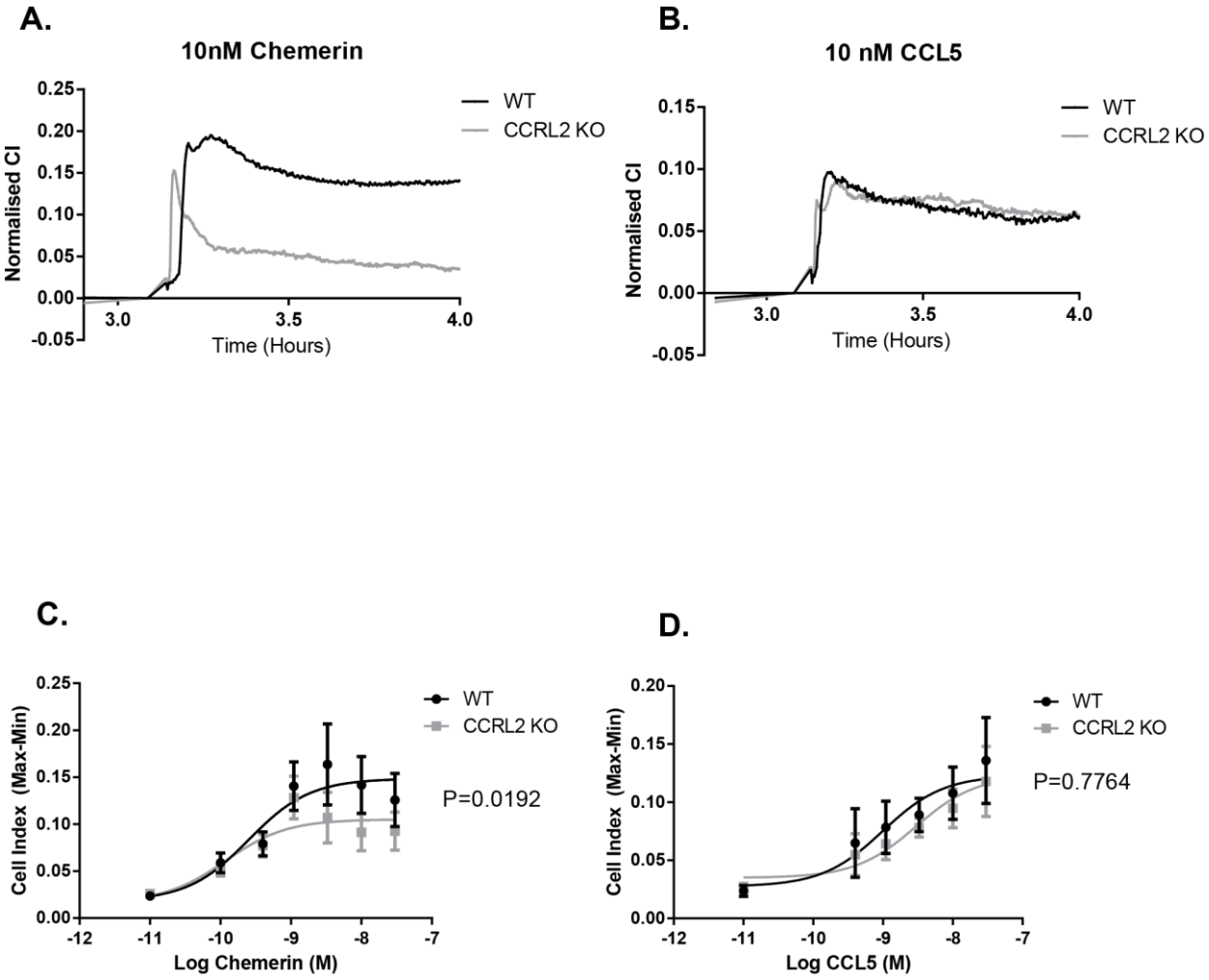


Figure 5.1 CCRL2 is required for optimal chemerin induced adhesion in the electrical impedance sensing platform.

8-10 week old male CCRL2 KO and aged matched C57Bl/6J mice were injected i.p. with 2% Bio-gel (polyacrylamide beads) and sacrificed 4 days later. Peritoneal cavities were lavaged with ice-cold PBS supplemented with 2mM EDTA. PECs (5.4×10^4) were allowed to adhere for 3 hours until no further increases in CI were observed. Cells were then challenged with a dose response of either CCL5 or chemerin. Raw traces of normalised (to vehicle) cell index responses of Bio-gel macrophages to chemerin (**A.**) or CCL5 (**B.**). Responses of macrophages were quantified using max-min values (**C.** and **D.**). Error bars represent S.E.M of 4 independent experiments. Non-linear regression analysis was performed and top values of the curves were compared.

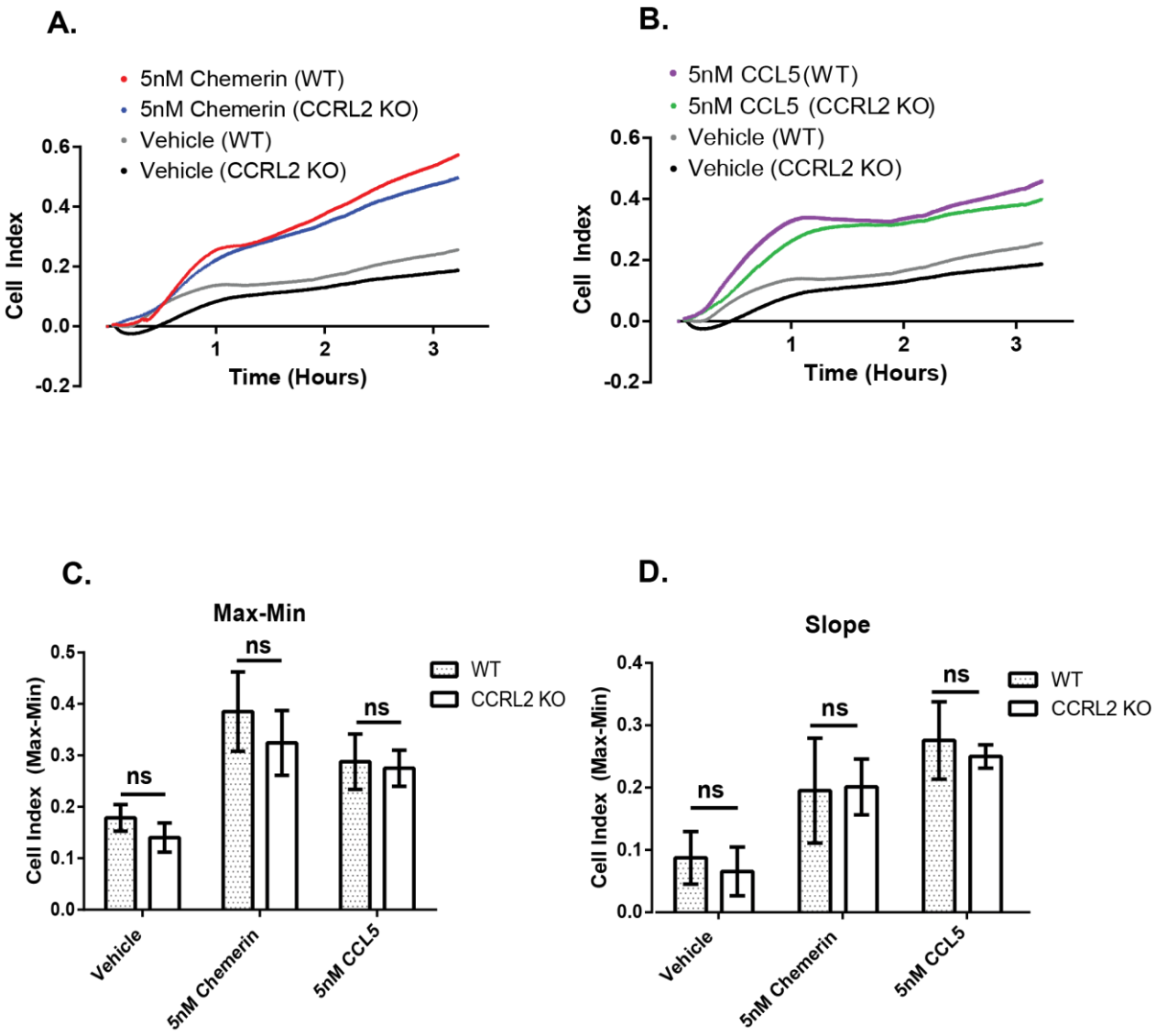


Figure 5.2 CCRL2 does not play a role in chemerin-induced chemotaxis of primary murine macrophages.

8-10 week old male CCRL2 KO mice and age matched C57Bl/6J mice were injected i.p. with 2% Bio-gel (polyacrylamide beads) and sacrificed 4 days later. Peritoneal cavities were lavaged with ice-cold PBS supplemented with 2mM EDTA. A gradient of either 5nM chemerin or CCL5 was allowed to form and chemotaxis was measured of $4x10^5$ cells (400,000 cells/well) for 3 hours. Representative traces of WT and CCRL2 KO macrophage chemotaxis to 5nM chemerin (**A.**) or 5nM CCL5. (**B.**). **C.**Max-Min analysis and **D.**slope analysis. Error bars are S.E.M. of 4 experiments with independent macrophage preparations. Significance was assessed using 2-way ANOVA with Sidak's multiple comparison test.

5.4.2 Phenotypic characterisation of naïve animals lacking the CCRL2 receptor

As mentioned earlier, there have been relatively few studies investigating the role of CCRL2 *in vivo.* However, there have been reports of some defects in animals lacking CCRL2 in the context of Th2 type immune responses [258, 259]. From my initial *in vitro* studies, macrophages deficient in CCRL2 exhibited impaired chemerin stimulated adhesion in the impedance platform. In order to assess whether CCRL2 might play a role in immune homeostasis, I began by characterising the cellular composition of different tissues of naïve animals lacking CCRL2. In my initial experiments, I noticed that animals lacking CCLR2 had significantly ($P \leq 0.05$) larger spleens relative to total body weight compared to WT animals (Figure 5.3A). To assess if this increase (17.6 %) was due to increased infiltration of a specific cell type, I performed flow cytometry on spleens from both WT and CCRL2 KO animals. I saw no difference in B cells (defined as $CD45^{+ve}$, $B220^{+ve}$, $CD19^{+ve}$) or macrophages ($CD45^{+ve}$, $F4/80^{+ve}$, $CD11b^{+ve}$) (Figure 5.3B-C). There was no difference in CD8 T cells (Figure 5.3F). However, there was a modest but significant decrease in CD4 T cells (16.3% of $CD45^{+ve}$ cells in WT compared to 14.1% of $CD45^{+ve}$ in CCLR2 KO) (Figure 5.3 D-E).

This observed splenomegaly did not seem to be due to a viral or bacterial infection as these animals had similar blood counts of different immune cells to the WT controls as well as the fact that both groups were bred in the same animal unit under the same conditions (Figure 5.4). There were no obvious differences between WT or CCRL2 KO animals in terms of circulating monocytes or neutrophils in the blood (Figure. 5.4 A-C). However, there did seem to be a trend towards decreased circulating T cells (~35% less in CCRL2 KO) (Figure 5.4 D-F).

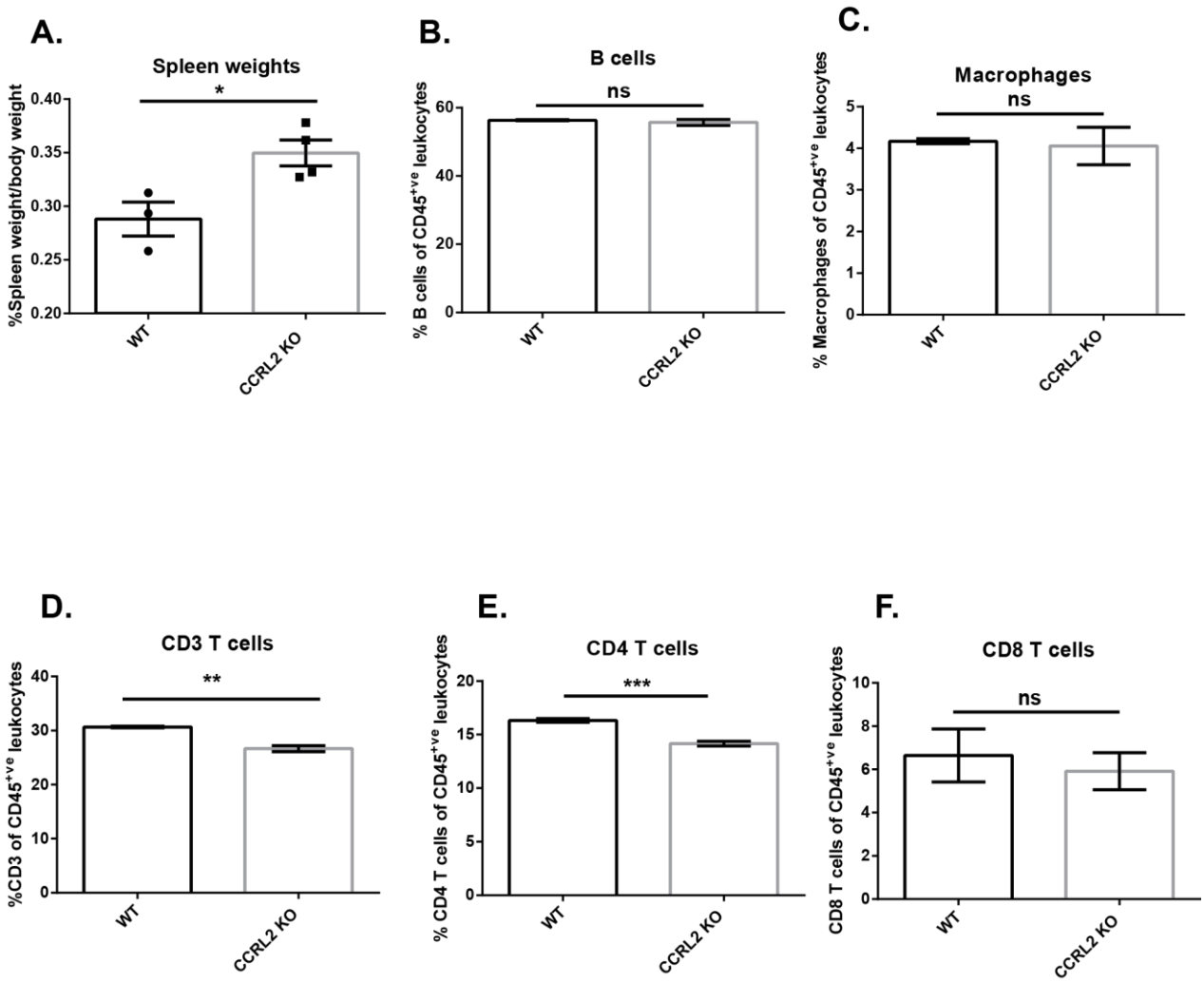


Figure 5.3 Animals lacking CCRL2 display larger spleens and decreased CD4 splenic T cell content under resting conditions.

8-10 week old male CCRL2 KO animals or age matched littermate C57Bl/6J mice were sacrificed and spleens were harvested. Total body weight and spleen weight was measured (**A.**). Spleens were digested in collagenase D (1mg/ml) in HBSS for 1 hour at 37° and passed through a 70 μm strainer to obtain a single cell suspension for flow cytometry analysis. Cell percentages are represented as percentage of total $CD45^{+ve}$ cells. **B.** B cells ($B220^{+ve}$, $CD19^{+ve}$). **C.** Macrophages ($F4/80^{+ve}$, $CD11b^{+ve}$). **D.** T cells ($CD3^{+ve}$). **E.** CD4 T cells ($CD3^{+ve}$, $CD4^{+ve}$). **F.** CD8 T cells ($CD3^{+ve}$, $CD8^{+ve}$). Error bars are S.E.M of 3-4 animals per group. Statistical significance was assessed using a students unpaired t-test. * $P \leq 0.05$, **$P \leq 0.01$, ***$P \leq 0.001$.

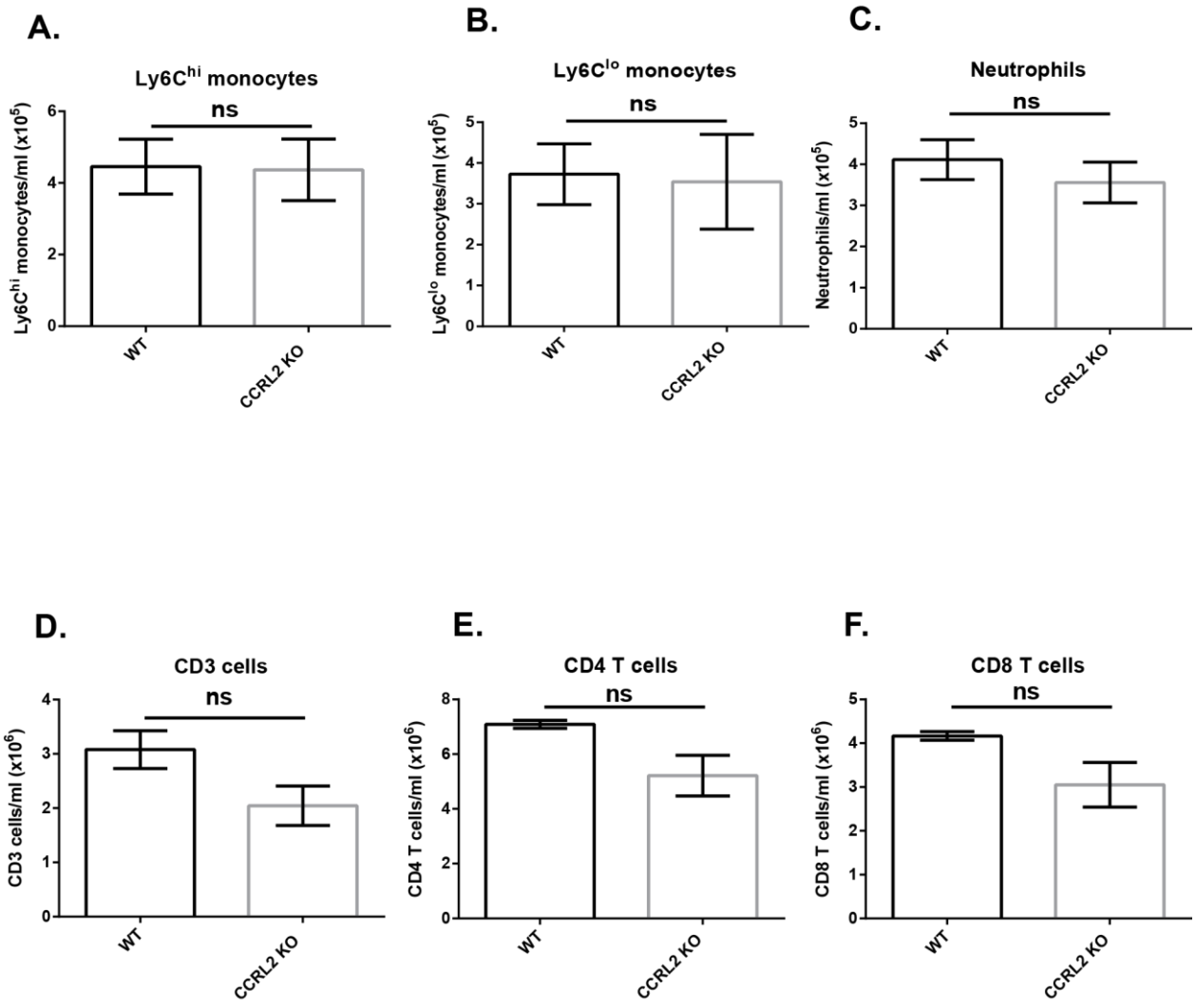


Figure 5.4 Animals lacking CCRL2 display no overt differences in circulating cells in the blood under resting conditions.

8-10 week old male CCRL2 KO animals or age matched littermate C57Bl/6J mice were sacrificed and blood was harvested via hepatic portal vein into EDTA coated vacutainers. Blood was lysed and analysed by flow cytometry and cell counts/ml were calculated using counting beads. All populations were gated on $CD45^{+ve}$. Ly6-C^{hi} (**A.**) and Ly6-C^{lo} (**B.**) monocytes ($CD115^{+ve}$, Ly6-C^{+ve}). **C.** Neutrophils ($CD11b^{+ve}$, LY6-G^{+ve}). **D.** T cells ($CD3^{+ve}$) E. CD4 T cells ($CD3^{+ve}$, $CD4^{+ve}$). F. (CD8 T cells ($CD3^{+ve}$, $CD8^{+ve}$). Error bars are S.E.M. of 2-4 animals/group. Statistical significance was assessed using a Students unpaired t-test.

I observed $3.1x10^5$ $CD3^{+ve}$ T cells/ml in WT animals and 2.0×10^5 $CD3^{+ve}$ T cells/ml in CCRL2 KO animals (Figure 5.4D).

When I examined the bone marrow of naïve CCRL2 and littermate control animals, there were no obvious differences in either monocyte or neutrophil numbers. WT animals had 0.7×10^6 monocytes/ml while CCRL2 KO animals had 0.51×10^6 monocytes/ml (Figure 5.5C). Similarly, WT animals had 1.8×10^6 neutrophils/ml and CCRL2 KO animals had 1.3×10^6 neutrophils/ml (Figure. 5.5D).

From this initial characterisation, CCRL2 KO animals exhibit large spleens in relation to total body weight compared to WT controls and there was a small but significant reduction in CD4 T cells in the spleen. There are no obvious differences in any other cell types within blood or bone marrow under resting conditions.

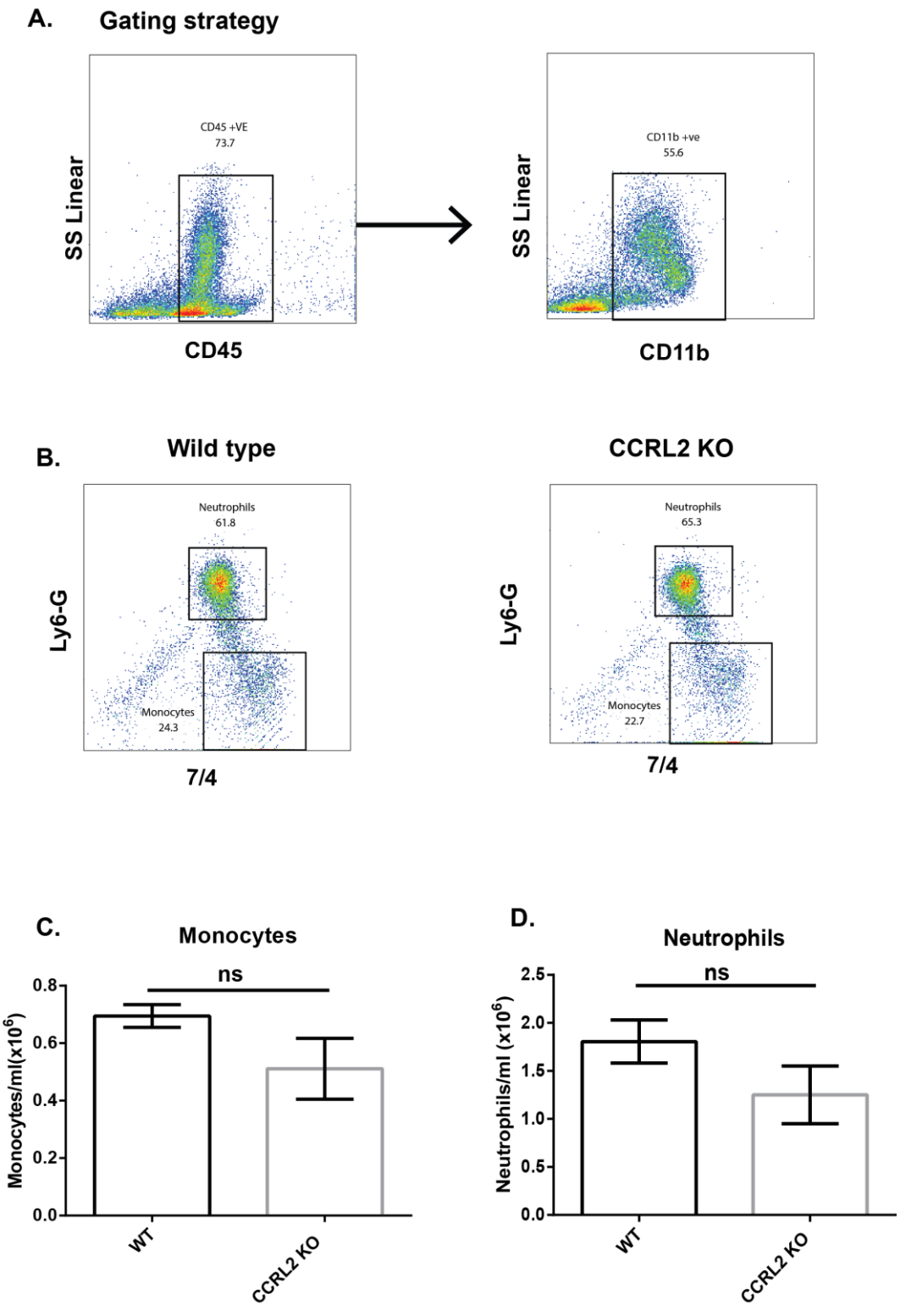


Figure 5.5 Animals lacking CCRL2 display no obvious differences in monocyte or neutrophil numbers in the bone marrow under resting conditions.

8-10 week old male CCRL2 KO animals or age-matched littermate C57Bl/6J animals were sacrificed and tibia and femurs were flushed with sterile PBS. Cell populations were analysed by flow cytometry and cell numbers were quantified using counting beads. **A**.Gating strategy used to gate on neutrophils and monocytes**.** (All cells were gated on $CD45^{+ve}$) **B.** Raw plots of WT and CCRL2 KO bone marrow. **C.** Monocytes ($CD11b^{+ve}$, $7/4^{+ve}$) **D.** Neutrophils ($CD11b^{+ve}$, $Ly6\text{-}G^{+ve}$). Error bars represent S.E.M. of 3-4 animals/group. Statistical significance was assessed using a students unpaired t-test.

5.4.3 Characterisation of inflammatory responses of animals lacking the CCRL2 receptor following challenge with zymosan.

Having established that there were no major differences between naïve WT and CCRL2 KO animals in immune cell populations in the tissues tested, I next sought to investigate what role if any, CCRL2 might play during inflammatory responses. One point to note is that previous experiments in this chapter used littermate animals as WT controls. In the *in vivo* experiments, I tested using both littermate controls and WT C57Bl/6J animals bred in the same animal unit and found that inflammatory responses were the same (data not shown). Thus, due to low animal numbers, some experiments where specified, used WT C57Bl/6J animals as controls, given that the CCRL2 KO animals had been backcrossed onto that background for 12 generations. Chemerin has previously been reported to be elevated in the blood of animals lacking CCRL2 with systemic inflammation [260]. I have demonstrated in the previous chapter that chemerin levels increase both locally and systemically following challenge with zymosan. Hence, this was the first inflammatory model I investigated with the CCRL2 KO animals. These experiments demonstrated a striking increase in monocyte and neutrophil recruitment to the peritoneum at 4 hours compared to WT controls (Figure 5.6.A-D). After zymosan challenge, there were 0.2 x 10^6 total monocytes recruited to the peritoneum of WT animals compared to 0.5 x 10^6 total monocytes recruited in CCRL2 KO animals ($P \leq 0.001$) (Figure. 5.6C). CCRL2 KO animals had a ~56% increase in neutrophil recruitment compared to WT controls (Figure 5.6D). Challenge of WT animals with 100 μg zymosan resulted in 3 x 10^6 total neutrophils while CCRL2 KO animals had 6.8 x 10^6 total neutrophils ($P \leq 0.0001$). I did not observe any differences in T and B cell numbers between WT and CCRL2 KO

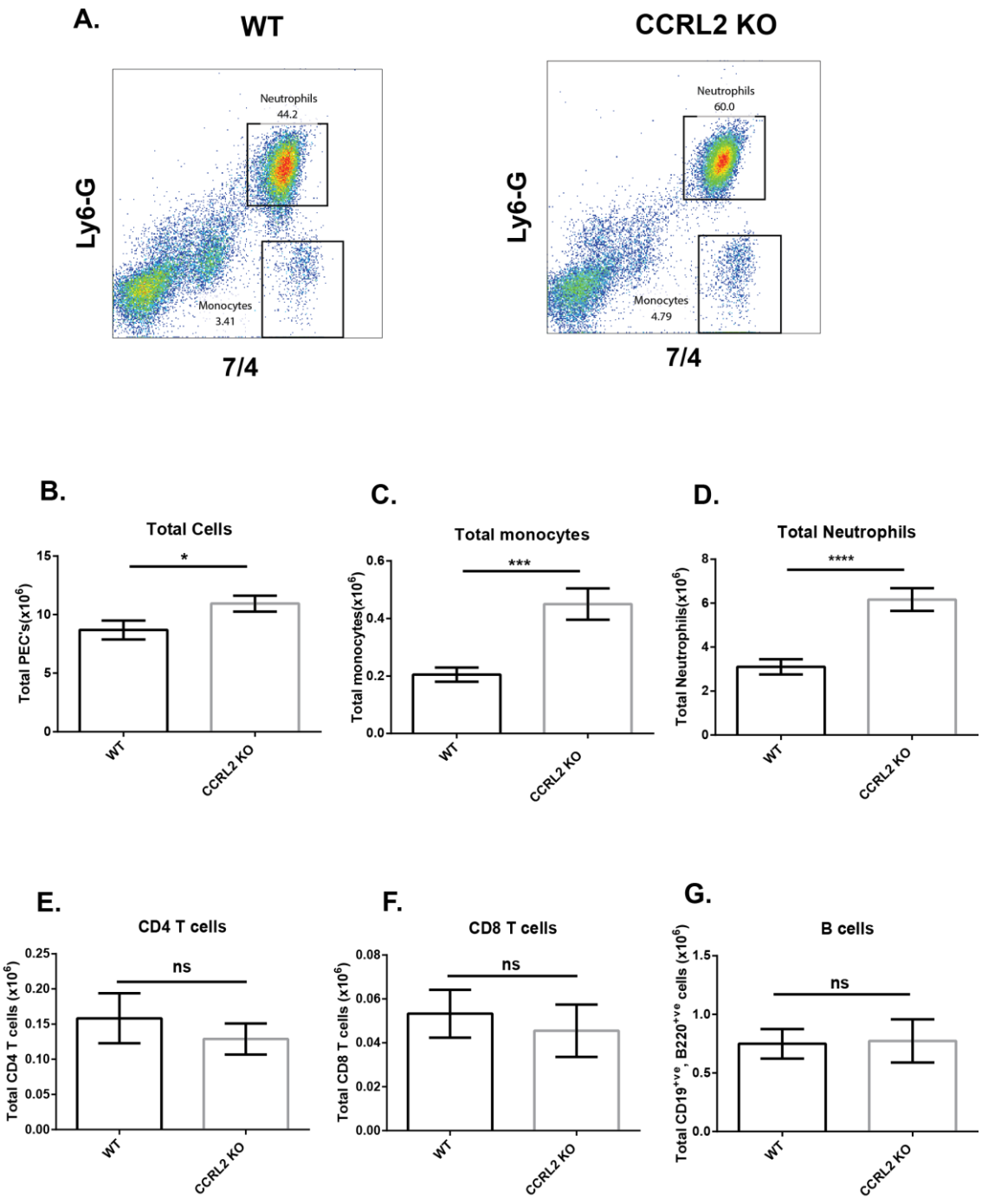


Figure 5.6 Animals lacking CCRL2 display exaggerated monocyte and neutrophil recruitment during zymosan induced peritonitis.

8-10 week old male CCRL2 KO or age matched C57Bl/6J animals were injected with zymosan i.p. (100 µg/animal) and 4 hours later, animals were sacrificed. Peritoneal cavities were lavaged with ice cold PBS supplemented with 2mM EDTA. Cells were quantified using counting beads and cell populations were analysed using flow cytometry. **A.** Representative flow cytometry plots of monocytes and neutrophils from WT and CCRL2 KO animals. **B.** Total cells recruited to cavity. **C.** Total monocytes. **D.** Total neutrophils. **E.** Total CD4 T cells. **F.**Total CD8 T cells. **G.**Total B cells. Error bars represent S.E.M. of 5-9 animals/group. Statistical significance was assessed using a students unpaired t-test. * $P \leq 0.05$, ** $P \leq 0.01$, *** $P \leq 0.001$, **** $P \leq 0.0001$.

animals (Figure. 5.6E-G). However, I know from the kinetic studies I performed in chapter 3 that both T and B cells numbers are very low at this time point. (Figure 3.4C). There was also an as yet unidentified population of cells in the peritoneum, which were $7/4^{lo}$ and Ly6-G^{hi}. This population seemed to be diminished in the CCRL2 KO animals however further stainings will be required to interrogate this population further.

In order to investigate whether these dramatic increases in monocyte and neutrophil recruitment were due to increased chemokine or cytokine levels in the peritoneum, I measured levels of a number of different mediators in the peritoneal exudate. Given previous reports that CCRL2 KO animals had increased circulating chemerin levels in the blood, I first measured endogenous chemerin levels in the peritoneum by ELISA. I saw no significant difference in chemerin levels between WT and CCRL2 KO animals (Figure. 5.7A). WT animals had 1.9 ± 0.4 ng/ml chemerin while CCRL2 KO animals had 2.1 ± 0.1 ng/ml chemerin (Figure. 5.7A). I also measured different mediator levels in the cavity using Luminex. Given the significant increases in monocyte and neutrophil numbers in the CCRL2 KO animals, one might have expected to see increased local mediator levels such as CCL2 or CXCL2. However, I did not observe any significant difference between the two groups (Figure 5.7B). CXCL1 levels at 4 hours post zymosan were unfortunately too low to accurately quantify. I measured a range of different mediators and saw no obvious differences between the two groups.

Given the increased spleen weights I observed in naïve CCRL2 KO animals, I examined spleen weights and cellular composition of the spleens of the animals following 4-hour challenge with zymosan. Firstly, in these experiments, I did not observe any difference in the ratio of spleen weight to body weight (WT=0.058 %, CCRL2 KO=0.068 % spleen weight/body weight). Similarly, when I interrogated different cell populations in the spleens of these animals, I did not observe any

differences in neutrophils, macrophages, DCs, B cells or T cells (Figure 5.8A-F). These results indicate that although there was a difference in spleen weight in the naïve animals between WT and CCRL2 KO animals, this observation may not play a functional role during this short-term model of inflammation.

When I examined the blood of these animals, there was significantly ($P \leq 0.05$) higher numbers of neutrophils in CCRL2 KO animals ($12.3 \pm 1.5 \times 10^5$ neutrophils/ml) compared to WT ($7 \pm 1.3 \times 10^5$ neutrophils/ml) (Figure. 5.9F). There were no significant differences in $Ly6C^{hi}$ or $Ly6C^{lo}$ monocytes between the two groups, although again there was a trend towards increased $Ly6C^{hi}$ monocytes in the blood of CCRL2 KO animals ($7.7 \pm 2 \times 10^5$ monocytes/ml in WT compared to $11.3 \pm 2.4 \times 10^5$ monocytes/ml) (Figure 5.9G-H). These increases were specific to monocytes and neutrophils as there were no differences observed in CD4 or CD8 T cells in the blood.

Simiarly to the peritoneum, when I examined the monocytes in the blood, there appeared to be an intermediate population between the $Ly6C^{hi}$ and $Ly6C^{lo}$ subsets, which may warrant further interrogation. However, given $Ly6C^{lo}$ monocytes differentiate from $Ly6C^{hi}$ monocytes in the blood, it seems proable this observed population is this intermediate stage [146].

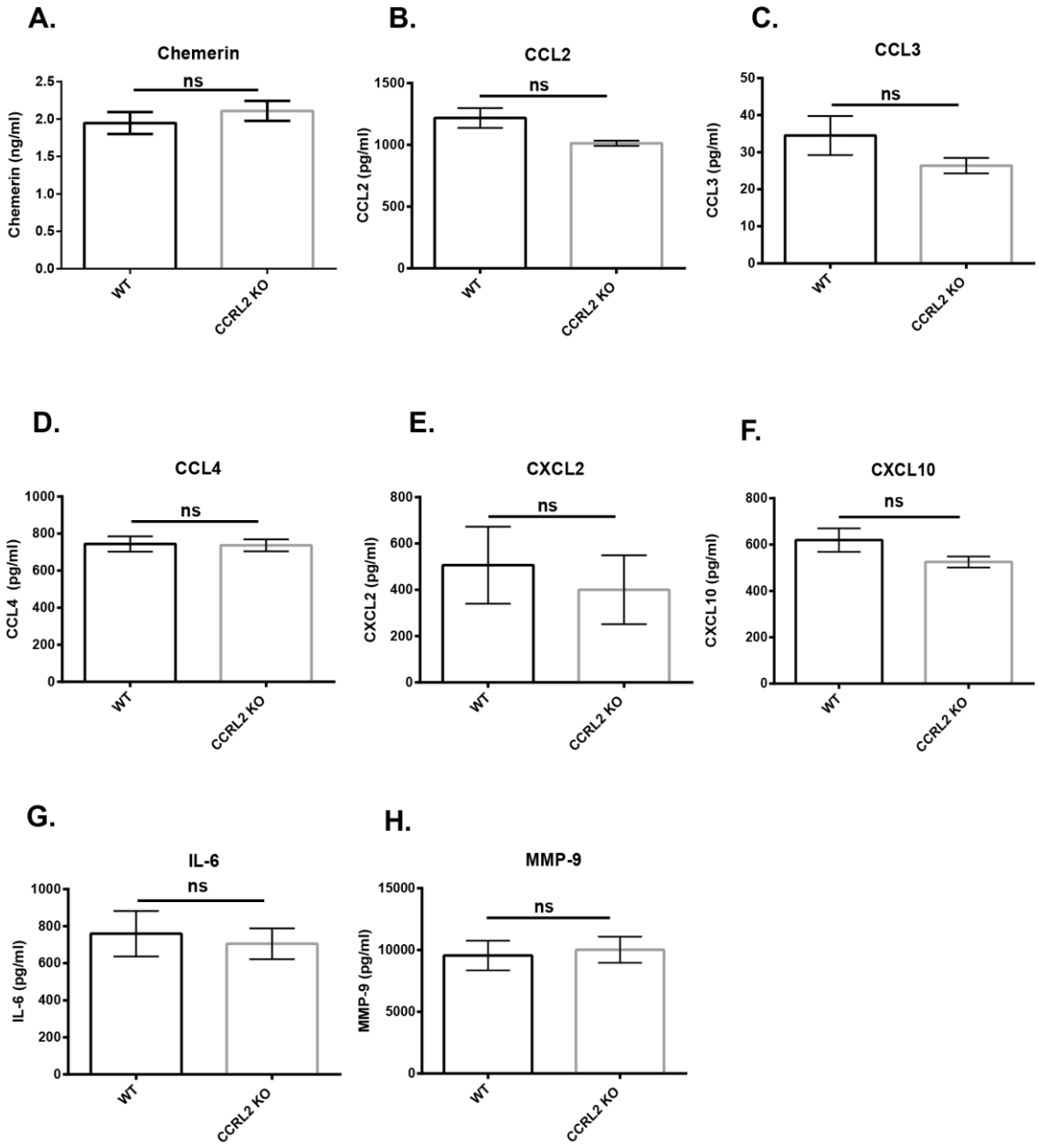


Figure 5.7 Cytokines and chemokines in the peritoneal cavity of CCRL2 KO animals and C57Bl/6J animals.

8-10 week old male CCRL2 KO or age matched C57Bl/6J controls were injected with zymosan i.p. (100 μg/animal) and 4 hours later, animals were sacrificed. Peritoneal cavities were lavaged with ice cold PBS supplemented with 2mM EDTA. Indicated mediators were measured by ELISA or Luminex. Statistical significance was assessed using a students unpaired t-test. Error bars represent mean ± S.E.M. of 9 animals/group.

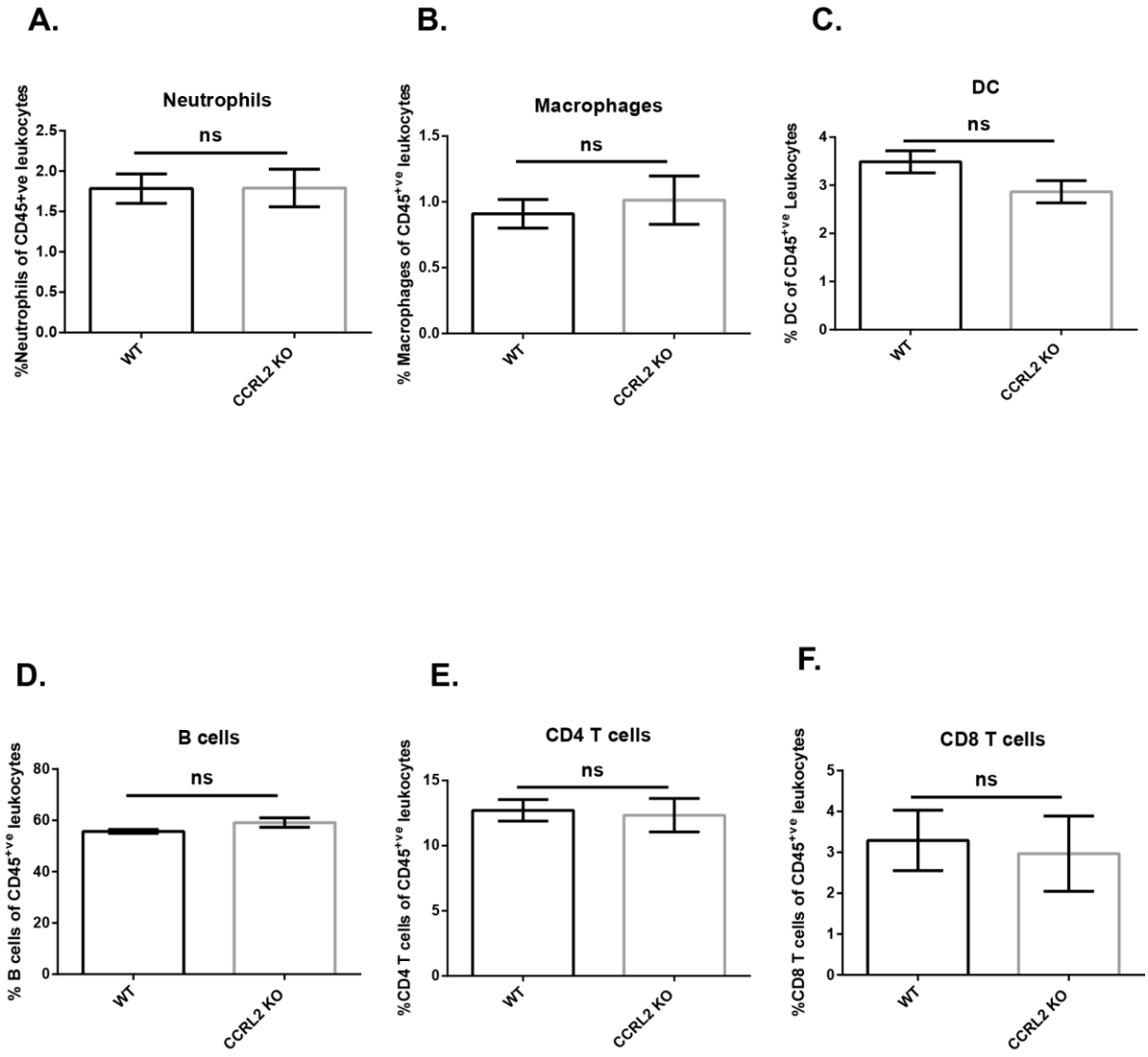


Figure 5.8 Animals lacking CCRL2 display no obvious differences in spleen weight or composition during 4-hour ZIP.

8-10 week old male CCRL2 KO animals or age matched C57Bl/6J mice injected with zymosan (100 µg/mouse) i.p. and 4 hours later were sacrificed. Spleens were harvested and total body weight and spleen weight was measured. Spleens were digested in collagenase D (1mg/ml) in HBSS for 1 hour at 37° and passed through a 70µm strainer to obtain a single cell suspension for flow cytometry analysis. Cell percentages are representd as percentage of $CD45^{+ve}$ cells. **A.** Neutrophils ($CD11b^{+ve}$, $Ly6\text{-}G^{+ve}$) **B.** Macrophages ($F4/80^{+ve}$, $CD11b^{+ve}$). **C.** Dendritic cells ($CD11c^{+ve}$, $MHC\text{-}II^{+ve}$). **D.** B cells ($B220^{+ve}$, $CD19^{+ve}$). **E.** CD4 T cells ($CD3^{+ve}$, $CD4^{+ve}$). **F.** CD8 T cells ($CD3^{+ve}$, $CD8^{+ve}$). Error bars represent S.E.M. of 4-6 animals/group. Statistical significance was assessed using a students unpaired t-test.

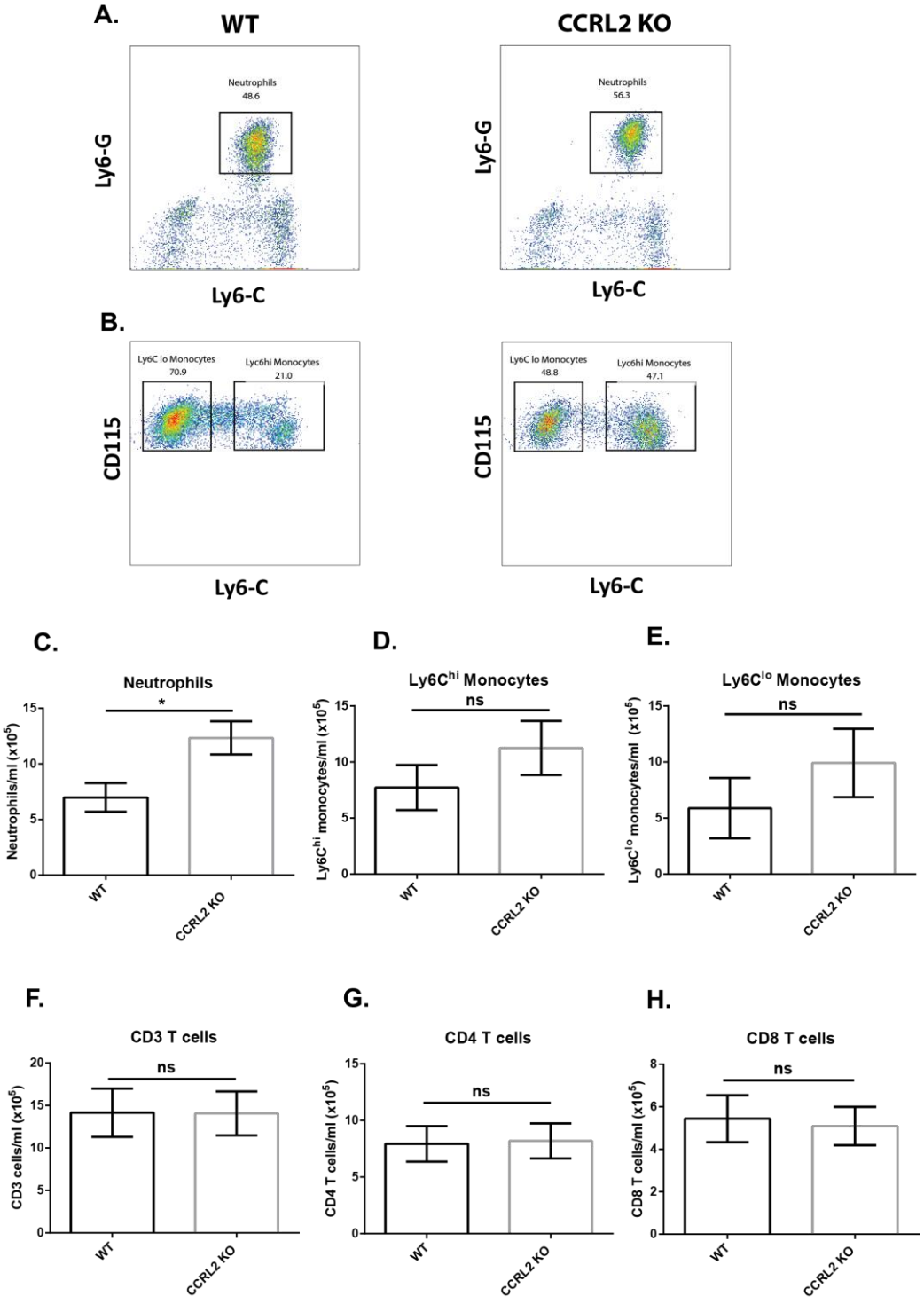


Figure 5.9 Animals lacking CCRL2 display increased neutrophil and Ly6-C^{hi} monocytes in the blood after 4-hour zymosan induced peritonitis.

8-10 week old male CCRL2 KO animals or age matched C57Bl/6J mice were injected with zymosan (100 µg/ml) i.p. and sacrificed 4 hours later. Blood was collected via hepatic portal vein into EDTA coated vacutainers and analysed by flow cytometry. Cell counts/ml were calculated using counting beads. All cells were gated on CD45^{+ve}. **A.** Representative flow cytometry plots of circulating neutrophils of WT and CCRL2 KO animals. **B.** Representative flow cytometry plots of Ly6-C^{hi} and Ly6-C^{lo} monocytes (gated on CD115^{+ve}). **C.** T cells/ml. **D.** CD4 T cells/ml. **E.** CD8 T cells/ml. **F.** Neutrophils/ml. **G.** Ly6-C^{hi} monocytes/ml. **H.** Ly6-C^{lo} monocytes/ml. Error bars represent S.E.M. of 4 animals/group. Statistical significance was assessed using a students unpaired t-test. * $P \leq 0.05$.

5.4.4 Animals lacking CCRL2 display increased CXCL1 production in the peritoneum during 1-hour thioglycollate challenge.

Animals lacking CCRL2 display increased neutrophil and monocyte recruitment to the peritoneum during local inflammation (Figure 5.6). In order to investigate this phenotype further, I used a short-term 1-hour challenge with 4% thioglycollate i.p.to specifically look at neutrophil recruitment to the peritoneal cavity. Injection of thioglycollate for 1 hour induced a small but distinct population of neutrophils recruited to the peritoneum but no monocytes (Figure. 5.10A). I observed no difference in total cell recruitment but there was a ~94% increase in neutrophil recruitment in the CCRL2 KO animals compared to WT ($0.08 \pm 0.03 \times 10^6$ neutrophils in WT compared to $1.3 \pm 0.02 \times 10^6$ neutrophils in CCRL2 KO animals) (Figure 5.10B-C). This did not reach significance because of low animal numbers per group. There was also a trend towards increased chemerin levels in the cavity of CCRL2 KO animals (7.6 ± 0.8 ng/ml) compared to WT animals (5.4 ± 0.5 ng/ml) (Figure 5.10D). Finally, animals lacking CCRL2 had significantly higher levels of CXCL1 compared to WT animals ($P \leq 0.05$). WT animals produced 142 ± 67 pg/ml while CCRL2 KO animals produced 502 ± 90 pg/ml (Figure 5.10E) (~72% increase in the CCRL2 KO animals).

Injection of thioglycollate is an established method for recruiting inflammatory macrophages to the cavity after 4 to 5 days [292]. I chose a 1-hour challenge because I was specifically interested in looking at neutrophil recruitment. Although this was a different inflammatory insult to zymosan, I observed increased neutrophil recruitment and increased inflammatory mediator production (CXCL1). In contrast to the 4-hour ZIP experiments however, there was a trend towards increased chemerin production in the cavity, possibly due to the larger inflammatory stimulus and shorter time point since chemerin levels seem to peak very rapidly following zymosan challenge (Fig 4.13A).

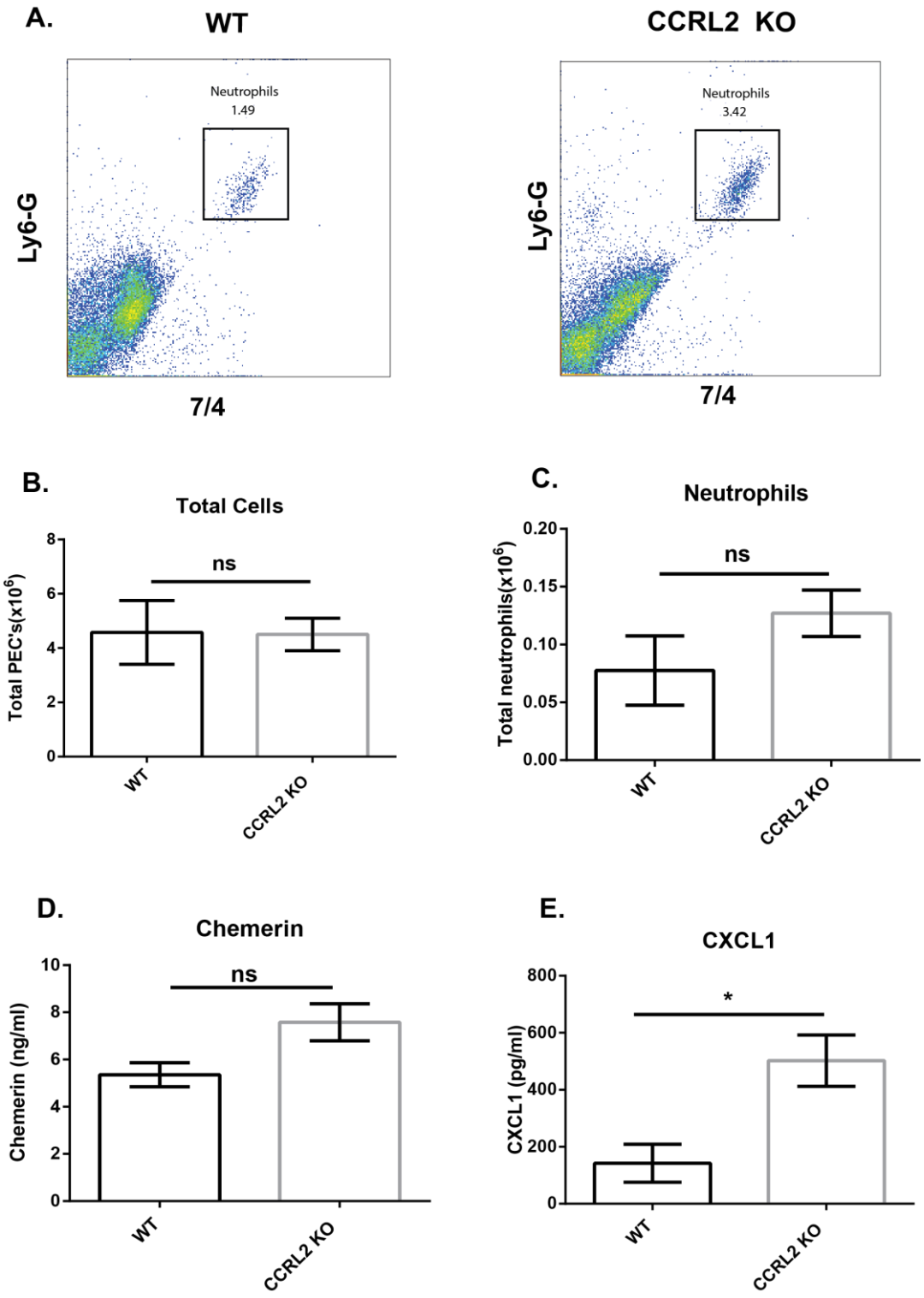


Figure 5.10 Animals lacking CCRL2 display increased CXCL1 levels after 1-hour challenge with thioglycollate.

8-10 week old male CCRL2 KO animals or age matched C57Bl/6J mice were injected with 1ml of 4% thioglycollate i.p.for 1 hour and sacrificed. Peritoneal cavities were lavaged with ice cold PBS supplemented with 2mM EDTA. Cells were quantified and neutrophils were analysed by flow cytometry. **A.** Raw flow cytometry plots of WT and CCRL2 KO cavities. **B.** Total cells recruited. **C.** Total neutrophils recruited. **D.** Chemerin levels were measured by ELISA**. E.** CXCL1 levels were measured by ELISA. Error bars represent S.E.M of 4 animals/group. Statistical significance was assessed using a students unpaired t-test.

5.4.5 Animals lacking CCRL2 display no difference in neutrophil recruitment to the lungs or liver during LPS induced endotoxemia.

The models used thus far have been mainly addressing local inflammatory responses. In order to assess if CCRL2 KO animals display exaggerated inflammation in the context of systemic inflammation, I investigated using LPS challenge as model of endotoxemia. LPS was identified as a key component of bacteria that caused inflammation and fever and is a well established TLR 4 agonist used for the study of acute inflammation in animals [391]. After injection of 1mg/kg of LPS i.p. for 2 hours, I observed robust neutrophil recruitment to the lungs and liver of both WT and CCRL2 KO animals (Figure 5.11A-E). I also measured monocyte recruitment and alveolar macrophage levels in the lungs. Despite robust inflammatory responses, I did not observe any differences in neutrophil recruitment in the lung between WT and CCRL2 KO animals (Figure 5.11A). WT animals had 35.6 ± 2.9 % neutrophils (of $CD45^{+ve}$ cells) while CCRL2 KO animals had 39.4 ± 3.0 % (of $CD45^{+ve}$ cells). Nor were there any differences in monocyte recruitment or in alveolar macrophages (Figure 5.11B-C). Similarly in the liver, there were no differences in neutrophil recruitment between WT and CCRL2 KO animals (Figure. 5.11D-E).

I measured cytokine levels in the serum and found no difference in CXCL2 levels (a murine neutrophil chemoattractant), which was unsurprising given that there were no differences in neutrophil recruitment at this time point (Figure 5.11G). However, CCRL2 KO animals displayed significantly ($P \leq 0.05$) less IL-6 in the blood compared to WT controls (5.11H). WT animals produced 40 ± 1.9 ng/ml IL-6 compared to 31.8 ± 2 ng/ml in CCRL2 KO animals. In line with the previously published report by Monnier *et al.*, CCRL2 KO animals displayed significantly higher chemerin levels in the serum after LPS challenge compared to WT animals (Figure. 5.11F) [260].

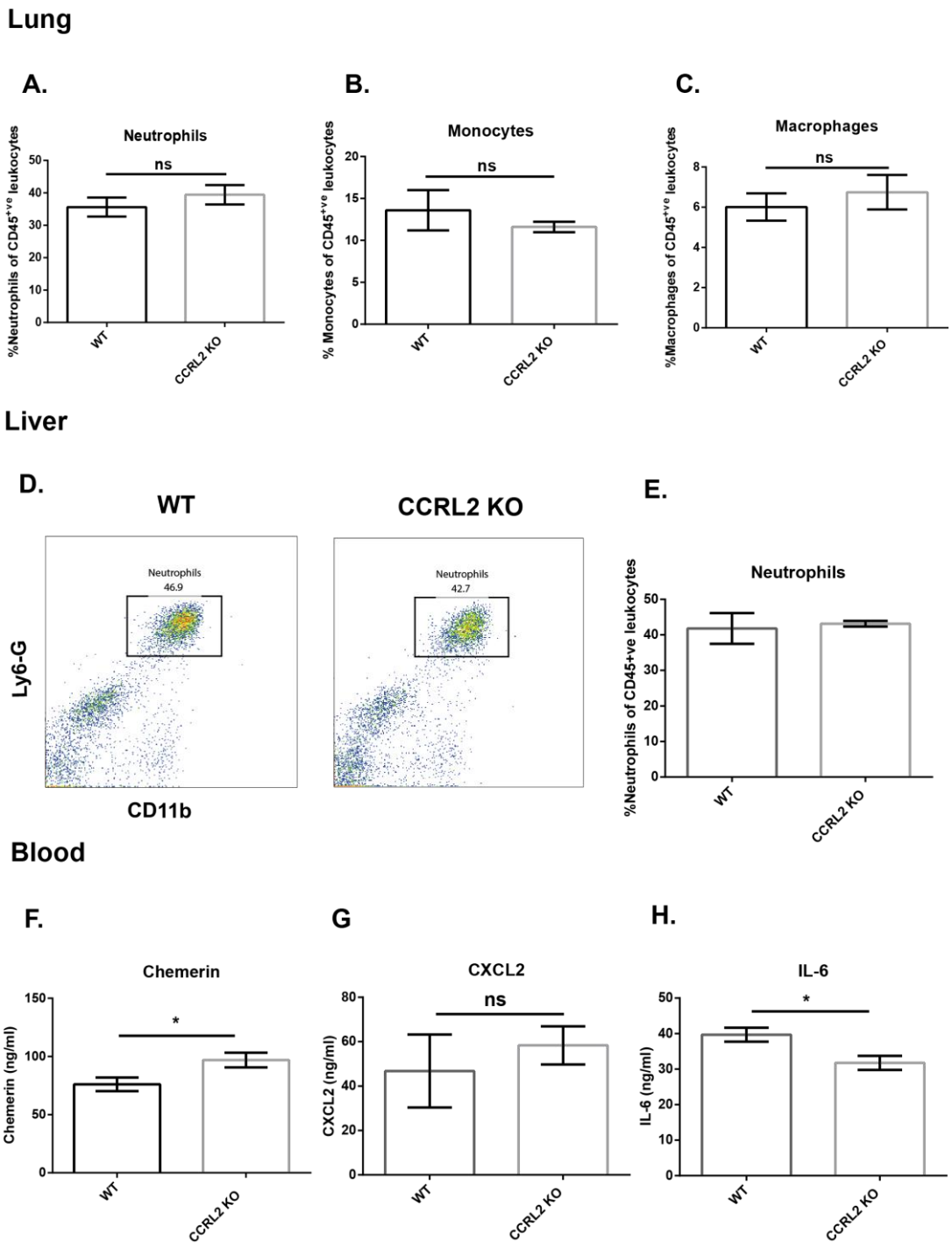


Figure 5.11 Animals lacking CCRL2 do not display an obvious difference in neutrophil recruitment to the liver or lungs following LPS challenge.

8-10 week old male CCRL2 KO animals or age matched C57Bl/6J mice were injected with 0.2 ml LPS (1mg/kg) for 2 hours and sacrificed. Blood was collected via hepatic portal vein into Eppendorf tubes and allowed to clot at 4°C for 3 hours prior to serum isolation **A.** Lungs were digested in collagenase D (1mg/ml) for 1 hour at 37°C and then passed through a 70µm filter to obtain a single cell suspension. Cell recruitment was quantified by flow cytometry (represented as % of $CD45^{+ve}$ cells). Neutrophils ($Ly6\text{-}G^{+ve}$,$CD11b^{+ve}$). **B.** Monocytes ($7/4^{+ve}$, $Ly6\text{-}G^{-ve}$). **C.** Alveolar macrophages ($CD11c^{+ve}$, $Siglic\text{-}F^{+ve}$). **D.** Livers were passed through a 70µm filter and analysed by flow cytometry. Representative flow cytometry plots of neutrophils in the liver. **E.** Neutrophils (% of $CD45^{+ve}$) Error bars represent S.E.M. of 7 animals/group. **F-H.** Indicated mediator levels were measured in the serum by ELISA. Error bars represent S.E.M. of 5-8 animals/group. Statistical significance was assessed using an unpaired students t-test. * $P \leq 0.05$.

5.4.6 Animals lacking CCRL2 experience exaggerated weight loss and enlarged spleens in a model of Dextran sodium sulphate (DSS) induced colitis.

Finally, I performed DSS induced colitis experiments using CCRL2 KO animals. DSS induced colitis is a well-established *in vivo* chemical model of colitis [272, 273]. DSS is thought to break down the mucosal barrier in the gut by directly destroying the surrounding epithelial cells leading to moderate inflammation of the colon, bloody diarrhea and weight loss. The microbiota of the gut plays an important role in this model, hence animals were co-housed for 2 weeks prior to DSS administration in order to exclude this as a variable [392]. Another important factor to note is that I used female animals in these experiments rather then males as previously published reports have demonstrated that males develop more severe disease [393]. Following the cohousing period, 2% DSS was administered in the drinking water for 7 days, followed by 3 days of normal drinking water. This is a longer-term model than the others I have presented so far (10 days total) and a different mechanism of inflammation induction. Another reason for this choice of model was that the adaptive immune system is not involved in the pathogenesis since RAG KO animals lacking T or B cells experience inflammation to the same degree as wild type animals [394]. Since the predominant phenotype of animals lacking CCRL2 seems to be on innate immune cells, this was considered advantageous.

During the 10 days of disease, both WT and CCRL2 KO animals lost weight. Interestingly, animals lacking CCRL2 lost significantly more weight on days 9 and 10 compared to WT ($P \leq 0.05$). On day 10, WT animals had lost 4.6 ± 1.9 % of their initial body weight whereas CCRL2 KO animals had lost 8.9 ± 2.8 % of their initial body weight (Figure 5.12A). Animals were inspected daily for clinical signs of disease including loose faeces, bloody stools and rectal bleeding. Loose faeces and

inflammation of the anus were the only overt clinical signs observed during these experiments. Another difference was a significantly ($P \leq 0.05$) increased spleen weight to body weight ratio in the CCRL2 KO animals (Figure 5.12C). This was reminiscent of the enlarged spleens I observed in naïve CCLR2 KO animals. Sections of the distal colon were fixed, stained with hematoxylin/eosin (H&E) and disease severity was visually assessed by an established disease scoring protocol [273]. Colon shortening was measured as a marker of colon inflammation and myeloperoxidase activity in the colon was used as a measure of neutrophil infiltration (Figure 5.12D-E). There were no obvious differences between WT and CCRL2 KO animals in any of these readouts. Histological scores did not differ between the two groups (Figure 5.12E).

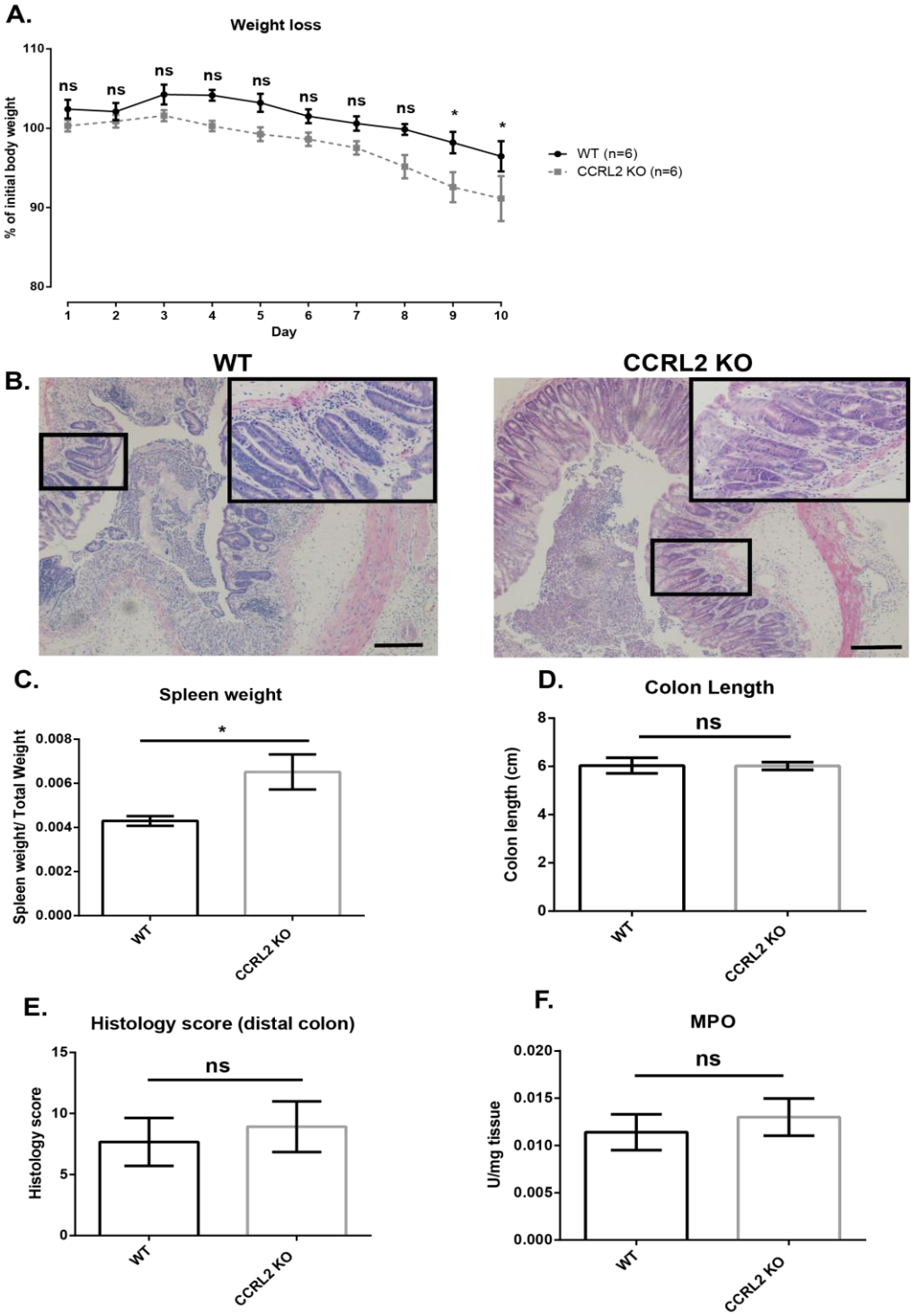


Figure 5.12 Animals lacking CCRL2 display exaggerated weight loss and splenomegaly in DSS induced colitis.

10-week-old female CCRL2 KO animals and age matched littermate C57Bl/6J animals were cohoused for 2 weeks before drinking water was replaced with 2% DSS. Fresh DSS drinking water was given every 2 days. On day 7 DSS was replaced with normal drinking water. **A.** Animals were weighed and clinical signs of disease were evaluated daily. On day 10, animals were sacrificed. Statistical significance was assessed using 2-way ANOVA with Bonferronis multiple comparison test. **B.** The distal colon was harvested and fixed in 4% formalin prior to H&E staining for histology Inset panel showing leukocyte infiltration and goblet cell destruction. Scale bar represents 200μm. **C.** Spleens were harvested and weighed. **D.** Colon length was measured. **E.** Disease scoring of distal colon by histology. **F.** MPO activity in distal colon. Error bars represent S.E.M. of 6 animals/group. Statistical significance was assessed using a students unpaired t-test. * $P \leq 0.05$. (**C-F**).

5.5 Discussion

5.5.1 CCRL2 plays a role in chemerin-induced adhesion of murine macrophages in the electrical impedance sensing platform but not in chemotaxis.

Chemerin has been demonstrated to induce robust adhesion of murine macrophages by a number of groups including our own [198]. ChemR23 is thought to be the predominant receptor involved in transducing downstream signals from chemerin binding. Experiments using macrophages from animals lacking the ChemR23 receptor in the previous chapter (Figure. 4.4D), demonstrated that the majority of chemerin-induced adhesion in the impedance platform does indeed seem to be due to ChemR23 dependent cytoskeletal rearrangements. The prevailing theory in the literature is that CCRL2 binds chemerin in order to concentrate it locally and present it to ChemR23 expressing cells [259, 260]. My *in vitro* studies using cells lacking CCRL2 largely agree with this model. While chemerin induced responses are not ablated in animals lacking CCLR2, they are significantly reduced. This result potentially supports a role for chemerin presentation by CCRL2 rather than direct signalling by this receptor which lacks the intracellular DRYLAIV motif required for downstream signalling [255]. Chemerin has been demonstrated to induce macrophage adhesion to fibronectin and VCAM-1 via integrin clustering. Hence, it is possible that CCRL2 may be affecting chemerin induced adhesion by interfering with this process [198]. However since the plates were not coated with any proteins, it is unclear whether integrins would play an important role in macrophage adhesion to plastic.

The fact that I did not observe a similar effect in real time chemotaxis assays is an interesting observation. Zabel *et al.* demonstrated that media containing chemerin that was first incubated with CCRL2 transfected cells induced less chemotaxis of

ChemR23 transfected cells, indicating that CCRL2 bound and scavenged chemerin from the medium [259]. In this context, one might have expected there to be more available chemerin for chemotaxis in the CCRL2 KO cells in my experiments and thus observe greater migration to chemerin. However, cells were not preincubated with media and these cells expressed ChemR23, so as they came in contact with chemerin they would have responded by migrating. The most likely function of binding of chemerin by CCRL2 is to present it to other ChemR23 expressing cells or even to heterodimerise with ChemR23 on the same cell. Although ChemR23 and CCRL2 have not yet been reported to dimerise, ChemR23 has been reported to dimierise with CXCR4 and CCR7, although without any obvious functional consequences [395]. Despite this potential mechanism of chemerin presentation, CCRL2 does not seem to play a role in chemotaxis. Another factor is the difference in what these two assays detect. As discussed in the previous chapter, I observed very different signalling properties of chemerin and chemerin-derived peptides between these two systems despite using the same primary cell types. The C17 peptide, for example, was 10-fold less potent in chemotaxis assays than full-length chemerin whereas it actually induced higher responses at equipotent concentrations in the impedance adhesion platform. These observations are in agreement with published literature, suggesting that CCRL2 does indeed play a role in chemerin induced adhesion [260]. There have not been any reports of CCRL2 playing any role in chemotaxis and my results indicate CCRL2 does not contribute to macrophage chemotaxis to chemerin and chemerin derived peptides.

5.5.2 Phenotypic characterisation of naïve animals lacking the CCRL2 receptor

There has been a number of reports detailing CCRL2 expression in a range of different cell types discussed in the introduction. The first report of animals lacking the CCRL2

receptor was from Zabel *et al.* who reported the involvement of this receptor in mast cell responses to antigen specific IgE mediated allergic inflammation [259]. In their initial characteristion of this mouse, they did not report any differences between naïve CCRL2 KO and WT animals, although they did not publish a detailed analysis of resident populations across different tissues. One difference between this study and the current set of experiments is that the CCRL2 KO animals they used were created by Lexicon Pharmaceuticals and contain a different mutation to the mouse used in this chapter. In a subsequent study, Otero *et al* did examine lymphoid organs and blood in CCRL2 KO animals and reported no significant differences under resting conditions [258]. However, they created their own CCRL2 KO mouse line and these animals were on a BALB/c background rather then a C57Bl/6J background.

To date, studies examining CCRL2 KO animals have used different mutations and different genetic backgrounds to the animals I have used. In addition, given that Zabel *et al* reported animals lacking CCLR2 (again on a BALB/c background) displayed higher circulating chemerin levels, it seemed logical to investigate whether there were any differences under resting conditions in the CCRL2 KO mice (Jackson Laboratoies) that I was using [260]. As detailed earlier in the results section, I did not observe any obvious differences in most resident cell populations in the spleen, blood or bone marrow in naïve animals. There was a modest decrease in CD4 T cells in the spleen as well as a trend towards decreased T cells in the blood, although this was not significant. Murine T cells have not been reported to express CCRL2 but Otero *et al*. reported impaired T cell recruitment in the bronchiolar lavage fluid in CCRL2 KO animals challenged with OVA [258]. Although CCRL2 may not be playing a direct role in T cell recruitment, it is possible it somehow dampens pro-inflammatory cytokine production locally. Since the observed decrease in T cells was specifically the CD4 T cell subset, it

is possible there is also decreased Treg cells in CCRL2 KO animals which may be contributing to the exaggerated inflammatory responses observed and this will be investigated.

5.5.3 Characterisation of inflammatory responses of animals lacking the CCRL2 receptor following challenge with zymosan.

Two of the three inflammatory models published using CCRL2 KO animals have been Th2 type allergic inflammation models. Both of these published studies reported modest decreases in antigen specific allergic inflammation with decreased leukocyte recruitment [258, 259]. These reports are interesting to think about in the context of my observations that animals lacking CCRL2 experienced increased neutrophil and monocyte recruitment upon zymosan challenge. These are very different types of models and are addressing different questions. The ZIP model induces a classical Th1 type inflammatory response, characterised by production of inflammatory cytokines including IL-6, IFN-γ and IL-1β amongst others (Figure 3.5). Another important point mentioned earlier, is that the CCRL2 KO animals used in the report by Otero *et al* (in which they reported impaired leukocyte recruitment and impaired migration of antigen loaded DC to draining lymph nodes) were on a BALB/c background [258]. BALB/c mice are predisposed to Th2 type immune responses characterised by increased IL-4 and IL-13 production in response to parasitic infections but impaired immune responses to intracellular pathogens. In contrast, C57Bl/6J mice are predisposed to classical Th1 type immune responses characterised by robust production of IFN-γ,TNF-α and IL-12 [396-398]. Similar phenotypes are observed with respect to macrophages from these strains with C57Bl/6J animals favoring M1 macrophages while BALB/c animals tending towards M2 macrophages [399]. Clearly the genetic background of mice affects the

observed phenotypes in preclinical disease models, therefore investigating CCRL2 KO animals on the same genetic background as those I used to validate the *in vivo* models was important.

To the best of my knowledge, this is the first report of CCRL2 KO animals to be tested in the ZIP model. The mechanism by which CCRL2 seems to dampen neutrophil and monocyte recruitment to the peritoneum during ZIP remains unclear. One possibility is that animals lacking CCRL2 may have higher circulating chemerin levels in the blood due to less chemerin binding to the vasculature (as demonstrated in Figure 5.11F) which may, in turn, activate endothelial cells during inflammation [260]. As mentioned, the current hypothesis in the literature proposes that CCRL2 serves to bind chemerin and present it to ChemR23 expressing cells to promote migration into inflamed tissues. If this were true in the ZIP model, one might have expected *decreased* inflammatory cell recruitment in animals lacking CCRL2. A recent report has demonstrated the ability of chemerin to induce pro-inflammatory signalling in microvascular endothelial and smooth muscle cells [244]. Chemerin treatment of smooth muscle cells increased mRNA expression of a number of pro-inflammatory mediators including CCL2, TNF-α and VCAM-1. Furthermore, chemerin treatment increased monocyte attachment to endothelial using an *in vitro* adhesion assay [244]. While intriguing, the fact that I did not observe higher chemerin levels in the peritoneum of CCRL2 KO animals suggests that increased chemerin levels may not be responsible for the increased inflammation (at least locally). It will however be important to compare chemerin bioactivity in CCRL2 KO and WT animals since, as stated previously, the commercial ELISA kit detects both pro-chemerin and active chemerin. Increased bioactive chemerin in CCRL2 KO animals may yet account for increased monocyte and neutrophil mobilisation. Adding further complexity, there has been a

previous report of chemerin exerting anti-inflammatory effects on endothelial cells. Chemerin treatment of HUVECs decreased TNF-α induced VCAM-1 protein expression and NF_KB phosphoylation [243]. Clearly, further investigation is required to elucidate exactly what effect chemerin has on endothelial cells.

Another decoy chemokine receptor, D6, displayed an interesting phenotype in the ZIP model. The authors observed increased macrophages in the peritoneum during the resolution phase, which was associated with increased efferocytosis. They did not report any differences in neutrophil recruitment [400]. While D6 and CCRL2 share similarities, D6 was demonstrated to efficiently bind and internalise a range of CC chemokines [401]. The only ligand reported for CCRL2 in the mouse to date is chemerin, which is not internalised upon binding. The mechanism of action of the CCRL2 receptor may be more subtle but seems likely that it will be related to its chemerin binding properties [259]. *In vivo* neutralisation of endogenous chemerin by anti-chemerin antibodies or anti-sense oligonucleotides in CCRL2 KO animals could address this.

CCRL2 KO animals exhibited higher circulating neutrophils and a trend towards higher $Ly6C^{hi}$ monocytes in the blood during ZIP so it is conceivable that the increased recruitment to the peritoneum is at least partially due to higher levels of monocytes and neutrophils being mobilised from the bone marrow during inflammation. An interesting experiment that could explore whether increased chemerin bioactivity was contributing to this would be to administer recombinant chemerin intravenously and measure neutrophil and monocyte mobilisation from the bone marrow into the blood. It will also be important to measure different cytokines and chemokines in the blood of CCRL2 KO animals during zymosan challenge to establish if there are systemic differences in any mediators which may explain this phenotype.

5.5.4 Animals lacking CCRL2 display increased neutrophil recruitment to the peritoneum and increased CXCL1 production during 1-hour thioglycollate challenge.

Thioglycollate produces a more potent inflammatory reaction than zymosan at the doses used and is a very different type of inflammatory stimulus. It is well established that it induces a robust recruitment of neutrophils at early time points after injection and this recruitment is mainly due to CXCL1 and CXCL2 production in the cavity [402, 403]. When I investigated CCRL2 KO animals using this model, the results were similar to the zymosan peritonitis experiments in that CCRL2 KO animals displayed exaggerated CXCL1 production in the peritoneum as well as a trend towards increased neutrophil recruitment. There was also a trend towards increased chemerin production in the peritoneum in CCRL2 KO animals. Higher chemerin levels could in turn activate surrounding endothelial cells or mesothelial cells and lead to increased local inflammatory mediator production as discussed earlier. The fact that I observed higher inflammatory mediators being produced in this very short term model but did not observe any differences in the 4-hour ZIP experiments is curious but may be a feature of the time points analysed. I know from my kinetic studies in chapter 3 (Figure 3.6) that most inflammatory mediators produced in the cavity peak by 4 hours or earlier after zymosan challenge, hence any differences in initial production may have been masked by 4 hours. It would therefore be informative to carry out a 2-hour zymosan challenge to compare mediator levels both in the peritoneum and in the blood using CCRL2 KO animals.

5.5.5 Animals lacking CCRL2 display no difference in neutrophil recruitment to the lungs or liver during LPS induced endotoxemia.

Chemerin has been reported to exert potent anti-inflammatory effects in LPS induced lung inflammation by Luangsay *et al.* Chemerin treatment (i.v) reduced neutrophil recruitment to the lungs as well as inflammatory mediator production in bronchiolar lavage fluid including IL-6, TNF-α and CXCL1 [241]. These effects were shown to be ChemR23 dependent. In a subsequent study mentioned earlier, Monnier *et al*. performed similar studies using animals lacking CCRL2 and reported higher levels of chemerin in the blood of CCRL2 KO animals treated with LPS compared to WT animals [260]. They reported no difference in neutrophil or T cell recruitment to the lungs but did observe impaired NK cell recruitment, which was attributed to loss of chemerin presentation by CCRL2 on endothelial cells in the lung to ChemR23 expressing NK cells [260].

Given the anti-inflammatory effects of chemerin reported previously in this model, it stood to reason that animals with higher circulating chemerin might exhibit reduced inflammatory responses when challenged with LPS. The experiments I performed using LPS challenge in CCRL2 KO animals differed from these above in a number of important ways. Firstly, LPS was administered intranasally for 12-18 hours in both the above studies whereas, I administered LPS i.p. for 2 hours. In addition, the CCRL2 KO animals used by Monnier *et al.* were on a BALB/c background rather then a C57Bl/6J background and so these experiments are not directly comparable [396, 404]. It is curious that these animals exhibited significantly higher monocyte and neutrophil recruitment to the peritoneum during ZIP but did not display marked differences in neutrophil or monocyte recruitment to the lungs or liver during LPS challenge. The ZIP model at this dose of zymosan (100 μg/mouse) induces a more targeted local

inflammatory response compared to LPS challenge (1 mg/kg), which induces a far more systemic inflammatory response. It is possible that the different responses are due to the differing magnitudes of inflammatory stimuli used. As Newson *et al.* have elegantly demonstrated, two different doses of zymosan induce very different inflammatory responses both in the immediate local cell recruitment as well as differential recruitment of immune cells during the resolution stages [55]. As shown in chapter 3, local chemerin levels increase rapidly following zymosan challenge. While blood levels of chemerin increase following LPS challenge, local levels of chemerin may not increase in the lungs or liver; thus CCRL2 may not have as obvious a function in local cell recruitment in this context.

Another interesting observation from my experiments was that IL-6 levels in the blood were significantly lower in CCRL2 KO animals. Given that IL-6 has been shown to play important regulatory roles during inflammation (particularly in shifting macrophages towards the M2 phenotype and limiting LPS induced endotoxemia), it is possible that lower levels of IL-6 indicate exaggerated systemic inflammation, although other inflammatory markers would need to be evaluated to confirm this was the case [405].

5.5.6 Animals lacking CCRL2 experience exaggerated weight loss and enlarged spleens in a model of dextran sodium sulphate (DSS) induced colitis.

There have been no published studies to date investigating the role of CCRL2 in the context of inflammatory bowel disease (IBD). There have however been two studies reporting elevated chemerin levels correlating with disease severity in patients suffering from IBD, while one study saw no correlation [208-210]. Lin *et al*. reported chemerin levels were elevated in animals undergoing DSS colitis compared to healthy controls. Administration of recombinant chemerin intraperitoneally increased disease severity and

inflammatory cytokine levels in the serum of these animals. Perhaps surprisingly, chemerin treatment did not result in increased cell recruitment to the colon but decreased M2 polarisation of macrophages, which resulted in increased tissue inflammation. Furthermore, they observed that blocking endogenous chemerin levels with a neutralising antibody decreased epithelial damage and decreased inflammatory cytokine levels in the serum while increasing M2 markers in the colon such as Arg-1 [210].

In a subsequent study Dranse *et al.* demonstrated that during DSS colitis, total chemerin levels actually decreased in the blood during colitis while bioactive chemerin levels increased. Importantly, chemerin production in the colon rather then systemic chemerin levels, seemed to correlate with disease severity. In contrast to the study by Lin *et al*., treatment with recombinant chemerin during these experiments did not have any effect on disease. Expanding on these results, they demonstrated that animals lacking ChemR23 exhibited less weight loss than the wild type controls and were slower to develop disease, although they did develop comparable disease by the end of the experiments [211]. There were no obvious differences in chemerin levels systemically, but colon explant cultures from animals lacking ChemR23 produced more chemerin compared to wild type animals. An interesting observation from these studies was that during DSS colitis, both ChemR23 and CCRL2 expression were significantly increased in the distal colon at the mRNA level, with CCRL2 being increased by ~15 fold [211]. ChemR23 has been reported to be protective in a number of lung inflammation models, highlighting the functions of chemerin and its receptors vary depending on the tissue and type of inflammation involved [241, 242].

When I investigated animals lacking CCRL2 in the DSS colitis model, I observed that CCRL2 KO animals lost more weight during disease than the wild type

controls. This is an interesting result given that animals lacking ChemR23 had been reported to have the opposite phenotype. Similarly to the study using ChemR23 KO animals, there were no obvious differences in disease scores or cell infiltration by histology or MPO assay. In contrast, I did observe a significant increase in spleen weight in the CCRL2 KO animals, which alongside weight loss can be used as markers of systemic inflammation. Therefore, although the lack of CCRL2 did not affect local tissue inflammation in the colon, it did seem to play a role in controlling systemic inflammation in animals experiencing DSS colitis.

5.5.7 Limitations and potential future studies

The first limitation of these studies is the lack of a reliable commercially available antibody against murine CCRL2. The other studies quoted above which examined murine CCRL2 expression across different tissues used an antibody that had been generated in house. As others have noted in the literature, thus far there is no widely available antibody, which specifically recognises murine CCRL2. However, others have characterised CCLR2 expression across different murine cell types [258-260].

Another limitation was generating sufficient homozygous CCRL2 KO animals and age matched WT controls for these experiments. For reasons of time and animal breeding, some of these studies have low animal numbers per treatment group and future studies will repeat some of these experiments with larger cohorts.

In order to address the mechanism of how CCRL2 dampens neutrophil and monocyte recruitment to the peritoneum during zymosan induced peritonitis, it would be interesting to knock down endogenous chemerin expression in CCRL2 KO animals and examine differences in neutrophil and monocyte mobilisation from the bone marrow into the blood. Given CCRL2 KO animals have more neutrophils in the blood, this

seems like a likely explanation. It will be important to analyse chemerin levels in the blood of these animals since chemerin levels in the peritoneum are similar between CCRL2 KO and WT animals.

It would also be interesting to analyse CCRL2 KO animals in longer term zymosan peritonitis models to investigate if this increased neutrophil influx at early time points affects the resolution phase of the model.

5.6 Summary

In summary, in this chapter I have demonstrated that CCRL2 plays a role in chemerin induced macrophage adhesion. I have characterised animals lacking the CCRL2 receptor under resting conditions and demonstrated that animals lacking CCRL2 display exaggerated inflammatory responses in a number of different models including ZIP, thioglycollate peritonitis, LPS endotoxemia and DSS colitis. These results imply that CCRL2 serves an as yet undefined regulatory function in the context of inflammation, dampening inflammatory cell recruitment.

6 Summary and Final Discussion

6.1 Key findings

The experiments in this thesis have focused on expanding our knowledge of the role of chemerin and chemerin peptides during inflammation as well as the role of the non-signalling receptor CCRL2. My key findings are outlined below:

- Chemerin pre-treatment during ZIP increased neutrophil recruitment to the peritoneum compared to PBS (Figure 4.7). The chemerin derived peptide, C17 in contrast decreased monocyte recruitment (Figure 4.7).
- Chemerin intervention, 2 hours after zymosan challenge, significantly decreased monocyte recruitment (Figure 4.8). Incubation of chemerin with neutrophil derived proteases results in production of chemerin peptides, which may be responsible for the anti-inflammatory effects observed in these experiments (Figure 4.12).
- Endogenous total chemerin levels increased during inflammation, as does chemerin bioactivity, although with different kinetics (Figure 4.13).
- Treatment with anti-inflammatory corticosteroids decreased chemerin expression *in vivo* (Figure 4.14).
- Inhibition of chemerin expression in vivo increases Ly6C^{hi} monocytes and neutrophils in the blood during ZIP, but does not result in increased recruitment to the peritoneum (Figure 4.17).
- Macrophages lacking CCRL2 displayed impaired chemerin stimulated adhesion (Figure 5.1).

- Naïve animals lacking CCRL2 displayed enlarged spleens and decreased CD4 T cells numbers in the spleen (Figure 5.3).
- Animals lacking CCRL2 displayed exaggerated neutrophil and monocyte recruitment to the peritoneum during ZIP as well as increased neutrophils in the blood (Figures 5.6 and 5.9)
- CCRL2 KO animals displayed exaggerated weight loss and enlarged spleens during DSS induced colitis (Figure 5.11).

6.2 Future directions

6.2.1 *In vivo* administration of chemerin administration during an ongoing inflammatory response.

In this thesis I have demonstrated that full-length active chemerin administered i.p. before zymosan challenge can increase neutrophil recruitment to the peritoneum. These results need to be explored further, particularly in light of the conflicting nature of the chemerin literature. Chemerin injection alone does not recruit neutrophils or monocytes to the peritoneum (data not shown and Rosie Hart, DPhil thesis, Oxford University, 2010). However, it is possible that bioactive chemerin is capable of syngergising with other mediators required for driving neutrophil mobilisation during inflammation in a similar manner to IL-17, which alone has minimal inflammatory effects but in combination with other inflammatory stimuli significantly enhances neutrophil recruitment [406-408]. To investigate this possibility, it would be interesting to administer chemerin intravenously during i.p zymosan challenge and measure neutrophil and monocyte numbers in the blood. Alternatively, administration of elastase, cathepsin-G or tryptase intravenously may cleave inactive pro-chemerin in the blood to active isoforms during ZIP, possibly increasing neutrophil and monocyte mobilisation from the

bone marrow. It will be important to perform these experiments in ChemR23 and CCRL2 KO animals as well to identify which receptors are important in this process. The dorsal air pouch model would be of use to investigate possible synergistic effects of chemerin with other mediators [409]. Using the dorsal air pouch model of sterile inflammation, chemerin could be injected directly into the pouch followed by inflammatory stimuli in order to assess whether the increased neutrophil numbers observed in the peritoneum during ZIP were due to direct effects on recruited leukocytes (since there are no resident macrophages and few other resident cells in the pouch) [409].

6.2.2 Identifying chemerin bioactivity at different inflammatory sites

From my thesis, I have shown that endogenous total chemerin levels increase during inflammation (Figure 4.13). Chemerin bioactivity at the ChemR23 receptor also increases but displays different kinetics, perhaps indicating that other chemerin isoforms or peptides are being generated. As has been shown in a number of reports, different chemerin isoforms are present at different sites of inflammation. For example, in patients with rheumatoid arthritis, the majority of chemerin present in the synovial fluid is chemerin^{158}, not pro-chemerin, whereas the majority of chemerin in ascites fluid was identified to be chemerin^{157} and the majority of chemerin circulating in the blood stream is pro-chemerin with some chemerin^{158} [170, 174]. These reports suggest there is differential cleavage of pro-chemerin at different anatomical sites during chronic inflammation. Gaining a better understanding of which isoforms are generated where, would be beneficial in terms of targeting specific isoforms as therapies in diseases like

rheumatoid arthritis, while leaving other isoforms which may be important for host defense intact.

In contrast to pre-treatment of animals with chemerin, administration of chemerin into an already inflamed peritoneal cavity produced anti-inflammatory effects on monocyte recruitment (Figure 4.8). This result coupled with my observation that *in vitro* incubation of chemerin with neutrophil derived proteases can generate shorter bioactive chemerin peptides (Figure 4.12) indicates that some chemerin cleavage products generated *in vivo* may possess anti-inflammatory properties. The lack of specific reagents capable of detecting these shorter peptides has hampered their identification. A student in the Greaves laboratory, Sophia Valaris in collaboration with UCB Celltech, is developing specific monoclonal antibodies against short chemerin derived peptides, which will be useful for studying chemerin peptides present in inflammatory exudates. Monoclonal antibodies that can specifically block these different peptides *in vivo,* will also shed light on their role in different inflammatory pathologies.

The function of chemerin during inflammatory diseases remains poorly understood. As I have discussed in chapter 4, chemerin levels have been reported to be elevated in a wide range of pathologies including rheumatoid arthritis, psoriasis, cardiovascular disease, metabolic diseases and inflammatory bowel disease amongst others. However, these studies have all used the commercial R&D ELISA kit to measure chemerin levels, which detects both inactive pro-chemerin and active chemerin. Unfortunately, this is not an accurate measure of chemerin bioactivity. As was demonstrated by both my results in Figure 4.13 and Dranse *et al.*, total chemerin levels as measured by ELISA do not translate to bioactive chemerin [211].

Previous studies reporting that total chemerin levels are reduced in patients treated with both anti-TNF-α antibodies and IL-6 receptor antagonists will be important to revisit with more specific reagents to detect specific chemerin isoforms and peptides [207, 214, 215]. In addition my own results demonstrated that the anti-inflammatory corticosteroid dexamethasone decreased total chemerin levels in mice after zymosan challenge (Figure 4.14). It is very possible these treatments are decreasing total chemerin levels but increasing the relative abundance of specific chemerin isoforms not detected by the commercial ELISA. Further investigation will elucidate which chemerin isoforms may be beneficial and which may be detrimental in the context of inflammatory diseases.

6.2.3 Targeting chemerin therapeutically

From the literature, one could argue that targeting chemerin would be of therapeutic benefit for the treatment of a number of inflammatory pathologies. Rheumatoid arthritis and psoriasis are two examples of diseases where there is a large body of evidence in support of this approach. Psoriasis is an inflammatory disease of the skin. The initial stages of plaque formation involve DCs, pDCs, T cells and neutrophils. Chronic long term established plaques are characterised by T cells, pDCs and DCs. CD8 T cells and Th17 T cells are the main T cell populations present in lesions, although CD4 T cells are also present [410]. IL-17 and IL-22 are produced at high levels within these lesions and IL-17 synergises with interferon-γ and TNF-α in order to further activate keratinocytes. A range of chemokines are also produced within the lesion as well as type 1 interferons (predominantly from pDCs) [411]. Patients suffering from psoriasis have been reported to exhibit higher chemerin levels which correlate with disease severity and treatment

with the anti-TNF-α antibody, Inflixamab, decreased total chemerin levels [206, 207]. Chemerin has also been demonstrated to colocalise with pDCs and NK cells in diseased skin [202, 205]. Because type 1 interferons play an important role in the initiation of this disease and pDCs are major producer of interferons, blocking chemerin in this context would seem a logical approach [411]. pDC express a limited number of functional chemokine receptors including CXCR3 (responds to CXCL10 and CXCL11), CXCR4 (responds to CXCL12) and ChemR23 (responds to chemerin) [194, 412]. Targeting CXCR3 and ChemR23 simultaneously in pre-clinical models would be interesting to explore as a novel approach to halt pDC recruitment to psoriatic plaques. Mouse models of psoriasis do not recapitulate the pathology as well as other disease models, however there have been a number of models developed which have led to important discoveries about this disease, including conclusively establishing the important role T cells play in this disease [413, 414]. Although no current mouse model recapitulates all aspects of psoriasis in humans, the K5-STAT3 transgenic mouse carries a targeted overexpression of STAT3 in keratinocytes and develops psoriasis like plaques characterised by lymphocyte and neutrophil infiltration [415]. It would be of interest to utilise this model in conjunction with neutralising chemerin antibodies or ChemR23 antagonists to investigate the efficacy of blocking chemerin as a therapy for patients suffering from psoriasis.

Rheumatoid arthritis is another inflammatory disease in which targeting chemerin could be of therapeutic benefit. Similarly to psoriasis, there have been reports of elevated chemerin levels in patients suffering from rheumatoid arthritis as well as reports of decreased systemic chemerin levels after treatment with anti-TNF-α antibodies and IL-6 receptor antagonists [213-215]. Local chemerin levels in the inflamed joints are probably more important to address however. Chemerin has been

demonstrated to be highly expressed in the diseased synovium and has been demonstrated to exert pro-inflammatory effects on human synoviocytes (increasing IL-6, CCL2, interferon-γ and matrix metalloproteanase production) [187, 203, 212]. It will be of interest to use blocking anti-chemerin antibodies in murine models of rheumatoid arthritis to examine potential therapeutic benefits, which to the best of my knowledge has not been done. Given Zhao *et al*. reported chemerin^{158} to be the dominant chemerin isoform present in inflamed joints of patients suffering from rheumatoid arthritis, specifically blocking this isoform in the joint may be the best approach, as this may avoid potential side effects of blocking all chemerin isoforms [174].

The therapeutic potential of blocking chemerin in other inflammatory diseases is perhaps less obvious. Chemerin may be important for glucose homeostasis, so blocking all chemerin isoforms systemically may have deleterious off target effects and increase the risk of metabolic disease [221, 223, 224]. However, chemerin has also been reported to promote metabolic disease progression in a number of studies and this requires further investigation before blocking chemerin could realistically be explored as a therapeutic strategy [172, 233, 416]. Chemerin has been reported to possess potent anti-bacterial properties and targeting chemerin therapeutically may also make patients more susceptible to bacterial infections [185, 235]. A final consideration is the possibility that chemerin is broken down into shorter chemerin derived peptides which exert anti-inflammatory effects as have been described by Cash *et al.* [225, 238, 239]. Data from section 4.4.5 of this thesis also supports this hypothesis. If true, blocking endogenous chemerin may also negate anti-inflammatory and anti-microbial effects of chemerin derived peptides produced in the resolution phase of an inflammatory response. This will need to be evaluated further in chemerin KO animals and by blocking antibodies against specific chemerin isoforms.

Administering exogenous chemerin or chemerin peptides may actually have beneficial effects in Th2 type allergic inflammatory diseases such as asthma or chronic obstructive pulmonary disorder (COPD). As discussed in chapter 4, both full-length chemerin and a lipidated chemerin C9 peptide have been reported to exert anti-inflammatory effects in allergic airway inflammation [245, 247]. The use of stabilised peptides in these disease contexts require further research but there is an unmet clinical need for good long term treatments for asthma and COPD [417]. Hence, chemerin or chemerin peptides either alone or in combination with current therapies like corticosteroids or β-adrenergic receptor agonists may prove beneficial in decreasing airway inflammation while avoiding off target effects of current therapies such as immunosuppression and resistance [418].

6.2.4 Elucidating the role of the CCRL2 chemerin receptor in innate immune cell recruitment to sites of inflammation.

In chapter 5, I demonstrated that animals lacking CCRL2 display increased neutrophil and monocyte recruitment to an inflamed peritoneum as well as increased neutrophil numbers in the blood. To the best of my knowledge, this is the first report of CCRL2 dampening monocyte and neutrophil mobilisation and recruitment to a local site of inflammation and points to a potentially novel regulatory role of this non-signalling receptor during inflammation. The exact mechanism of how CCRL2 dampens neutrophil and monocyte mobilisation in normal physiology remains to be determined. The most obvious explanation was increased chemerin levels in animals lacking CCRL2 given data from Monnier *et al*. and my own data from section 5.5.5 showing animals lacking CCRL2 had higher serum chemerin levels following LPS challenge [260]. However, during zymosan challenge, there were no significant differences in chemerin

levels either in the peritoneum or in the plasma as measured by ELISA. It is however possible that there are higher levels of other chemerin isoforms and peptides generated during zymosan challenge, that were not detected by the ELISA. Hence, it will be important to test these same samples in the β-arrestin recruitment bioassay I used in section 4 4.6 to confirm if bioactivity at the ChemR23 receptor is different between CCRL2 KO animals and wild type animals. If this is the case, it seems likely that higher levels of bioactive chemerin in the CCRL2 KO animals syngerise with other inflammatory mediators, given my results that chemerin pre-treatment in ZIP significantly increased neutrophil recruitment (Figure 4.7C).

Another possible explanation could be decreased Treg cell numbers in CCRL2 KO animals. Given I observed fewer CD4 T cells in the spleen of naïve animals lacking CCRL2, it is possible this decrease was due to a defect in Treg cell development. It will also be of interest to interrogate Treg cell populations in these animals both under resting conditions and during inflammation to establish whether this population is contributing to the observed phenotype. Although there may be decreased Treg cell numbers in CCRL2 KO animals, it seems unlikely this defect would manifest in short term inflammatory models like a 4-hour zymosan challenge. However, they may be more important in longer-term chronic inflammatory models such as the 10-day DSS colitis experiments or 13-day challenge with zymosan and this requires further investigation.

CCRL2 and chemerin are both highly expressed in the inflamed synovium of patients suffering from rheumatoid arthritis [212, 263]. Given chemerin levels are increased in CCRL2 KO animals during LPS challenge as well, it would be useful to test animals lacking CCRL2 in murine arthritis models such as the K/BxN serum transfer

model [419, 420]. The advantage of this model is that it can be performed on the CCRL2 KO colony already established in the Pathology Support Building.

In order to elucidate the mechanism of action of CCRL2 the following experiments will be informative:

- Compare chemerin bioactivity in the peritoneum and in the blood of wild type and CCRL2 KO animals during ZIP to establish if there are differences, that may contribute to this phenotype.
- Knock down endogenous chemerin expression in wild type and CCRL2 KO animals to confirm whether the increased monocyte and neutrophil recruitment is due to increased chemerin bioactivity.
- Evaluate inflammatory mediators in the plasma of CCRL2 KO animals during zymosan challenge to assess any systemic differences in mediators that may also be contributing to the inflammatory phenotype.
- Irradiate CCRL2 KO animals and make bone marrow chimeras to assess whether the increased mobilisation and recruitment is due to differences on the hematopoietic compartment or on other cell types.

6.3 Final summary and conclusions

From this thesis, I have demonstrated that chemerin levels increase during inflammation as detected by ELISA but bioactivity at the ChemR23 receptor displays different kinetics indicating the presence of other chemerin products not detected by ELISA. I have also demonstrated that incubation of recombinant active murine chemerin with neutrophil derived proteases results in further cleavage to short bioactive peptides.

The role played by chemerin in inflammation remains controversial and context specific. Further research is required to establish chemerin's role in inflammation but it seems likely to perform different functions during different phases of the inflammatory response as well as in different types of inflammation. I believe that targeting specific chemerin isoforms will be of therapeutic benefit in at least some inflammatory diseases such as rheumatoid arthritis and psoriasis. Blocking chemerin in psoriasis for example, may inhibit pDC recruitment to plaques, decreasing interferon-α production. Blocking chemerin in rheumatoid arthritis may decrease neutrophil recruitment by inhibiting synergistic effects of chemerin^{158} with other inflammatory mediators such as IL-6, CCL2 and MMP3 [187].

CCRL2 has been thought of as a decoy chemerin receptor with little function during inflammation apart from concentrating chemerin on the cell surface [259]. The results from this thesis indicate that CCRL2 plays a non-redundant role in dampening monocyte and neutrophil mobilisation from bone marrow and recruitment during inflammatory responses. The mechanism by which it achieves this remains unknown but it seems likely it will be related to chemerin bioactivity.

In conclusion, the exact role of chemerin in health and disease remains a complicated and controversial subject. Exogenous chemerin treatment may prove beneficial for some diseases such as asthma, COPD and melanoma but chemerin blockade may be the best approach in other diseases such as arthritis, psoriaisis and inflammatory bowel disease. Further research is required to fully understand the plethora of functions this protein performs in order to safely target it therapeutically. Given different chemerin isoforms seem to be involved in different diseases it will be interesting to see if chemerin isoform specific therapies can be developed and tested in pre-clinical models and what benefits they will bring to patients.

References

1. Serhan, C.N. and J. Savill, *Resolution of inflammation: the beginning programs the end.* Nat Immunol, 2005. **6**(12): p. 1191-7.
2. Kumar, V., Cotran, R.S., Robbins, S.L., *Robbins Basic Pathology*. 2003.
3. Levy, B.D., et al., *Lipid mediator class switching during acute inflammation: signals in resolution.* Nat Immunol, 2001. **2**(7): p. 612-9.
4. Li, M.O., et al., *Transforming growth factor-beta regulation of immune responses.* Annu Rev Immunol, 2006. **24**: p. 99-146.
5. Nathan, C. and A. Ding, *Nonresolving inflammation.* Cell, 2010. **140**(6): p. 871-82.
6. Ley, K., et al., *Getting to the site of inflammation: the leukocyte adhesion cascade updated.* Nat Rev Immunol, 2007. **7**(9): p. 678-89.
7. Kansas, G.S., *Selectins and their ligands: current concepts and controversies.* Blood, 1996. **88**(9): p. 3259-87.
8. von Hundelshausen, P., et al., *RANTES deposition by platelets triggers monocyte arrest on inflamed and atherosclerotic endothelium.* Circulation, 2001. **103**(13): p. 1772-7.
9. Johnson, Z., A.E. Proudfoot, and T.M. Handel, *Interaction of chemokines and glycosaminoglycans: a new twist in the regulation of chemokine function with opportunities for therapeutic intervention.* Cytokine Growth Factor Rev, 2005. **16**(6): p. 625-36.
10. Berlin, C., et al., *alpha 4 integrins mediate lymphocyte attachment and rolling under physiologic flow.* Cell, 1995. **80**(3): p. 413-22.
11. Salas, A., et al., *Rolling adhesion through an extended conformation of integrin alphaLbeta2 and relation to alpha I and beta I-like domain interaction.* Immunity, 2004. **20**(4): p. 393-406.
12. Chesnutt, B.C., et al., *Induction of LFA-1-dependent neutrophil rolling on ICAM-1 by engagement of E-selectin.* Microcirculation, 2006. **13**(2): p. 99-109.
13. Constantin, G., et al., *Chemokines trigger immediate beta2 integrin affinity and mobility changes: differential regulation and roles in lymphocyte arrest under flow.* Immunity, 2000. **13**(6): p. 759-69.
14. Wiig, H., *Pathophysiology of tissue fluid accumulation in inflammation.* J Physiol, 2011. **589**(Pt 12): p. 2945-53.
15. Kolaczkowska, E. and P. Kubes, *Neutrophil recruitment and function in health and inflammation.* Nat Rev Immunol, 2013. **13**(3): p. 159-75.
16. Peters, A.M., *Just how big is the pulmonary granulocyte pool?* Clin Sci (Lond), 1998. **94**(1): p. 7-19.
17. Summers, C., et al., *Neutrophil kinetics in health and disease.* Trends Immunol, 2010. **31**(8): p. 318-24.
18. Cassatella, M.A., *Neutrophil-derived proteins: selling cytokines by the pound.* Adv Immunol, 1999. **73**: p. 369-509.
19. Mantovani, A., et al., *Neutrophils in the activation and regulation of innate and adaptive immunity.* Nat Rev Immunol, 2011. **11**(8): p. 519-31.
20. Nathan, C., *Neutrophils and immunity: challenges and opportunities.* Nat Rev Immunol, 2006. **6**(3): p. 173-82.
21. Klebanoff, S.J., *Myeloperoxidase: friend and foe.* J Leukoc Biol, 2005. **77**(5): p. 598-625.
22. Faurschou, M. and N. Borregaard, *Neutrophil granules and secretory vesicles in inflammation.* Microbes Infect, 2003. **5**(14): p. 1317-27.
23. Brinkmann, V., et al., *Neutrophil extracellular traps kill bacteria.* Science, 2004. **303**(5663): p. 1532-5.
24. Lee, T.D., et al., *CAP37, a neutrophil-derived inflammatory mediator, augments leukocyte adhesion to endothelial monolayers.* Microvasc Res, 2003. **66**(1): p. 38-48.
25. Gautam, N., et al., *Heparin-binding protein (HBP/CAP37): a missing link in neutrophil-evoked alteration of vascular permeability.* Nat Med, 2001. **7**(10): p. 1123-7.

26. Pahlman, L.I., et al., *Streptococcal M protein: a multipotent and powerful inducer of inflammation.* J Immunol, 2006. **177**(2): p. 1221-8.
27. Chertov, O., et al., *Identification of human neutrophil-derived cathepsin G and azurocidin/CAP37 as chemoattractants for mononuclear cells and neutrophils.* J Exp Med, 1997. **186**(5): p. 739-47.
28. Taekema-Roelvink, M.E., et al., *Proteinase 3 enhances endothelial monocyte chemoattractant protein-1 production and induces increased adhesion of neutrophils to endothelial cells by upregulating intercellular cell adhesion molecule-1.* J Am Soc Nephrol, 2001. **12**(5): p. 932-40.
29. Kasama, T., et al., *Expression and regulation of human neutrophil-derived macrophage inflammatory protein 1 alpha.* J Exp Med, 1993. **178**(1): p. 63-72.
30. Dale, D.C., L. Boxer, and W.C. Liles, *The phagocytes: neutrophils and monocytes.* Blood, 2008. **112**(4): p. 935-45.
31. Shi, C. and E.G. Pamer, *Monocyte recruitment during infection and inflammation.* Nat Rev Immunol, 2011. **11**(11): p. 762-74.
32. Cooper, D., et al., *The effect of galectins on leukocyte trafficking in inflammation: sweet or sour?* Ann N Y Acad Sci, 2012. **1253**: p. 181-92.
33. Bondue, B., V. Wittamer, and M. Parmentier, *Chemerin and its receptors in leukocyte trafficking, inflammation and metabolism.* Cytokine Growth Factor Rev, 2011. **22**(5-6): p. 331-8.
34. Nahrendorf, M., et al., *The healing myocardium sequentially mobilizes two monocyte subsets with divergent and complementary functions.* J Exp Med, 2007. **204**(12): p. 3037-47.
35. Leuschner, F., et al., *Rapid monocyte kinetics in acute myocardial infarction are sustained by extramedullary monocytopoiesis.* J Exp Med, 2012. **209**(1): p. 123-37.
36. Grage-Griebenow, E., H.D. Flad, and M. Ernst, *Heterogeneity of human peripheral blood monocyte subsets.* J Leukoc Biol, 2001. **69**(1): p. 11-20.
37. Galli, S.J., et al., *Mast cells as "tunable" effector and immunoregulatory cells: recent advances.* Annu Rev Immunol, 2005. **23**: p. 749-86.
38. Nilsson, G., et al., *C3a and C5a are chemotaxins for human mast cells and act through distinct receptors via a pertussis toxin-sensitive signal transduction pathway.* J Immunol, 1996. **157**(4): p. 1693-8.
39. Dawicki, W. and J.S. Marshall, *New and emerging roles for mast cells in host defence.* Curr Opin Immunol, 2007. **19**(1): p. 31-8.
40. Saluja, R., et al., *The role of the IL-33/IL-1RL1 axis in mast cell and basophil activation in allergic disorders.* Mol Immunol, 2015. **63**(1): p. 80-5.
41. Weller, C.L., et al., *Leukotriene B4, an activation product of mast cells, is a chemoattractant for their progenitors.* J Exp Med, 2005. **201**(12): p. 1961-71.
42. Kaufmann, S.H., *Immunology's foundation: the 100-year anniversary of the Nobel Prize to Paul Ehrlich and Elie Metchnikoff.* Nat Immunol, 2008. **9**(7): p. 705-12.
43. Davies, L.C., et al., *Tissue-resident macrophages.* Nat Immunol, 2013. **14**(10): p. 986-95.
44. Schulz, C., et al., *A lineage of myeloid cells independent of Myb and hematopoietic stem cells.* Science, 2012. **336**(6077): p. 86-90.
45. Yona, S., et al., *Fate mapping reveals origins and dynamics of monocytes and tissue macrophages under homeostasis.* Immunity, 2013. **38**(1): p. 79-91.
46. Lavin, Y., et al., *Tissue-resident macrophage enhancer landscapes are shaped by the local microenvironment.* Cell, 2014. **159**(6): p. 1312-26.
47. Gosselin, D., et al., *Environment drives selection and function of enhancers controlling tissue-specific macrophage identities.* Cell, 2014. **159**(6): p. 1327-40.
48. Bain, C.C., et al., *Resident and pro-inflammatory macrophages in the colon represent alternative context-dependent fates of the same Ly6Chi monocyte precursors.* Mucosal Immunol, 2013. **6**(3): p. 498-510.
49. Bain, C.C., et al., *Constant replenishment from circulating monocytes maintains the macrophage pool in the intestine of adult mice.* Nat Immunol, 2014. **15**(10): p. 929-37.

50. Taylor, P.R., et al., *Macrophage receptors and immune recognition.* Annu Rev Immunol, 2005. **23**: p. 901-44.
51. Akira, S., K. Takeda, and T. Kaisho, *Toll-like receptors: critical proteins linking innate and acquired immunity.* Nat Immunol, 2001. **2**(8): p. 675-80.
52. Inohara, N. and G. Nunez, *NODs: intracellular proteins involved in inflammation and apoptosis.* Nat Rev Immunol, 2003. **3**(5): p. 371-82.
53. Yoneyama, M., et al., *The RNA helicase RIG-I has an essential function in double-stranded RNA-induced innate antiviral responses.* Nat Immunol, 2004. **5**(7): p. 730-7.
54. Cailhier, J.F., et al., *Conditional macrophage ablation demonstrates that resident macrophages initiate acute peritoneal inflammation.* J Immunol, 2005. **174**(4): p. 2336-42.
55. Newson, J., et al., *Resolution of acute inflammation bridges the gap between innate and adaptive immunity.* Blood, 2014.
56. Jenkins, S.J., et al., *Local macrophage proliferation, rather than recruitment from the blood, is a signature of TH2 inflammation.* Science, 2011. **332**(6035): p. 1284-8.
57. Davies, L.C., et al., *Distinct bone marrow-derived and tissue-resident macrophage lineages proliferate at key stages during inflammation.* Nat Commun, 2013. **4**: p. 1886.
58. Rosas, M., et al., *The transcription factor Gata6 links tissue macrophage phenotype and proliferative renewal.* Science, 2014. **344**(6184): p. 645-8.
59. Savill, J., *Apoptosis in resolution of inflammation.* J Leukoc Biol, 1997. **61**(4): p. 375-80.
60. Hansson, G.K. and P. Libby, *The immune response in atherosclerosis: a double-edged sword.* Nat Rev Immunol, 2006. **6**(7): p. 508-19.
61. Glass, C.K. and J.L. Witztum, *Atherosclerosis. the road ahead.* Cell, 2001. **104**(4): p. 503-16.
62. Tabas, I., K.J. Williams, and J. Boren, *Subendothelial lipoprotein retention as the initiating process in atherosclerosis: update and therapeutic implications.* Circulation, 2007. **116**(16): p. 1832-44.
63. Steinberg, D., *Low density lipoprotein oxidation and its pathobiological significance.* J Biol Chem, 1997. **272**(34): p. 20963-6.
64. Cominacini, L., et al., *Oxidized low density lipoprotein (ox-LDL) binding to ox-LDL receptor-1 in endothelial cells induces the activation of NF-kappaB through an increased production of intracellular reactive oxygen species.* J Biol Chem, 2000. **275**(17): p. 12633-8.
65. Cybulsky, M.I. and M.A. Gimbrone, Jr., *Endothelial expression of a mononuclear leukocyte adhesion molecule during atherogenesis.* Science, 1991. **251**(4995): p. 788-91.
66. Boring, L., et al., *Decreased lesion formation in CCR2-/- mice reveals a role for chemokines in the initiation of atherosclerosis.* Nature, 1998. **394**(6696): p. 894-7.
67. Mestas, J. and K. Ley, *Monocyte-endothelial cell interactions in the development of atherosclerosis.* Trends Cardiovasc Med, 2008. **18**(6): p. 228-32.
68. Moore, K.J., F.J. Sheedy, and E.A. Fisher, *Macrophages in atherosclerosis: a dynamic balance.* Nat Rev Immunol, 2013. **13**(10): p. 709-21.
69. Harris, A.K., et al., *GM-CSF deficiency delays neointima formation in a normolipidemic mouse model of endoluminal endothelial damage.* Immunol Cell Biol, 2009. **87**(2): p. 122-30.
70. Takahashi, M., et al., *Human monocyte-endothelial cell interaction induces synthesis of granulocyte-macrophage colony-stimulating factor.* Circulation, 1996. **93**(6): p. 1185-93.
71. Peiser, L., S. Mukhopadhyay, and S. Gordon, *Scavenger receptors in innate immunity.* Curr Opin Immunol, 2002. **14**(1): p. 123-8.
72. Stewart, C.R., et al., *CD36 ligands promote sterile inflammation through assembly of a Toll-like receptor 4 and 6 heterodimer.* Nat Immunol, 2010. **11**(2): p. 155-61.

73. Greaves, D.R. and S. Gordon, *Thematic review series: the immune system and atherogenesis. Recent insights into the biology of macrophage scavenger receptors.* J Lipid Res, 2005. **46**(1): p. 11-20.
74. Duewell, P., et al., *NLRP3 inflammasomes are required for atherogenesis and activated by cholesterol crystals.* Nature, 2010. **464**(7293): p. 1357-61.
75. Robbins, C.S., et al., *Local proliferation dominates lesional macrophage accumulation in atherosclerosis.* Nat Med, 2013. **19**(9): p. 1166-72.
76. Swirski, F.K., *Monocyte recruitment and macrophage proliferation in atherosclerosis.* Kardiol Pol, 2014. **72**(4): p. 311-4.
77. Tang, J., et al., *Inhibiting macrophage proliferation suppresses atherosclerotic plaque inflammation.* Sci Adv, 2015. **1**(3).
78. Zhang, S.H., et al., *Spontaneous hypercholesterolemia and arterial lesions in mice lacking apolipoprotein E.* Science, 1992. **258**(5081): p. 468-71.
79. Jonasson, L., et al., *Regional accumulations of T cells, macrophages, and smooth muscle cells in the human atherosclerotic plaque.* Arteriosclerosis, 1986. **6**(2): p. 131-8.
80. Paulsson, G., et al., *Oligoclonal T cell expansions in atherosclerotic lesions of apolipoprotein E-deficient mice.* Arterioscler Thromb Vasc Biol, 2000. **20**(1): p. 10-7.
81. Stemme, S., et al., *T lymphocytes from human atherosclerotic plaques recognize oxidized low density lipoprotein.* Proc Natl Acad Sci U S A, 1995. **92**(9): p. 3893-7.
82. Zhou, X., et al., *Transfer of CD4(+) T cells aggravates atherosclerosis in immunodeficient apolipoprotein E knockout mice.* Circulation, 2000. **102**(24): p. 2919-22.
83. Mallat, Z., et al., *Induction of a regulatory T cell type 1 response reduces the development of atherosclerosis in apolipoprotein E-knockout mice.* Circulation, 2003. **108**(10): p. 1232-7.
84. Ait-Oufella, H., et al., *Natural regulatory T cells control the development of atherosclerosis in mice.* Nat Med, 2006. **12**(2): p. 178-80.
85. Pastrana, J.L., et al., *Regulatory T cells and Atherosclerosis.* J Clin Exp Cardiolog, 2012. **2012**(Suppl 12): p. 2.
86. Watanabe, M., et al., *Distribution of inflammatory cells in adventitia changed with advancing atherosclerosis of human coronary artery.* J Atheroscler Thromb, 2007. **14**(6): p. 325-31.
87. Lauber, K., et al., *Apoptotic cells induce migration of phagocytes via caspase-3-mediated release of a lipid attraction signal.* Cell, 2003. **113**(6): p. 717-30.
88. Fadok, V.A., et al., *Exposure of phosphatidylserine on the surface of apoptotic lymphocytes triggers specific recognition and removal by macrophages.* J Immunol, 1992. **148**(7): p. 2207-16.
89. Festjens, N., T. Vanden Berghe, and P. Vandenabeele, *Necrosis, a well-orchestrated form of cell demise: signalling cascades, important mediators and concomitant immune response.* Biochim Biophys Acta, 2006. **1757**(9-10): p. 1371-87.
90. Iyer, S.S., et al., *Necrotic cells trigger a sterile inflammatory response through the Nlrp3 inflammasome.* Proc Natl Acad Sci U S A, 2009. **106**(48): p. 20388-93.
91. Serhan, C.N., N. Chiang, and T.E. Van Dyke, *Resolving inflammation: dual anti-inflammatory and pro-resolution lipid mediators.* Nat Rev Immunol, 2008. **8**(5): p. 349-61.
92. Dennis, E.A. and P.C. Norris, *Eicosanoid storm in infection and inflammation.* Nat Rev Immunol, 2015. **15**(8): p. 511-23.
93. Williams, T.J. and M.J. Peck, *Role of prostaglandin-mediated vasodilatation in inflammation.* Nature, 1977. **270**(5637): p. 530-2.
94. Legler, D.F., et al., *Prostaglandin E2 at new glance: novel insights in functional diversity offer therapeutic chances.* Int J Biochem Cell Biol, 2010. **42**(2): p. 198-201.
95. Minami, T., et al., *Characterization of EP receptor subtypes responsible for prostaglandin E2-induced pain responses by use of EP1 and EP3 receptor knockout mice.* Br J Pharmacol, 2001. **133**(3): p. 438-44.

96. Kalinski, P., *Regulation of immune responses by prostaglandin E2.* J Immunol, 2012. **188**(1): p. 21-8.
97. Jing, H., E. Vassiliou, and D. Ganea, *Prostaglandin E2 inhibits production of the inflammatory chemokines CCL3 and CCL4 in dendritic cells.* J Leukoc Biol, 2003. **74**(5): p. 868-79.
98. Busse, W.W., *Leukotrienes and inflammation.* Am J Respir Crit Care Med, 1998. **157**(6 Pt 1): p. S210-3.
99. Brach, M.A., et al., *Leukotriene B4 transcriptionally activates interleukin-6 expression involving NK-chi B and NF-IL6.* Eur J Immunol, 1992. **22**(10): p. 2705-11.
100. Freire-de-Lima, C.G., et al., *Apoptotic cells, through transforming growth factor-beta, coordinately induce anti-inflammatory and suppress pro-inflammatory eicosanoid and NO synthesis in murine macrophages.* J Biol Chem, 2006. **281**(50): p. 38376-84.
101. Maderna, P. and C. Godson, *Lipoxins: resolutionary road.* Br J Pharmacol, 2009. **158**(4): p. 947-59.
102. Serhan, C.N., M. Hamberg, and B. Samuelsson, *Lipoxins: novel series of biologically active compounds formed from arachidonic acid in human leukocytes.* Proc Natl Acad Sci U S A, 1984. **81**(17): p. 5335-9.
103. Serhan, C.N. and K.A. Sheppard, *Lipoxin formation during human neutrophil-platelet interactions. Evidence for the transformation of leukotriene A4 by platelet 12-lipoxygenase in vitro.* J Clin Invest, 1990. **85**(3): p. 772-80.
104. Claria, J. and C.N. Serhan, *Aspirin triggers previously undescribed bioactive eicosanoids by human endothelial cell-leukocyte interactions.* Proc Natl Acad Sci U S A, 1995. **92**(21): p. 9475-9.
105. Colgan, S.P., et al., *Lipoxin A4 modulates transmigration of human neutrophils across intestinal epithelial monolayers.* J Clin Invest, 1993. **92**(1): p. 75-82.
106. Godson, C., et al., *Cutting edge: lipoxins rapidly stimulate nonphlogistic phagocytosis of apoptotic neutrophils by monocyte-derived macrophages.* J Immunol, 2000. **164**(4): p. 1663-7.
107. Chiang, N., M. Arita, and C.N. Serhan, *Anti-inflammatory circuitry: lipoxin, aspirin-triggered lipoxins and their receptor ALX.* Prostaglandins Leukot Essent Fatty Acids, 2005. **73**(3-4): p. 163-77.
108. Serhan, C.N., et al., *Novel functional sets of lipid-derived mediators with antiinflammatory actions generated from omega-3 fatty acids via cyclooxygenase 2-nonsteroidal antiinflammatory drugs and transcellular processing.* J Exp Med, 2000. **192**(8): p. 1197-204.
109. Arita, M., et al., *Stereochemical assignment, antiinflammatory properties, and receptor for the omega-3 lipid mediator resolvin E1.* J Exp Med, 2005. **201**(5): p. 713-22.
110. Schwab, J.M., et al., *Resolvin E1 and protectin D1 activate inflammation-resolution programmes.* Nature, 2007. **447**(7146): p. 869-74.
111. Serhan, C.N., et al., *Protectins and maresins: New pro-resolving families of mediators in acute inflammation and resolution bioactive metabolome.* Biochim Biophys Acta, 2015. **1851**(4): p. 397-413.
112. Serhan, C.N., et al., *Maresins: novel macrophage mediators with potent antiinflammatory and proresolving actions.* J Exp Med, 2009. **206**(1): p. 15-23.
113. Serhan, C.N., N. Chiang, and J. Dalli, *The resolution code of acute inflammation: Novel pro-resolving lipid mediators in resolution.* Semin Immunol, 2015. **27**(3): p. 200-15.
114. Ouyang, W., et al., *Regulation and functions of the IL-10 family of cytokines in inflammation and disease.* Annu Rev Immunol, 2011. **29**: p. 71-109.
115. Bogdan, C., Y. Vodovotz, and C. Nathan, *Macrophage deactivation by interleukin 10.* J Exp Med, 1991. **174**(6): p. 1549-55.
116. Fiorentino, D.F., M.W. Bond, and T.R. Mosmann, *Two types of mouse T helper cell. IV. Th2 clones secrete a factor that inhibits cytokine production by Th1 clones.* J Exp Med, 1989. **170**(6): p. 2081-95.

117. Fadok, V.A., et al., *Macrophages that have ingested apoptotic cells in vitro inhibit proinflammatory cytokine production through autocrine/paracrine mechanisms involving TGF-beta, PGE2, and PAF.* J Clin Invest, 1998. **101**(4): p. 890-8.
118. Huynh, M.L., V.A. Fadok, and P.M. Henson, *Phosphatidylserine-dependent ingestion of apoptotic cells promotes TGF-beta1 secretion and the resolution of inflammation.* J Clin Invest, 2002. **109**(1): p. 41-50.
119. Gorelik, L. and R.A. Flavell, *Abrogation of TGFbeta signaling in T cells leads to spontaneous T cell differentiation and autoimmune disease.* Immunity, 2000. **12**(2): p. 171-81.
120. Cazac, B.B. and J. Roes, *TGF-beta receptor controls B cell responsiveness and induction of IgA in vivo.* Immunity, 2000. **13**(4): p. 443-51.
121. Tsunawaki, S., et al., *Deactivation of macrophages by transforming growth factor-beta.* Nature, 1988. **334**(6179): p. 260-2.
122. Yegutkin, G.G., *Nucleotide- and nucleoside-converting ectoenzymes: Important modulators of purinergic signalling cascade.* Biochim Biophys Acta, 2008. **1783**(5): p. 673-94.
123. Cronstein, B.N., et al., *Adenosine: an endogenous inhibitor of neutrophil-mediated injury to endothelial cells.* J Clin Invest, 1986. **78**(3): p. 760-70.
124. Nemeth, Z.H., et al., *Adenosine augments IL-10 production by macrophages through an A2B receptor-mediated posttranscriptional mechanism.* J Immunol, 2005. **175**(12): p. 8260-70.
125. Hasko, G., et al., *An agonist of adenosine A3 receptors decreases interleukin-12 and interferon-gamma production and prevents lethality in endotoxemic mice.* Eur J Pharmacol, 1998. **358**(3): p. 261-8.
126. Pinhal-Enfield, G., et al., *An angiogenic switch in macrophages involving synergy between Toll-like receptors 2, 4, 7, and 9 and adenosine A(2A) receptors.* Am J Pathol, 2003. **163**(2): p. 711-21.
127. Hasko, G. and P. Pacher, *Regulation of macrophage function by adenosine.* Arterioscler Thromb Vasc Biol, 2012. **32**(4): p. 865-9.
128. Rhen, T. and J.A. Cidlowski, *Antiinflammatory action of glucocorticoids--new mechanisms for old drugs.* N Engl J Med, 2005. **353**(16): p. 1711-23.
129. Goulding, N.J., et al., *Anti-inflammatory lipocortin 1 production by peripheral blood leucocytes in response to hydrocortisone.* Lancet, 1990. **335**(8703): p. 1416-8.
130. Morand, E.F., et al., *Detection of intracellular lipocortin 1 in human leukocyte subsets.* Clin Immunol Immunopathol, 1995. **76**(2): p. 195-202.
131. Perretti, M., et al., *Mobilizing lipocortin 1 in adherent human leukocytes downregulates their transmigration.* Nat Med, 1996. **2**(11): p. 1259-62.
132. Perretti, M., et al., *Annexin I is stored within gelatinase granules of human neutrophil and mobilized on the cell surface upon adhesion but not phagocytosis.* Cell Biol Int, 2000. **24**(3): p. 163-74.
133. Wein, S., et al., *Mediation of annexin 1 secretion by a probenecid-sensitive ABC-transporter in rat inflamed mucosa.* Biochem Pharmacol, 2004. **67**(6): p. 1195-202.
134. Perretti, M. and R.J. Flower, *Annexin 1 and the biology of the neutrophil.* J Leukoc Biol, 2004. **76**(1): p. 25-9.
135. Lim, L.H., et al., *Promoting detachment of neutrophils adherent to murine postcapillary venules to control inflammation: effect of lipocortin 1.* Proc Natl Acad Sci U S A, 1998. **95**(24): p. 14535-9.
136. Chatterjee, B.E., et al., *Annexin 1-deficient neutrophils exhibit enhanced transmigration in vivo and increased responsiveness in vitro.* J Leukoc Biol, 2005. **78**(3): p. 639-46.
137. Perretti, M., et al., *Endogenous lipid- and peptide-derived anti-inflammatory pathways generated with glucocorticoid and aspirin treatment activate the lipoxin A4 receptor.* Nat Med, 2002. **8**(11): p. 1296-302.
138. Perretti, M. and J. Dalli, *Exploiting the Annexin A1 pathway for the development of novel anti-inflammatory therapeutics.* Br J Pharmacol, 2009. **158**(4): p. 936-46.

139. Stables, M.J., et al., *Transcriptomic analyses of murine resolution-phase macrophages.* Blood, 2011. **118**(26): p. e192-208.
140. Rajakariar, R., et al., *Novel biphasic role for lymphocytes revealed during resolving inflammation.* Blood, 2008. **111**(8): p. 4184-92.
141. Semerad, C.L., et al., *G-CSF is an essential regulator of neutrophil trafficking from the bone marrow to the blood.* Immunity, 2002. **17**(4): p. 413-23.
142. Eash, K.J., et al., *CXCR2 and CXCR4 antagonistically regulate neutrophil trafficking from murine bone marrow.* J Clin Invest, 2010. **120**(7): p. 2423-31.
143. Suratt, B.T., et al., *Role of the CXCR4/SDF-1 chemokine axis in circulating neutrophil homeostasis.* Blood, 2004. **104**(2): p. 565-71.
144. Bendall, L.J. and K.F. Bradstock, *G-CSF: From granulopoietic stimulant to bone marrow stem cell mobilizing agent.* Cytokine Growth Factor Rev, 2014. **25**(4): p. 355-67.
145. Wengner, A.M., et al., *The coordinated action of G-CSF and ELR + CXC chemokines in neutrophil mobilization during acute inflammation.* Blood, 2008. **111**(1): p. 42-9.
146. Ginhoux, F. and S. Jung, *Monocytes and macrophages: developmental pathways and tissue homeostasis.* Nat Rev Immunol, 2014. **14**(6): p. 392-404.
147. Geissmann, F., S. Jung, and D.R. Littman, *Blood monocytes consist of two principal subsets with distinct migratory properties.* Immunity, 2003. **19**(1): p. 71-82.
148. Wiktor-Jedrzejczak, W. and S. Gordon, *Cytokine regulation of the macrophage (M phi) system studied using the colony stimulating factor-1-deficient op/op mouse.* Physiol Rev, 1996. **76**(4): p. 927-47.
149. Serbina, N.V. and E.G. Pamer, *Monocyte emigration from bone marrow during bacterial infection requires signals mediated by chemokine receptor CCR2.* Nat Immunol, 2006. **7**(3): p. 311-7.
150. Jia, T., et al., *Additive roles for MCP-1 and MCP-3 in CCR2-mediated recruitment of inflammatory monocytes during Listeria monocytogenes infection.* J Immunol, 2008. **180**(10): p. 6846-53.
151. Serbina, N.V., et al., *Selective expansion of the monocytic lineage directed by bacterial infection.* J Immunol, 2009. **183**(3): p. 1900-10.
152. Swirski, F.K., et al., *Identification of splenic reservoir monocytes and their deployment to inflammatory sites.* Science, 2009. **325**(5940): p. 612-6.
153. Ingersoll, M.A., et al., *Monocyte trafficking in acute and chronic inflammation.* Trends Immunol, 2011. **32**(10): p. 470-7.
154. Zipfel, P.F. and C. Skerka, *Complement regulators and inhibitory proteins.* Nat Rev Immunol, 2009. **9**(10): p. 729-40.
155. Schiffmann, E., B.A. Corcoran, and S.M. Wahl, *N-formylmethionyl peptides as chemoattractants for leucocytes.* Proc Natl Acad Sci U S A, 1975. **72**(3): p. 1059-62.
156. Dorward, D.A., et al., *The role of formylated peptides and formyl peptide receptor 1 in governing neutrophil function during acute inflammation.* Am J Pathol, 2015. **185**(5): p. 1172-84.
157. White, G.E., A.J. Iqbal, and D.R. Greaves, *CC chemokine receptors and chronic inflammation--therapeutic opportunities and pharmacological challenges.* Pharmacol Rev, 2013. **65**(1): p. 47-89.
158. Schall, T.J. and A.E. Proudfoot, *Overcoming hurdles in developing successful drugs targeting chemokine receptors.* Nat Rev Immunol, 2011. **11**(5): p. 355-63.
159. Bardi, G., et al., *The T cell chemokine receptor CCR7 is internalized on stimulation with ELC, but not with SLC.* Eur J Immunol, 2001. **31**(11): p. 3291-7.
160. White, G.E., et al., *Site-directed mutagenesis of the CC chemokine binding protein 35K-Fc reveals residues essential for activity and mutations that increase the potency of CC chemokine blockade.* Mol Pharmacol, 2011. **80**(2): p. 328-36.
161. McNeill, E., et al., *Contrasting in vitro vs. in vivo effects of a cell membrane-specific CC-chemokine binding protein on macrophage chemotaxis.* J Mol Med (Berl), 2014.
162. Gilbert, J., et al., *Effect of CC chemokine receptor 2 CCR2 blockade on serum C-reactive protein in individuals at atherosclerotic risk and with a single nucleotide*

polymorphism of the monocyte chemoattractant protein-1 promoter region. Am J Cardiol, 2011. **107**(6): p. 906-11.
163. Keshav, S., et al., *A randomized controlled trial of the efficacy and safety of CCX282-B, an orally-administered blocker of chemokine receptor CCR9, for patients with Crohn's disease.* PLoS One, 2013. **8**(3): p. e60094.
164. Nagpal, S., et al., *Tazarotene-induced gene 2 (TIG2), a novel retinoid-responsive gene in skin.* J Invest Dermatol, 1997. **109**(1): p. 91-5.
165. Adams, A.E., et al., *1,25 dihydroxyvitamin D3 and dexamethasone induce the cyclooxygenase 1 gene in osteoclast-supporting stromal cells.* J Cell Biochem, 1999. **74**(4): p. 587-95.
166. Zabel, B.A., et al., *Chemoattractants, extracellular proteases, and the integrated host defense response.* Exp Hematol, 2006. **34**(8): p. 1021-32.
167. Lehrer, R.I. and T. Ganz, *Defensins of vertebrate animals.* Curr Opin Immunol, 2002. **14**(1): p. 96-102.
168. Gantz, I., et al., *Molecular cloning of a novel receptor (CMKLR1) with homology to the chemotactic factor receptors.* Cytogenet Cell Genet, 1996. **74**(4): p. 286-90.
169. Samson, M., et al., *ChemR23, a putative chemoattractant receptor, is expressed in monocyte-derived dendritic cells and macrophages and is a coreceptor for SIV and some primary HIV-1 strains.* Eur J Immunol, 1998. **28**(5): p. 1689-700.
170. Wittamer, V., et al., *Specific recruitment of antigen-presenting cells by chemerin, a novel processed ligand from human inflammatory fluids.* J Exp Med, 2003. **198**(7): p. 977-85.
171. Meder, W., et al., *Characterization of human circulating TIG2 as a ligand for the orphan receptor ChemR23.* FEBS Lett, 2003. **555**(3): p. 495-9.
172. Bozaoglu, K., et al., *Chemerin is a novel adipokine associated with obesity and metabolic syndrome.* Endocrinology, 2007. **148**(10): p. 4687-94.
173. Rourke, J.L., H.J. Dranse, and C.J. Sinal, *Towards an integrative approach to understanding the role of chemerin in human health and disease.* Obes Rev, 2013. **14**(3): p. 245-62.
174. Zhao, L., et al., *Chemerin158K protein is the dominant chemerin isoform in synovial and cerebrospinal fluids but not in plasma.* J Biol Chem, 2011. **286**(45): p. 39520-7.
175. Wittamer, V., et al., *Neutrophil-mediated maturation of chemerin: a link between innate and adaptive immunity.* J Immunol, 2005. **175**(1): p. 487-93.
176. Zabel, B.A., et al., *Chemerin activation by serine proteases of the coagulation, fibrinolytic, and inflammatory cascades.* J Biol Chem, 2005. **280**(41): p. 34661-6.
177. Wittamer, V., et al., *The C-terminal nonapeptide of mature chemerin activates the chemerin receptor with low nanomolar potency.* J Biol Chem, 2004. **279**(11): p. 9956-62.
178. Muruganandan, S., et al., *Chemerin, a novel peroxisome proliferator-activated receptor gamma (PPARgamma) target gene that promotes mesenchymal stem cell adipogenesis.* J Biol Chem, 2011. **286**(27): p. 23982-95.
179. Maheshwari, A., et al., *Epithelial cells in fetal intestine produce chemerin to recruit macrophages.* Am J Physiol Gastrointest Liver Physiol, 2009. **297**(1): p. G1-G10.
180. Gonzalvo-Feo, S., et al., *Endothelial cell-derived chemerin promotes dendritic cell transmigration.* J Immunol, 2014. **192**(5): p. 2366-73.
181. Horton, J.D., et al., *Activation of cholesterol synthesis in preference to fatty acid synthesis in liver and adipose tissue of transgenic mice overproducing sterol regulatory element-binding protein-2.* J Clin Invest, 1998. **101**(11): p. 2331-9.
182. Bauer, S., et al., *Sterol regulatory element-binding protein 2 (SREBP2) activation after excess triglyceride storage induces chemerin in hypertrophic adipocytes.* Endocrinology, 2011. **152**(1): p. 26-35.
183. Tan, B.K., et al., *Insulin and metformin regulate circulating and adipose tissue chemerin.* Diabetes, 2009. **58**(9): p. 1971-7.
184. Parlee, S.D., et al., *Serum chemerin levels vary with time of day and are modified by obesity and tumor necrosis factor-{alpha}.* Endocrinology, 2010. **151**(6): p. 2590-602.

185. Banas, M., et al., *The expression and regulation of chemerin in the epidermis.* PLoS One, 2015. **10**(2): p. e0117830.
186. Kralisch, S., et al., *Interleukin-1beta induces the novel adipokine chemerin in adipocytes in vitro.* Regul Pept, 2009. **154**(1-3): p. 102-6.
187. Kaneko, K., et al., *Chemerin activates fibroblast-like synoviocytes in patients with rheumatoid arthritis.* Arthritis Res Ther, 2011. **13**(5): p. R158.
188. De Palma, G., et al., *The possible role of ChemR23/Chemerin axis in the recruitment of dendritic cells in lupus nephritis.* Kidney Int, 2011. **79**(11): p. 1228-35.
189. Guillabert, A., et al., *Role of neutrophil proteinase 3 and mast cell chymase in chemerin proteolytic regulation.* J Leukoc Biol, 2008. **84**(6): p. 1530-8.
190. Kulig, P., et al., *Regulation of chemerin chemoattractant and antibacterial activity by human cysteine cathepsins.* J Immunol, 2011. **187**(3): p. 1403-10.
191. Kulig, P., et al., *Staphylococcus aureus-derived staphopain B, a potent cysteine protease activator of plasma chemerin.* J Immunol, 2007. **178**(6): p. 3713-20.
192. Du, X.Y., et al., *Regulation of chemerin bioactivity by plasma carboxypeptidase N, carboxypeptidase B (activated thrombin-activable fibrinolysis inhibitor), and platelets.* J Biol Chem, 2009. **284**(2): p. 751-8.
193. Jungi, T.W., *Assay of chemotaxis by a reversible Boyden chamber eliminating cell detachment.* Int Arch Allergy Appl Immunol, 1975. **48**(3): p. 341-52.
194. Zabel, B.A., A.M. Silverio, and E.C. Butcher, *Chemokine-like receptor 1 expression and chemerin-directed chemotaxis distinguish plasmacytoid from myeloid dendritic cells in human blood.* J Immunol, 2005. **174**(1): p. 244-51.
195. Vermi, W., et al., *Role of ChemR23 in directing the migration of myeloid and plasmacytoid dendritic cells to lymphoid organs and inflamed skin.* J Exp Med, 2005. **201**(4): p. 509-15.
196. Parolini, S., et al., *The role of chemerin in the colocalization of NK and dendritic cell subsets into inflamed tissues.* Blood, 2007. **109**(9): p. 3625-32.
197. Zabel, B.A., et al., *Chemokine-like receptor 1 expression by macrophages in vivo: regulation by TGF-beta and TLR ligands.* Exp Hematol, 2006. **34**(8): p. 1106-14.
198. Hart, R. and D.R. Greaves, *Chemerin contributes to inflammation by promoting macrophage adhesion to VCAM-1 and fibronectin through clustering of VLA-4 and VLA-5.* J Immunol, 2010. **185**(6): p. 3728-39.
199. Iqbal, A.J., et al., *A Real Time Chemotaxis Assay Unveils Unique Migratory Profiles amongst Different Primary Murine Macrophages.* PLoS One, 2013. **8**(3): p. e58744.
200. Albanesi, C., et al., *Chemerin expression marks early psoriatic skin lesions and correlates with plasmacytoid dendritic cell recruitment.* J Exp Med, 2009. **206**(1): p. 249-58.
201. Vermi, W., et al., *Cutaneous distribution of plasmacytoid dendritic cells in lupus erythematosus. Selective tropism at the site of epithelial apoptotic damage.* Immunobiology, 2009. **214**(9-10): p. 877-86.
202. Skrzeczynska-Moncznik, J., et al., *Potential role of chemerin in recruitment of plasmacytoid dendritic cells to diseased skin.* Biochem Biophys Res Commun, 2009. **380**(2): p. 323-7.
203. Berg, V., et al., *Human articular chondrocytes express ChemR23 and chemerin; ChemR23 promotes inflammatory signalling upon binding the ligand chemerin(21-157).* Arthritis Res Ther, 2010. **12**(6): p. R228.
204. Parlee, S.D., et al., *Elastase and tryptase govern TNFα-mediated production of active chemerin by adipocytes.* PLoS One, 2012. **7**(12): p. e51072.
205. Skrzeczyńska-Moncznik, J., et al., *Chemerin and the recruitment of NK cells to diseased skin.* Acta Biochim Pol, 2009. **56**(2): p. 355-60.
206. Nakajima, H., et al., *Circulating level of chemerin is upregulated in psoriasis.* J Dermatol Sci, 2010. **60**(1): p. 45-7.
207. Gisondi, P., et al., *Serum chemerin is increased in patients with chronic plaque psoriasis and normalizes following treatment with infliximab.* Br J Dermatol, 2013. **168**(4): p. 749-55.

208. Weigert, J., et al., *Circulating levels of chemerin and adiponectin are higher in ulcerative colitis and chemerin is elevated in Crohn's disease.* Inflamm Bowel Dis, 2010. **16**(4): p. 630-7.
209. Waluga, M., et al., *Serum adipokines in inflammatory bowel disease.* World J Gastroenterol, 2014. **20**(22): p. 6912-7.
210. Lin, Y., et al., *Chemerin aggravates DSS-induced colitis by suppressing M2 macrophage polarization.* Cell Mol Immunol, 2014. **11**(4): p. 355-66.
211. Dranse, H.J., et al., *Local chemerin levels are positively associated with DSS-induced colitis but constitutive loss of CMKLR1 does not protect against development of colitis.* Physiol Rep, 2015. **3**(8).
212. Eisinger, K., et al., *Chemerin induces CCL2 and TLR4 in synovial fibroblasts of patients with rheumatoid arthritis and osteoarthritis.* Exp Mol Pathol, 2012. **92**(1): p. 90-6.
213. Ha, Y.J., et al., *Plasma chemerin levels in rheumatoid arthritis are correlated with disease activity rather than obesity.* Joint Bone Spine, 2014. **81**(2): p. 189-90.
214. Herenius, M.M., et al., *Anti-TNF therapy reduces serum levels of chemerin in rheumatoid arthritis: a new mechanism by which anti-TNF might reduce inflammation.* PLoS One, 2013. **8**(2): p. e57802.
215. Makrilakis, K., et al., *Chemerin and cardiovascular risk in rheumatoid arthritis after interleukin 6 receptor blockade.* J Rheumatol, 2015. **42**(2): p. 349.
216. Pachynski, R.K., et al., *The chemoattractant chemerin suppresses melanoma by recruiting natural killer cell antitumor defenses.* J Exp Med, 2012. **209**(8): p. 1427-35.
217. Graham, K.L., et al., *Chemokine-like receptor-1 expression by central nervous system-infiltrating leukocytes and involvement in a model of autoimmune demyelinating disease.* J Immunol, 2009. **183**(10): p. 6717-23.
218. Graham, K.L., et al., *A novel CMKLR1 small molecule antagonist suppresses CNS autoimmune inflammatory disease.* PLoS One, 2014. **9**(12): p. e112925.
219. Goralski, K.B., et al., *Chemerin, a novel adipokine that regulates adipogenesis and adipocyte metabolism.* J Biol Chem, 2007. **282**(38): p. 28175-88.
220. Roh, S.G., et al., *Chemerin--a new adipokine that modulates adipogenesis via its own receptor.* Biochem Biophys Res Commun, 2007. **362**(4): p. 1013-8.
221. Takahashi, M., et al., *Chemerin enhances insulin signaling and potentiates insulin-stimulated glucose uptake in 3T3-L1 adipocytes.* FEBS Lett, 2008. **582**(5): p. 573-8.
222. Sell, H., et al., *Chemerin is a novel adipocyte-derived factor inducing insulin resistance in primary human skeletal muscle cells.* Diabetes, 2009. **58**(12): p. 2731-40.
223. Takahashi, M., et al., *Chemerin regulates beta-cell function in mice.* Sci Rep, 2011. **1**: p. 123.
224. Wargent, E.T., et al., *Evidence from studies in rodents and in isolated adipocytes that agonists of the chemerin receptor CMKLR1 may be beneficial in the treatment of type 2 diabetes.* PeerJ, 2015. **3**: p. e753.
225. Cash, J.L., et al., *Synthetic chemerin-derived peptides suppress inflammation through ChemR23.* J Exp Med, 2008. **205**(4): p. 767-75.
226. Rourke, J.L., et al., *Gpr1 is an active chemerin receptor influencing glucose homeostasis in obese mice.* J Endocrinol, 2014. **222**(2): p. 201-15.
227. Rouger, L., et al., *ChemR23 knockout mice display mild obesity but no deficit in adipocyte differentiation.* J Endocrinol, 2013. **219**(3): p. 279-89.
228. Landgraf, K., et al., *Chemerin as a mediator between obesity and vascular inflammation in children.* J Clin Endocrinol Metab, 2012. **97**(4): p. E556-64.
229. Weigert, J., et al., *Systemic chemerin is related to inflammation rather than obesity in type 2 diabetes.* Clin Endocrinol (Oxf), 2010. **72**(3): p. 342-8.
230. Bozaoglu, K., et al., *Chemerin is associated with metabolic syndrome phenotypes in a Mexican-American population.* J Clin Endocrinol Metab, 2009. **94**(8): p. 3085-8.
231. Ji, Q., et al., *Chemerin is a novel biomarker of acute coronary syndrome but not of stable angina pectoris.* Cardiovasc Diabetol, 2014. **13**: p. 145.

232. Lehrke, M., et al., *Chemerin is associated with markers of inflammation and components of the metabolic syndrome but does not predict coronary atherosclerosis.* Eur J Endocrinol, 2009. **161**(2): p. 339-44.
233. Bobbert, T., et al., *Chemerin and prediction of Diabetes mellitus type 2.* Clin Endocrinol (Oxf), 2015.
234. Stejskal, D., et al., *Chemerin is an independent marker of the metabolic syndrome in a Caucasian population--a pilot study.* Biomed Pap Med Fac Univ Palacky Olomouc Czech Repub, 2008. **152**(2): p. 217-21.
235. Banas, M., et al., *Chemerin is an antimicrobial agent in human epidermis.* PLoS One, 2013. **8**(3): p. e58709.
236. Cash, J.L., A.R. Christian, and D.R. Greaves, *Chemerin peptides promote phagocytosis in a ChemR23- and Syk-dependent manner.* J Immunol, 2010. **184**(9): p. 5315-24.
237. Bondue, B., et al., *The chemerin/ChemR23 system does not affect the pro-inflammatory response of mouse and human macrophages ex vivo.* PLoS One, 2012. **7**(6): p. e40043.
238. Cash, J.L., et al., *Chemerin15 inhibits neutrophil-mediated vascular inflammation and myocardial ischemia-reperfusion injury through ChemR23.* EMBO Rep, 2013. **14**(11): p. 999-1007.
239. Cash, J.L., et al., *Resolution mediator chemerin15 reprograms the wound microenvironment to promote repair and reduce scarring.* Curr Biol, 2014. **24**(12): p. 1406-14.
240. Chang, C., et al., *Chemerin15-Ameliorated Cardiac Ischemia-Reperfusion Injury Is Associated with the Induction of Alternatively Activated Macrophages.* Mediators Inflamm, 2015. **2015**: p. 563951.
241. Luangsay, S., et al., *Mouse ChemR23 is expressed in dendritic cell subsets and macrophages, and mediates an anti-inflammatory activity of chemerin in a lung disease model.* J Immunol, 2009. **183**(10): p. 6489-99.
242. Bondue, B., et al., *ChemR23 dampens lung inflammation and enhances anti-viral immunity in a mouse model of acute viral pneumonia.* PLoS Pathog, 2011. **7**(11): p. e1002358.
243. Yamawaki, H., et al., *A novel adipocytokine, chemerin exerts anti-inflammatory roles in human vascular endothelial cells.* Biochem Biophys Res Commun, 2012. **423**(1): p. 152-7.
244. Neves, K.B., et al., *Chemerin Regulates Crosstalk Between Adipocytes and Vascular Cells Through Nox.* Hypertension, 2015. **66**(3): p. 657-66.
245. Zhao, L., et al., *Chemerin suppresses murine allergic asthma by inhibiting CCL2 production and subsequent airway recruitment of inflammatory dendritic cells.* Allergy, 2014. **69**(6): p. 763-74.
246. Shimamura, K., et al., *Identification of a stable chemerin analog with potent activity toward ChemR23.* Peptides, 2009. **30**(8): p. 1529-38.
247. Doyle, J.R., et al., *Development of a membrane-anchored chemerin receptor agonist as a novel modulator of allergic airway inflammation and neuropathic pain.* J Biol Chem, 2014. **289**(19): p. 13385-96.
248. Joost, P. and A. Methner, *Phylogenetic analysis of 277 human G-protein-coupled receptors as a tool for the prediction of orphan receptor ligands.* Genome Biol, 2002. **3**(11): p. RESEARCH0063.
249. Rourke, J.L., H.J. Dranse, and C.J. Sinal, *CMKLR1 and GPR1 Mediate Chemerin Signaling Through the RhoA/ROCK Pathway.* Mol Cell Endocrinol, 2015.
250. Herova, M., et al., *ChemR23, the receptor for chemerin and resolvin E1, is expressed and functional on M1 but not on M2 macrophages.* J Immunol, 2015. **194**(5): p. 2330-7.
251. Serhan, C.N., N. Chiang, and T.E. Van Dyke, *Resolving inflammation: dual anti-inflammatory and pro-resolution lipid mediators.* Nat Rev Immunol, 2008. **8**(5): p. 349-61.
252. Ohira, T., et al., *Resolvin E1 receptor activation signals phosphorylation and phagocytosis.* J Biol Chem, 2010. **285**(5): p. 3451-61.

253. Arita, M., et al., *Resolvin E1 selectively interacts with leukotriene B4 receptor BLT1 and ChemR23 to regulate inflammation.* J Immunol, 2007. **178**(6): p. 3912-7.
254. Barnea, G., et al., *The genetic design of signaling cascades to record receptor activation.* Proc Natl Acad Sci U S A, 2008. **105**(1): p. 64-9.
255. Shimada, T., et al., *A novel lipopolysaccharide inducible C-C chemokine receptor related gene in murine macrophages.* FEBS Lett, 1998. **425**(3): p. 490-4.
256. Brouwer, N., et al., *Induction of glial L-CCR mRNA expression in spinal cord and brain in experimental autoimmune encephalomyelitis.* Glia, 2004. **46**(1): p. 84-94.
257. Oostendorp, J., et al., *Localization and enhanced mRNA expression of the orphan chemokine receptor L-CCR in the lung in a murine model of ovalbumin-induced airway inflammation.* J Histochem Cytochem, 2004. **52**(3): p. 401-10.
258. Otero, K., et al., *Nonredundant role of CCRL2 in lung dendritic cell trafficking.* Blood, 2010. **116**(16): p. 2942-9.
259. Zabel, B.A., et al., *Mast cell-expressed orphan receptor CCRL2 binds chemerin and is required for optimal induction of IgE-mediated passive cutaneous anaphylaxis.* J Exp Med, 2008. **205**(10): p. 2207-20.
260. Monnier, J., et al., *Expression, Regulation, and Function of Atypical Chemerin Receptor CCRL2 on Endothelial Cells.* J Immunol, 2012. **189**(2): p. 956-67.
261. Migeotte, I., et al., *Distribution and regulation of expression of the putative human chemokine receptor HCR in leukocyte populations.* Eur J Immunol, 2002. **32**(2): p. 494-501.
262. Patel, L., et al., *Expression and functional analysis of chemokine receptors in human peripheral blood leukocyte populations.* Cytokine, 2001. **14**(1): p. 27-36.
263. Galligan, C.L., et al., *Up-regulated expression and activation of the orphan chemokine receptor, CCRL2, in rheumatoid arthritis.* Arthritis Rheum, 2004. **50**(6): p. 1806-14.
264. Hartmann, T.N., et al., *Human B cells express the orphan chemokine receptor CRAM-A/B in a maturation-stage-dependent and CCL5-modulated manner.* Immunology, 2008. **125**(2): p. 252-62.
265. Fra, A.M., et al., *Cutting edge: scavenging of inflammatory CC chemokines by the promiscuous putatively silent chemokine receptor D6.* J Immunol, 2003. **170**(5): p. 2279-82.
266. Douglas, R.M., et al., *Chemokine receptor-like 2 is involved in ischemic brain injury.* J Exp Stroke Transl Med, 2013. **6**: p. 1-6.
267. Yin, F., et al., *Elevated chemokine CC-motif receptor-like 2 (CCRL2) promotes cell migration and invasion in glioblastoma.* Biochem Biophys Res Commun, 2012. **429**(3-4): p. 168-72.
268. Doherty, N.S., et al., *Intraperitoneal injection of zymosan in mice induces pain, inflammation and the synthesis of peptidoleukotrienes and prostaglandin E2.* Prostaglandins, 1985. **30**(5): p. 769-89.
269. Li, Y.M., et al., *Glycation products in aged thioglycollate medium enhance the elicitation of peritoneal macrophages.* J Immunol Methods, 1997. **201**(2): p. 183-8.
270. Dy, M., et al., *Effect of thioglycollate on macrophage lysosomal enzymes.* Biomedicine, 1978. **29**(5): p. 167-70.
271. Karima, R., et al., *The molecular pathogenesis of endotoxic shock and organ failure.* Mol Med Today, 1999. **5**(3): p. 123-32.
272. Okayasu, I., et al., *A novel method in the induction of reliable experimental acute and chronic ulcerative colitis in mice.* Gastroenterology, 1990. **98**(3): p. 694-702.
273. Wirtz, S., et al., *Chemically induced mouse models of intestinal inflammation.* Nat Protoc, 2007. **2**(3): p. 541-6.
274. Davies, J.Q. and S. Gordon, *Isolation and culture of murine macrophages.* Methods Mol Biol, 2005. **290**: p. 91-103.
275. Tomida, M., Y. Yamamoto-Yamaguchi, and M. Hozumi, *Purification of a factor inducing differentiation of mouse myeloid leukemic M1 cells from conditioned medium of mouse fibroblast L929 cells.* J Biol Chem, 1984. **259**(17): p. 10978-82.

276. Sun, M., et al., *A dynamic real-time method for monitoring epithelial barrier function in vitro.* Anal Biochem, 2012. **425**(2): p. 96-103.
277. Olson, K.R. and R.M. Eglen, *Beta galactosidase complementation: a cell-based luminescent assay platform for drug discovery.* Assay Drug Dev Technol, 2007. **5**(1): p. 137-44.
278. Oliver, K.G., J.R. Kettman, and R.J. Fulton, *Multiplexed analysis of human cytokines by use of the FlowMetrix system.* Clin Chem, 1998. **44**(9): p. 2057-60.
279. Suzuki, K., et al., *Assay method for myeloperoxidase in human polymorphonuclear leukocytes.* Anal Biochem, 1983. **132**(2): p. 345-52.
280. Gratama, J.W., et al., *Validation of the single-platform ISHAGE method for CD34(+) hematopoietic stem and progenitor cell enumeration in an international multicenter study.* Cytotherapy, 2003. **5**(1): p. 55-65.
281. Voskuhl, R., *Sex differences in autoimmune diseases.* Biol Sex Differ, 2011. **2**(1): p. 1.
282. Coxon, A., et al., *A novel role for the beta 2 integrin CD11b/CD18 in neutrophil apoptosis: a homeostatic mechanism in inflammation.* Immunity, 1996. **5**(6): p. 653-66.
283. Rao, T.S., et al., *In vivo characterization of zymosan-induced mouse peritoneal inflammation.* J Pharmacol Exp Ther, 1994. **269**(3): p. 917-25.
284. Paul-Clark, M.J., et al., *15-epi-lipoxin A4-mediated induction of nitric oxide explains how aspirin inhibits acute inflammation.* J Exp Med, 2004. **200**(1): p. 69-78.
285. Kono, H., et al., *Uric acid promotes an acute inflammatory response to sterile cell death in mice.* J Clin Invest, 2010. **120**(6): p. 1939-49.
286. Serhan, C.N., et al., *Resolvins: a family of bioactive products of omega-3 fatty acid transformation circuits initiated by aspirin treatment that counter proinflammation signals.* J Exp Med, 2002. **196**(8): p. 1025-37.
287. Navarro-Xavier, R.A., et al., *A new strategy for the identification of novel molecules with targeted proresolution of inflammation properties.* J Immunol, 2010. **184**(3): p. 1516-25.
288. Tager, A.M., et al., *BLTR mediates leukotriene B(4)-induced chemotaxis and adhesion and plays a dominant role in eosinophil accumulation in a murine model of peritonitis.* J Exp Med, 2000. **192**(3): p. 439-46.
289. Kipari, T., et al., *Lymphocytes modulate peritoneal leukocyte recruitment in peritonitis.* Inflamm Res, 2009. **58**(9): p. 553-60.
290. Louahed, J., et al., *Interleukin 9 promotes influx and local maturation of eosinophils.* Blood, 2001. **97**(4): p. 1035-42.
291. Lam, D., D. Harris, and Z. Qin, *Inflammatory mediator profiling reveals immune properties of chemotactic gradients and macrophage mediator production inhibition during thioglycollate elicited peritoneal inflammation.* Mediators Inflamm, 2013. **2013**: p. 931562.
292. Zhang, X., R. Goncalves, and D.M. Mosser, *The isolation and characterization of murine macrophages.* Curr Protoc Immunol, 2008. **Chapter 14**: p. Unit 14.1.
293. Cody, C.S., et al., *Protective anti-lipopolysaccharide monoclonal antibodies inhibit tumor necrosis factor production.* J Surg Res, 1992. **52**(4): p. 314-9.
294. Reddy, R.C., et al., *Selective inhibition of COX-2 improves early survival in murine endotoxemia but not in bacterial peritonitis.* Am J Physiol Lung Cell Mol Physiol, 2001. **281**(3): p. L537-43.
295. Martin, W.J., et al., *Monosodium urate monohydrate crystal-recruited noninflammatory monocytes differentiate into M1-like proinflammatory macrophages in a peritoneal murine model of gout.* Arthritis Rheum, 2011. **63**(5): p. 1322-32.
296. Chen, C.J., et al., *Identification of a key pathway required for the sterile inflammatory response triggered by dying cells.* Nat Med, 2007. **13**(7): p. 851-6.
297. Ajuebor, M.N., et al., *Investigation of the functional role played by the chemokine monocyte chemoattractant protein-1 in interleukin-1-induced murine peritonitis.* Br J Pharmacol, 1998. **125**(2): p. 319-26.

298. Witowski, J., et al., *Synthesis of C-X-C and C-C chemokines by human peritoneal fibroblasts: induction by macrophage-derived cytokines.* Am J Pathol, 2001. **158**(4): p. 1441-50.
299. Syam, S., et al., *β Mangostin suppress LPS-induced inflammatory response in RAW 264.7 macrophages in vitro and carrageenan-induced peritonitis in vivo.* J Ethnopharmacol, 2014. **153**(2): p. 435-45.
300. Michaud, J., D.S. Im, and T. Hla, *Inhibitory role of sphingosine 1-phosphate receptor 2 in macrophage recruitment during inflammation.* J Immunol, 2010. **184**(3): p. 1475-83.
301. Hla, T., *Physiological and pathological actions of sphingosine 1-phosphate.* Semin Cell Dev Biol, 2004. **15**(5): p. 513-20.
302. Matloubian, M., et al., *Lymphocyte egress from thymus and peripheral lymphoid organs is dependent on S1P receptor 1.* Nature, 2004. **427**(6972): p. 355-60.
303. Cash, J.L., G.E. White, and D.R. Greaves, *Chapter 17. Zymosan-induced peritonitis as a simple experimental system for the study of inflammation.* Methods Enzymol, 2009. **461**: p. 379-96.
304. Beutler, B.A., *TLRs and innate immunity*. Blood, 2009. **113**(7): p. 1399-407.
305. Brown, G.D., et al., *Dectin-1 is a major beta-glucan receptor on macrophages.* J Exp Med, 2002. **196**(3): p. 407-12.
306. Ajuebor, M.N., et al., *Role of resident peritoneal macrophages and mast cells in chemokine production and neutrophil migration in acute inflammation: evidence for an inhibitory loop involving endogenous IL-10.* J Immunol, 1999. **162**(3): p. 1685-91.
307. van Vugt, E., et al., *Morphological and functional characteristics of rat steady state peritoneal dendritic cells.* Immunobiology, 1991. **184**(1): p. 14-24.
308. Boring, L., et al., *Impaired monocyte migration and reduced type 1 (Th1) cytokine responses in C-C chemokine receptor 2 knockout mice.* J Clin Invest, 1997. **100**(10): p. 2552-61.
309. Kurihara, T., et al., *Defects in macrophage recruitment and host defense in mice lacking the CCR2 chemokine receptor.* J Exp Med, 1997. **186**(10): p. 1757-62.
310. Tsou, C.L., et al., *Critical roles for CCR2 and MCP-3 in monocyte mobilization from bone marrow and recruitment to inflammatory sites.* J Clin Invest, 2007. **117**(4): p. 902-9.
311. Ajuebor, M.N., et al., *Endogenous monocyte chemoattractant protein-1 recruits monocytes in the zymosan peritonitis model.* J Leukoc Biol, 1998. **63**(1): p. 108-16.
312. Perretti, M., E. Solito, and L. Parente, *Evidence that endogenous interleukin-1 is involved in leukocyte migration in acute experimental inflammation in rats and mice.* Agents Actions, 1992. **35**(1-2): p. 71-8.
313. Woo, P., *Systemic juvenile idiopathic arthritis: diagnosis, management, and outcome.* Nat Clin Pract Rheumatol, 2006. **2**(1): p. 28-34.
314. Alten, R., et al., *The human anti-IL-1 beta monoclonal antibody ACZ885 is effective in joint inflammation models in mice and in a proof-of-concept study in patients with rheumatoid arthritis.* Arthritis Res Ther, 2008. **10**(3): p. R67.
315. Corp, N.P., *Ilaris [prescribing information]. East Hanover, NJ*. 2013.
316. Lefkowith, J.B., *Essential fatty acid deficiency inhibits the in vivo generation of leukotriene B4 and suppresses levels of resident and elicited leukocytes in acute inflammation.* J Immunol, 1988. **140**(1): p. 228-33.
317. Sun, Y.P., et al., *Anti-inflammatory and pro-resolving properties of benzo-lipoxin A(4) analogs.* Prostaglandins Leukot Essent Fatty Acids, 2009. **81**(5-6): p. 357-66.
318. Arita, M., et al., *Stereochemical assignment, antiinflammatory properties, and receptor for the omega-3 lipid mediator resolvin E1.* J Exp Med, 2005. **201**(5): p. 713-22.
319. Serhan, C.N., et al., *Anti-inflammatory actions of neuroprotectin D1/protectin D1 and its natural stereoisomers: assignments of dihydroxy-containing docosatrienes.* J Immunol, 2006. **176**(3): p. 1848-59.
320. O'Sullivan, T.P., et al., *Aromatic lipoxin A4 and lipoxin B4 analogues display potent biological activities.* J Med Chem, 2007. **50**(24): p. 5894-902.

321. Dufton, N., et al., *Anti-inflammatory role of the murine formyl-peptide receptor 2: ligand-specific effects on leukocyte responses and experimental inflammation.* J Immunol, 2010. **184**(5): p. 2611-9.
322. Arita, M., et al., *Metabolic inactivation of resolvin E1 and stabilization of its anti-inflammatory actions.* J Biol Chem, 2006. **281**(32): p. 22847-54.
323. Perretti, M. and F. D'Acquisto, *Annexin A1 and glucocorticoids as effectors of the resolution of inflammation.* Nat Rev Immunol, 2009. **9**(1): p. 62-70.
324. Getting, S.J., R.J. Flower, and M. Perretti, *Inhibition of neutrophil and monocyte recruitment by endogenous and exogenous lipocortin 1.* Br J Pharmacol, 1997. **120**(6): p. 1075-82.
325. Scotland, R.S., et al., *Sex differences in resident immune cell phenotype underlie more efficient acute inflammatory responses in female mice.* Blood, 2011. **118**(22): p. 5918-27.
326. Alcamí, A., et al., *Blockade of chemokine activity by a soluble chemokine binding protein from vaccinia virus.* J Immunol, 1998. **160**(2): p. 624-33.
327. Buatois, V., et al., *Pan-CC chemokine neutralization restricts splenocyte egress and reduces inflammation in a model of arthritis.* J Immunol, 2010. **185**(4): p. 2544-54.
328. Hodges, B.L. and R.K. Scheule, *Hydrodynamic delivery of DNA.* Expert Opin Biol Ther, 2003. **3**(6): p. 911-8.
329. Sebestyén, M.G., et al., *Mechanism of plasmid delivery by hydrodynamic tail vein injection. I. Hepatocyte uptake of various molecules.* J Gene Med, 2006. **8**(7): p. 852-73.
330. Berland, R. and H.H. Wortis, *Origins and functions of B-1 cells with notes on the role of CD5.* Annu Rev Immunol, 2002. **20**: p. 253-300.
331. Combadière, C., et al., *Combined inhibition of CCL2, CX3CR1, and CCR5 abrogates Ly6C(hi) and Ly6C(lo) monocytosis and almost abolishes atherosclerosis in hypercholesterolemic mice.* Circulation, 2008. **117**(13): p. 1649-57.
332. Iqbal, A.J., et al., *Human CD68 promoter GFP transgenic mice allow analysis of monocyte to macrophage differentiation in vivo.* Blood, 2014. **124**(15): p. e33-44.
333. Progatzky, F., M.J. Dallman, and C. Lo Celso, *From seeing to believing: labelling strategies for in vivo cell-tracking experiments.* Interface Focus, 2013. **3**(3): p. 20130001.
334. Webster, J.I., L. Tonelli, and E.M. Sternberg, *Neuroendocrine regulation of immunity.* Annu Rev Immunol, 2002. **20**: p. 125-63.
335. van der Velden, V.H., *Glucocorticoids: mechanisms of action and anti-inflammatory potential in asthma.* Mediators Inflamm, 1998. **7**(4): p. 229-37.
336. Clark, A.R., *Anti-inflammatory functions of glucocorticoid-induced genes.* Mol Cell Endocrinol, 2007. **275**(1-2): p. 79-97.
337. Perretti, M. and R.J. Flower, *Modulation of IL-1-induced neutrophil migration by dexamethasone and lipocortin 1.* J Immunol, 1993. **150**(3): p. 992-9.
338. Marnett, L.J., et al., *Arachidonic acid oxygenation by COX-1 and COX-2. Mechanisms of catalysis and inhibition.* J Biol Chem, 1999. **274**(33): p. 22903-6.
339. Masferrer, J.L., et al., *Selective regulation of cellular cyclooxygenase by dexamethasone and endotoxin in mice.* J Clin Invest, 1990. **86**(4): p. 1375-9.
340. Peshavariya, H.M., et al., *Annexin peptide Ac2-26 suppresses TNFα-induced inflammatory responses via inhibition of Rac1-dependent NADPH oxidase in human endothelial cells.* PLoS One, 2013. **8**(4): p. e60790.
341. Bystrom, J., et al., *Resolution-phase macrophages possess a unique inflammatory phenotype that is controlled by cAMP.* Blood, 2008. **112**(10): p. 4117-27.
342. Lloyd, C.M., et al., *Role of MCP-1 and RANTES in inflammation and progression to fibrosis during murine crescentic nephritis.* J Leukoc Biol, 1997. **62**(5): p. 676-80.
343. Burns, J.M., et al., *Comprehensive mapping of poxvirus vCCI chemokine-binding protein. Expanded range of ligand interactions and unusual dissociation kinetics.* J Biol Chem, 2002. **277**(4): p. 2785-9.

344. Bursill, C.A., et al., *Adenoviral-mediated delivery of a viral chemokine binding protein blocks CC-chemokine activity in vitro and in vivo.* Immunobiology, 2003. **207**(3): p. 187-96.
345. Bursill, C.A., et al., *Broad-spectrum CC-chemokine blockade by gene transfer inhibits macrophage recruitment and atherosclerotic plaque formation in apolipoprotein E-knockout mice.* Circulation, 2004. **110**(16): p. 2460-6.
346. Nayak, S. and R.W. Herzog, *Progress and prospects: immune responses to viral vectors.* Gene Ther, 2010. **17**(3): p. 295-304.
347. Moreland, L.W., et al., *Recombinant soluble tumor necrosis factor receptor (p80) fusion protein: toxicity and dose finding trial in refractory rheumatoid arthritis*. J Rheumatol, 1996. **23**(11): p. 1849-55.
348. Terkeltaub, R., et al., *Monocyte-derived neutrophil chemotactic factor/interleukin-8 is a potential mediator of crystal-induced inflammation.* Arthritis Rheum, 1991. **34**(7): p. 894-903.
349. Mizuno, M., et al., *Zymosan, but not lipopolysaccharide, triggers severe and progressive peritoneal injury accompanied by complement activation in a rat peritonitis model.* J Immunol, 2009. **183**(2): p. 1403-12.
350. Dong, B., W. Ji, and Y. Zhang, *Elevated serum chemerin levels are associated with the presence of coronary artery disease in patients with metabolic syndrome.* Intern Med, 2011. **50**(10): p. 1093-7.
351. Taylor, L., et al., *Primary Macrophage Chemotaxis Induced by Cannabinoid Receptor 2 Agonists Occurs Independently of the CB2 Receptor.* Sci Rep, 2015. **5**: p. 10682.
352. Fauve, R.M., H. Jusforgues, and B. Hevin, *Maintenance of granuloma macrophages in serum-free medium.* J Immunol Methods, 1983. **64**(3): p. 345-51.
353. Atlas, S.J. and S. Lin, *Dihydrocytochalasin B. Biological effects and binding to 3T3 cells.* J Cell Biol, 1978. **76**(2): p. 360-70.
354. Wu, D., G.J. LaRosa, and M.I. Simon, *G protein-coupled signal transduction pathways for interleukin-8.* Science, 1993. **261**(5117): p. 101-3.
355. Sullivan, T.J., et al., *Experimental evidence for the use of CCR2 antagonists in the treatment of type 2 diabetes.* Metabolism, 2013. **62**(11): p. 1623-32.
356. Murray, P.J., et al., *Macrophage activation and polarization: nomenclature and experimental guidelines.* Immunity, 2014. **41**(1): p. 14-20.
357. Nicola, N.A., et al., *Purification of a factor inducing differentiation in murine myelomonocytic leukemia cells. Identification as granulocyte colony-stimulating factor.* J Biol Chem, 1983. **258**(14): p. 9017-23.
358. Stanley, E.R., D.M. Chen, and H.S. Lin, *Induction of macrophage production and proliferation by a purified colony stimulating factor.* Nature, 1978. **274**(5667): p. 168-70.
359. Kaur, J., et al., *Identification of chemerin receptor (ChemR23) in human endothelial cells: chemerin-induced endothelial angiogenesis.* Biochem Biophys Res Commun, 2010. **391**(4): p. 1762-8.
360. Frokjaer, S. and D.E. Otzen, *Protein drug stability: a formulation challenge.* Nat Rev Drug Discov, 2005. **4**(4): p. 298-306.
361. Wang, J.M., et al., *Human recombinant macrophage inflammatory protein-1 alpha and -beta and monocyte chemotactic and activating factor utilize common and unique receptors on human monocytes.* J Immunol, 1993. **150**(7): p. 3022-9.
362. Wolpe, S.D. and A. Cerami, *Macrophage inflammatory proteins 1 and 2: members of a novel superfamily of cytokines.* FASEB J, 1989. **3**(14): p. 2565-73.
363. Combadiere, C., et al., *Cloning and functional expression of CC CKR5, a human monocyte CC chemokine receptor selective for MIP-1(alpha), MIP-1(beta), and RANTES.* J Leukoc Biol, 1996. **60**(1): p. 147-52.
364. Michie, H.R., et al., *Detection of circulating tumor necrosis factor after endotoxin administration.* N Engl J Med, 1988. **318**(23): p. 1481-6.
365. Moore, J.P., et al., *M2 MACROPHAGE ACCUMULATION IN THE AORTIC WALL DURING ANGIOTENSIN II INFUSION IN MICE IS ASSOCIATED WITH FIBROSIS,*

ELASTIN LOSS AND ELEVATED BLOOD PRESSURE. Am J Physiol Heart Circ Physiol, 2015: p. ajpheart.00821.2014.
366. Dalli, J., et al., *Annexin A1 N-terminal derived Peptide ac2-26 exerts chemokinetic effects on human neutrophils.* Front Pharmacol, 2012. **3**: p. 28.
367. Garrouste, F., et al., *Nonspecific binding by macrophages: different modulation of adhesive properties of rat peritoneal cells after plating on a glass or a plastic surface.* J Reticuloendothel Soc, 1982. **31**(5): p. 415-22.
368. Liu, Y. and W.J. Kao, *Human macrophage adhesion on fibronectin: the role of substratum and intracellular signalling kinases.* Cell Signal, 2002. **14**(2): p. 145-52.
369. Lee, C.M. and J. Hu, *Cell density during differentiation can alter the phenotype of bone marrow-derived macrophages.* Cell Biosci, 2013. **3**: p. 30.
370. Leung, K.P., et al., *Heterogeneity among macrophages cultured from mouse bone marrow. Morphologic, cytochemical and flow cytometric analyses.* Cell Tissue Res, 1985. **239**(3): p. 693-701.
371. Prystowsky, M.B., et al., *Multiple hemopoietic lineages are found after stimulation of mouse bone marrow precursor cells with interleukin 3.* Am J Pathol, 1984. **117**(2): p. 171-9.
372. Lobato, N.S., et al., *The adipokine chemerin augments vascular reactivity to contractile stimuli via activation of the MEK-ERK1/2 pathway.* Life Sci, 2012.
373. Ganju, R.K., et al., *Beta-chemokine receptor CCR5 signals via the novel tyrosine kinase RAFTK.* Blood, 1998. **91**(3): p. 791-7.
374. Patel, J., et al., *RGS1 regulates myeloid cell accumulation in atherosclerosis and aortic aneurysm rupture through altered chemokine signalling.* Nat Commun, 2015. **6**: p. 6614.
375. Chou, C.C., et al., *Pharmacological characterization of the chemokine receptor, hCCR1 in a stable transfectant and differentiated HL-60 cells: antagonism of hCCR1 activation by MIP-1beta.* Br J Pharmacol, 2002. **137**(5): p. 663-75.
376. Basu, S. and H.E. Broxmeyer, *CCR5 ligands modulate CXCL12-induced chemotaxis, adhesion, and Akt phosphorylation of human cord blood CD34+ cells.* J Immunol, 2009. **183**(11): p. 7478-88.
377. Gouwy, M., et al., *Synergy between coproduced CC and CXC chemokines in monocyte chemotaxis through receptor-mediated events.* Mol Pharmacol, 2008. **74**(2): p. 485-95.
378. Mellado, M., et al., *Chemokine receptor homo- or heterodimerization activates distinct signaling pathways.* EMBO J, 2001. **20**(10): p. 2497-507.
379. Bellingan, G.J., et al., *Adhesion molecule-dependent mechanisms regulate the rate of macrophage clearance during the resolution of peritoneal inflammation.* J Exp Med, 2002. **196**(11): p. 1515-21.
380. Hoover, D.L. and C.A. Nacy, *Macrophage activation to kill Leishmania tropica: defective intracellular killing of amastigotes by macrophages elicited with sterile inflammatory agents.* J Immunol, 1984. **132**(3): p. 1487-93.
381. Mårtensson, U.E., et al., *The mouse chemerin receptor gene, mcmklr1, utilizes alternative promoters for transcription and is regulated by all-trans retinoic acid.* Gene, 2005. **350**(1): p. 65-77.
382. Perretti, M., et al., *Endogenous lipid- and peptide-derived anti-inflammatory pathways generated with glucocorticoid and aspirin treatment activate the lipoxin A4 receptor.* Nat Med, 2002. **8**(11): p. 1296-302.
383. Lahiri, S., T. Sen, and G. Palit, *Involvement of glucocorticoid receptor and peroxisome proliferator activated receptor-gamma in pioglitazone mediated chronic gastric ulcer healing in rats.* Eur J Pharmacol, 2009. **609**(1-3): p. 118-25.
384. Johnson, T.E., et al., *Thiazolidinedione effects on glucocorticoid receptor-mediated gene transcription and differentiation in osteoblastic cells.* Endocrinology, 1999. **140**(7): p. 3245-54.
385. Warren, M.S., et al., *Results of a proof of concept, double-blind, randomized trial of a second generation antisense oligonucleotide targeting high-sensitivity C-reactive protein (hs-CRP) in rheumatoid arthritis.* Arthritis Res Ther, 2015. **17**(1): p. 80.

386. Gaudet, D., et al., *Antisense Inhibition of Apolipoprotein C-III in Patients with Hypertriglyceridemia.* N Engl J Med, 2015. **373**(5): p. 438-47.
387. Weigert, J., et al., *Circulating levels of chemerin and adiponectin are higher in ulcerative colitis and chemerin is elevated in Crohn's disease.* Inflamm Bowel Dis, 2010. **16**(4): p. 630-7.
388. Kolaczkowska, E., et al., *Resident peritoneal leukocytes are important sources of MMP-9 during zymosan peritonitis: superior contribution of macrophages over mast cells.* Immunol Lett, 2007. **113**(2): p. 99-106.
389. Monnier, J., et al., *Expression, regulation, and function of atypical chemerin receptor CCRL2 on endothelial cells.* J Immunol, 2012. **189**(2): p. 956-67.
390. Del Prete, A., et al., *Molecules regulating migration: CCRL2, a fringe member of the atypical chemoattractant receptor family.* Eur J Immunol, 2013.
391. Beutler, B. and E.T. Rietschel, *Innate immune sensing and its roots: the story of endotoxin.* Nat Rev Immunol, 2003. **3**(2): p. 169-76.
392. Brinkman, B.M., et al., *Gut microbiota affects sensitivity to acute DSS-induced colitis independently of host genotype.* Inflamm Bowel Dis, 2013. **19**(12): p. 2560-7.
393. Babickova, J., et al., *Sex Differences in Experimentally Induced Colitis in Mice: a Role for Estrogens.* Inflammation, 2015.
394. Dieleman, L.A., et al., *Dextran sulfate sodium-induced colitis occurs in severe combined immunodeficient mice.* Gastroenterology, 1994. **107**(6): p. 1643-52.
395. de Poorter, C., et al., *Consequences of ChemR23 heteromerization with the chemokine receptors CXCR4 and CCR7.* PLoS One, 2013. **8**(2): p. e58075.
396. Watanabe, H., et al., *Innate immune response in Th1- and Th2-dominant mouse strains.* Shock, 2004. **22**(5): p. 460-6.
397. Gessner, A., H. Blum, and M. Rollinghoff, *Differential regulation of IL-9-expression after infection with Leishmania major in susceptible and resistant mice.* Immunobiology, 1993. **189**(5): p. 419-35.
398. Schulte, S., G.K. Sukhova, and P. Libby, *Genetically programmed biases in Th1 and Th2 immune responses modulate atherogenesis.* Am J Pathol, 2008. **172**(6): p. 1500-8.
399. Kuroda, E., T. Kito, and U. Yamashita, *Reduced expression of STAT4 and IFN-gamma in macrophages from BALB/c mice.* J Immunol, 2002. **168**(11): p. 5477-82.
400. Pashover-Schallinger, E., et al., *The atypical chemokine receptor D6 controls macrophage efferocytosis and cytokine secretion during the resolution of inflammation.* FASEB J, 2012. **26**(9): p. 3891-900.
401. Mantovani, A., R. Bonecchi, and M. Locati, *Tuning inflammation and immunity by chemokine sequestration: decoys and more.* Nat Rev Immunol, 2006. **6**(12): p. 907-18.
402. Call, D.R., et al., *Ratio of local to systemic chemokine concentrations regulates neutrophil recruitment.* Am J Pathol, 2001. **158**(2): p. 715-21.
403. Cacalano, G., et al., *Neutrophil and B cell expansion in mice that lack the murine IL-8 receptor homolog.* Science, 1994. **265**(5172): p. 682-4.
404. Alm, A.S., et al., *Variation of lipopolysaccharide-induced acute lung injury in eight strains of mice.* Respir Physiol Neurobiol, 2010. **171**(2): p. 157-64.
405. Mauer, J., et al., *Signaling by IL-6 promotes alternative activation of macrophages to limit endotoxemia and obesity-associated resistance to insulin.* Nat Immunol, 2014. **15**(5): p. 423-30.
406. Griffin, G.K., et al., *IL-17 and TNF-alpha sustain neutrophil recruitment during inflammation through synergistic effects on endothelial activation.* J Immunol, 2012. **188**(12): p. 6287-99.
407. Badalyan, V., et al., *TNF-alpha/IL-17 synergy inhibits IL-13 bioactivity via IL-13Ralpha2 induction.* J Allergy Clin Immunol, 2014. **134**(4): p. 975-8 e5.
408. Maione, F., et al., *Interleukin 17 sustains rather than induces inflammation.* Biochem Pharmacol, 2009. **77**(5): p. 878-87.
409. Edwards, J.C., A.D. Sedgwick, and D.A. Willoughby, *The formation of a structure with the features of synovial lining by subcutaneous injection of air: an in vivo tissue culture system.* J Pathol, 1981. **134**(2): p. 147-56.

410. Bowcock, A.M. and J.G. Krueger, *Getting under the skin: the immunogenetics of psoriasis.* Nat Rev Immunol, 2005. **5**(9): p. 699-711.
411. Nestle, F.O., et al., *Plasmacytoid predendritic cells initiate psoriasis through interferon-alpha production.* J Exp Med, 2005. **202**(1): p. 135-43.
412. Vanbervliet, B., et al., *The inducible CXCR3 ligands control plasmacytoid dendritic cell responsiveness to the constitutive chemokine stromal cell-derived factor 1 (SDF-1)/CXCL12.* J Exp Med, 2003. **198**(5): p. 823-30.
413. Wagner, E.F., et al., *Psoriasis: what we have learned from mouse models.* Nat Rev Rheumatol, 2010. **6**(12): p. 704-14.
414. Gudjonsson, J.E., et al., *Mouse models of psoriasis.* J Invest Dermatol, 2007. **127**(6): p. 1292-308.
415. Sano, S., et al., *Stat3 links activated keratinocytes and immunocytes required for development of psoriasis in a novel transgenic mouse model.* Nat Med, 2005. **11**(1): p. 43-9.
416. Ernst, M.C., et al., *Chemerin exacerbates glucose intolerance in mouse models of obesity and diabetes.* Endocrinology, 2010. **151**(5): p. 1998-2007.
417. Barnes, P.J., *Immunology of asthma and chronic obstructive pulmonary disease.* Nat Rev Immunol, 2008. **8**(3): p. 183-92.
418. Barnes, P.J., *New anti-inflammatory targets for chronic obstructive pulmonary disease.* Nat Rev Drug Discov, 2013. **12**(7): p. 543-59.
419. Korganow, A.S., et al., *From systemic T cell self-reactivity to organ-specific autoimmune disease via immunoglobulins.* Immunity, 1999. **10**(4): p. 451-61.
420. Monach, P.A., D. Mathis, and C. Benoist, *The K/BxN arthritis model.* Curr Protoc Immunol, 2008. **Chapter 15**: p. Unit 15 22.

Appendix 1: Published work

Patel J, McNeill E, Douglas G, Hale AB, de Bono J, Lee R, Iqbal AJ, **Regan-Komito D**, Stylianou E, Greaves DR, Channon KM.
RGS1 regulates myeloid cell accumulation in atherosclerosis and aortic aneurysm rupture through altered chemokine signalling.
Nat Commun. 2015 Mar 18;6:6614. doi: 10.1038/ncomms7614.

McNeill E, Iqbal AJ, Patel J, White GE, **Regan-Komito D**, Greaves DR, Channon KM.
Contrasting in vitro vs. in vivo effects of a cell membrane-specific CC-chemokine binding protein on macrophage chemotaxis.
J Mol Med (Berl). 2014 Aug 1. [Epub ahead of print]

Iqbal AJ, McNeill E, Kapellos TS, **Regan-Komito D**, Norman S, Burd S, Smart N, Machemer DE, Stylianou E, McShane H, Channon KM, Chawla A, Greaves DR.
Human CD68 promoter GFP transgenic mice allow analysis of monocyte to macrophage differentiation in vivo.
Blood. 2014 Oct 9;124(15):e33-44. doi: 10.1182/blood-2014-04-568691.

Iqbal AJ, **Regan-Komito D**, Christou I, White GE, McNeill E, Kenyon A, Taylor L, Kapellos TS, Fisher EA, Channon KM, Greaves DR.
A real time chemotaxis assay unveils unique migratory profiles amongst different primary murine macrophages..
PLoS One. 2013;8(3):e58744. doi: 10.1371/journal.pone.0058744. Epub 2013 Mar 14.